Evaluation of the catecholaminergic system in recognition memory

Stephanie Tran

A dissertation submitted to the University of Bristol in accordance with the requirements for award of the degree of Doctor of Philosophy in the Faculty of Life Sciences

December 2021

Word count 44,409

Abstract

Associative recognition memory depends on a network of brain regions, which includes: the hippocampus (HPC), medial prefrontal cortex (mPFC) and nucleus reuniens (NRe). How noradrenaline modulates these brain regions during associative recognition memory has not been thoroughly characterised. In addition, little is known about the anatomical organisation of the noradrenergic (as well as dopaminergic) systems in the NRe. This thesis aims to characterise the anatomy of the catecholaminergic system in the NRe as well as explore the functional role of noradrenaline originating from the locus coeruleus (LC), in the NRe, HPC and mPFC, in long-term associative recognition memory.

The first results chapter employs anatomical techniques, revealing that the entire rostral-caudal axis of the NRe is innervated with catecholaminergic-positive fibers. The chapter further demonstrates that the NRe receives its dopaminergic input from the A13 cell group and noradrenergic input from the LC.

The second results chapter utilises a pharmacological approach to explore the functional role of noradrenergic neurotransmission in the NRe, HPC and mPFC in long-term object-in-place memory. It revealed that antagonism of α1- and agonism of α2- adrenoceptors in the NRe impaired the retrieval but not encoding of object-in-place memory. In contrast, in the HPC, agonism of α2- and antagonism of β- adrenoceptors impaired memory encoding but not retrieval, while in the mPFC manipulation of the adrenergic receptors were without effect on memory performance.

The third results chapter employs an optogenetic approach to explore whether inputs from the LC to the NRe and HPC are critical for recognition memory. In line with the pharmacology results, it is revealed that LC to NRe inputs are critical for the retrieval but not encoding of object-in-place memory while LC to HPC inputs are critical for the encoding but not retrieval of object-in-place memory.

Together, the results of this thesis indicate that the NRe is more extensively innervated with catecholaminergic fibers than previously characterised. Further, the

data also demonstrates that noradrenaline originating from the LC, has dissociable effects at different stages of associative memory processing in the NRe, HPC and mPFC.

Dedication and Acknowledgements

I would like to start by thanking my primary supervisor Clea Warburton, for giving me the opportunity in the first place to do this PhD. Thank you for the continuous support throughout my PhD and allowing me to grow as a scientist by trusting me and giving me freedom to run with my ideas, even if they didn't always go according to plan! I would also like to thank my second supervisor John Aggleton for providing support, insight and reassurance during my PhD.

Thank you to Gareth Barker and Mathias Mathiasen for teaching me all the techniques that I have used in this thesis. In particular, Gareth who has mentored me throughout my PhD and also provided endless support and encouragement.

Thanks to all the members of the Bashir/ Warburton group (past and present) for their technical support, being a lovely bunch of people and making the office and lab an enjoyable place to work.

Another thank you to all the SWBio gals in Bristol. In particular, Naomi and Megan for always being available for spontaneous coffee breaks and providing a great support network for the last 4 years.

Finally, I would like to thank my family for their constant support. To my partner Callum, for always being a source of fun and laughter and taking my mind off the PhD. My siblings, Shufan and Michael, for being available whenever for chats about utter nonsense. Dad, for letting me do my own thing without any pressure. Mum, thank you for giving me the nudge that I needed all those years ago to apply myself.

Author's Declaration

I declare that the work in this dissertation was carried out in accordance with the requirements of the University's Regulations and Code of Practice for Research Degree Programmes and that it has not been submitted for any other academic award. Except where indicated by specific reference in the text, the work is the candidate's own work. Work done in collaboration with, or with the assistance of, others, is indicated as such. Any views expressed in the dissertation are those of the author.

SIGNED: ..... DATE:.....

Contents

List of Figures

List of Tables

Abbreviations

3V Third ventricle

4V 4th ventricle

6-OHDA 6-hydroxydopamine

A1-7 A1-7 noradrenaline cells

A8-17 A8-17 dopamine cells

AHA Anterior hypothalamic area, anterior part

AHP Anterior hypothalamic area, posterior part

AM Anteromedial thalamic nucleus

AMV Anteromedial thalamic nucleus, ventral part

ANS Accessory neurosecretory nuclei

AP Anterior-posterior

Bar Barrington's nucleus

BLA Basolateral amygdala

CA1-3 Cornu ammonis 1-3

CB Calbindin

CCK Cholecystokinin

CGA Central gray, alpha part

CGB Central gray, beta part

CGG Central gray, gamma part

CGO Central gray, nucleus O

CGPn Central gray of the pons

CGRP Calcitonin gene-related peptide

ChR2 Channelrhodopsin-2

CM Central medial thalamic nucleus

COMT Catechol-O-methyltransferase

CR Calretinin

CTB Cholera-toxin b

CTT Central tegmental tract

D1-5 Dopamine 1-5 receptor

DA Dorsal hypothalamic area

DAT Dopamine transporter

DBH Dopamine beta-hydroxylase

DG Dentate gyrus

DMC Dorsomedial hypothalamic nucleus, compact part

DMD Dorsomedial hypothalamic nucleus, dorsal part

DMSO Dimethyl sulfoxide

DMV Dorsomedial hypothalamic nucleus, ventral part

DNB Dorsal noradrenergic bundle

DNMS Delayed non-matching-to-sample task

DSP-4 N-(2-choloro-ethyl)-N-ethyl)-2-bromobenzylamine

DV Dorsoventral

EEG Electroencephalogram

Eve Nucleus of origin of efferents of the vestibular nerve

F Fornix

FB Fast blue

FG FluoroGold

fMRI Functional magnetic resonance imaging

GABA γ-Aminobutyric acid

GPCR G protein-coupled receptor

HPC Hippocampus

HPLC-ECD High-pressure liquid chromatography with electrochemical detection

IAD Interanterodorsal thalamic nucleus

IAM Interanteromedial thalamic nucleus

JLPH Juxtaparaventricular part of lateral hypothalamus

$\mathbf{K_d}$ Dissociation constant

$\mathbf{K_i}$ Inhibitory constant

L-Enk Leucin-enkephalin

LC Locus coeruleus

LDTg Laterodorsal tegmental nucleus

LPB Lateral parabrachial nucleus

LPBI Lateral parabrachial nucleus, internal part

LPbV Lateral parabrachial nucleus, ventral part

LTP Long term potentiation

MAO Monamine Oxidase

MD Mediodorsal thalamus

Me5 Mesencephalic trigeminal nucleus

MFB Medial forebrain bundle

ML Mediolateral

MPA Medial preoptic area

MPB Medial parabrachial nucleus

mPFC Medial prefrontal cortex

MT Medial terminal nucleus of the accessory optic tract

MVeMC Medial vestibular nucleus, magnocellular part

MVePC Medial vestibular nucleus, parvicellular part

NET Noradrenaline transporter

NMDA N-methyl-D-aspartate

NPY Neuropeptide Y

NRe Nucleus reuniens

PaAP Paraventricular hypothalamic nucleus, anterior parvicellular part

PaDC Paraventricular hypothalamic nucleus, dorsal cap

PaLM Paraventricular hypothalamic nucleus, lateral magnocellular part

PaMP Paraventricular hypothalamic nucleus, medial parvicellular part

PaPo Paraventricular hypothalamic nucleus, posterior part

PaXi Paraxiphoid nucleus of thalamus

PBS Phosphate-buffered saline

PBST Phosphate-Buffered Saline/Tween

PDTg Posterodorsal tegmental nucleus

Pe Periventricular hypothalamic nucleus

PeFLH Perifornical part of lateral hypothalamus

PFA Paraformadehyde

PFC Prefrontal cortex

PH Posterior hypothalamic nucleus

PHD Posterior hypothalamic area, dorsal part

PRH Perirhinal cortex

PT Paratenial thalamic nucleus

PV Parvalbium

PVA Paraventricular thalamic nucleus, anterior part

Re Reuniens thalamic nucleus

Rh Rhomboid thalamic nucleus

Scp Superior cerebellar peduncle (brachium conjunctivum)

Scpd Superior cerebellar peduncle, descending limb

SEM Standard error of mean

SGe Supragenual nucleus

SMV Superior medullary velum

SNc Substantia nigra pars compacta

SOM Somatostatin

SP Substance P

Sph Sphenoid nucleus

Stg Stigmoid hypothalamic nucleus

STMPM Bed nucleus of the stria terminalis, medialdivision, posteromedial part

Su5 Supratrigeminal nucleus

Sub Submedius thalamic nucleus

SubCD Subcoeruleus nucleus, dorsal part

SubD Submedius thalamic nucleus, dorsal part

SubV Submedius thalamic nucleus, ventral part

SuVe Superior vestibular nucleus

TH tyrosine hydroxylase

TRN Thalamic reticular nucleus

Veme Vestibulomesencephalic tract

VIP Vasoactive intestinal polypeptide

VM Ventromedial thalamic nucleus

VMAT Vesicular monamine transporter

VNAB Ventral noradrenergic bundle

VPm Ventral posteromedial nucleus

VRe Ventral reuniens thalamic nucleus

VTA Ventral tegmental area

Xi Xiphoid thalamic nucleus

ZID Zona incerta, dorsal part

ZIR Zona incerta, rostral part

1 General Introduction

1.1 Recognition memory

Recognition memory refers to the ability to determine whether a stimulus (e.g. a face, object or place) has been previously experienced (Brown & Aggleton, 2001; Eichenbaum et al., 1994; Eichenbaum et al., 2007). Recognition memory judgements can be made based on different types of information. For example, discriminations can be based on item recognition, which requires one to make judgments based on whether an item is novel or familiar; associative recognition, which involves determining whether a familiar item has been already encountered with a context or spatial location; or recency memory, which requires determining which object has been experienced more recently. It is evident that recognition memory consists of multiple component processes which depend on the features of information to be processed. In agreement with this view, a prominent model of recognition memory, the dual process model, suggests that two functionally separate mechanisms, familiarity and recollection, are supported by different brain regions - the perirhinal cortex (PRH) for the familiarity component and the hippocampus (HPC) as well as other brain regions for the recollective component (Brown & Aggleton, 2001; Eichenbaum et al., 2007). In contrast to the dual process model of recognition memory, the single process model suggests that recollection and familiarity are not distinct memory processes but instead consist of a unitary process. That is, recognition memory is a continuous memory process whereby recollection and familiarity represent differences in memory strength, strong and weak memories, respectively (Squire et al., 2007). While the experiments conducted in the thesis do not explicitly explore differences between the single and dual process models of recognition memory, a vast body of human and rodent literature (as reviewed in the next section) have indicated that different brain regions make separable contributions to recognition memory, thus providing support for the dual process model of recognition memory.

1.1.1 Recognition memory in humans

Clinical studies examining recognition memory in neurophysiological patients have provided evidence that separate components of recognition memory depend on different brain regions. For instance, in human amnesic patients with HPC damage, studies have revealed that patients are unable to make recognition memory judgements which involve the recollection of associated information but not when they require recognition of single-items (Adlam et al., 2009; Baddeley et al., 2001; Bastin et al., 2004; Mayes et al., 2002; Patai et al., 2015; Turriziani et al., 2008) (but see (Cipolotti et al., 2006; Manns et al., 2003; Wais et al., 2006) for contradictory evidence suggesting that the HPC is involved in both familiarity and recollective components of recognition memory). Beyond the HPC, studies have shown that in one amnesic patient with PRH damage, familiarity but not recollection is impaired (Bowles et al., 2007; Köhler & Martin, 2020). Furthermore, it has also been demonstrated that patients with left thalamic infarcts (with damage mainly focused in the mediodorsal thalamus; MD) show impaired recollection but persevered familiarity (Danet et al., 2017). In further support of the double dissociation between recollection and familiarity, studies utilising task-based functional magnetic resonance imaging (fMRI) and electroencephalogram (EEG) recordings have also reported that distinct brain regions are differentially engaged during familiarity- and recollective-based recognition (Kafkas et al., 2017; Staresina et al., 2012; Staresina et al., 2013).

While the human literature outlined above has provided important insights to the brain regions underling recognition memory, studies involving humans do have several limitations. For instance, in amnesic human patients, brain damage is often not localised to a single brain region but instead involves damage to multiple brain regions, thus conclusions concerning a specific brain region are limited. In addition, fMRI and EEG studies only offer correlative evidence regarding the role of a brain region to recognition memory processing (Bell & Bultitude, 2018). As a result, a considerable amount of research concerned with the neural substrates involved in recognition memory has focused on animals, in particular, in rodents. The use of

animals allows researchers to induce permanent lesions or reversible inactivation's, therefore allowing one to unravel the precise contribution of a given brain region while also ruling out compensatory mechanisms. Research involving animals over the years has therefore both complemented and extended findings from human studies.

1.1.2 Recognition memory in rodents

1.1.2.1 Spontaneous recognition memory tasks

To investigate recognition memory in rodents, the spontaneous recognition memory tasks are commonly used (Ennaceur & Delacour, 1988). The spontaneous recognition memory tasks take advantage of an animal's natural propensity to explore novelty over familiarity, in doing so the animal demonstrates that it has memory for familiar aspects of the environment and is therefore able to successfully discriminate novel from familiar, thus demonstrating recognition memory. The spontaneous recognition memory tasks therefore do not require rule learning or reinforcement and instead rely on an animal's spontaneous exploratory behaviour. In the classic spontaneous recognition memory task, the novel object recognition task, it comprises of sample and test phase separated by a delay period – a short delay to test short-term memory or a long delay to test long-term memory (Figure 1.1). During the sample phase, animals are encountered with two identical objects and permitted to explore the objects. Following a delay period, at test, animals are exposed to two objects, a novel object and a copy of the sample object, and once again allowed to freely explore the objects. Therefore, an animal with intact object recognition memory will demonstrate a greater amount of novel object exploration over the familiar object. Since the initial description of the novel object recognition task by Ennaceur & Delacour (1988), the experimental paradigm has been adapted by Ennaceur and others to test other types of recognition memory which involve discriminations based on spatial and contextual features of an environment (Dix & Aggleton, 1999; Eacott & Norman, 2004; Ennaceur & Aggleton, 1994; Mitchell & Laiacona, 1998). The spontaneous recognition memory tasks that the current thesis is concerned with

are: novel object recognition, object location and object-in-place (see Section 2.3.6 for more details about task procedure). The next section will primarily summarise literature that has utilised the spontaneous recognition memory tasks to explore the involvement of the HPC, medial prefrontal cortex (mPFC) and nucleus reuniens (NRe) in recognition memory, as the current thesis conducts a functional investigation of these structures.

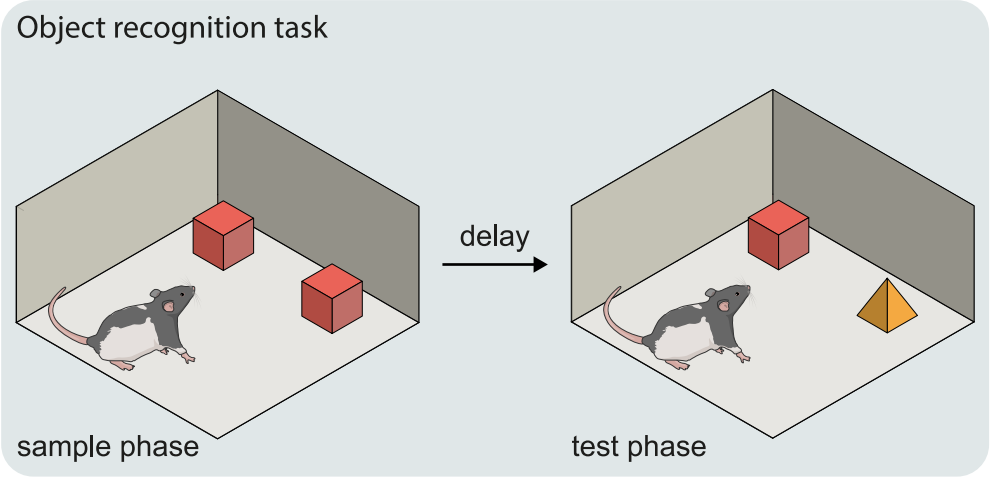

Figure 1.1. Illustration of the object recognition task. In the sample phase an animal is presented with two identical objects and allowed to freely explore these objects. Following a delay period, the animal is returned to the arena where it encounters a novel object (yellow pyramid) and the previously encountered familiar object (red cube). An animal with intact object recognition memory demonstrates preferential exploration of the novel object over the familiar object.

1.1.2.2 Hippocampus

Studies employing the spontaneous recognition memory paradigm have revealed an important role for the HPC in remembering spatial and temporal aspects of when stimuli were previously encountered. For example, studies have established hippocampal involvement in the object location task (Barker & Warburton, 2011; López et al., 2016; Mumby et al., 2002; Tuscher et al., 2018), which is in agreement with the substantial evidence implicating the HPC in spatial navigation (Morris et al., 1982; O'Keefe & Nadel, 1978). Furthermore, the hippocampus has also been demonstrated to be involved in recognising the relative recency of objects and

integrating object-place associations as evidenced by deficits in the temporal order task and object-in-place task, respectively (Barker & Warburton, 2011).

While the above evidence provides conclusive evidence regarding the importance of the HPC when object discriminations are based on temporal, spatial or associative information, literature concerning hippocampal involvement in object recognition memory is less consistent. For instance, while a large proportion of literature agrees that lesions of the HPC do not impact an animals ability to recognise objects when testing conditions involve exploration of two identical objects during the sample phase (Ainge et al., 2006; Barker & Warburton, 2011; Forwood et al., 2005; Good et al., 2007; Langston & Wood, 2010; López et al., 2016; Mumby et al., 2002; Mumby et al., 2005; Winters et al., 2004), in contrast, conflicting evidence exists implicating the HPC in object recognition memory (Broadbent et al., 2010; Clark et al., 2000; Cohen et al., 2013; Hammond et al., 2004; Tuscher et al., 2018). Attempts have been made to provide an explanation for these discrepant findings, suggesting that factors such as extent of HPC lesions, amount of exploration during the sample phase, or length of retention delay may perhaps explain these conflicting results. However, a general consensus has not been reached and as a result whether the HPC is critical for object recognition memory processing is still much debated (Aggleton & Nelson, 2020; Ainge et al., 2006; Chao et al., 2020).

1.1.2.3 Medial prefrontal cortex

Lesions of the mPFC have been revealed to disrupt object-in-place memory and temporal order memory but not object recognition and object location memory (Barker et al., 2007; Ennaceur et al., 1997; Hannesson et al., 2004; Mitchell & Laiacona, 1998). Furthermore, optogenetic stimulation of mPFC glutamatergic neurons after the sample phase were shown to specifically enhance object-in-place memory, however, object recognition and object location memory were unaffected (Benn et al., 2016). In addition, in a variant of the delayed non-matching-to-sample task (DNMS), rats with selective mPFC lesions showed preserved item recognition memory but impaired recollection-based recognition memory (Farovik et al., 2008).

While the foregoing evidence does indicate that the mPFC is critically required for recognition memory tasks that require object-place associations and recency discriminations and not when tasks require discriminations based on object identity only. It should be noted that there are contradictory reports suggesting that the mPFC is involved in object recognition and object location memory (Tuscher et al., 2018). Tuscher et al. (2018) revealed that following chemogenetic inactivation of the mPFC in mice during the delay phase of the object recognition and object location task, that memory was impaired in both tasks when tested at a 4- or 24-hour delay. Given that previous studies reporting null results in the object recognition and object location task, when animals have been subject to mPFC lesions, employed shorter delays of <2 hours (Barker et al., 2007; Benn et al., 2016; Ennaceur et al., 1997; Hannesson et al., 2004), it has been suggested that the mPFC becomes requisite for the consolidation of object recognition and object location memories when tested at a long delay between the sample and test phase but not following a short delay (Chao et al., 2020; Mathis, 2018; Tuscher et al., 2018).

1.1.2.4 Nucleus reuniens

More recent behavioural evidence has included the NRe as an additional brain region implicated in recognition memory. Barker & Warburton (2018) tested animals with excitotoxic lesions of the NRe on variants of the spontaneous exploration tasks (novel object recognition, object-in-place and object location). Such lesions of the NRe were found to impair object-in-place recognition memory when animals were tested at a 3-hour delay but not following a 5-minute delay. Furthermore, object recognition memory and object location memory were without effect. In the same study, to further examine at which stage of associative recognition memory processing (encoding or retrieval) that the NRe is required for, a pharmacological approach was adopted. This involved infusing a number of agonists and antagonists that target specific receptors into the NRe. It was revealed that: infusion of muscimol (GABA agonist) impaired object-in-place memory when tested at a long but not short delay when infusions were made both before the sample and test phase; infusion of AP5

(NMDAR antagonist) was without effect; infusions of scopolamine and mecamylamine (muscarinic and nicotinic cholinergic antagonists, respectively) impaired the encoding of long-term object-in-place memory but did not affect retrieval; and finally, infusion of anisomycin (protein synthesis inhibitor) impaired the encoding of object-in-place memory following a 24-hour delay but not a 3-hour delay.

Although the interaction between the NRe and the HPC and mPFC was not functionally tested in the study, given the extensive behavioural evidence that indicates that object-in-place memory involves the cooperative actions of the HPC and mPFC (see Section 1.1.2.5), and the anatomical evidence that indicates that the NRe shares strong connections with the mPFC and HPC (see Section 1.2.3), Barker & Warburton (2018) proposed that the NRe serves as a key component part of a neural circuit that includes the HPC and mPFC, that is critical for associative recognition memory. Furthermore, given the time-dependent involvement of the NRe in object-in-place memory it was also suggested that the NRe does not simply serve to only transfer information between the HPC and mPFC but instead is also important in directly coordinating communication between the HPC and mPFC. Taken together, these data indicate that the NRe serves as a key node part of the long-term associative recognition memory network.

1.1.2.5 A neural network that includes the hippocampus, medial prefrontal cortex and nucleus reuniens in associative recognition memory

The studies outlined thus far have described the individual contributions of the HPC, mPFC and NRe in recognition memory. Taking into consideration the extensive anatomical connectivity between the HPC, mPFC and NRe (see Section 1.2.3), it is unsurprising that direct functional evidence for the interactions between these brain structures has been demonstrated for associative recognition memory.

In an initial study, the interaction between the HPC and mPFC was investigated using a functional disconnection paradigm (i.e., lesions that involve removal of one brain region in one hemisphere and the removal a second brain region in the opposite

hemisphere) (Barker & Warburton, 2011). To this end, it was revealed that crossed unilateral lesions of the HPC and mPFC impaired object-in-place and temporal order memory but not object recognition or object location memory (Barker & Warburton, 2011). Therefore, demonstrating that HPC and mPFC interactions support associative recognition memory and temporal order memory. Extending these observations, in a recent study, Barker et al. (2017) identified a functional dissociation in the output pathways of the CA1 region of the HPC to the mPFC. It was revealed that the dorsal CA1 to mPFC pathway is required for temporal order memory, while the intermediate CA1 to mPFC pathway is crucial for object-in-place memory. More recent experiments employing chemogenetic and optogenetic techniques have integrated the NRe as an additional node in this neural network for associative recognition memory and at the same time revealed the specific pathways between the HPC, mPFC and NRe that support different memory stages of associative recognition memory (Barker et al., unpublished data). In these series of experiments, it was demonstrated that inputs from the NRe to dorsal and intermediate CA1, NRe to mPFC, and inputs from the intermediate CA1 to mPFC are involved in the acquisition of associative recognition memory but not the retrieval, in contrast, inputs from the mPFC to NRe and NRe to intermediate CA1 are required for the retrieval but not encoding of associative recognition memory. These findings clearly demonstrate that specific directional interactions between the HPC, mPFC and NRe are differentially engaged during different stages of associative memory processing.

1.2 Nucleus reuniens

Until recently the NRe of the midline thalamus has been considered a 'non-specific' thalamic nuclei proposed to only relay sensorimotor information to the cortex (Groenewegen & Berendse, 1994). However, this notion is no longer supported due to the recent appreciation of the strong anatomical connections that the NRe shares with limbic-associated structures, such as the HPC and mPFC, and the accumulating functional evidence implicating the NRe in several cognitive domains (reviewed in

Cassel et al., 2013; Dolleman-Van Der Weel et al., 2019). This section will provide an overview of the general anatomical features of the NRe, the anatomical connections between the NRe, HPC and mPFC as well as functional evidence concerning the NRe with respect to behavioural functions which require the cooperative actions of the HPC and mPFC.

1.2.1 Anatomical subdivisions of the nucleus reuniens

The NRe is located on the midline of the thalamus above the third ventricle, extending the entire rostro-caudal axis of the thalamus. The size and shape of the NRe varies across its rostro-caudal extent (Figure 1.2). The rostral-most portion of the NRe is divided into two separate components, located by the third ventricle. Caudally, the two separate components merge in the midline, above the third ventricle. At this caudal level, the NRe comprises of a medial portion and lateral portion (often referred to as lateral wings of the NRe or peri-reuniens) (Groenewegen & Berendse, 1994; Paxinos & Watson, 2006).

1.2.2 Neuronal sub-types in the nucleus reuniens

The NRe is thought to consist of predominantly glutamatergic cells, where anatomical studies have demonstrated that the NRe sends dense excitatory afferents to the HPC, mPFC and entorhinal cortex (Bokor et al., 2002; Dolleman-Van der Weel & Witter, 2000; Hur & Zaborszky, 2005; Wouterlood et al., 2008; Wouterlood et al., 1990). More recently, the presence of dopaminergic-positive neurons has been identified in the NRe, thought to belong to the A13 dopaminergic cell group (Ogundele et al., 2017). Immunohistochemical experiments have revealed that the NRe contains the calcium-binding proteins calretinin (CR) and calbindin (CB) but not parvalbumin (PV). More specifically, the NRe contains cells that only express CR or CB as well as cells that co-express both CR and CB (Arai et al., 1994; Bokor et al., 2002; Viena et al., 2021). Moreover, the NRe does not contains cells immunopositive for somatostatin (SOM), cholecystokinin (CCK), neuropeptide Y (NPY), leucin-enkephalin (L-Enk), substance P (SP), calcitonin gene-related peptide

(CGRP) and vasoactive intestinal polypeptide (VIP) (Bokor, 2002). A proportion of CR and CB positive neurons in the NRe appear to be co-expressed with the excitatory amino acids, glutamate and aspartate (Frassoni et al., 1997; Wouterlood et al., 2008). Interestingly, recent observations have demonstrated a role for this neurochemical heterogeneity within the thalamus (Lara-Vásquez et al., 2016). In this study, Lara-Vásquez et al. (2016) made simultaneous recordings from dorsal hippocampal neurons and midline thalamic neurons (including the NRe) and revealed a dissociation in neural activity between CR-positive and CR-negative neurons of the thalamus during specific hippocampal network oscillations. Specifically, CR-negative neurons were found to fire spontaneously at higher levels compared to CR-negative neurons. During hippocampal theta, CR-negative neurons increased their firing while CR-positive neurons did not. Lastly, during sharp wave-ripples, firing activity of CR-negative neurons was unaffected while activity of CR-positive neurons was inhibited. Given that different hippocampal network oscillations have been associated with different stages of memory, i.e., theta oscillations with memory encoding and sharp-wave ripples with memory consolidation (Buzsáki & da Silva, 2012; Ego-Stengel & Wilson, 2010), these results suggest that midline thalamic projection neurons, based on their neurochemical identity, may be able to support different stages of memory processing.

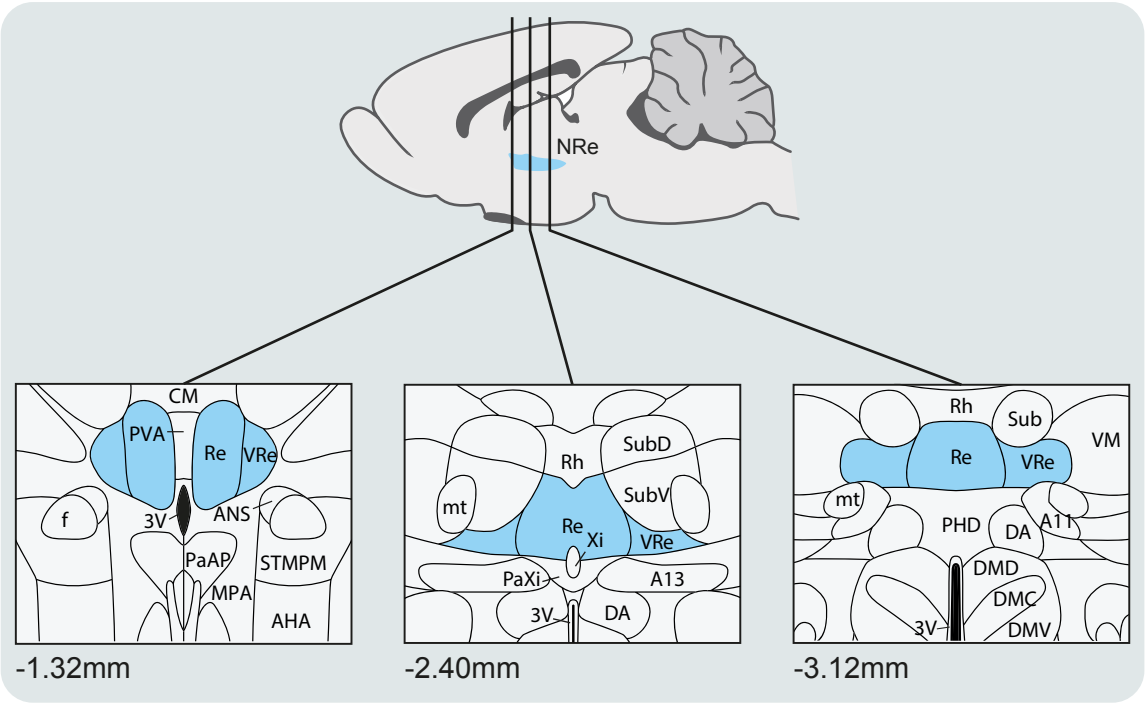

Figure 1.2. Anatomical arrangement of the NRe at the rostral (-1.32mm), intermediate/middle (-2.40mm) and caudal (-3.12mm) levels relative to bregma. The NRe is highlighted in blue. Abbreviations: 3V, third ventricle; A11, A11 dopamine cells; A13, A13 dopamine cells; AHA, anterior hypothalamic area, anterior part; ANS, accessory neurosecretory nuclei; CM, central medial thalamic nucleus; DA, dorsal hypothalamic area; DMC, dorsomedial hypothalamic nucleus, compact part; DMD, dorsomedial hypothalamic nucleus, dorsal part; DMV, dorsomedial hypothalamic nucleus, ventral part; f, fornix; MPA, medial preoptic area; mt, medial terminal nucleus of the accessory optic tract; PaAP, paraventricular hypothalamic nucleus, anterior parvicellular part; PaXi, paraxiphoid nucleus of thalamus; PHD, posterior hypothalamic area, dorsal part; PVA, paraventricular thalamic nucleus, anterior part; Re, nucleus reuniens; Rh, rhomboid thalamic nucleus; Sub, submedius thalamic nucleus; SubD, submedius thalamic nucleus, dorsal part; SubV, submedius thalamic nucleus, ventral part; STMPM, bed nucleus of the stria terminalis, medialdivision, posteromedial part; VM, ventromedial thalamic nucleus; VRe, ventral reuniens thalamic nucleus; Xi, xiphoid thalamic nucleus. Figure is adapted from Cassel et al. (2013). Brain atlas figures are adapted from Paxinos & Watson (2006).

1.2.3 Anatomical connections between the nucleus reuniens, hippocampus and medial prefrontal cortex

A prominent anatomical feature of the NRe is that it receives widespread afferents from many brain structures, but in turn, sends rather selective efferents (Vertes et al., 2015). For instance, the NRe receives widespread input from the cortex, amygdala, basal forebrain, hypothalamus and brain stem (Herkenham, 1978; McKenna & Vertes, 2004; Sesack et al., 1989; Vertes, 2002, 2004; Wouterlood et al., 1990), but sends dense projections to virtually only the HPC and limbic cortical structures (such as the PRH, entorhinal cortex, insular cortex, anterior piriform, and the mPFC) with sparser projections to other brain regions (Herkenham, 1978; Vertes, 2006; Vertes et al., 2006). Of note, are the prominent anatomical connections between the NRe, HPC and mPFC which are of relevance to the aims of the experiments in this thesis. Therefore, this section will summarise the anatomical tracing studies which have revealed the precise input-output organisation of the NRe in relation to its connectivity with the HPC and mPFC (summarised in Figure 1.3).

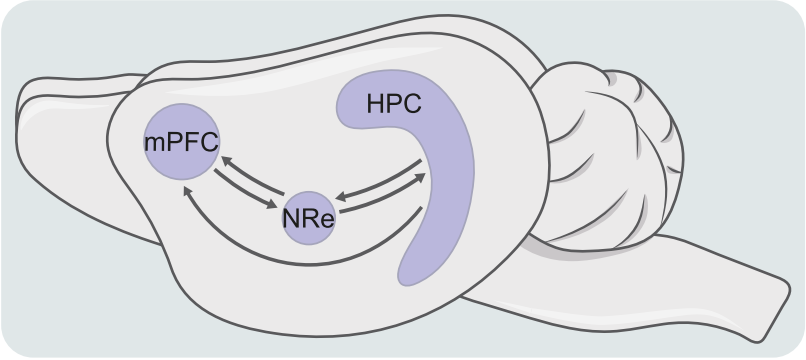

Figure 1.3. Anatomical connections between the NRe, mPFC and HPC. Note, the brain structures have not been anatomically subdivided, arrows are positioned generally to represent the whole brain region. The HPC sends dense projections to the mPFC, however only the anterior cingulate subdivision of the mPFC sends a weak afferent to the HPC (not shown). The NRe shares strong bidirectional connections with the HPC and mPFC.

Anterograde tracing studies have revealed that of the four subregions of the mPFC (medial agranular cortex, anterior cingulate cortex, prelimbic cortex, infralimbic cortex), the NRe heavily projects to the infralimbic, prelimbic and anterior cingulate cortex subregions, with the densest projection terminating in layers 1 and 5/6 (Condé et al., 1995; Vertes et al., 2006; Wouterlood et al., 1990). Specifically, a large proportion of NRe projections to mPFC originate from the caudal NRe, particularly in the lateral wings of the NRe (Hoover & Vertes, 2012; Varela et al., 2014). In turn, it has been demonstrated that all four subregions of the mPFC send projections to the NRe, with the terminals distributing densely to the lateral wings of the NRe (McKenna & Vertes, 2004; Vertes, 2002). Moreover, the NRe sends strong projections to the HPC, heavily innervating the stratum lacosum-moleculare of the CA1 region of the HPC and the molecular layer of the subiculum (Bokor et al., 2002; Herkenham, 1978; Vertes et al., 2006; Wouterlood et al., 1990), with a denser projection to the ventral HPC compared to the dorsal HPC (Hoover & Vertes, 2012; Varela et al., 2014). The NRe does not however project to the dentate gyrus (DG) or CA2/CA3 subregions of the HPC (Vertes et al., 2006; Wouterlood et al., 1990). Furthermore, NRe to HPC projections are found to arise predominantly from the rostral NRe, in particular, the medial aspect of the NRe (Hoover & Vertes, 2012; Varela et al., 2014). HPC projections to the NRe originate from the CA1 region of the ventral HPC and ventral subiculum (McKenna & Vertes, 2004). Interestingly, a small proportion ($\sim$3-9%) of NRe neurons sends projections to both the HPC and mPFC via axon collaterals (Hoover & Vertes, 2012; Varela et al., 2014), therefore placing the NRe in a central location to co-ordinate HPC and mPFC neural activity.

Hippocampal afferents to the mPFC, which primarily originate from the ventral CA1 and ventral subiculum, target the infralimbic and prelimbic subregions. In addition, there is an absence of projections from DG to the mPFC (Jay & Witter, 1991; Vertes et al., 2007). Despite strong HPC to mPFC projections, only weak afferents from the anterior cingulate subdivision of the mPFC to the HPC have been reported (Rajasethupathy et al., 2015). Given the lack of anatomical connections from other mPFC cortices (i.e., infralimbic and prelimbic) to the HPC, it has been

suggested that the NRe, based on the anatomical evidence indicating that the NRe receives strong afferents from the mPFC and that the NRe also provides strong efferents to the HPC, serves as a crucial indirect route for the mPFC to convey information to the HPC (Vertes, 2002). Indeed, direct anatomical evidence for the mPFC-NRe-HPC pathway has been provided. Vertes et al. (2007) paired injections of anterograde and retrograde tracers into the mPFC and HPC, respectively, and revealed that in the NRe, mPFC fibres make synaptic contacts with NRe neurons that send projections to the HPC.

Taken together, the anatomical connections outlined above suggests that the NRe appears to be in a key position to influence the HPC and mPFC. Accordingly, behavioural studies are beginning to provide functional evidence for this anatomical arrangement.

1.2.4 The role of the nucleus reuniens in hippocampal- prefrontal associated cognitive functions

Based on the anatomical features shared between the NRe, mPFC and HPC, described above, the NRe has been implicated in hippocampal-medial prefrontal cortical related cognitive processes. Indeed, behavioural studies are beginning to show that the NRe becomes requisite in memory processes that require the co-operation between the HPC and mPFC but not when such processes only require the HPC but not the mPFC and vice versa (Cassel et al., 2013; Dolleman-van der Weel et al., 2019).

In line with this idea, a number of experiments have now identified that the NRe is required for working memory, demonstrating that lesions or transient inactivation of the NRe impaired performance in a win-shift radial arm maze task (Hembrook & Mair, 2011) and a delayed non-match-to position task (Hembrook et al., 2012) - tasks which are both sensitive to HPC and mPFC lesions (Mair et al., 1998; McDonald & White, 2013; Porter et al., 2000; Porter & Mair, 1997). However, inactivation of the NRe in the hippocampal dependent varying choice delayed-nonmatching task did not have an effect of task performance (Hembrook et al., 2012; Porter et al., 2000). Moreover, using a double-H maze, a task which involves both strategy

shifting and spatial memory components, functions associated with the mPFC and HPC, respectively (Floresco et al., 2008; Morris et al., 1982; O'Keefe & Nadel, 1978; Ragozzino et al., 2003), it was demonstrated that NRe lesioned animals were impaired (Cholvin et al., 2013).

Furthermore, Griffin and colleagues, across a series of experiments using variants of the delayed T-maze paradigm, a task that is known to recruit the mPFC and HPC (Churchwell & Kesner, 2011; Wang & Cai, 2006), have provided further support for NRe involvement in working memory. Hallock et al. (2013) provided the first line of evidence, demonstrating working memory deficits following disruption of the NRe. The role of the NRe in working memory was further extended by Layfield et al. (2015), revealing a delay-dependent involvement of the NRe, suggesting that longer delays between sample and choice phase require greater engagement of the NRe compared to shorter delays. Work by others have also reported spatial working deficits using a T-maze following NRe inactivation (Viena et al., 2018). More recently, using an optogenetic approach, disruption of NRe neural activity at certain timepoints of the T-maze task (i.e., sample, delay or choice phase), selectively impaired performance when the NRe was suppressed during the sample phase but not during the delay or choice phase, implicating the NRe in the encoding of task-relevant information during working memory (Maisson et al., 2018). In addition, in a recent electrophysiology study, inactivation of the NRe not only impaired task performance in a working memory task but also interrupted the well characterised HPC-mPFC synchrony that is observed during successful task performance. These results suggest that the NRe is pivotal in co-ordinating HPC and mPFC neural activity during spatial working memory (Hallock et al., 2016).

In addition to the NRe's role in working memory, the NRe has also been associated with memory consolidation. Loureiro et al. (2012) tested animals with NRe lesions in a Morris water maze task to investigate NRe involvement in recent and remote spatial memory. It was found that NRe lesions specifically impaired task performance when rats were tested at a long delay (25-days post acquisition) but not when they were tested at a shorter delay (5-days post acquisition), suggesting that the NRe is required

for transforming recent memories to remote memories. Given the well-established role for the HPC and mPFC in memory consolidation (Frankland & Bontempi, 2005), and that the NRe shares strong anatomical connections with the HPC and mPFC (see Section 1.2.3), it has therefore been suggested that the NRe is actively involved in modulating HPC-mPFC dialogue that is central for memory consolidation, and that the pattern of results observed by Loureiro et al. (2012), following lesions of the NRe, may be due to disconnection of the HPC from the mPFC (de Vasconcelos & Cassel, 2015). This notion that the NRe is involved in the consolidation of memories is also further supported by studies looking at fear learning, whereby manipulation of NRe function in contextual fear conditioning paradigms have been shown to disrupt the consolidation and retrieval of fear memories (Quet et al., 2020; Troyner et al., 2018; Vetere et al., 2017; Xu & Südhof, 2013).

Collectively, these studies highlight that the NRe is involved in different types of memory that are dependent on the hippocampal-mPFC circuit, whereby the NRe serves to transfer information and co-ordinate activity between the HPC and mPFC, which occurs online during ongoing behaviour and also offline during memory consolidation.

1.3 Noradrenaline

Noradrenaline, also called norepinephrine, is part of the catecholamine family which includes epinephrine (adrenaline) and dopamine. In the central nervous system, noradrenaline containing cell bodies are found in clusters scattered throughout the brainstem and send widespread projections to almost every brain region. The broad projection pattern of the noradrenergic system allows noradrenaline activating via the G-protein coupled adrenergic receptors to modulate many diverse functions, such as arousal, memory, pain and more (Berridge, 2008; Sara, 2009; Schwarz & Luo, 2015).

This section will summarise the noradrenaline system in the central nervous system, and its role in recognition memory with particular focus on the NRe, HPC

and mPFC.

1.3.1 Noradrenaline synthesis

Synthesis of noradrenaline occurs at noradrenergic nerve terminals where enzymes responsible for catalysing the conversion of noradrenaline from the aromatic amino acid L-tyrosine are present in high concentrations. Noradrenaline is synthesised in the following enzymatic steps: tyrosine → dopa → dopamine → noradrenaline (Figure 1.4). Following synthesis, noradrenaline is packaged into synaptic vesicles located in the synaptic terminal by the vesicular monamine transporter (VMAT). Noradrenaline released from the noradrenergic neuron binds to the adrenoceptors located on the post-synaptic neuron or the pre-synaptic neuron (autoreceptors) to initiate intracellular signalling cascades. Depending on the specific receptor that noradrenaline has bound to different effects are elicited (see section 1.3.3 for a more detailed description of the adrenoceptors). While some of the released noradrenaline in the synaptic cleft is degraded by the enzyme catechol-O-methyltransferase (COMT), most of the released noradrenaline is eventually taken back into the pre-synaptic terminal by the noradrenaline transporter (NET). In the pre-synaptic terminal noradrenaline either undergoes degradation, which is catalysed by the enzyme monamine oxidase (MAO), or repackaged into vesicles (Szabadi, 2013) (Figure 1.4).

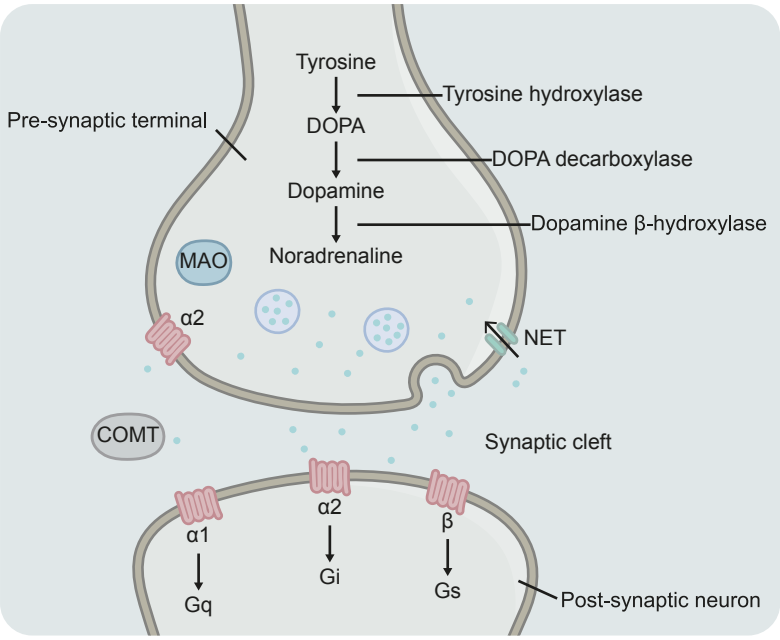

Figure 1.4. Schematic representation of the biosynthesis pathway of noradrenaline at the noradrenergic synapse. Noradrenaline is synthesised from tyrosine though a series of enzymatic steps and stored in synaptic vesicles. Each step is catalysed by a specific enzyme. Upon appropriate electrical stimulation (not shown), the synaptic vesicle binds to the membrane and releases noradrenaline into the synaptic cleft. Released noradrenaline binds to the adrenergic receptors located pre- and post- synaptically to initiate various intracellular signalling cascades. Noradrenaline that has exerted its function or noradrenaline that has not bound to any receptor can either be taken back into the pre-synaptic terminal by NET or degraded by COMT. In the pre-synaptic terminal, noradrenaline can either be repackaged into synaptic vesicles or degraded by the enzyme MAO. Figure adapted from Kvetnansky et al. (2009).

1.3.2 The central noradrenergic system

The anatomy of the noradrenergic system in the central nervous system has been studied in great detail. Advances in the glyoxylic acid histofluorescence method in the 1960s allowed Dahlstrom & Fuxe (1964) to provide the first description of the anatomical arrangement of noradrenergic neurons in the rat brain. In this pioneering study the authors identified noradrenergic nuclei located in the dorsal pons and medulla and classified them into seven cell groups, designated the A1-A7

noradrenergic cell groups (Dahlström & Fuxe, 1964). Among these noradrenergic cell groups, the A6 cell group (locus coeruleus; LC) has received most attention. The LC contains the majority of noradrenergic cell bodies in the central nervous system and sends afferents to virtually every region of the brain (Samuels & Szabadi, 2008). Fibre projections originating from the LC project via three pathways: the dorsal noradrenergic bundle; the cerebellar pathway; and the descending pathway. The dorsal noradrenergic bundle either sends projections to the thalamus directly or along with the central tegmental tract, joins the medial forebrain bundle to project to the thalamus as well as other brain regions, such as the HPC, amygdala and cortex. The noradrenergic cells groups A1, A3, A5 and A7 form the lateral tegmental system and project via the central tegmental track and ventral noradrenergic bundle. Descending (bulbospinal) projections from the lateral tegmental system project to the spinal cord while ascending projections target structures located in the brainstem, telencephalon, and diencephalon. Finally, while evidence does implicate the A2 cell group as part of the lateral tegmental group it is often thought of as a separate system (Kvetnansky et al., 2009; Szabadi, 2013) (Figure 1.5).

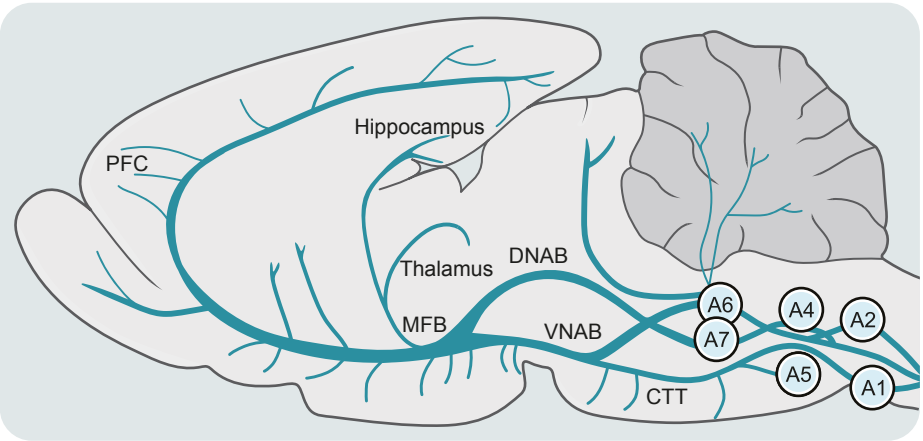

Figure 1.5. Sagittal section of the rat brain showing location of noradrenergic cell bodies and central noradrenergic pathways. Abbreviations: CTT, Central tegmental tract; DNAB, dorsal noradrenergic bundle; PFC, prefrontal cortex; MFB, medial forebrain bundle; VNAB, ventral noradrenergic bundle. Figure adapted from Kvetnansky et al. (2009).

1.3.2.1 Noradrenergic innervation of the nucleus reuniens

To date, no report has investigated in detail the pattern of distribution of noradrenergic fibres to the rat NRe, however, studies examining the general distribution of noradrenergic fibres in the central nervous system have indicated that the NRe receives rather limited projections (Lindvall et al., 1974; Swanson & Hartman, 1975). It is interesting to note, that in the macaque thalamus, a recent report has revealed that midline thalamic nuclei, including the NRe, are densely innervated with noradrenergic fibres (Pérez-Santos et al., 2021). Given the dense noradrenergic fibre distribution in the macaque thalamus, it is likely that noradrenergic afferents to the rat thalamus are denser than current descriptions in literature suggest, thus an anatomical re-appraisal of the distribution of noradrenergic fibres in the rat NRe is warranted. The only report concerning the origin of noradrenergic afferents to the NRe is based on experimental lesions, whereby the LC was identified as the source of noradrenergic innervation to the NRe (Lindvall et al., 1974). However, it is unknown if the NRe receives noradrenergic input from other noradrenergic cells groups. It is noteworthy to mention that anatomical studies have demonstrated that the NRe receives afferents from other noradrenergic cell groups, such as the pontine tegmentum (A7 cell group) (McKenna & Vertes, 2004), however, the neurochemical identity of this projection was not addressed in the study. Therefore, there is a possibility that the NRe may receive modulatory input from the A7 cell group as well as the LC.

Overall, it is evident that knowledge of the noradrenergic anatomy of the rat NRe is poor and a re-evaluation of the pattern of distribution and neuronal source of noradrenaline in the NRe using modern tract tracing and immunohistochemical techniques is required.

1.3.2.2 Noradrenergic innervation of the hippocampus

The LC has been reported as the only source of noradrenaline to the HPC (Loy et al., 1980). Studies using Falck-Hillarp fluorescence histochemistry and DBH immunohistochemistry have indicated that all hippocampal subfields are densely

innervated with noradrenergic fibres in which regional and laminar differences in density exist (Blackstad et al., 1967; Loy et al., 1980; Oleskevich et al., 1989). Using a radioautographic approach, it has been reported that in the ventral HPC, the DG receives the densest input while the CA1 region shows the lightest overall density in comparison to other hippocampal areas. In each hippocampal subfield the densest inputs are observed in stratum moleculare in CA1, stratum radiatum in CA3 and the polymorph layer in DG (Oleskevich et al., 1989). In the dorsal HPC studies using cell-type specific anatomical tracing combined with immunohistochemical methods have provided inconsistent results regarding which hippocampal subfield receives the densest input, therefore making it difficult to ultimately determine whether any topography exists regarding noradrenergic innervation to the dorsal HPC (Kempadoo et al., 2016; Takeuchi et al., 2016; Wagatsuma et al., 2018).

1.3.2.3 Noradrenergic innervation of the medial prefrontal cortex

The mPFC is densely innervated with noradrenergic fibres and similar to the HPC, neurons from the LC provide the sole source of noradrenaline to the mPFC (Agster et al., 2013; Berridge & Waterhouse, 2003). In a recent immunohistochemical analysis, the organisation of noradrenergic innervation to the mPFC was described. In this report it was revealed that while the majority of the mPFC receives a homogeneous noradrenergic innervation, a rostro-caudal topography in the infralimbic subregion was observed, with denser inputs at the caudal compared to rostral levels of the mPFC (Cerpa et al., 2019).

1.3.3 Adrenergic receptors

The modulatory effects of noradrenaline are mediated via the G-protein coupled adrenergic receptors, whereby binding of noradrenaline to the adrenergic receptors activates various signalling cascades. Classification of adrenergic receptors was initially based on pharmacological properties before being further refined by molecular cloning techniques (Bylund, 2005). It is now well established that three major families of adrenoceptors exist, known as $\alpha 1$, $\alpha 2$ and β. $\alpha 1$- and β- adrenergic receptors

are primarily located on the postsynaptic membrane whereas $\alpha 2$ adrenoceptors are located pre- and post-synaptically (Schwarz & Luo, 2015). Each family of adrenoceptors comprises of multiple subtypes and are defined as follows: $\alpha 1$ ($\alpha 1$A, $\alpha 1$B, $\alpha 1$D), $\alpha 2$ ($\alpha 2$A, $\alpha 2$B, $\alpha 2$C) and β ($\beta 1$, $\beta 2$, $\beta 3$) (Bylund, 2005; Calzada & de Artiñano, 2001). Accordingly, $\alpha 1$ adrenoceptors couple to Gq proteins and activate phospholipase C and phosphatidyl inositol intracellular signalling pathways, producing faciliatory effects. In contrast, $\alpha 2$ adrenoceptors are Gi-coupled and function as inhibitory autoreceptors, therefore activation of $\alpha 2$ receptors inhibits adenylyl cyclase production and cAMP signalling. Finally, β adrenoceptors couple to Gs proteins and stimulate adenylyl cyclase and increase cAMP signalling, producing faciliatory effects (Finch et al., 2006; Johnson & Minneman, 1985; MacDonald et al., 1997) (Figure 1.4).

Noradrenaline displays different affinities to the three adrenoceptor subtypes, it has the highest affinity for $\alpha 2$ (K_d 50 nM), followed by $\alpha 1$ (K_d 300 nM), and the lowest affinity for β (K_d 700 nM) (Atzori et al., 2016; Ramos & Arnsten, 2007).

Methods commonly employed to characterise the presence of adrenergic receptors in the central nervous system are autoradiographic techniques, in situ hybridisation and immunohistochemistry. Using such techniques, several studies have identified that all adrenergic receptor subtypes are found throughout the central nervous system, in which region-specific variations of receptor expression are present.

1.3.3.1 Expression in the nucleus reuniens

All three adrenoceptor families have been identified in the NRe but at varying expression levels. The NRe shows abundant expression of $\alpha 1$- (Sargent et al., 1984), moderate expression of $\alpha 2$- and light expression of β-adrenoceptors (Boyajian et al., 1987; Palacios & Kuhar, 1982). Of the $\alpha 1$ family the NRe shows high expression of $\alpha 1$B but light expression of $\alpha 1$A and $\alpha 1$D (Day et al., 1997; Domyancic & Morilak, 1997; McCune et al., 1993; Pieribone et al., 1994); of the $\alpha 2$ adrenoceptors the NRe demonstrates high expression of $\alpha 2$B and light to moderate of $\alpha 2$A and $\alpha 2$C (McCune et al., 1993; Scheinin et al., 1994; Talley et al., 1996); and lastly both $\beta 1$

and β2 expression is reportedly light in the NRe (Nicholas et al., 1993b; Paschalis et al., 2009; Wanaka et al., 1989). However, whether any topographical differences in expression density exists within each adrenoceptor family in the NRe has not been examined.

1.3.3.2 Expression in the hippocampus

α1 adrenergic receptors can be found throughout the HPC (Loy et al., 1980; Sargent et al., 1984; Tayrien & Loy, 1984; Young & Kuhar, 1980). Both α1A and α1D subtypes are densely expressed in the HPC, however, reports regarding the presence of α1B indicate that this subtype may be absent/ lightly expressed in the HPC (Day et al., 1997; Domyancic & Morilak, 1997; McCune et al., 1993; Pieribone et al., 1994). Interestingly, studies have demonstrated that α1 adrenoceptors are mainly expressed in CA1 interneurons (Hillman, Doze, et al., 2005, 2007; Hillman, Knudson, et al., 2005). The HPC also contains α2 adrenergic receptors, which belong mainly to the α2A subtype while α2C expression is reportedly lighter (Boyajian et al., 1987; Milner et al., 1998; Nicholas et al., 1993b; Scheinin et al., 1994; Sherman & Guillery, 2006; Talley et al., 1996; Young & Kuhar, 1980). All three β adrenergic receptors are expressed at high to moderate levels in the HPC. Furthermore, immunohistochemical techniques have revealed that the majority of β1 and β2 adrenoceptors are expressed in pyramidal neurons with some β adrenergic receptor expression found in GABAergic interneurons (Alexander et al., 1975; Booze et al., 1993; Bylund & Snyder, 1976; Cox et al., 2008; Guo & Li, 2007; Minneman et al., 1979; Nicholas et al., 1993a; Palacios & Kuhar, 1982; Paschalis et al., 2009; Rainbow et al., 1984; Summers et al., 1995; Wanaka et al., 1989).

1.3.3.3 Expression in the medial prefrontal cortex

The mPFC shows dense expression of α1 adrenoceptors and double in situ hybridisation experiments have demonstrated that all three subtypes of α1 adrenergic receptors are found in both GABAergic and pyramidal neurons (Santana et al., 2013). The mPFC displays densest expression of α1A and α1D subtype while α1B expression is

low (Pieribone et al., 1994; Santana & Artigas, 2017; Santana et al., 2013). Of the α2 adrenoceptors, the mPFC shows high expression of α2A and α2C while α2B appears to be light/ absent (Nicholas et al., 1993b; Rosin et al., 1996; Scheinin et al., 1994; Talley et al., 1996). The mPFC contains dense expression of all three β adrenergic receptor subtypes. In addition, β1 and β2 subtypes have also been demonstrated to be expressed in GABAergic interneurons and pyramidal neurons (Liu et al., 2014; Nicholas et al., 1993a; Palacios & Kuhar, 1982; Paschalis et al., 2009; Wanaka et al., 1989).

1.3.4 Noradrenergic modulation of cognitive function

Given the extensive projections of the noradrenergic system described above, it is unsurprising that the noradrenergic system has been associated with modulating a variety of functions, such as memory and attention (Berridge, 2008; Berridge & Waterhouse, 2003; Sara, 2009; Schwarz & Luo, 2015).

Results from rodent studies have demonstrated that manipulating the noradrenergic system can alter attentional processes. For instance, it has been shown that systemic administration of the noradrenaline reuptake inhibitor, atomoxetine, can improve attentional performance (Cain et al., 2011; Jentsch et al., 2009; Robinson, 2012), while lesioning of the dorsal noradrenergic bundle causes detrimental effects on attentional performance in the 5-choice reaction time task (Carli et al., 1983). Studies have also shown that degeneration of noradrenergic neurons using the neurotoxin N-(2-choloro-ethyl)-N-ethyl)-2-bromobenzylamine (DSP-4) impairs working memory (Sontag et al., 2008). Impairments in cognitive flexibility, tested on an attentional set-shifting paradigm, have also been demonstrated following depletion of noradrenaline (Tait et al., 2007), while treatment with desipramine, a noradrenaline reuptake inhibitor, enhances performance (Lapiz & Morilak, 2006).

Pharmacological studies have extended these investigations regarding the role of noradrenaline in mediating cognitive functions, revealing the specific receptor subtypes and brain regions involved. For example, extensive research has identified a pivotal role for noradrenergic neurotransmission in the mPFC in working memory,

revealing the interplay between α1 and α2 receptors, demonstrating that activation of postsynaptic α2A receptors in the mPFC enhances working memory while activation of α1 receptors impairs working memory (Berridge & Spencer, 2016; Ramos & Arnsten, 2007). In spatial memory, intra-hippocampal infusions of the α1 adrenergic receptor antagonist prazosin impairs spatial memory while infusion of the α2 receptor antagonist yohimbine facilitates spatial learning (Torkaman-Boutorabi et al., 2014). Furthermore, administration of β adrenergic receptor antagonists into the amygdala has been revealed to impair the consolidation of auditory fear memory (Qu et al., 2008).

Overall, these findings highlight the diverse cognitive functions that are modulated by the noradrenergic system, revealing that the effect of noradrenergic modulation of cognition is receptor- and brain region-dependent.

1.3.5 Noradrenergic modulation of recognition memory

Exploration of novelty, as occurs within an object recognition task, requires an animal to detect and memorise details about the object and its spatial configuration (Ennaceur, 2010). Interestingly, neurons within the LC, the major source of noradrenaline, have been demonstrated to respond to both novel objects and contexts. Single unit recording studies of the LC have shown that exposure to a novel stimulus causes phasic firing of LC neurons that rapidly decreases (Sara et al., 1994; Vankov et al., 1995). Considering that the noradrenergic system has been implicated in novelty processing and that the spontaneous exploration tasks used to assess recognition memory requires an animal to detect novelty, this suggests an important role for noradrenergic modulation of recognition memory. Below literature concerning noradrenergic modulation of recognition memory in the NRe, HPC and mPFC is reviewed.

1.3.5.1 Noradrenergic modulation of nucleus reuniens

To date, no study has evaluated the involvement of noradrenergic neurotransmission in the NRe in recognition memory or indeed in other NRe-dependent cognitive

functions. Given the presence of adrenergic receptors in the NRe (see Section 1.3.3.1) it seems likely that release of noradrenaline in the NRe may have important functional implications. It is therefore necessary that research should be conducted to begin exploration of noradrenergic modulation of the NRe in recognition memory.

1.3.5.2 Noradrenergic modulation of hippocampus

Although limited, current literature indicates a role for noradrenergic modulation of the HPC in recognition memory. Using a pharmacological approach, Mellos-Carpes et al. (2016) tested animals on a variant of the object recognition task which involves exposing animals to non-identical objects during the sample phase – a version of the object recognition task that has been demonstrated to involve hippocampal function (Ameen-Ali et al., 2015; Warburton et al., 2013) – and reported that post-sample intra-HPC infusion of timolol, the β adrenergic antagonist, impaired object recognition memory when animals were tested with a 24-hour delay. Moreover, it has also been demonstrated that infusion of propranolol into the HPC before the sample phase impairs the spatial component of an episodic-like memory task that is based on the spontaneous exploration paradigm (Lemon et al., 2009).

However, evidence concerning whether noradrenergic neurotransmission is involved in modulating the HPC during long-term object location memory is inconclusive. For instance, in a recent study employing tyrosine hydroxylase (TH)-Cre mice, it was demonstrated that optogenetic activation of hippocampal TH-positive fibres originating from the LC during memory encoding could enhance learning in the object location task tested at a 24-hour delay. Furthermore, it was found that this enhancement in learning was blocked by pre-sample pharmacological inactivation of the D1-like receptors but not β adrenergic receptors, suggesting a role for dopamine but not noradrenaline in spatial recognition memory when tested at long delays of 24-hours (Kempadoo et al., 2016). However, in another study, it was revealed using in vivo microdialysis that concurrent release of noradrenaline as well as dopamine is observed in the HPC during the object location task (Moreno-Castilla et al., 2017). In the same study, when catecholaminergic lesions of the HPC were made

using the neurotoxin 6-hydroxydopamine (6-OHDA), in accordance with the in vivo microdialysis results, animals with 6-OHDA lesions were unable to discriminate in the object location task when tested at a 24-hour delay, thus providing causal evidence for the role of catecholaminergic modulation of the HPC during long-term object location memory (Moreno-Castilla et al., 2017)). While the use of 6-OHDA employed by Moreno-Castilla et al. (2017) does not allow one to differentiate the effects of noradrenaline from dopamine, the in vivo microdialysis results do indicate that noradrenaline was released in the HPC during object location task, indicating some involvement of hippocampal noradrenaline. However, it is also possible that release of noradrenaline has no functional role and that the concurrent release of dopamine observed is sufficient for normal object location memory (Moreno-Castilla et al., 2017). Thus, the reason for these discrepant findings is uncertain and more testing is required to resolve this issue regarding hippocampal-noradrenergic involvement in long-term object location memory.

1.3.5.3 Noradrenergic modulation of medial prefrontal cortex

To our knowledge, no study has evaluated the involvement of noradrenergic neurotransmission in the mPFC in recognition memory. It is interesting to note however that while the specific question concerning the role of noradrenaline has not been addressed, the role of catecholaminergic (that is both dopamine and noradrenaline) neurotransmission in the mPFC in recognition memory has been examined. For example, Nelson et al. (2011) found that animals with 6-OHDA lesions of the mPFC were impaired in the temporal order recognition memory task but showed intact performance in the object recognition and object location task. While this study does not dissociate the involvement of noradrenaline from dopamine, these results are indicative of a role for noradrenergic modulation of the mPFC in recognition memory.

1.4 The Dopaminergic System

The dopaminergic system consists of groups of dopamine-synthesising neurons dispersed throughout the central nervous system. The location and pathways of the dopaminergic cell groups has been well characterised. Dopaminergic neurons form a continuum extending from the ventral midbrain through the preoptic area and up to the periaqueductal gray. Dopamine has widespread actions and its circuits have been associated in modulating a broad range of cognitive functions, such as motor control, memory, and motivation. This section provides a brief description of the dopaminergic system focusing on current knowledge about the NRe as well as the functional role of dopaminergic neuromodulation in recognition memory.

1.4.1 Dopamine synthesis

Dopamine shares the same metabolic pathway as noradrenaline (described in detail in Section 1.3.1), however, at the dopaminergic nerve terminal, synthesis of dopamine ends with the enzyme DOPA decarboxylase catalysing the conversion of DOPA to dopamine (Figure 1.6). Following synthesis, dopamine is packaged into synaptic vesicles for storage. Released dopamine binds to the G-protein coupled dopamine receptors. Re-uptake of dopamine into the pre-synaptic terminal is primarily mediated by the dopamine transporter (DAT). Dopamine undergoes degradation by the enzymes MAO and COMT (Ayano, 2016; Daubner et al., 2011).

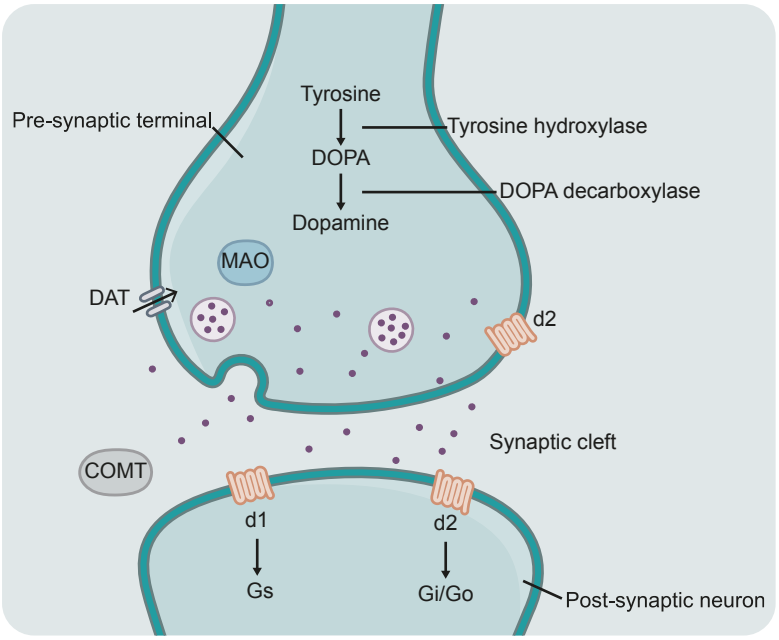

Figure 1.6. Schematic representation of the dopamine synthesis pathway at the dopaminergic synapse. Dopamine is synthesised from the amino acid tyrosine, each step in the biosynthesis pathway is catalysed by a specific enzyme. Upon nerve stimulation (not shown), the synaptic vesicle binds to the membrane and releases dopamine into the synaptic cleft. Released dopamine binds to the dopamine receptors. Dopamine action is terminated by re-uptake into the pre-synaptic terminal by DAT. Degradation of dopamine is catalysed by COMT and MAO. Figure adapted from Ranjbar-Slamloo & Fazlali (2020).

1.4.2 The central dopaminergic system

In the same study conducted by Dahlstrom & Fuxe (1964) that provided detailed descriptions of the noradrenergic system in the central nervous system (see Section 1.3.2), the first descriptions of the dopaminergic system were also provided. Dopaminergic containing cell bodies are designated into groups A8-A17. Modern immunohistochemical techniques used to visualise dopaminergic cell bodies and fibres commonly employ antibodies against TH (the rate limiting enzyme responsible for catalysing the biosynthesis of catecholamines) and DAT.

The dopaminergic cell bodies are organised into groups mesencephalic (A8, A9 and A10), diencephalic (A11, A12, A13, A14 and A15) and those located in the telencephalon (A16 and A17) (Dahlström & Fuxe, 1964; Kvetnansky et al.,

2009). The mesencephalic system comprises of three major ascending pathways: the mesostriatal pathway which consists of pathways that arise in the substantia nigra pars compacta (SNc; A9 cell group) and sends afferents to the dorsal striatum; the mesolimbic pathway which originates in the ventral tegmental area (VTA; A10 cell group) that sends afferents to the hippocampus, septum and nucleus accumbens; and the mesocortical pathway which also arises in the A10 cell group but innervates limbic cortical structures such as mPFC, entorhinal cortex and cingulate cortex (Bentivoglio & Morelli, 2005; Björklund & Dunnett, 2007; Dahlström & Fuxe, 1964). Dopaminergic neurons of the retrorubral field (A8 cell group) also contribute to the mesencephalic pathways described above, sending afferents to striatal, cortical and limbic regions (Bentivoglio & Morelli, 2005). The A11 cell group, located in the posterior hypothalamus, sends projections to the brainstem and spinal cord. The A13 cell group (zona incerta) projects to the amygdala and hypothalamus. Dopaminergic neurons in groups A12 (arcuate nucleus) and A14 (paraventricular hypothalamus) sends afferents to the median eminence and the posterior lobe of the pituitary (Björklund et al., 1973). Projections of the A15 cell group (anterior hypothalamus) have not been well characterised. Lastly, the A16 cell group of the olfactory bulb sends restricted projections to the periglomerular interneurons while the A17 cell group of the retina projects to amacrine interneurons (Prakash & Wurst, 2006) (Figure 1.7).

Based on the distinct projection pattern of each dopaminergic cell group, each pathway has been associated in modulating specific brain functions. For example, the mesocortical pathway has been implicated in decision making and cognition, while the mesostriatial pathway has been demonstrated to be involved in motor control (Ayano, 2016; Björklund & Dunnett, 2007).

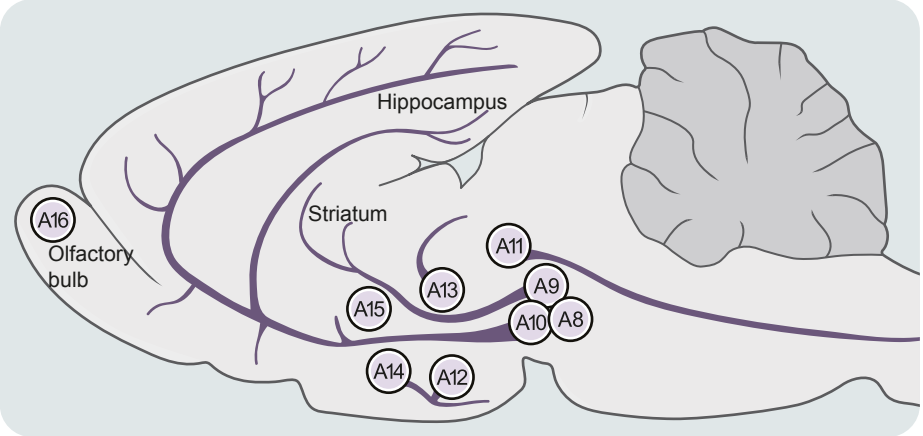

Figure 1.7. Sagittal section of the rat brain showing location of dopaminergic cell bodies and central dopaminergic pathways. Figure adapted from Kvetnansky et al. (2009).

1.4.2.1 Dopaminergic innervation of the nucleus reuniens

It should be noted that no study to date has described the pattern of dopaminergic innervation to the NRe in the rodent thalamus. Studies commonly use techniques that detect both dopamine and noradrenaline, therefore limiting conclusions based solely on dopamine. Nonetheless, these studies have proved to be insightful, for example, in an early report employing histofluorescence techniques, sparse labelling of catecholaminergic positive fibres were detected in the NRe (Lindvall et al., 1974). In addition, in a recent report the existence of TH-positive neurons (part of the A13 dopaminergic cell group) has also been reported in the NRe (Ogundele et al., 2017).

Interestingly, in a recent study it was revealed that the NRe receives a dopaminergic input from the A13 cell group, however, this study did not thoroughly examine all potential sources of dopaminergic afferents to the NRe, thus it is currently unknown whether the NRe receives additional dopaminergic input from other sources (Venkataraman et al., 2021). For instance, while the neurochemical identity of these projections were not identified, it has been demonstrated that the NRe receives inputs from a number of other brain regions which contain dopaminergic cell bodies, such as the VTA (A10) and SNc (A9) to name a few (McKenna & Vertes, 2004). It is clear that more detailed studies should be conducted to thoroughly characterise the neuronal source(s) of dopaminergic input to the NRe.

1.4.3 Dopamine receptor expression in the nucleus reuniens

Dopamine exerts its neuromodulatory influence on central nervous system function via two classes of G-protein coupled dopamine receptors: the D1-like receptor family which includes the D1 and D5 receptors; and the D2-like receptor family which includes the D2, D3 and D4 receptors. Several studies have characterised the expression of dopamine receptors in the rat brain, however, the specific pattern of expression in the NRe is unclear. While these studies do indicate that the NRe contains light expression of each dopamine receptor subtype, many of these studies conducted brain-wide analysis, therefore specific conclusions concerning the expression of dopamine receptors in the NRe are difficult to tease out (Bouthenet et al., 1991; Mansour et al., 1990). Furthermore, there seems to be a discrepancy between species regarding the presence or absence of certain dopamine receptor subtypes in the NRe. For instance, evidence from the Allen Mouse Brain Atlas indicates that D1 (Experiment 352) but not D2 (Experiment 357) is expressed in the NRe (Lein et al., 2007), in contrast, in the human brain, various thalamic nuclei (including the NRe) have been demonstrated to show dense expression of the D2-like receptors (Rieck et al., 2004). It is clear that anatomical characterisation of the distribution and density of dopamine receptor expression in the rat thalamus with particular focus on the NRe is required before one proceeds with functional analysis.

1.4.4 Dopaminergic modulation of recognition memory

To our knowledge, no study has evaluated the functional role of dopaminergic modulation of the NRe in recognition memory, however, existing evidence suggests that dopamine neurotransmission is critical for recognition memory processing. In an early report, manipulation of dopamine levels via systemic administration of a D1 agonist were demonstrated to alter performance in an object recognition, object location and temporal order memory task (Hotte et al., 2005). More recently, across a series of experimental manipulations, Savalli et al. (2015) investigated the functional role of dopamine neurotransmission acting via the D1-like receptors in the mPFC,

HPC and PRH. Interestingly only intra-mPFC infusion of D1-like antagonists affected object-in-place recognition memory, impairing the encoding but not retrieval, while intra-HPC and intra-PRH infusions were without effect. Furthermore, as previously mentioned (see Section 1.3.5.2), recent optogenetic and in vivo microdialysis studies have also implicated a role for dopamine neurotransmission in the HPC in object location memory (Kempadoo et al., 2016; Moreno-Castilla et al., 2017).

Taken together, given that the NRe has been demonstrated to have a role in recognition memory and the anatomical evidence outlined above suggests that the NRe receives dopaminergic input from the A13 cell group, it is likely that dopamine may have a pivotal role in modulating the NRe in recognition memory – a dopamine modulated behaviour. However, it is also evident that detailed anatomical descriptions of the dopaminergic system in the NRe are lacking.

1.5 Summary

The literature summarised in the general introduction has highlighted the significant advancements made in recent years in unravelling the contribution of the NRe in higher-order cognitive functions, including associative recognition memory. In particular, the studies outlined have identified the NRe as a critical node within neural circuits that involve the HPC and mPFC. However, despite the substantial progress, our understanding of the NRe is still far from comprehensive. One aspect that is currently underexplored is information concerning the catecholaminergic system in the NRe, at both the anatomical and functional level.

In addition to literature concerning the NRe, the evidence outlined in the general introduction also revealed that in comparison to other neuromodulatory systems, such as cholinergic and dopaminergic systems, the function of noradrenergic neuromodulation in the HPC and mPFC in recognition memory is currently underexplored. While some evidence does exist to suggest that noradrenergic neurotransmission in the HPC and mPFC is involved in recognition memory, these studies offer an incomplete picture regarding the exact conditions that require noradrenaline signalling in the

HPC and mPFC during recognition memory processing.

1.5.1 Thesis aims and organisation

To address the gaps in knowledge highlighted above the thesis aims are:

1. To provide an anatomical description of catecholaminergic neuromodulatory system in the NRe

2. To investigate the role of noradrenergic neurotransmission in the NRe, HPC and mPFC in recognition memory

3. To investigate the role of LC inputs to the HPC and NRe in recognition memory

To investigate the anatomy of the catecholaminergic system in the NRe, the experiments in Chapter 3 employed immunohistochemical methods using antibodies against TH to stain for catecholaminergic fibres in the NRe. Retrograde tract tracing combined with TH immunohistochemistry was also employed to determine the neuronal source of catecholaminergic input to the NRe.

To determine the role of noradrenergic neurotransmission in the NRe, HPC and mPFC in recognition memory, a pharmacological approach was employed in Chapter 4. The experiments involved infusing various adrenergic agonists and antagonists separately into the NRe, HPC and mPFC at distinct timepoints of the spontaneous recognition memory tasks to manipulate encoding or retrieval processes.

Finally, based on the anatomical observation that the LC provides the sole source of noradrenergic input to the NRe (see Chapter 3) and previous reports indicating that the LC is the only source of noradrenergic input to the HPC (Loy et al., 1980), and the current demonstration that direct pharmacological manipulation of noradrenergic neurotransmission in the NRe and HPC but not mPFC results in specific deficits in recognition memory (see Chapter 4), the experiments in Chapter 5 aimed to test whether inputs from the LC to the NRe or HPC are involved in recognition memory.

2 General Methods

2.1 Animals

2.1.1 Animals used for behavioural studies

Male lister hooded rats (Harlan Laboratories, UK) weighing 300-400g at the start of experimentation were used. Rats were group housed (2-4 per cage) and kept on 12-hour light/dark cycle (light phase, 18:00 to 06:00). All animals had ad libitum access to water and standard chow. Compliance with the Animals (Scientific Procedures) Act, 1986 was ensured.

2.1.2 Animals used for anatomical studies

Male Lister Hooded rats (Envigo, UK) weighing 297-307g were used at the start of experimentation were used. Rats were group housed (2-4 per cage) kept on 12-hour light/dark cycle (light phase, 06:00 to 18:00). Compliance with the Animals (Scientific Procedures) Act, 1986 was ensured and all procedures were approved by the local ethics committee at Cardiff University.

2.2 Surgical procedures

For injection of anatomical tracers, implantation of infusion cannula, injection of viruses and implantation of optical fibres, the following surgical procedures were performed. Animals were anaesthetised using isoflurane (induction 4%, maintenance 2%). The scalp of the animals was shaved before they were positioned in a stereotaxic frame, the incisor bar was adjusted to achieve a flat skull (Kopf Instruments, USA). Before the start of surgery animals received eye drops (0.1% sodium hyaluronate; Hycosan, UK) and topical application of both lidocaine (5% m/m; TEVA; UK) and chlorhexidine on the scalp. Following surgery, the skin was sutured and antibiotic

wound powder (2% w/w; Battle, UK) was applied. Immediately post-surgery animals received eye drops (0.1% sodium hyaluronate; Hycosan, UK), subcutaneous injection of 5ml glucose saline (sodium chloride 0.9% w/v with glucose 5% w/v), intramuscular injection of 0.05ml vetergesic (0.3 mg/ml buprenorphine; Ceva Animal Health, UK) and intramuscular injection of 0.1ml Clamoxyl (150mg/ml; Zoetis, UK).

2.2.1 Anatomical tracer injections

To investigate the origin of catecholaminergic input to the NRe, anatomical tracers were injected into the NRe. Surgical procedures outlined in Section 2.2 were followed. Co-ordinates used were determined using the rat brain atlas of Paxinos & Watson (2006) (see Table 3.1 for list of cases analysed and injection co-ordinates used). The retrograde tracers used were fast blue (FB; 3% in PBS; Sigma-Aldrich, Gillingham, UK), cholera-toxin b (CTB, 1% in dH_20; List Biological Laboratories Inc, Campbell, CA, USA) and FluoroGold (FG, 4% in dH_2O; Santa Cruz Biotechnology, Santa Cruz, CA, USA) (see Table 2.1 for an overview of tracers used). For pressure injections, FB and CTB were mechanically injected via a 1μl Hamilton syringe (Hamilton, Bonaduz, Switzerland), 55nl was injected per site at a rate of 20nl/min. The syringe was left in situ for 3 minutes prior to injection and 10 minutes after injection to minimise leakage of tracer. For iontophoretic injections, CTB and FG were injected using a glass micropipette (tip diameter 15-20μm). A positive pulsed current (2μA for 6 minutes followed by 6μA for 6 minutes and finally 7μA for 6 minutes) was applied using Digital Midgard Precision Current Source iontophoretic pump (Stoelting Co, Wood Dale, USA) on a cycle of 6 seconds on/ 6 seconds off. After the injection period, the glass micropipette was left in situ for 3 minutes to minimise leakage of tracer. During withdrawal of the micropipette a negative current was applied.

Table 2.1. Overview of anatomical tracers used for retrograde tract tracing.

Tracer	Supplier	Cat no.
Fast blue	Polysciences	17740-1
Cholera Toxin B Subunit	List biological Laboratories	#104
FluoroGold	Santa Cruz Biotechnology	SC-358883

2.2.2 Cannulation

To study the role of noradrenergic neuromodulation in recognition memory in the NRe, HPC and mPFC, animals were implanted with guide cannula to allow infusion of noradrenergic agonists and antagonists at distinct time points of the spontaneous recognition memory tasks. Surgical procedures outlined in Section 2.2 were followed. Burr holes were drilled into the skull to allow implantation of stainless-steel guide cannula (26 gauge; Plastics One, Bilaney, UK). Four stainless steel screws (Plastics One, Bilaney, UK) and dental cement were used to anchor the cannula. To target the NRe, animals were implanted with bilateral cannula using the following co-ordinates: anterior-posterior (AP) -1.8mm and -2.4mm; mediolateral (ML) ±1.7mm, dorsoventral (DV) -6.4mm. All cannula were implanted 15° from the ML plane. To target the HPC or mPFC, animals were implanted with bilateral cannula to target both brain regions. Therefore, for a given animal 4 infusion cannula were implanted (2 aimed at the HPC and 2 aimed at the mPFC). To target the HPC, the co-ordinates were: AP -4.3mm, ML ±2.5mm, DV -2.8mm (dura). To target the mPFC, the co-ordinates were: AP +3.2mm; ML ±0.75mm, DV -3.5mm. To prevent contamination/cannulae blockages, dummy cannula were inserted into the guide cannula and for the mPFC dust caps were also used.

2.2.3 Viral injections and implantation of optical fibres

To study the role of LC inputs to the NRe and HPC in recognition memory, various viruses were piloted (see Table 2.2). Surgical procedures outlined in Section 2.2

were followed. The co-ordinates used for injections to target the LC were calculated relative to bregma, these were: AP -9.6mm, ML ±1.4mm, DV -7.4mm. In one animal (see Section 5.3.1.1), injections were made into the VTA. The co-ordinates used for injections to target the VTA were calculated relative to bregma, these were: AP -5.6mm, ML ±1.0mm, DV -7.8mm. Each animal received 2 injections (1 in each hemisphere) of virus through a 5μl Hamilton syringe. Each virus was injected at a rate of 0.2μl/min using a Micro4 controller infusion pump (World Precision Instruments, USA), attached to the arm of the stereotaxic frame. The needle was left in situ for a further 10 minutes before being withdrawn. Various combinations and volumes of virus were injected dependent on the experiment (see Table 5.1).

Table 2.2. Overview of viruses used.

Virus/ plasmid	Volume injected	Original titre	Supplier	Cat no.
AAV5-Camkii-eArch3.0-EYFP	1ul/per hemisphere	3.4×10^{12} vg/ml	UNC Vector Core	N/A
AAV5-Camkii-EYFP	1ul/per hemisphere	3.6×10^{12} vg/ml	UNC Vector Core	N/A
AAV9-TH-PI-Cre.SV40	0.3ul/per hemisphere	1×10^{13} vg/ml	A gift from James M. Wilson	#107788
AAV5-EF1a-DIO-eArch3.0-EYFP	0.3ul/per hemisphere	5×10^{12} vg/ml	UNC Vector Core	N/A
AAV9-PRSX8-eArchT3.0-EYFP	1ul/per hemisphere	1.56×10^{12} GC/ml	Vectorbuilder	N/A
pLenti-PRSX8 eArchT3.0-EYFP	N/A	N/A	A gift from Ruth Stornetta	#89538

For the behavioural experiments, animals received a bilateral injection of AAV5-CaMKII-eArchT3.0-EYFP or AAV5-CaMKII-EYFP into the LC (see above for injection procedure) and were immediately implanted with bilateral optical fibres to target both the NRe and HPC. Therefore, for a given animal 4 optical fibres were

implanted (2 aimed at the NRe and 2 aimed at the HPC). To implant optical fibres, burr holes were drilled into the skull to allow implantation of optical fibre (core = 200μm, numerical aperture = 0.22, (MFC_200/240-0.22_SM3_C45 Mono Fiberoptic Cannula); Doric Lenses, Quebec, Canada). Four stainless steel screws (Plastics One, Bilaney, UK) and dental cement were used to anchor the optical fibres. To target the NRe animals were implanted with bilateral optical fibre (length: 7mm) using the following co-ordinates: AP -1.8mm, ML ±2mm, DV -6.6mm. All optical fibres were implanted 15° from the ML plane. To target the HPC animals were implanted with bilateral optical fibre (length: 5.5mm) using the following coordinates: AP -5.4mm, ML ±2.7mm, DV -2.8mm. All optical fibres were implanted 25° from the AP plane.

2.3 Spontaneous object exploration behavioural testing

2.3.1 Apparatus

Behavioural testing was conducted in an open-topped (90cm x 100 cm x 50cm) arena constructed from wood. The floor of the arena was covered in sawdust. The walls of the arena were painted black on one side and grey on the other side making them interchangeable depending on the task. The arena was surrounded with a black cloth which was hung from a height of 1.5m. The room was lit with two floor lamps situated at either side of the arena. A webcam was located above the arena to record behaviour. For all tasks, the black cloth on the west and east side of the arena was removed to provide the animal with distal cues. The arena was configured so that the west wall was black and the other 3 walls (north, east and south) were grey in colour.

2.3.2 Habituation

2.3.2.1 Animals with cannula

Habituation took place over 4 consecutive days. No objects were present during the habituation period. At the start of each day animals were individually habituated to the infusion procedure before being individually placed in the arena to freely explore for 5 minutes. For habituation to the infusion procedure a specific procedure was followed. On day 1 animals were placed on the lap of the experimenter for 5 minutes, during this time animals were allowed to roam freely for 4.5 minutes and held in position for 30s. Day 2 consisted of a 1 minute hold and 4 minutes of free roaming. Day 3 involved a 2.5 minute hold and 2.5 minute free roam. The infusion pump was also triggered during the 5 minute duration for 30s and dummy cannula were lightly manipulated. On day 4 animals were held for 4 minutes and allowed to roam for 1 minute, during which the infusion pump was triggered for 1 minute and dummy cannula were lightly manipulated.

2.3.2.2 Animals with optical fibre

Animals were handled extensively prior to habituation. Animals underwent two separate habituation procedures. No objects were present during the habituation period. The first habituation procedure consisted of 4 days and involved placing animals on the lap of the experimenter for 5 minutes, during this time animals were gently handled, and dust caps manipulated. Animals were subsequently individually placed in the arena to freely explore for 5 minutes. The second habituation procedure consisted of 4 days and involved placing animals on the lap of the experimenter for 5 minutes, during this time animals were gently handled, and dust caps manipulated.

2.3.3 Objects

Objects were constructed from Duplo blocks (Lego, Denmark). Objects varied in size (ranging from 16x16x8cm to 20x20x25cm), colour and shape. Objects were placed 10cm from the edges of the arena and cleaned with 100% ethanol during the delay

period between sample and test and also between animals to remove olfactory cues.

2.3.4 Drugs and infusion procedure for cannulation experiments

The following drugs were used: the $\alpha 2$ adrenergic agonist UK 14,304 (2466, Tocris, UK); the $\alpha 2$ antagonist RS 79948 (0987, Tocris, UK); the $\alpha 1$ antagonist prazosin (0623, Tocris, UK); and the β adrenergic antagonist propranolol (0834, Tocris, UK) (see Table 2.3 for an overview). UK 14,304, propranolol and RS 79949 were dissolved in 0.9% sterile saline solution and infused at the following concentrations: UK 14,304 (10μM); propranolol (10μM); and RS 79948 (1μM). Prazosin was initially dissolved in 100% dimethyl sulfoxide (DMSO), the stock solution was subsequently diluted with 0.9% sterile saline solution, yielding an infusion concentration of 1μM prazosin in 0.1% DMSO. For the NRe experiments, vehicle control animals received either 0.9% sterile saline solution (UK 14,304 and RS 79948 experiment) or 0.9% sterile saline solution with 0.1% DMSO (prazosin and propranolol experiment). For the HPC-mPFC experiments, vehicle control animals received 0.9% sterile saline solution. Drug doses used were based on published IC_{50} values (Atlas et al., 1974; Bylund & Snyder, 1976; Greengrass & Bremmer, 1979; Lefkowitz et al., 1976; U'Prichard et al., 1978; Van Meel et al., 1981).

Table 2.3. Overview of drugs.

Drug	Receptor selectivity	Concentration	Supplier	Cat no.
UK 14,304	$\alpha 2$	$10\mu M$	Tocris	2466
RS 79948	$\alpha 2$	$1\mu M$	Tocris	0987
Prazosin	$\alpha 1$	$1\mu M$	Tocris	0623
Propranolol	β	$10\mu M$	Tocris	0834

Drugs were infused via 33-gauge cannula (Plastic Ones, Bilaney, UK) attached to a 25μl Hamilton syringe by polyethylene tubing. Rate of infusion was controlled using an infusion pump (Harvard, UK). For the NRe, animals were infused with 0.3μl

of drug or saline per hemisphere at a rate of 0.3μl/min. For the HPC, animals were infused with 1μl of drug or saline per hemisphere at a rate of 0.5μl/min. For mPFC infusions, animals were infused with 0.5μl of drug or saline per hemisphere at a rate of 0.25μl/min. Following infusion, cannulae were left in place for 5 minutes. Infusions were given 15 minutes before the sample phase to test the effects on encoding or 15 minutes before the test phase to assess the effects on retrieval.

2.3.5 Stimulation protocol for optogenetic experiments

Laser light for optical stimulation was generated using a diode laser (Omicron LuxX® 515-100 laser (515nm), Photonlines, UK). The laser was attached to a fibre optic rotary joint with beam splitter (FRJ_1X2i_FC-2FC, Doric Lenses, Quebec, Canada) via a fibre-optic patch cord (core = 200μm, numerical aperture = 0.22, FG200LEA, ThorLabs, Newton, NJ, USA). Two fibre-optic patch cords (core = 200μm, numerical aperture = 0.22, FC-CM3, Doric Lenses, Quebec, Canada) were attached to the rotary joint at one end while the other end was used to connect to the optical implant on the animal's head. The power output of the laser was adjusted so that 10mW was measured at the tip of each optical fibre. Optical stimulation was either given during the sample phase to test the effects on encoding or during the test phase to test the effect on retrieval. Laser stimulation was delivered at a frequency of 30 Hz and a duration of 10ms using a custom protocol on WinLTP (2.20 M/X-Series, WinLTP Ltd.). Stimulation parameters were chosen based on a previous in vitro electrophysiological study conducted in acute brain slices demonstrating that laser stimulation using the abovementioned parameters resulted in a robust decrease in resting membrane potential (Banks et al., unpublished).

2.3.6 Spontaneous exploration tasks

2.3.6.1 Object-in-place task

The object-in-place task comprised of a sample and test phase, with a 3-hour delay period between each phase. The sample phase was 5 minutes in duration, during this

time animals were allowed to freely explore 4 different objects placed at a distance of 10cm away from the walls of the arena (Figure 2.1A). After 5 minutes had elapsed, the animals were removed from the testing arena and placed back into their home cage for the full duration of the delay period. At test phase, 2 objects were exchanged positions and the animals were given 3 minutes to explore. If an animal demonstrates object-in-place memory it should preferentially explore the 2 objects which have exchanged positions (the novel configuration) over the 2 objects which have remained in the same position (familiar configuration). Thus, in Figure 2.1A, the 2 objects on the right-hand side of the arena at test.

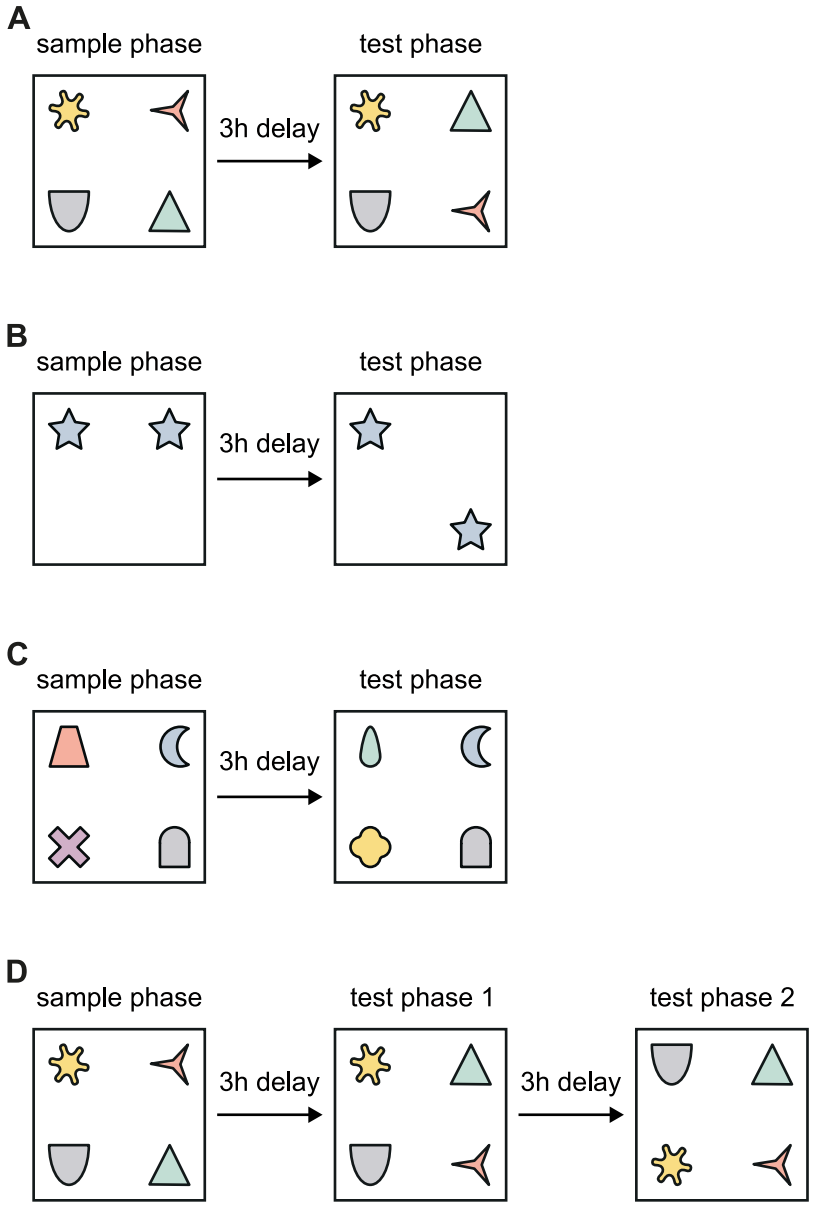

Figure 2.1. Schematic diagram of the spontaneous exploration memory tasks. (A) Object-in-place task. (B) Object location task. (C) Object recognition task based on the object-in-place task. (D) Object-in-place task with 2 test phases.

2.3.6.2 Object location task

This task employed similar methods to the object-in-place task as described above, except the sample phase was only 4 minutes in duration and animals were only presented with 2 identical objects at the sample and test phases. In addition, at test, object location was changed (Figure 2.1B). Successful object location memory is demonstrated by greater exploration of the familiar object in the new location (novel

configuration) over the familiar object in the familiar location (familiar configuration). Therefore, as illustrated in Figure 2.1B, the object positioned to the right of the arena at test.

2.3.6.3 Object recognition task based on the object-in-place task

This task employed similar methods to the object-in-place task as described above, except at test, 2 objects, were replaced with novel objects. Intact object recognition memory is demonstrated by greater exploration of the novel objects (novel configuration) over the familiar objects (familiar configuration). Therefore, as illustrated in Figure 2.1C, the objects positioned to the left of the arena at test.

2.3.6.4 Object-in-place task with two test phases

This task employed similar methods to the object-in-place task as described above, except it consisted of 2 test phases. At test phase 1, 2 objects, either both on the left or right side, exchanged positions, and the animals were given 5 minutes to explore. At test phase 2, 2 objects either both on the left or right side, exchanged positions, and the animals were given 3 minutes to explore. If during test phase 1, objects to the left exchanged positions, then during test phase 2, objects to the right exchanged positions and vice versa. If an animal demonstrates successful object-in-place memory it should preferentially explore the 2 objects which have exchanged positions (the novel configuration) over the 2 objects which have remained in the same position (familiar configuration). Thus, in Figure 2.1D, at test phase 1, the objects on the right-hand side of the arena and at test phase 2, the objects on the left-hand side of the arena.

2.3.7 Data acquisition, scoring and analysis

Total exploration time of the objects in the sample and test phases was measured using a custom software. The experimenter was blind to the experimental condition of the animal when scoring exploratory behaviour. In all tasks the positioning and/or identity of the objects in the sample and test phases in each task was

counterbalanced between the animals. Exploration of an object was measured in seconds and defined as when the animal's nose was directed towards the object while actively sniffing. Sitting on top of the object or using the object for supported rearing was not scored as exploratory behaviour. All animals were required to display a minimum total exploration time in the sample and test phase (15 seconds and 10 seconds, respectively). Data from an animal that did not meet this criterion was excluded from analysis for that specific behavioural test. To measure an animal's ability to discriminate between the novel configuration compared to the familiar configuration, a discrimination ratio was calculated. The following formula was used to calculate the discrimination ratio for each animal in each task: discrimination ratio = (exploration of novel object configuration (s) – exploration of familiar object configuration (s))/ total exploration time (s). A value of zero indicates that the animal has no preference for the novel or familiar object/configuration. A positive discrimination ratio value indicates that an animal has preference for the novel object/configuration, while a negative value indicates that the animal has a preference for the familiar object/configuration.

In all behavioural experiments, statistical analysis was performed to compare discrimination ratios, sample phase exploration times and test phase exploration times between conditions (see Methods in Chapter 4 and Chapter 5 for detailed descriptions about the statistical tests performed).

In addition, in all experiments to determine whether the discrimination ratio for each condition was significantly different from chance (a discrimination ratio of zero), one-sample t-tests were conducted.

Alpha was set at 0.05 for all analysis. IBM SPSS Statistics 25 software (IBM, USA) was used to perform all statistical analysis. Graphs were created using R 3.6.1 (R Core Team, Austria). Data are presented as mean ± standard error of mean (SEM).

2.4 Histology

2.4.1 Tissue fixation

On completion of experiments animals received an intraperitoneal injection of sodium pentobarbital (Euthatal, Merial, Harlow, UK). Animals were transcardially perfused with 0.1M phosphate-buffered saline (PBS) followed by 4% paraformaldehyde (PFA) in 0.1M PBS or 4% formal saline. Brains were removed and post-fixed with PFA for a minimum of 4 hours or with formal saline for a minimum of 1 week before being transferred to 25% sucrose in 0.1M PBS for 24 hours. It should be noted that animals that underwent anatomical tracing, viral injections and optical fibre implantation were perfused and post-fixed with PFA while cannulated animals were perfused and post-fixed with formal saline.

2.4.2 Tissue preparation for anatomical tracers

Following the tissue fixation procedures outlined in Section 2.4.1, brains were sectioned using a freezing microtome (Leica 1400, Germany) into 50μm coronal sections, four series were taken. The first tissue series was directly mounted onto gelatin-subbed slides for cresyl violet staining (see Section 2.4.5). The second tissue series was stained with various antibodies (see Table 2.4). A Leica DM5000B microscope with a Leica DFC310FX digital camera was used to image the samples.

Table 2.4. Overview of antibodies used.

Antibody	Dilution	Supplier	Cat no.
Anti-TH antibody, Rabbit polyclonal to TH	1:1000	Chemicon	AB152
Anti-TH antibody, Chicken polyclonal to TH	1:1000	Abcam	AB76442
Anti-GFP antibody, Chicken polyclonal to GFP	1:1000	Aves Labs	GFP-1020
Anti-CTB antibody, Rabbit polyclonal to CTB	1:3000	Sigma-aldrich	C30620
Goat Anti-Rabbit Antibody Biotinylated	1:500	Vector	BA-1000
Alexa Fluor 488 Goat Anti-Chicken antibody	1:500	Invitrogen	A-11039
Alexa Fluor 594 Goat Anti-Rabbit antibody	1:500	Invitrogen	A-11037
Alexa Fluor 594 Goat Anti-Chicken antibody	1:500	Invitrogen	A-11042

2.4.3 Tissue preparation for cannulated animals

Following the tissue fixation procedures outlined in Section 2.4.1, brains were sectioned using a cryostat (Leica CM3050S, Milton Keynes, UK) into 40μm coronal sections and directly mounted onto gelatin-subbed slides and air dried before staining with cresyl violet (see Section 2.4.5). A Leica DM6 B microscope mounted with a Hamamatsu C13440 digital camera was used to image the samples.

2.4.4 Tissue preparation for viral injections and optical fibre implantations

Following the tissue fixation procedures outlined in Section 2.4.1, brains were sectioned using a cryostat (Leica CM3050S, Milton Keynes, UK) into 40μm coronal sections. Two series were taken. The first tissue series was stained with various antibodies (see Table 2.4). A Leica DM6 B microscope mounted with a Hamamatsu C13440 digital camera was used to image the samples.

2.4.5 Cresyl violet staining procedure

Cresyl violet staining consisted of dehydrating sections in increasing concentrations of alcohol (50%, 70%, 90%, 2 x 100%), clearing in xylene and coverslipping with DPX mountant.

2.4.6 Immunohistochemical procedure

For an overview of antibodies used (see Table 2.4). Immunohistochemical staining was performed on free-floating sections. Sections were washed with 0.1M PBS (3 x 10 minutes). Sections were incubated in blocking solution (5% animal serum, 2.5% bovine serum albumin, 0.2% Triton x-100 in 0.1M PBS (PBST)) for 1 hour before incubation with primary antibodies diluted in blocking solution overnight at room temperature. Sections were then washed in 0.1M PBST (4 x 10 minutes) before incubation in secondary antibodies diluted in blocking buffer for 2 hours at room temperature. Sections were given a final wash with PBS (4 x 10 minutes) and mounted on gelatin-subbed slides and coverslipped with Fluoromount (Sigma-Aldrich, F4680, St. Louis, MO, USA).

2.5 Analysis for anatomical tracing

2.5.1 Anatomical nomenclature

Anatomical boundaries and nomenclature follow the rat brain atlas of Paxinos & Watson (2006), except for terminology regarding dopamine and noradrenaline-positive neurons which follows the well described nomenclature (Björklund & Dunnett, 2007; Fuxe, 1964; Hokfelt, 1984; Lindvall, 1983). To determine the origin of catecholaminergic input to the NRe, only catecholaminergic cell groups which have previously described projections to the NRe were examined for double-labelled neurons (i.e., those that demonstrate co-staining of both the retrograde tracer and TH antibody) (McKenna & Vertes, 2004). The catecholaminergic cell groups evaluated and not evaluated are summarised in Table 3.2.

2.5.2 Cell Counts and quantification

For cell counts, the region of interest was determined by the presence of TH-positive cells. All TH-positive cells, retrogradely transported cells and double-labelled cells within the region of interest were counted for each animal. Olympus cellSens Dimension Desktop Software was used to perform manual cell counts.

2.6 Cell counts for viral pilots

For cell counts, the region of interest was determined by the presence of TH-positive cells. All TH-positive cells, YFP-positive cells, and double-labelled cells within the region of interest were counted for each animal. ImageJ (Schindelin et al., 2012) was used to perform manual cell counts.

3 An anatomical investigation of the catecholaminergic system in the nucleus reuniens

3.1 Introduction

Despite the growing number of studies identifying the NRe as a pivotal structure involved in higher-order cognitive functions (Cassel et al., 2013; Dolleman-van der Weel et al., 2019), including recognition memory (Barker & Warburton, 2018), our understanding of this thalamic structure, and the neurotransmitter systems involved in regulating NRe function is still far from comprehensive.

In general, descriptions to date indicate that the rodent NRe receives a rather limited catecholaminergic innervation, and recent evidence suggests the existence of catecholaminergic-positive neurons in the NRe (Björklund et al., 1973; Lindvall et al., 1974; Ogundele et al., 2017; Swanson & Hartman, 1975). It is important to note that these descriptions stem from brain-wide analyses, therefore detailed anatomic maps concerning the NRe were not provided. It is therefore likely that the density of catecholaminergic innervation to the NRe is more extensive than has been previously described. Additional evidence that the NRe may receive a more significant catecholaminergic innervation stems from radioligand binding and in situ hybridisation studies indicating that the NRe contains dense to moderate expression levels of the adrenergic receptors (see Section 1.3.3.1), and also radioimmunoassay analysis demonstrating that the NRe contains moderate levels of both dopamine and noradrenaline (Versteeg et al., 1976).

A handful of studies have identified the sources of noradrenergic and dopaminergic afferents to the rodent NRe. Lesion studies have demonstrated that the NRe receives its noradrenergic input from the LC (Lindvall et al., 1974; Swanson & Hartman,

1975), although this technique lacks spatial precision and sensitivity. More recent evidence in the mouse, has indicated that the A13 dopaminergic cell group provides dopaminergic innervation to the NRe (Venkataraman et al., 2021). However, both abovementioned studies only focused on noradrenergic and dopaminergic inputs from one cell body group (Lindvall et al., 1974; Venkataraman et al., 2021). Thus it is currently unknown whether the NRe receives catecholaminergic input from additional sources. For instance, while the neurochemical identity of these projections was not determined, anatomical tract tracing studies have indicated that the NRe receives input from other catecholaminergic cell groups, such as the VTA, SNc and pontine reticular formation (McKenna & Vertes, 2004), thus any one of these brain regions could provide an additional source of catecholaminergic input to the NRe.

Interestingly, a functional role for A13 projections to the NRe in the extinction recall of fear memories has been demonstrated (Venkataraman et al., 2021). Thus, the catecholamine system could serve to modulate other NRe-associated functions, including recognition memory. However, to fully understand the functional role of catecholaminergic neuromodulation in the NRe it is necessary to have a detailed account of the organisation of the catecholaminergic system in the NRe, this includes details about the pattern of innervation and the origin of catecholaminergic fibres. Therefore, in the experiments within this Chapter, an antibody against TH, the rate limiting enzyme for dopamine synthesis, was used to visualise the distribution of catecholaminergic fibres in the NRe. In addition, retrograde tract tracing combined with TH immunohistochemistry was also conducted to identify the origin of catecholaminergic input to the NRe.

3.2 Methods

3.2.1 Animals

A total of 8 male Lister Hooded rats (Envigo, UK) weighing between 297-307g were used, 1 animal was used to describe the distribution of TH-positive fibres and 7 animals were used for the anatomical tract tracing experiments. See Section 2.1 for

full details about animals.

3.2.2 Surgery

All animals underwent surgical procedures as described in Section 2.2. Each animal received a unilateral injection of an anatomical tracer into the NRe (see Section 2.2.1 for full injection procedure). All tracer injections were given at a 6° angle from the mediolateral plane. The stereotaxic co-ordinates were derived from the rat brain atlas of Paxinos & Watson (2006). As the NRe lies directly ventral to the sagittal sinus, mediolateral co-ordinates used were aimed to target as close to the side of the sagittal sinus as possible. See Table 3.1 for a list of cases including details of the co-ordinates used, anatomical tracer used and spread of anatomical tracer. All animals were allowed to recover for 7 days before being sacrificed for subsequent histological processing.

3.2.3 Histology

See Section 2.4 for details of histological procedures to fix brain tissue for subsequent immunohistochemical processing.

Table 3.1. Overview of individual cases with details of retrograde tracers used, method of injection and anatomical spread of tracer deposit.

Case #	Tracer	Co-ordinates	Method of injection	Main site of tracer deposit	Spread of tracer to other nuclei
222#3	FB	AP: -1.9, ML: sinus, DV: -7.4	Pressure	Rostral NRe	PaXi
7#5	CTB	AP: -1.9, ML: sinus, DV: -7.5	Pressure	Rostral NRe	N/A
7#7	CTB	AP: -1.9, ML: sinus, DV: -7.5	Pressure	Rostral NRe	Rh, Xi
216#4	CTB	AP: -1.9, ML: sinus, DV: -6.8 (dura)	Iontophoretic	Rostral NRe	Rh, CM, PaXi
225#2	CTB	AP: -2.4, ML: sinus, DV: -6.9 (dura)	Iontophoretic	Intermediate to caudal NRe	N/A
216#9	FG	AP: -2.6, ML: sinus, DV: -6.8 (dura)	Iontophoretic	Intermediate to caudal NRe	PHD
216#5	CTB	AP: -2.6, ML: sinus, DV: -6.7 (dura)	Iontophoretic	Intermediate to caudal NRe	N/A

Abbreviations: A11, A11 dopamine cells; A13, A13 dopamine cells; CTB, cholera toxin subunit B; CM, central medial thalamic nucleus; DA, dorsal hypothalamic area; FB, fast blue; FG, fluorogold; PaXi, paraxiphoid nucleus of thalamus; PHD, posterior hypothalamic area, dorsal part; NRe, nucleus reuniens; Rh, rhomboid thalamic nucleus; Xi, xiphoid nucleus.

3.2.4 Immunohistochemical procedures

Immunohistochemical procedures are described in Section 2.4.6. For an overview of antibodies used see Table 2.4. To characterise the distribution of TH-positive fibres, sections were stained with a TH antibody (rabbit, 1:1000, Chemicon, AB152) and the secondary antibody biotinylated anti-rabbit (goat, 1:500, Vector, BA-1000). For the tract tracing experiments, sections from cases which involved FB and FG injections were stained with an antibody against-TH (chicken, 1:1000, Abcam, AB76442) and secondary antibody anti-chicken Alexa Fluor 594 (goat, 1:500, Invitrogen, A-11042) or anti-chicken Alexa Fluor 488 (goat, 1:500, Invitrogen, A11039). In cases which involved CTB injection, a cocktail of antibodies was used: primary antibodies anti-TH (chicken, 1:1000, Abcam, AB76442) and anti-CTB (rabbit, 1:3000, Sigma-Aldrich, C30620); and secondary antibodies anti-chicken Alexa Fluor 488 (goat, 1:500, Invitrogen, A-11039) and anti-rabbit Alexa Fluor 594, (goat, 1:500, Invitrogen, A-11037).

3.2.5 Anatomical nomenclature concerning the catecholaminergic cell groups

Nomenclature adopted for identification of the catecholaminergic cell groups is described in Section 2.5.1, except for the A6 cell group which will be herein referred to as LC. Only catecholaminergic cell groups which occupy brain regions which have established projections to the NRe were evaluated for the presence of double-labelled cells (i.e., those that express both the retrograde tracer and TH antibody) (McKenna & Vertes, 2004). The catecholaminergic cell groups evaluated and not evaluated for the presence of double-labelled cells is summarised in Table 3.2.

Table 3.2. Overview of catecholaminergic cells evaluated and not evaluated.

Cell group	Anatomical location	Analysed
A1	lateral reticular nucleus	x
A2	dorsal motor nucleus of the vagus nerve in the medulla	x
A4	tegmen ventriculi quarti (along the ventral surface of the cerebellum)	x
A5	lateral to the superior olivary complex in the pontine tegmentum	x
A6	locus coeruleus	✓
A7	pontine reticular formation	✓
A8	retrorubral field, occupying the caudal mesencephalic reticular formation	✓
A9	substantia nigra pars compacta, pars reticulata and pars lateralis	✓
A10	ventral tegmental area (VTA)	✓
A10 dorsocaudal	ventral periaqueductal gray (PAG), dorsal raphe nucleus	✓
A10 ventrorostral	supramammillary nucleus, rostral PAG to dorsal and caudal hypothalamus adjacent to the mammillothalamic tract	✓
A11	rostral PAG to the posterior hypothalamus adjacent to the mammillothalamic tract	✓
A12	arcuate nucleus	x
A13	medial zona incerta	✓
A14	hypothalamus, along the third ventricle and including the posterior part of the paraventricular hypothalamic nucleus	x
A15	anterior hypothalamus, above the optic chiasm/ supraoptic nucleus	✓

"✓" indicates that the cell body was analysed, and "x" indicates that the cell body was not analysed for the presence of double-labelled cells.

3.2.6 Anatomical nomenclature and borders concerning the nucleus reuniens and adjacent nuclei

Anatomical boundaries used in the present experiments follow those described in Paxinos & Watson (2006). The NRe is located above the third ventricle and extends the entire rostro-caudal axis of the thalamus. At the most rostral level, the NRe is separated into two structures where it is bordered dorsally by the central medial thalamic nucleus, anteromedial thalamic nucleus and anteromedial thalamic nucleus, ventral part. Caudally, the two structures merge in the midline, and consist of a medial and lateral portion, the lateral portion is often referred to as the NRe or peri-reuniens. At more intermediate levels of the NRe, it is bordered dorsally by the rhomboid thalamic nucleus and submedius thalamic nucleus, and ventrally by the paraxiphoid nucleus of thalamus. As the NRe moves caudally, the ventral portion borders against the posterior hypothalamus dorsal part and the dorsal portion eventually becomes bordered against the central medial thalamic nucleus (Groenewegen & Witter, 2004; Paxinos & Watson, 2006).

3.2.7 Figures

Figures were prepared using ImageJ (Schindelin et al., 2012) and Adobe Illustrator (version 25.4.1, San Jose, CA, USA). Graphs were created using the R package ggplot2 (Hadley, 2016). Brain atlas figures are adapted from Paxinos & Watson (2006).

3.3 Results

3.3.1 Distribution of catecholaminergic fibres in the nucleus reuniens

To visualise the distribution of catecholaminergic innervation to the NRe, an antibody against TH was used (Figure 3.1). The entire rostrocaudal axis of the NRe contained

TH-immunopositive fibres that were fine and spindly in nature. Visually it appeared that the distribution of TH-positive fibres is non-uniform throughout the NRe. At the rostral-most level of the NRe, moderate levels of labelled fibres were observed, whereas fewer labelled fibres were observed in the intermediate to caudal levels of the NRe. In addition, no apparent variation in density of catecholaminergic fibres was observed in the medio-lateral plane.

3.3.2 Injection sites

Figure 3.2 provides a schematic overview of injection sites and illustrates the extent of tracer spread for all cases analysed. In two cases (7#5 and 216#5), spread of tracer was located exclusively in the NRe. Case 7#5 covered rostral regions of the NRe while case 216#5 covered caudal and lateral portions of the NRe. Case 7#7 covered rostral regions of the NRe and contained some minor involvement of the rhomboid. In two cases (222#3 and 216#4), injections were centred in the rostral NRe with some minor involvement of the paraxiphoid nucleus of thalamus in case 222#3 and minor involvement of the rhomboid, central medial thalamic nucleus and paraxiphoid nucleus of thalamus in case 216#4. In two cases (225#2 and 216#9), injections were centred in the intermediate to caudal levels of the NRe with some spread to the posterior hypothalamic area, dorsal part in case 216#9.

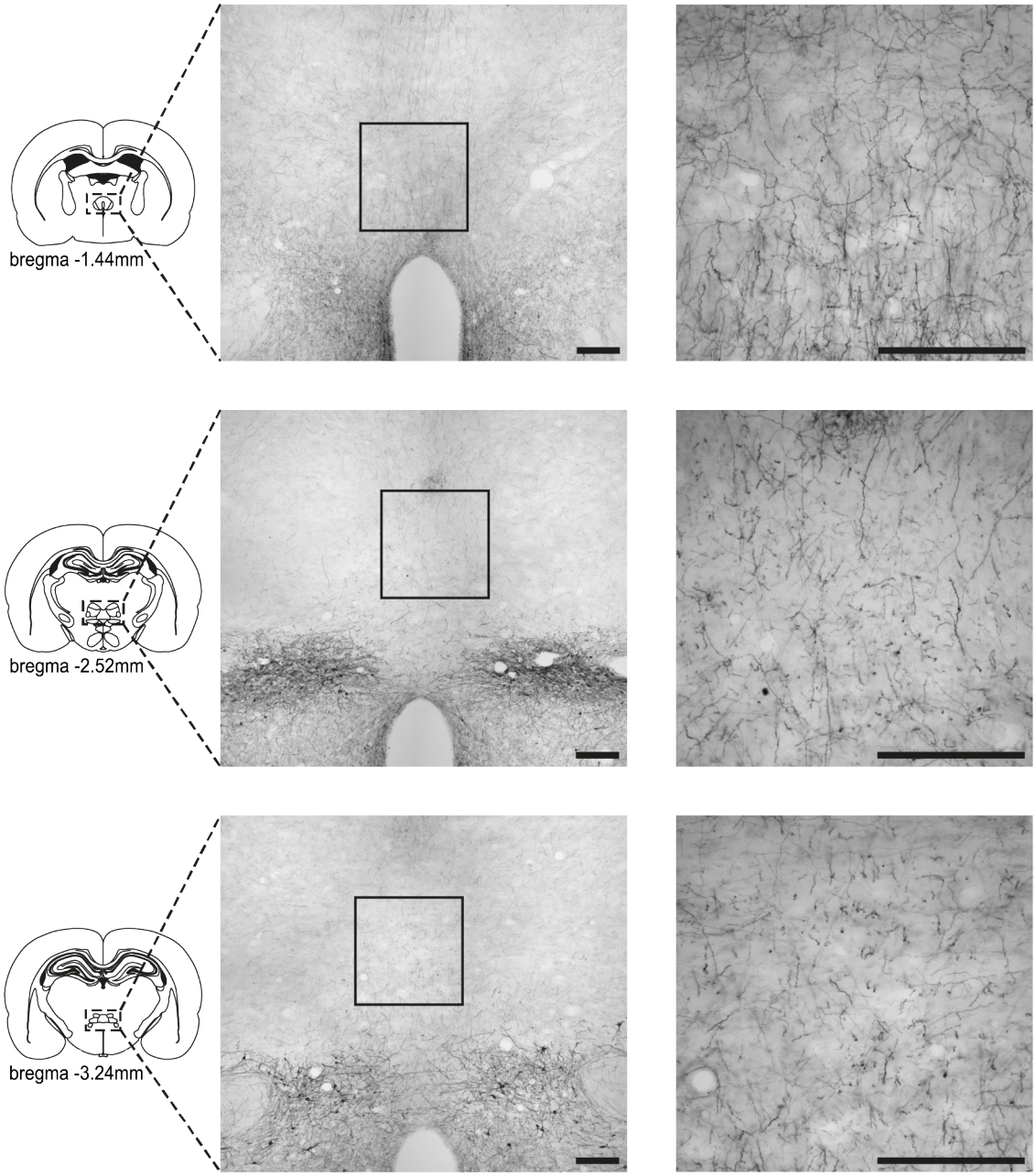

Figure 3.1. Distribution of TH-positive fibres in the NRe. Left panel includes schematics of the brain atlas at three anterior-posterior levels with enclosed dashed box indicating region in which photomicrographs were taken. Middle panel includes low magnification photomicrographs with regions enclosed by black boxes indicating areas in which photomicrographs of higher magnification images were taken on the right panel. Scale bars: 200μm. Figures adapted from Paxinos & Watson (2006).

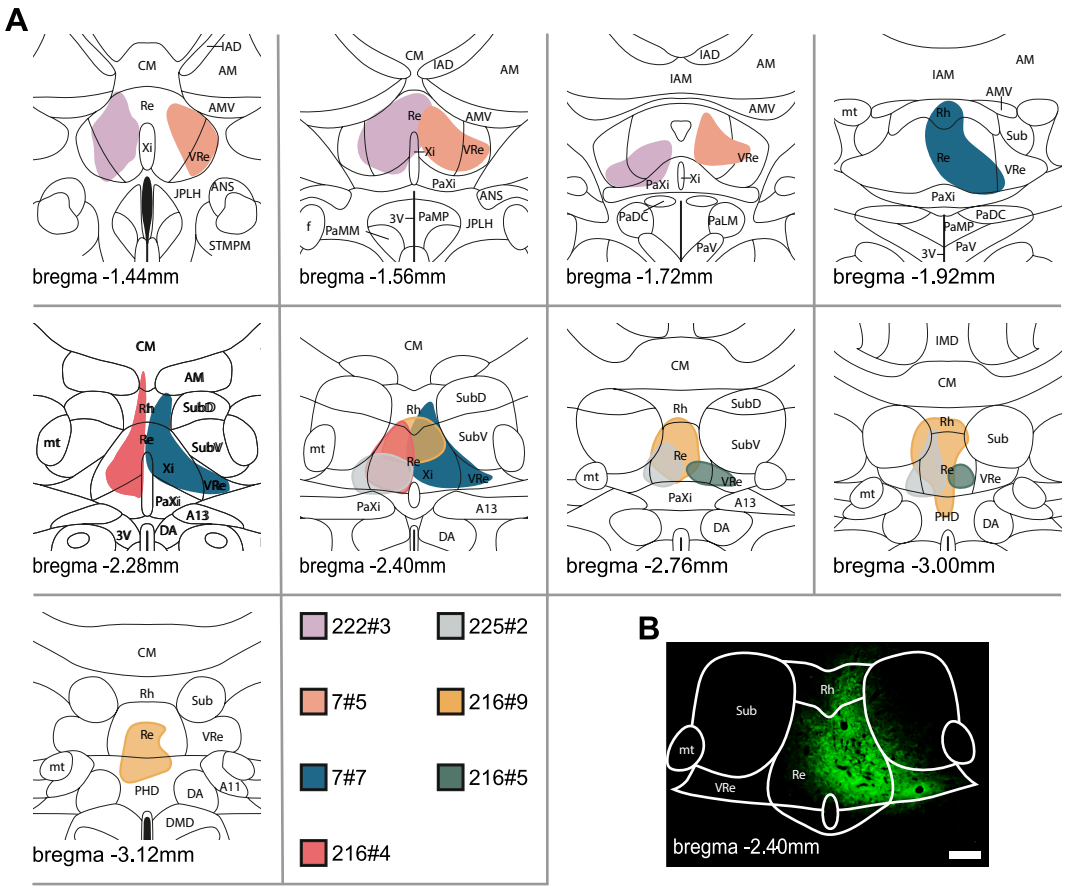

Figure 3.2. Schematic overview of cases. (A) Schematic drawings of retrograde tracer injection spread in each case. Each individual case is colour coded: 222#3 (purple), 7#5 (pink), 7#7 (dark blue), 216#4 (red), 225#2 (grey), 216#9 (yellow), and 216#5 (green). (B) Representative case 7#7 showing spread of CTB tracer in the NRe. Scale bar: 200μm. Abbreviations: A11, A11 dopamine cells; A13, A13 dopamine cells; AHP, anterior hypothalamic area, posterior part; AM, anteromedial thalamic nucleus; AMV, anteromedial thalamic nucleus, ventral part; ANS, accessory neurosecretory nuclei; CM, central medial thalamic nucleus; DA, dorsal hypothalamic area; DMD, dorsomedial hypothalamic nucleus, dorsal part; IAD, interanterodorsal thalamic nucleus; IAM, interanteromedial thalamic nucleus; JLPH, juxtaparaventricular part of lateral hypothalamus; MT, medial terminal nucleus of the accessory optic tract; PaDC, paraventricular hypothalamic nucleus, dorsal cap; PaLM, paraventricular hypothalamic nucleus, lateral magnocellular part; PaMP, paraventricular hypothalamic nucleus, medial parvicellular part; PaXi, paraxiphoid nucleus of thalamus; Pe, periventricular hypothalamic nucleus; PH, posterior hypothalamic nucleus; PHD, posterior hypothalamic area, dorsal part; PT, paratenial thalamic nucleus; PVA, paraventricular thalamic nucleus, posterior part; Re, reuniens thalamic nucleus; Rh, rhomboid thalamic nucleus; Stg, stigmoid hypothalamic nucleus;

Figure 3.2 ***(continued).*** Sub, submedius thalamic nucleus; SubD, submedius thalamic nucleus, dorsal part; SubV, submedius thalamic nucleus, ventral part; VM, ventromedial thalamic nucleus; VRe, ventral reuniens thalamic nucleus; Xi, xiphoid thalamic nucleus. Figures adapted from Paxinos & Watson (2006).

3.3.3 Distribution of double-labelled neurons

3.3.3.1 A13 cell group

In all cases analysed, double-labelled neurons, i.e., neurons immunopositive for both retrograde tracer and TH antibody, were dispersed throughout the dopaminergic A13 cell group (see Figure 3.3A for representative case 216#9). A significant number of double-labelled neurons were observed at the intermediate level of the A13 cell group ($\sim$ -2.40mm from bregma). Figure 3.3B shows the distribution of double-labelled cells in two cases (222#3 and 7#7). The number of double-labelled neurons, retrogradely transported neurons and the proportion of double-labelled neurons relative to the number of retrogradely transported neurons in the A13 region for all cases is shown in Figure 3.3C. The fraction of double-labelled neurons remained relatively consistent among the cases despite tracer injections targeting different rostrocaudal portions of the NRe. For example, cases which involved the rostral NRe (222#3 and 216#4), 12.9% and 12.2% of the retrogradely transported neurons were double-labelled, respectively. Similarly, cases which involved tracer in intermediate to caudal levels of the NRe (225#2 and 216#9), 15.4% and 10.5% of the retrogradely transported neurons were double-labelled, respectively. Overall, these data reveal that the A13 cell group provides dopaminergic input to the NRe.

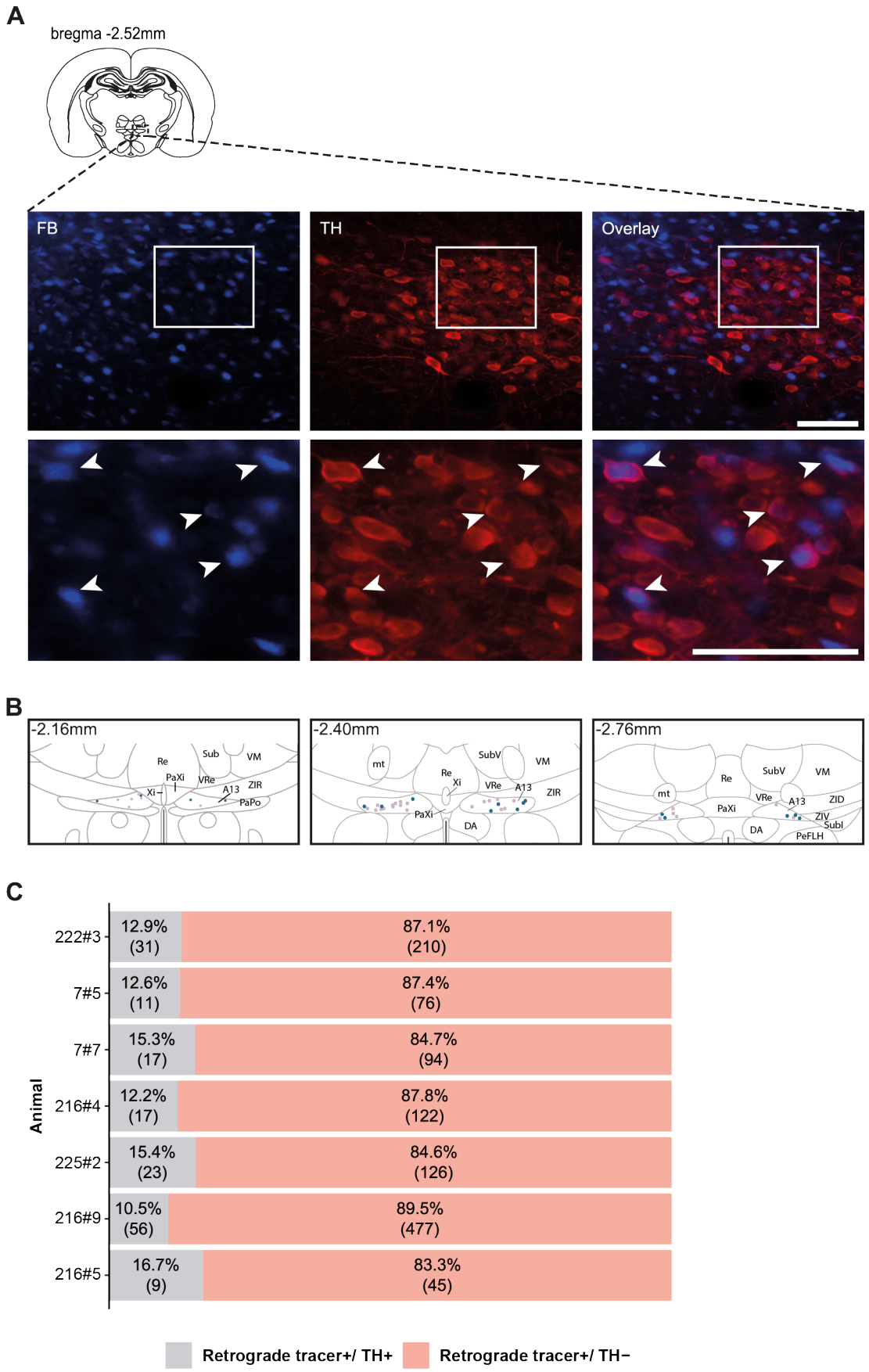

Figure 3.3 Double-labelled neurons in the A13 cell group. (A) Top, schematic of the brain atlas at the approximate anterior-posterior level in which photomicrographs were taken

Figure 3.3 ***(continued).*** with area enclosed by the dashed box indicating location of images. Middle, photomicrographs show representative case 216#9 showing retrogradely transported FB neurons (blue), TH-positive neurons (red) and an overlay of the two images in the A13 cell group. Bottom, higher magnification images of the regions outlined by the white boxes in the middle panel are shown. Example of double-labelled neurons are highlighted by the arrowheads. (B) Schematic overview of the distribution of double-labelled cells in the A13 cell group spanning three anterior-posterior levels in two representative cases, 222#3 (dark blue dots) and 7#7 (pink dots). Each dot represents one double-labelled neuron. (C) Raw numbers are in brackets and percentages show the proportion of double-labelled neurons (grey) relative to the number of retrogradely transport transported neurons (pink) in the A13 region for each case. Scale bars: images to the top (50μm), images to the bottom (25μm). Abbreviations: A13, A13 dopamine cells; DA, dorsal hypothalamic area; mt, mammillothalamic tract; PaPo, paraventricular hypothalamic nucleus, posterior part; Paxi, paraxiphoid nucleus of thalamus; PeFLH, perifornical part of lateral hypothalamus; Re, reuniens thalamic nucleus; Sub, submedius thalamic nucleus; SubV, submedius thalamic nucleus, ventral part; VM, ventromedial thalamic nucleus; VRe, ventral reuniens thalamic nucleus; Xi, xiphoid thalamic nucleus; ZID, zona incerta, dorsal part; ZIR, zona incerta, rostral part. Figures adapted from Paxinos & Watson (2006).

3.3.3.2 Locus coeruleus

The presence of double-labelled cells in the LC was variable among the cases analysed. Injections which involved the rostral NRe (cases 222#3, 7#5, 7#7 and 216#4), retrogradely and double-labelled neurons were reliably observed in the LC (Figure 3.4A shows representative case 222#3). While double-labelled cells were still observed in cases which involved tracer deposit in the caudal NRe (cases 225#2, 216#9 and 216#5), the total number of retrogradely transported cells was considerably lower than the rostral NRe cases (Figure 3.4A shows representative case 216#9). Due to the low levels of retrogradely transported cells in the LC following intermediate to caudal NRe injections, further analysis to describe the pattern of projections was not conducted. However, in cases with tracer spread in the rostral NRe, double-labelled

neurons were found scattered throughout the anterior-posterior and medio-lateral axis of the LC with no apparent topography. Mapping of the distribution of double-labelled cells in two rostral cases (222#3 and 7#7) highlights the lack of topography (Figure 3.4B). The number of double-labelled neurons, retrogradely transported neurons and the proportion of double-labelled neurons relative to the number of retrogradely transported neurons in the LC between cases is shown in Figure 3.4C. Together, these data indicate that noradrenergic LC projections to the NRe are topographically organised, such that rostral NRe receives denser LC cell inputs than caudal NRe.

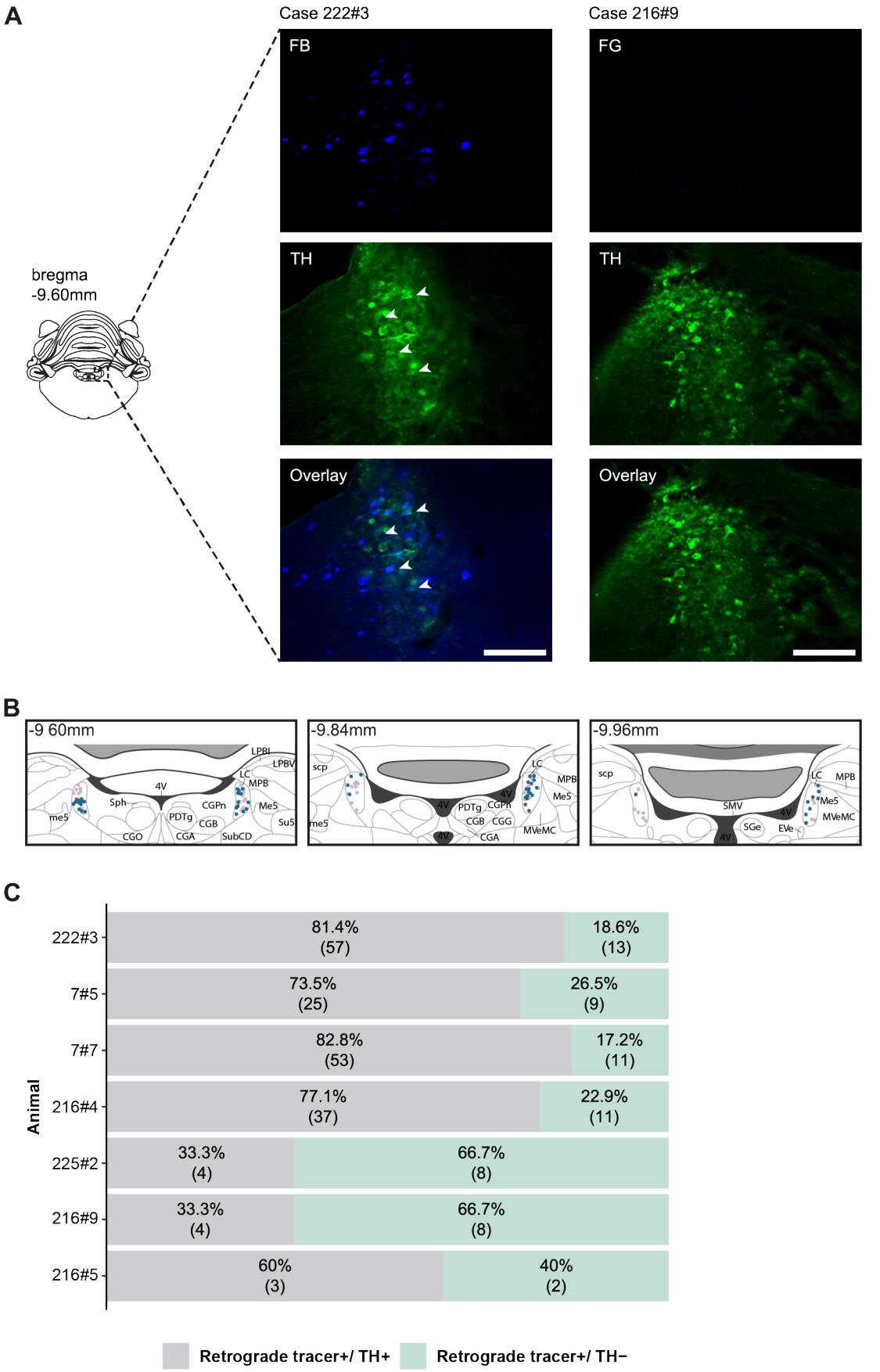

Figure 3.4 Comparison of double-labelled neurons in the LC. (A) Left, schematic of the brain atlas at the approximate anterior-posterior level in which photomicrographs

Figure 3.4 ***(continued).*** were taken with area enclosed by the dashed box indicating location of images. Middle, fluorescent photomicrographs of case 222#3 showing retrogradely transported FB neurons (blue), TH-positive neurons (green) and an overlay of the two images in the LC. Double labelled neurons are visibly present in case 222#3, indicated by white arrowheads. Right, fluorescent photomicrographs of case 216#9, a lack of both retrogradely transported neurons and double-labelled neurons was observed. (B) Schematic overview of the distribution of double-labelled cells in the LC spanning three anterior-posterior levels in two rostral NRe cases, 222#3 (dark blue dots) and 7#7 (pink dots). Each dot represents one double-labelled neuron. (C) Raw numbers are in brackets and percentages show the proportion of double-labelled neurons (grey) relative to the number of retrogradely transport transported cells (green) in the LC for each case. Scale bars: 100μm. Abbreviations: 4V, 4th ventricle; CGA, central gray, alpha part; CGB, central gray, beta part; CGG, central gray, gamma part; CGO, central gray, nucleus O; CGPn, central gray of the pons; Eve, nucleus of origin of efferents of the vestibular nerve; LC, locus coeruleus; LPBI, lateral parabrachial nucleus, internal part; LPbV, lateral parabrachial nucleus, ventral part; Me5, mesencephalic trigeminal nucleus; MPB, medial parabrachial nucleus; MVeMC, medial vestibular nucleus, magnocellular part; PDTg, posterodorsal tegmental nucleus; scp, superior cerebellar peduncle (brachium conjunctivum); SMV, superior medullary velum; Sph, sphenoid nucleus; Su5, supratrigeminal nucleus; SubCD, subcoeruleus nucleus, dorsal part; SGe, supragenual nucleus. Figure adapted from Paxinos & Watson (2006).

3.3.3.3 Other catecholaminergic cell groups

The other eight catecholaminergic cell groups were also evaluated for the presence of double-labelled neurons (see Table 3.1 for full list), however, in all eight cell groups analysed, double-labelled neurons were virtually absent. For instance, in the more extensively studied dopaminergic cells groups, such as the midbrain dopaminergic cell groups, the VTA (A10 cell group) and SNc (A9 cell group), virtually no double-labelled cells were observed. Retrogradely transported cells and TH-positive cells seemed to be distributed in separate regions of the VTA and SNc (Figure 3.5). In addition, in the noradrenergic pontine reticular formation (A7 cell group), retrogradely

transported cells and TH-positive cells were found intermingled within the A7 cell group anatomical boundaries but never overlapping (Figure 3.6). Together, this pattern of labelling shows that the NRe receives catecholaminergic input exclusively from two sources, the A13 cell group and the LC.

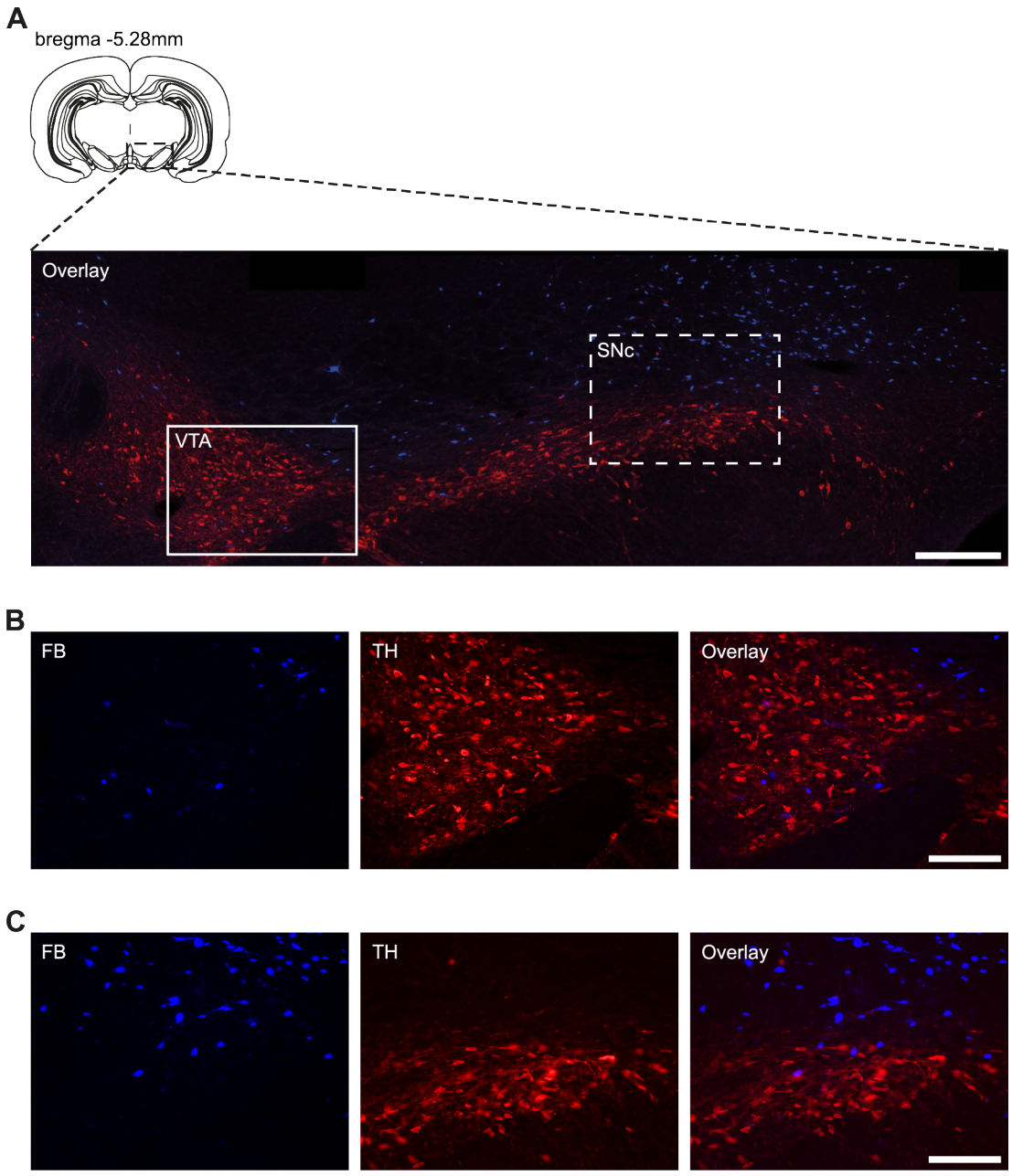

Figure 3.5. Absence of double-labelled neurons in other dopaminergic cell groups. Fluorescent photomicrographs of representative case 216#9. (A) Top, schematic of the brain atlas at the approximate anterior-posterior level in which photomicrographs were taken with area enclosed by the dashed box indicating location of images. Bottom, an overlay of retrogradely transported neurons (blue) and TH-positive neurons (red) in the VTA (A10) and SNc (A9). Higher magnification images of the regions enclosed by the white boxes highlight the lack of double-labelled neurons in (B) VTA and (C) SNc. Scale bars: (A) 200μm, (B and C) 100μm. Abbreviations: SNc, substantia nigra; VTA, ventral tegmental area. Figures adapted from Paxinos & Watson (2006).

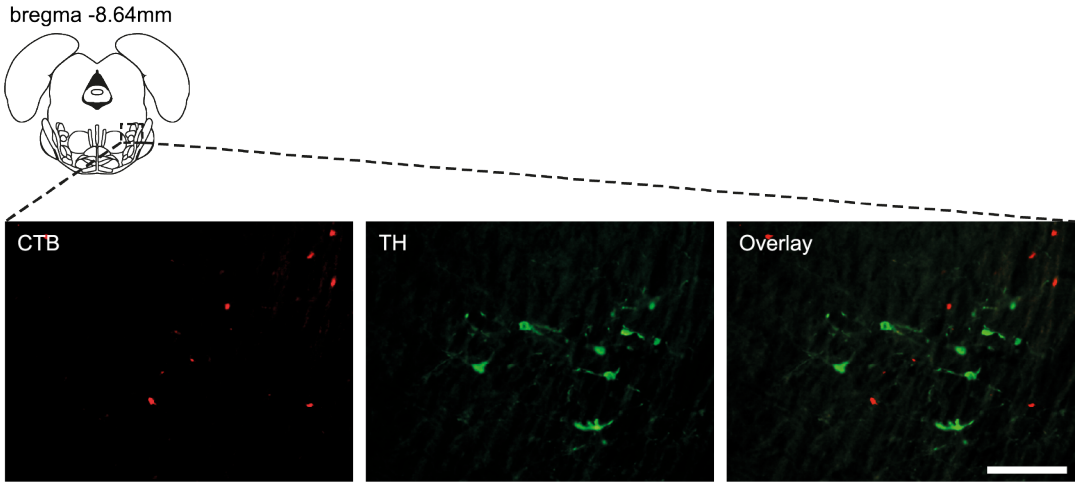

Figure 3.6. Absence of double-labelled neurons in other noradrenergic cell groups. Fluorescent photomicrographs of representative case 216#4 in the A7 cell group. Top, schematic of the brain atlas at the approximate anterior-posterior level in which photomicrographs were taken with area enclosed by the dashed box indicating location of images. Photomicrographs show retrogradely transported CTB neurons (red), TH-positive neurons (green), and an overlay (right). Scale bar: 100μm. Figures adapted from Paxinos & Watson (2006).

3.4 Discussion

The present findings revealed that the rostrocaudal axis of the NRe contains TH-positive fibres but at varying density. It was observed that the rostral NRe contains fibres with slightly greater TH immunoreactivity compared to the caudal NRe. In addition, by employing retrograde tract tracing with TH immunohistochemistry, the source of catecholaminergic fibres was revealed. The A13 cell group (located in the medial aspect of the zona incerta), and the LC were identified as the sources of catecholaminergic input to the NRe. The anatomical tract tracing experiments revealed that dopaminergic input from the A13 cell group seems to uniformly target the entire neuroaxis of the NRe, whereas LC noradrenergic input to the NRe distributes more densely to the rostral NRe than to the intermediate to caudal NRe.

3.4.1 Methodological considerations

When anatomical retrograde tracers are injected into discrete brain regions there is often spread of the tracer to adjacent nuclei and therefore conclusions may not be based solely on the brain region of interest. Although several of the cases involved tracer spread outside of the NRe, with respect to the A13 projection to the NRe, there are a number of arguments that suggest that such tracer spread made a minimal contribution to the conclusions of the current chapter. For example, in some cases (see Table 3.1 and Figure 3.2) minor spread to midline nuclei adjacent to the NRe was observed, however, it has been previously reported that neurons (not necessarily TH-positive) within the A13 cell group do not project heavily to structures, such as the paraventricular hypothalamic nucleus, intermediodorsal thalamic nucleus, central medial thalamic nucleus and anteromedial thalamic nucleus (Sita et al., 2007). While the A13 cell group displays a distinct projection pattern to thalamic structures, the LC projects to virtually every structure in the central nervous system (Aston-Jones & Waterhouse, 2016), therefore there is a possibility that tracer deposit outside of the NRe also contributed to the number of double-labelled cells observed in the LC. However, given that cases which involved tracer deposit located exclusively in the NRe demonstrated a similar pattern of double-labelled cells to cases which involved minimal leakage of tracer to neighbouring structures, it seems unlikely that tracer spread outside of the NRe had a significant impact on the current results. For example, case 222#3 which involved tracer injections exclusively confined to the NRe, a similar pattern of retrogradely transported cells and double-labelled cells in the LC was found to case 216#4 which involved some leakage of tracer deposit outside the NRe, (see Table 3.1 and Figure 3.2). Taking the above evidence into consideration, it seems that tracer spread to thalamic nuclei adjacent to the NRe had a minimal contribution to the conclusions in the current study, thus the pattern of A13 and LC projections reported here are specific to the NRe.

Following injection of the retrograde tracers, to determine whether a projection was catecholaminergic in nature, an antibody against TH was used. Thus, only cell

bodies that were clearly labelled with both the retrograde tracer and TH antibody were counted as double-labelled cells. However, there is a possibility that some TH-positive neurons were not detected, perhaps due to low expression levels of the TH antibody (an issue associated with all immunohistochemical techniques), thus the number of double-labelled cells may be higher than reported here. Indeed, this may be the case regarding descriptions concerning the noradrenergic projection from the LC reported in the current chapter. We only found 80% of neurons in the LC to be double-labelled, while reports indicate that the majority of neurons within the LC are TH-positive (Aston-Jones et al., 2004). However, at the same time, the current finding that only 80% of LC neurons are double-labelled may not be a gross underestimation as there is also a possibility that non-TH-positive cells innervate the NRe, given the recent descriptions of LC-GABA neurons found intermingled within LC-TH neurons (Breton-Provencher & Sur, 2019).

The current chapter also demonstrated, for the first time, that LC projections innervate the rostral NRe more densely than the caudal NRe. It could be argued that in the present study that the difference in the number of retrogradely transported cells is not due to a topographical projection pattern but instead explained by other factors such as differences between transduction efficiency of the retrograde tracers used or the method of injection used. However, several lines of evidence suggest that these technical factors did not affect the results of the present study. For instance, in one case (216#9), which involved tracer deposit covering intermediate to caudal levels of the NRe, the retrograde tracer FG was used. FG is considered to be a highly sensitive tracer with very good transduction efficiency and thus able to label a large number of neurons (Schofield, 2008). Taking these properties of FG into consideration, the fact that relatively few retrogradely transported cells in the LC following FG injection was observed, suggests that the LC does not project as strongly to the intermediate and caudal NRe compared to the rostral NRe. Moreover, it is unlikely that case 216#9 suffered from insufficient uptake of FG tracer as a pronounced number of retrogradely transported cells was observed in the A13 cell group (Figure 3.3).

This study employed a number of different retrograde tracers and injection techniques (Table 3.1). Regardless of the tracer used or method of injection employed, a similar pattern of results among cases that had similar spread of tracer deposit was observed, e.g., rostral NRe case 222#3 pressure injected with FB revealed a similar proportion of double-labelled LC neurons compared to rostral NRe case 7#7 injected with CTB via pressure injection, 81.4% and 82.8%, respectively. Thus, the replicability between cases using different tracers and injection procedures provides further support to the conclusions of the current study.

3.4.2 Catecholaminergic fibres in the nucleus reuniens

It is generally presumed that catecholaminergic input to the rodent thalamus is weak. For instance, García-Cabezas et al. (2009) demonstrated sparse labelling of DAT in the rodent thalamus, while Groenewegen (1988) and Papadopoulos & Parnavelas (1990), using an antibody against dopamine, reported weak immunoreactivity in the MD and lateral geniculate nucleus in rats, respectively. With respect to the NRe, two early reports conducted in rats, one using an antibody against dopamine beta-hydroxylase (DBH) (Swanson & Hartman, 1975), and the other using glyoxylic acid fluorescence (Lindvall et al., 1974), indicated that midline thalamic nuclei are only innervated with a scattering of noradrenergic and catecholaminergic fibres, respectively. It is important to note however, that the abovementioned studies employed immunostaining procedures that have several drawbacks. For example, the use of the DAT antibody by García-Cabezas et al. (2009) does not consider input from DAT-negative dopaminergic cell groups, while the dopamine antibody employed by Groenewegen (1988) and Papadopoulos & Parnavelas (1990) is reportedly technically challenging to use and also lacks sensitivity (Garcıa-Cabezas et al., 2007). Furthermore, while the DBH antibody is still widely used, newer, more sensitive variants of the DBH antibody have been developed. These new variants have a much higher detection threshold, therefore it is likely that the results reported by Swanson & Hartman (1975) provided an underestimation of the density of DBH-positive fibres present in the NRe. Finally, while the glyoxylic acid fluorescence

technique used by Lindvall et al. (1974) serves as an excellent marker for detecting the catecholaminergic system in the central nervous system, more recent modern-day antibodies directed against the catecholamine synthesis enzyme (such as the TH antibody used in the current study), have been developed that allow for visualisation of the catecholaminergic system in greater detail (Björklund & Dunnett, 2007).

In the current study, using the TH antibody, which can detect fibres originating from non-DAT and DAT expressing dopaminergic cell bodies, as well as noradrenergic cell bodies, it was revealed that the NRe contains a higher density of TH-positive fibres than previously reported. It therefore seems likely that the difference in results can be explained by the poorer detection thresholds of the immunochemical procedures used in previous studies compared to modern-day antibodies and the use of antibodies that do not account for dopaminergic innervation from all dopamine cell groups (i.e., the DAT antibody). While catecholaminergic innervation to the NRe is by no means dense, especially in comparison to other brain structures, e.g., the mPFC (Cerpa et al., 2019), the results of the current study and the evidence outlined above regarding antibody choice suggest that catecholaminergic innervation to the NRe is much more extensive than previously described and that the notion that the rodent thalamus (in particular the NRe) only receives a scattering of catecholaminergic fibres should be updated.

It is interesting to note that until recently the primate thalamus was also not recognised to receive a significant catecholaminergic input. However, in a series of experiments employing a number of catecholaminergic markers, (TH, dopamine and DAT), it was revealed that the primate thalamus is in fact widely innervated with catecholaminergic fibres (Garcıa-Cabezas et al., 2009; Garcıa-Cabezas et al., 2007; Sánchez-González et al., 2005). The authors also reported that midline thalamic nuclei (including the NRe) demonstrated dense immunoreactivity of the TH and dopamine antibodies, and to a lesser extent the DAT antibody. Thus, the anatomical studies conducted in the primate thalamus further highlight that appropriate antibody choice is pivotal when drawing conclusions regarding the extent of catecholaminergic innervation to the thalamus, and that by employing these sensitive antibodies, the

authors were able to demonstrate that contrary to the common assumption that the primate thalamus is only weakly innervated with catecholaminergic fibres, that it does in fact receive dense catecholaminergic innervation (Sánchez-González et al., 2005).

The current results also indicated that catecholaminergic innervation to the NRe is non-uniform. It was observed that rostral portions of the NRe contained slightly denser TH immunolabelling compared to the intermediate to caudal NRe. It is important to note that conclusions based on the density of TH-positive fibres were based on visual inspection, thus these are only preliminary observations. To ultimately confirm these findings, further work is required. For example, it would be necessary to stain more cases with the TH antibody followed by quantitative approaches to measure the density of TH-positive fibres in the NRe. Regardless, it is interesting to note that the anatomical tract tracing experiments demonstrated that following tracer injections into the NRe, LC projections followed a similar topography, with rostral NRe injections resulting in greater numbers of retrogradely and double-labelled cells in the LC region compared to intermediate to caudal NRe injections. Moreover, given that the proportion of A13 double-labelled cells remained relatively consistent regardless of whether tracer spread was confined to more rostral or caudal portions of the NRe, it is unlikely that dopaminergic inputs to the NRe contributed to this topography. Altogether it seems that the denser labelling of TH-positive fibres in the rostral NRe reflects the denser noradrenergic inputs arising from the LC.

It is noteworthy to mention that in a recent study conducted in mice, it has been proposed that the NRe contains TH-positive neurons, thought to be part of the A13 dopaminergic cell group (Ogundele et al., 2017). However, in the current study, TH-positive neurons were not observed within the anatomical boundaries of the NRe. This discrepancy regarding the presence of TH-positive cell bodies in the NRe could be due to classification of anatomical boundaries between species or indeed between different atlases, therefore providing ambiguity in precise anatomical boundaries of certain brain regions (Paxinos & Franklin, 2019; Paxinos & Watson, 2006; Swanson,

2004).

3.4.3 Dopaminergic input to the nucleus reuniens

The current results indicate that the full rostro-caudal axis of the NRe receives dopaminergic innervation from the A13 cell group. A relatively consistent proportion of double-labelled cells was observed among the cases, with an average of 13.2% of cells counted as double-labelled. The A13 cell group, due to its close proximity to the zona incerta, has often been classified together with the zona incerta as a singular structure. However, Sita et al. (2007) demonstrated that A13 neurons display a distinct projection pattern compared to other neurons within the zona incerta and proposed that the A13 dopaminergic cell group should be considered as an anatomically distinct region from the zona incerta and instead be considered as part of the medial hypothalamic system. Accordingly, by targeting anterograde tracers specifically into the A13 cell group area, it was demonstrated that neurons in the medial hypothalamic system send very dense projections to the NRe, however, the neurochemical identity of these projections was not confirmed to be dopaminergic (Sita et al., 2007). More recently, by injecting Cre-dependent viruses into the A13 cell group of TH-Cre transgenic mice, it was confirmed that the dopaminergic neurons of the A13 cell group project to the NRe (Venkataraman et al., 2021). Thus, the current findings are in accordance with these studies and extend these observations by demonstrating that the A13 cell group provides the sole source of dopamine to the NRe as the NRe does not receive dopaminergic inputs from any additional sources such as the midbrain dopaminergic cells groups (A8, A9 and A10 cell group).

Interestingly, in a retrograde tract tracing study conducted in monkeys, as well as identifying that midline thalamic nuclei are innervated with dopaminergic fibres originating from the A13 cell group, the authors also observed that midline thalamic nuclei receive additional sources of dopaminergic innervation (Sanchez-Gonzalez, 2005). This finding contrasts with the current results indicating that the A13 cell group is the only source of dopaminergic afferents to the NRe, however, this discrepancy is likely explained by the large injection sites of Sanchez-Gonzalez et al.

(2005) which covered all midline thalamic nuclei while our injections were confined to the NRe.

3.4.4 Noradrenergic input to the nucleus reuniens

The LC was previously identified as a source of noradrenergic input to the NRe (Lindvall et al., 1974), which was confirmed in the present study, using a more sensitive approach. Thus, instead of using lesions, here retrograde tract tracing was combined with TH immunohistochemistry. While co-localisation of cells in the LC was observed in all our cases, quantification of the number of double-labelled and retrogradely transported cells revealed that projections arising from the LC to the NRe are topographically organised. We found that LC neurons seem to distribute more densely to the rostral NRe than to the intermediate to caudal NRe, as demonstrated by the greater number of retrogradely transported cells, and generally a greater proportion of double-labelled cells in cases which involved tracer deposit covering the rostral NRe (cases 222#3, 7#5, 7#7 and 216#4), compared to cases which involved tracer deposit covering intermediate to caudal levels of the NRe (cases 225#2, 216#9 and 216#5). While previous retrograde tracing studies have identified that the LC sends afferents to the NRe, no such topographical projection pattern has been previously described (Krout et al., 2002; McKenna & Vertes, 2004). As mentioned above (Section 3.4.2), in accordance with the topography described from the retrograde tracing results, the pattern of catecholaminergic fibre labelling in the NRe as visualised by TH immunohistochemistry in the present study also indicated denser immunolabelling in rostral NRe compared to intermediate to caudal NRe (Figure 3.1), thus supporting this notion that LC projections to the NRe are topographically organised. It is interesting to note, in a recent report describing the distrbution of noradrenergic fibres in the macaque NRe, no rostro-caudal differences in density were noted by the authors (Pérez-Santos et al., 2021). Thus it is likely that species differences exist in the distribution of noradrenergic fibres in the thalamus. However, to ultimately confirm whether a topographical projection pattern exists, an alternative approach would be to inject a “SynaptoTag” virus into the LC. The

SynaptoTag AAV expresses two fluorescent proteins, one which is expressed in axon terminals and the other which is fused to synaptobrevin-2 (the synaptic vesicle protein), and thus expresses in synaptic terminals (Huerta-Ocampo et al., 2020; Xu & Südhof, 2013). Therefore, by using this approach, it would allow one to quantitively determine whether LC axons primarily establish synapses in the rostral NRe compared to the intermediate to caudal NRe.

The current chapter also revealed that in cases in which the injection was confined to the rostral NRe, there was no clear topography in the pattern of retrogradely transported cells in the LC. We found double-labelled cells scattered throughout the anterior-posterior and medio-lateral axis of the LC. In contrast, previous reports have indicated that LC projections to the thalamus primarily arise from the posterior LC with few projections originating from the anterior LC (Mason & Fibiger, 1979; Schwarz & Luo, 2015), however, in the study conducted by Mason & Fibiger (1979), the authors regarded the thalamus as one structure, and the NRe was not specifically examined. It therefore seems that these descriptions regarding the pattern of LC projections to the thalamus should be updated, and each thalamic structure should be considered individually.

In addition, by analysing the presence of double-labelled cells in other noradrenergic cell groups with known projections to the NRe (McKenna & Vertes, 2004), it was revealed that these other cell groups, such as the pontine reticular formation (A7 cell group), do not send noradrenergic afferents to the NRe, indicating that the LC is the exclusive source of noradrenaline to the NRe.

3.4.5 Functional considerations

3.4.5.1 Dopaminergic modulation of the nucleus reuniens

Until recently, direct functional evidence for a role for the A13 cell group had not been established, however, in a recent study, as mentioned in the introduction (Section 3.1), the A13 cell group has been identified to send dopaminergic projections to the NRe that were demonstrated to be critical for fear extinction recall (Venkataraman

et al., 2021). This finding is intriguing as it indicates that projections from the A13 cell group to the NRe are indeed functional and suggests that such projections may be involved in other NRe-mediated cognitive functions. However, whether A13 projections to the NRe have the potential to be involved in recognition memory is unclear. For instance, other structures within the recognition memory neural circuit that are closely linked to the NRe, i.e., the HPC and mPFC, receive their dopaminergic input from distinct sources, the VTA and SNc (Gasbarri et al., 1997; Lindvall et al., 1974). In addition, some evidence also indicates that the LC provides an additional source of dopamine to the HPC and mPFC due to the LC's ability to co-release dopamine and noradrenaline (Devoto & Flore, 2006; Kempadoo et al., 2016; Takeuchi et al., 2016). Therefore, considering that the origin of dopaminergic afferents to the NRe originates from a distinct source (the A13 cell group), compared to the HPC and mPFC, it is unclear whether dopamine will play a role in regulating the NRe in recognition memory processing, as the A13 cell group, unlike the VTA and LC, has not been associated with recognition memory and novelty processing (Kempadoo et al., 2016; Lemon et al., 2009; Moreno-Castilla et al., 2017; Savalli et al., 2015). Instead, the A13 cell group, based on its anatomic connections and the abovementioned functional study, has been more closely associated with the regulation of fear memory and avoidance behaviour (Bolton et al., 2015; Eaton et al., 1994; Liu et al., 2014; Messanvi et al., 2013; Sharma et al., 2018; Venkataraman et al., 2021). Thus, functional investigation of the A13 projection to the NRe during recognition memory processing could reveal some interesting insights and add to the relatively new literature concerning the behavioural functions of the A13 cell group.

3.4.5.2 Noradrenergic modulation of the nucleus reuniens

While functional evidence for the role of the A13 cell group is scarce, a substantial body of evidence indicates a pivotal role for the LC in many diverse functions, such as modulating memory, arousal, attention and more (Berridge, 2008; Berridge & Waterhouse, 2003; Sara, 2009; Schwarz & Luo, 2015). Interestingly, the LC has been shown to fire in a phasic manner upon exposure to a novel stimulus or context

(Sara et al., 1994; Vankov et al., 1995), and a number of studies have indicated a critical role for LC noradrenaline in recognition memory (Lemon et al., 2009; Mello-Carpes et al., 2016; Moreno-Castilla et al., 2017). In this regard, it is likely that noradrenergic LC inputs to the NRe may serve an important role in modulating the NRe in recognition memory processing.

The anatomical arrangement observed in the present study, i.e., denser noradrenergic inputs to the rostral compared to caudal NRe, likely reflects a functional topographical organisation within the NRe. Interestingly, previous anatomical tracing studies have also suggested a rostrocaudal functional segregation within the NRe, demonstrating that NRe projecting hippocampal cells are principally located in the rostral NRe (Dolleman-van der Weel et al., 2019; Hoover & Vertes, 2012; Varela et al., 2014). Thus, it seems that LC noradrenaline inputs to the NRe are well organised to preferentially modulate the activity of NRe projecting HPC neurons, and thus affect behaviours dependent on projections from the NRe to the HPC. However, further studies are required to support this proposal, such experiments would initially involve anatomical techniques, such as the use of transsynaptic tracing techniques (Saleeba et al., 2019) to empirically demonstrate that LC neurons project to hippocampal projecting NRe neurons, before functional perturbation of this pathway is conducted.

3.4.6 Conclusion

The current chapter has provided an anatomical foundation for the functional exploration of the catecholaminergic system in the NRe. The source of catecholaminergic input to the NRe was revealed to originate from two distinct sources, the A13 cell group and the LC. More experiments are required to determine the precise functional role of the catecholaminergic system in the NRe and more specifically, the contribution of these two distinct pathways to NRe-associated behaviours. As a first step in determining the role of catecholaminergic neuromodulation in the NRe in recognition memory, the next chapter focuses on the role of noradrenergic neurotransmission.

4 Investigating the role of noradrenergic neurotransmission in the nucleus reuniens, hippocampus and medial prefrontal cortex in recognition memory

4.1 Introduction

As previously described in the general introduction (see Section 1.1.2.5), recent experimental evidence has indicated that the NRe serves as a key brain region within a neural circuit for associative recognition memory, however, our functional understanding of the NRe is still limited. For instance, the underlying neurotransmitter systems involved in modulating NRe function during recognition memory are not well characterised.

In Chapter 3, the anatomy of the catecholaminergic innervation of the NRe was re-evaluated. It was revealed that contrary to the notion that the rodent thalamus is weakly innervated with catecholaminergic fibres, that the NRe receives a denser catecholaminergic innervation than previously described. It was also found that the NRe receives both dopaminergic and noradrenergic inputs, from the A13 cell group and LC, respectively, therefore indicating that release of either neurotransmitter may serve as an important modulator of NRe-dependent functions.

Another aim of the current chapter was to investigate the role of noradrenergic neurotransmission in other brain regions crucial for associative recognition memory through their interaction with the NRe, namely the HPC and mPFC. As stated in the general introduction (see Section 1.3.3.2 and 1.3.3.3), $\alpha 1$, $\alpha 2$ and β adrenergic receptor subtypes, are expressed in both the HPC and mPFC, and anatomical studies have demonstrated that the LC is the exclusive source of noradrenaline to both these

brain regions (Agster et al., 2013; Berridge & Waterhouse, 2003; Loy et al., 1980). While several studies have demonstrated that other neuromodulatory systems, such as the cholinergic and dopaminergic systems, in the HPC and mPFC are involved in recognition memory (Barker & Warburton, 2009; Sabec et al., 2018; Savalli et al., 2015), only a handful of studies have examined the role of noradrenaline. Although the studies that have evaluated the involvement of noradrenergic neuromodulation in the HPC and mPFC have indicated a role for HPC and mPFC noradrenaline in recognition memory processing (see Section 1.3.5.2 and 1.3.5.3 for summary) (Lemon et al., 2009; Mello-Carpes et al., 2016; Moreno-Castilla et al., 2017; Nelson et al., 2011), these studies either do not offer causal evidence for a role for noradrenaline or do not provide a comprehensive picture regarding the precise conditions which require noradrenergic neurotransmission in the HPC and mPFC during recognition memory. For instance, questions related to the role of each adrenergic receptor subtype has not been established and the role of these subtypes during the different phases of recognition memory processing has not been explored.

Given the limited functional evidence but strong anatomical evidence for the presence of the noradrenergic system in the NRe, HPC and mPFC, the current chapter investigated the role of noradrenergic neurotransmission, mediated via $\alpha 1$, $\alpha 2$ and β adrenoceptors in the NRe, HPC and mPFC, on the encoding and retrieval of recognition memory. To achieve this, drugs specific for the $\alpha 1$, $\alpha 2$ or β adrenergic receptors were infused directly into each brain region separately during distinct timepoints of the recognition memory task. To investigate the effect of a drug on the encoding or retrieval of memory, drugs were infused either prior to the sample phase or prior to the retrieval phase, respectively. To target the $\alpha 2$ adrenergic receptors, the agonist UK 14,304 or the antagonist RS 79948 was infused. $\alpha 2$ receptors are mainly found on the pre-synaptic membrane, therefore via inhibitory autoreceptor mechanisms, activation of $\alpha 2$ adrenoceptors inhibits noradrenaline release in brain regions such as the amygdala and frontal cortex (Dalley & Stanford, 1995; Ferry et al., 2015; Van Veldhuizen et al., 1993), however, the precise cellular location of $\alpha 2$ adrenoceptors in all brain regions under current investigation, such as the

NRe, has not been determined. While it is still predicted that the $\alpha 2$ agonist UK 14,304 should result in a decrease in noradrenaline release in the NRe, given that $\alpha 2$ adrenoceptors are predominantly located on the pre-synaptic membrane in the central nervous system (Langer, 1974; Starke, 2001; Talley et al., 1996), it is also possible that post-synaptic $\alpha 2$ adrenoceptors may be recruited following infusion of UK 14,304. As a result, any potential memory enhancing effects would be difficult to detect under the current testing protocol employed and would manifest as a null result. Therefore, the effects of the $\alpha 2$ adrenergic receptor antagonist RS 79948 were also tested. Thus if there is a possibility of any potential post-synaptic effects, infusion of RS 79948 is predicted to impair memory (Zhang et al., 2009). In addition, to explore the effect of inhibiting noradrenergic neurotransmission via the $\alpha 1$ and β adrenergic receptors, the current chapter infused the $\alpha 1$ and β adrenergic antagonists prazosin and propranolol, respectively.

4.2 Methods

4.2.1 Animals

36 male Lister hooded rats (Harlan Laboratories, UK) weighing $\sim$350g at the start of experimentation were used. See Section 2.1 for full details about animals. Animals were split into 3 cohorts, thus each cohort consisted of 12 rats. Cohort 1 had cannulae bilaterally implanted into the NRe and cohorts 2 and 3 had cannulae bilaterally implanted into both the HPC and mPFC (a total of 4 cannulae per animal). An overview of cohorts used in each experiment is provided in Table 4.1

Table 4.1. Overview of animals.

Cohort no.	Infusion location	Exp no.	Drug infused	Task	Infusion timing
1	NRe	1	UK 14,304	Object-in-place	Pre-sample
					Pre-test
1	NRe	2	RS 79948	Object-in-place	Pre-sample
					Pre-test
1	NRe	3	Prazosin	Object-in-place	Pre-sample
					Pre-test
1	NRe	3	Propranolol	Object-in-place	Pre-sample
					Pre-test
2	HPC and PFC	4	UK 14,304	Object-in-place	Pre-sample
					Pre-test
3	HPC and PFC	5	RS 79948	Object-in-place	Pre-sample
					Pre-test
3	HPC and PFC	6	Prazosin	Object-in-place	Pre-sample
					Pre-test
2	HPC and PFC	7	Propranolol	Object-in-place	Pre-sample
					Pre-test
3	HPC	8	UK 14,304	Object location	Pre-sample
					Pre-test
3	HPC	8	Propranolol	Object location	Pre-sample
					Pre-test
3	HPC	9	UK 14,304	Object recognition	Pre-sample
3	HPC	9	Propranolol	Object recognition	Pre-sample
3	HPC	10	Propranolol	Object-in-place	Pre-sample

4.2.2 Surgery

All animals underwent surgical procedures as described in Section 2.2. For cohort 1, 12 animals were implanted with bilateral cannula aimed at the NRe using the

following co-ordinates calculated relative to bregma: AP -1.8mm and -2.4mm; ML ±1.7mm, DV -6.4mm, all cannulae were implanted 15° from the ML plane. For cohorts 2 and 3, 24 animals were implanted with bilateral cannula aimed at both the HPC and mPFC with co-ordinates calculated relative to bregma. To target the HPC, the following co-ordinates were used: AP -4.3mm; ML ±2.5mm; and DV -2.8mm (dura). To target the mPFC, the following co-ordinates were used: AP +3.2mm; ML ±0.75mm; and DV -3.5mm. Animals were singly housed for seven days post-surgery and given two weeks to recover before behavioural testing commenced.

4.2.3 Drugs

Details of the drugs used are summarised in Table 2.3.

UK 14,304

The selective α2 agonist UK 14,304 was infused at a concentration of 10μM. This dose was chosen based on published IC_{50} values at α2 adrenergic receptors (indicating an IC_{50} of 3.6nM) (Van Meel et al., 1981), and previous microdialysis studies demonstrating that infusion of UK 14,304 at a dose of 10μM in the amygdala, and at doses ranging from 0.5-10μM in the frontal cortex, causes a robust decrease in noradrenaline (Dalley & Stanford, 1995; Ferry et al., 2015; Van Veldhuizen et al., 1993).

RS 79948

The α2 antagonist RS 79948 was infused at a concentration of 1μM. The published K_d values of RS 79948 at the α2 adrenoceptors subtypes are: 0.18nM at α2B, 0.19nM at α2C and 0.42nM at α2A. Thus, 1μM RS 79948 is well above its K_d values to target all three α2 adrenoceptor subtypes. In addition, microdialysis studies have indicated that a concentration of 1μM results in a robust increase in noradrenaline release (Fernández-Pastor & Meana, 2002; Horrillo et al., 2019).

Prazosin

The α1 antagonist prazosin was infused at a concentration of 1μM. Studies have

indicated that prazosin has a K_i value of 0.1-0.49nM at α1 adrenergic receptors (Greengrass & Bremmer, 1979; U'Prichard et al., 1978) and an IC_{50} value at α1 adrenoceptors of 0.6-1.68nM (Nagatomo et al., 1985; Van Meel et al., 1981). Furthermore, studies have reported behavioural deficits following intra-amygdala infusion of prazosin at a concentration of 0.2nM (Ferry et al., 1999a, 1999b). Thus, infusion of prazosin at a dose of 1μM should provide robust inhibition of α1 adrenoceptors.

Propranolol

The β antagonist propranolol was infused at a concentration of 10μM because the IC_{50} value at β adrenergic receptors is 2.1nM (Bylund and Snyder, 1976).

4.2.3.1 Infusion Procedure

For NRe infusions, animals were infused with 0.3μl of drug or saline per hemisphere at a rate of 0.3μl/min. For HPC infusions, animals were infused with 1μl of drug or saline per hemisphere at a rate of 0.5μl/min. For mPFC infusions, animals were infused with 0.5μl of drug or saline per hemisphere at a rate of 0.25μl/min. For full details of infusion procedure see Section 2.3.4.

4.2.4 Behavioural testing

Recognition memory was tested using the following spontaneous exploration tasks: object-in-place (3-hour delay), object location (3-hour delay) and novel object preference task, with four objects to parallel the number of stimuli in the object-in-place task (3-hour delay). To test whether a given drug is required for memory encoding, the drug was infused 15 minutes before the start of the sample phase. To test whether a given drug is required for memory retrieval, the drug was infused 15 minutes before the start of the test phase (Figures 4.2B, 4.5B, 4.6B, 4.7B and 4.8B). See Section 2.3 for full details of habituation procedure, objects used, apparatus and testing procedures.

4.2.5 Data acquisition, scoring and analysis

For full details see Section 2.3.7. The experiments were run with a cross-over design, thus for a given experiment, each animal received both drug and saline infusions. For the HPC-mPFC implanted animals, saline infusion into the HPC or mPFC was counterbalanced between infusion timing, e.g., for a given drug, if an animal received a pre-sample infusion of saline into the HPC, for the pre-test infusion, the same animal would receive saline infusion into the mPFC or vice versa. In all experiments, statistical analysis was performed to compare discrimination ratios, sample phase exploration times and test phase exploration times between conditions. In experiments 1, 2, 3 and 8, mixed model ANOVAs were conducted with drug (vehicle versus drug) as the within-subjects factor and infusion timing (encoding versus retrieval) as the between-subjects factor. In experiments 4, 5, 6, and 7, mixed model ANOVAs were conducted with infusion region (control versus HPC versus mPFC) as the within-subjects factor and infusion timing (encoding versus retrieval) as the between-subjects factor. When appropriate, Bonferroni-corrected post-hoc comparisons were performed. In experiments comparing discrimination ratios and exploration times (sample and test) between two groups (experiments 9 and 10), paired samples t-tests were conducted. See Table 4.1 for an overview of experiments). In all experiments to determine whether the discrimination ratio for each condition was significantly different from chance (a discrimination ratio of zero), one-sample t-tests were conducted. Loss of an animal is indicted by fewer degrees of freedom. Alpha was set at 0.05. All statistical analysis was conducted with IBM SPSS Statistics 25 software (IBM, USA).

4.2.6 Histology

For full details of histological procedures see Section 2.4. Following completion of behavioural testing animals were sacrificed and underwent histological procedures in preparation for cresyl violet staining to confirm cannula placement.

4.2.7 Figures

Figures were edited using Adobe Illustrator (version 25.4.1, San Jose, CA, USA) and graphs were created using the R package ggplot2 (Hadley, 2016). Brain atlas figures are adapted from Paxinos & Watson (2006).

4.3 Results

4.3.1 Noradrenergic neurotransmission in the nucleus reuniens

As stated in the general introduction (see Section 1.1.2.4), evidence suggests that the NRe is critically involved in object-in-place recognition memory when tested at a long but not short delay (Barker & Warburton, 2018), therefore in all experiments, the NRe cannulated animals were tested following a 3-hour delay.

4.3.1.1 Nucleus reuniens histology

Histological analysis revealed that all cannulae were located in the NRe. Schematic representation of the location of the cannula tips is shown in Figure 4.1.

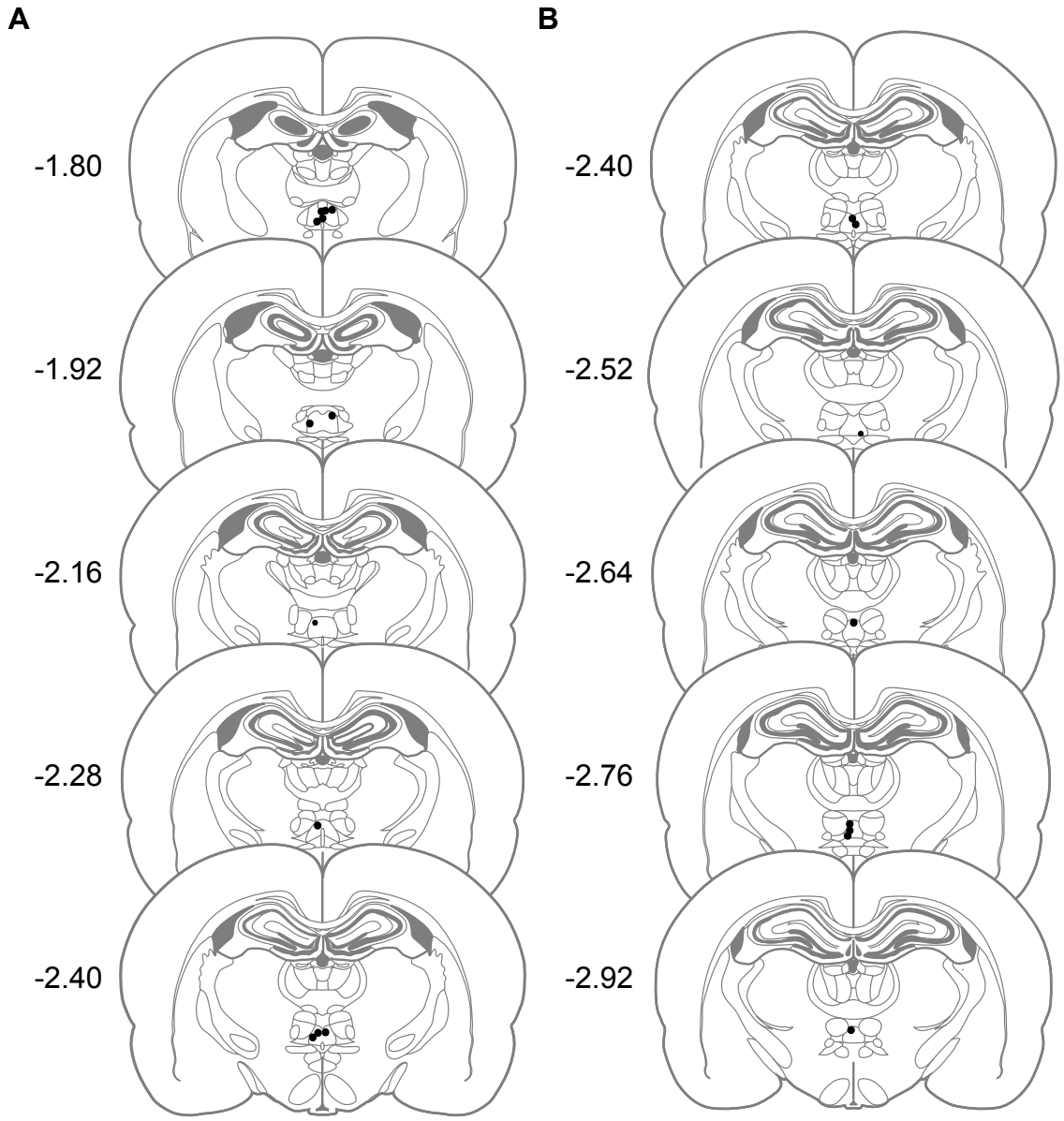

Figure 4.1. Schematic representation of placements of individual cannula for each animal targeting the NRe. (A) Rostral NRe. (B) Caudal NRe. Numbers indicate distance from bregma, and black dots indicate location of the tips of the cannula. Figures adapted from Paxinos & Watson (2006).

4.3.1.2 The role of nucleus reuniens α2 adrenergic receptors in object-in-place memory

4.3.1.2.1 Experiment 1: Activation of nucleus reuniens α2 adrenergic receptors selectively impairs retrieval of object-in-place memory

Mean discrimination ratios in the object-in-place task following infusions of either vehicle or the α2 agonist UK 14,304 is shown in Figure 4.2C. Pre-test but not pre-sample infusions of UK 14,304 into the NRe significantly impaired discrimination (drug x infusion timing interaction: ($F(1,18) = 6.29$, $p = .022$); post-hoc comparisons: pre-test infusion (vehicle versus UK 14,304: ($t(9) = 3.62$, $p = .006$)), pre-sample infusion (vehicle versus UK 14,304: ($t(9) = -.462$, $p = .655$)). No significant main effects of drug ($F(1,18) = 3.11$, $p = .095$) or infusion timing ($F(1,18) = 3.58$, $p = .075$). Comparison of discrimination performance against chance confirmed this pattern of results. Animals that received saline infusions demonstrated significant discrimination (pre-sample: ($t(9) = 5.05$, $p = .001$); pre-test: ($t(9) = 4.32$, $p = .002$)), while UK 14,304-infused animals only demonstrated significant discrimination when infusions were given before the sample phase but not test phase (pre-sample: ($t(9) = 3.64$, $p = .005$), pre-test: ($t(9) = .092$, $p = .928$).

Infusion of UK 14,304 did not affect the overall exploration levels during the sample phase (drug x infusion timing interaction: ($F(1,18) = .516$, $p = .482$); main effect of drug: ($F(1,18) = .062$, $p = .806$); main effect of infusion timing: ($F(1,18) = 4.02$, $p = .060$)). However, while analysis of total test phase exploration revealed a non-significant main effect of drug ($F(1,18) = .203$, $p = .658$) and drug x infusion timing interaction ($F(1,18) = .026$, $p = .874$), a significant main effect of infusion timing ($F(1,18) = 4.75$, $p = .043$) was found. Further analysis indicated that the significant main effect of infusion timing was due to the greater amount of exploration observed in both vehicle- and UK 14,304- infused animals when pre-test infusions were given (Table 4.2).

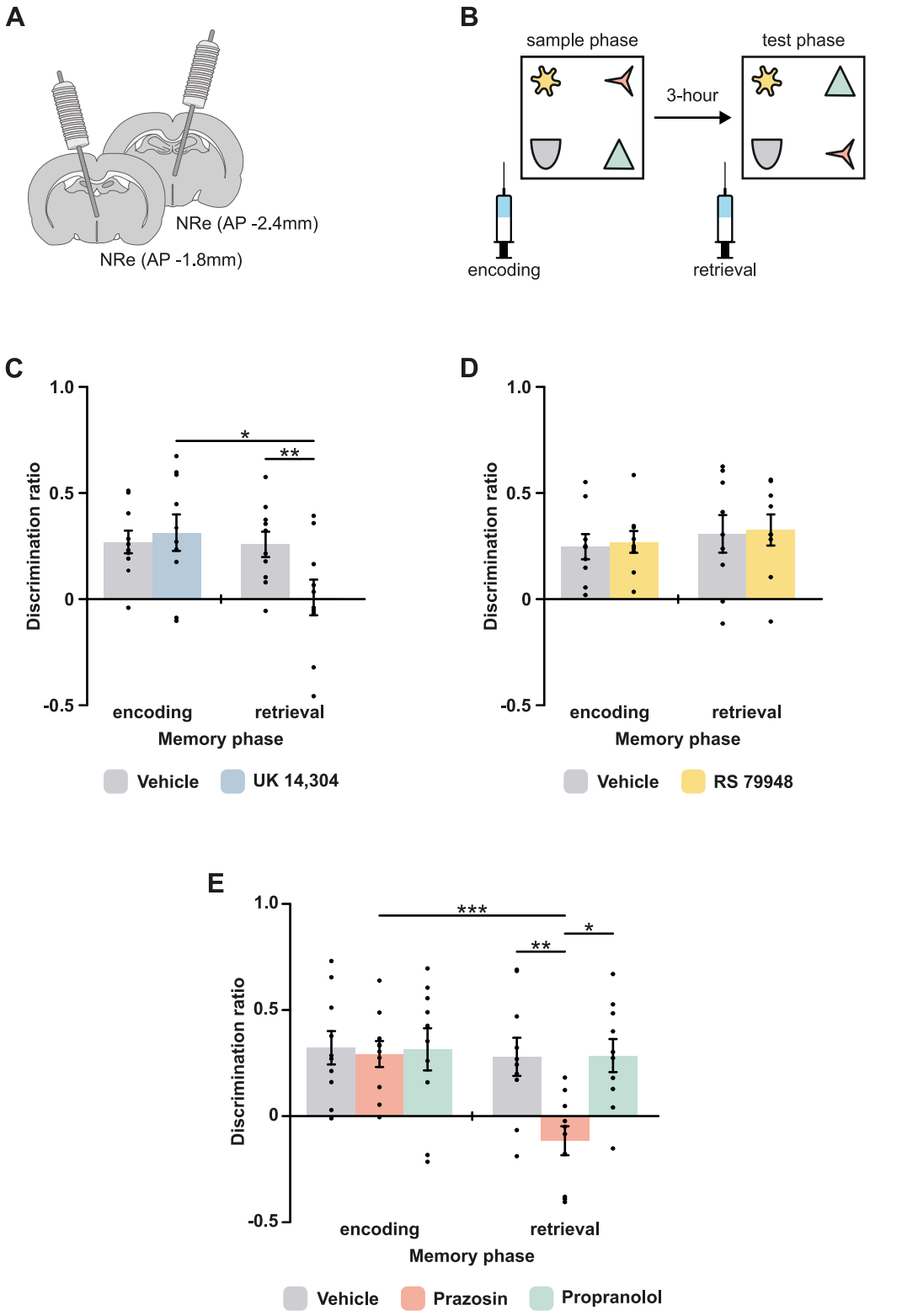

Figure 4.2. Noradrenergic neurotransmission in the NRe is critical for the retrieval but not encoding of object-in-place memory. (A) Schematic of experiment. Infusions were made into the NRe. (B) Schematic of the object-in-place task. Drugs were infused either before the sample phase or before the test phase. (C) Pre-test infusion of UK 14,304 impaired memory. (D) Infusion of RS 79948 before the sample or test phase did not affect memory.

Figure 4.2 ***(continued).*** (E) Prazosin infusion given before the test phase but not sample phase impaired long-term object-in-place memory. Propranolol infusions were without effect when given at both infusion timepoints. Data are represented as mean ± SEM. * p < .05, **p < .01, ***p < .001.

Table 4.2. Mean exploration times ± SEM in the sample and test phases of NRe-infused animals.

Experiment	Infusion timing	Condition	Exploration in sample phase (s) (300s max)	Exploration in test phase (s) (180s max)
1 (UK 14,304)	Pre-sample	Vehicle	76.9 ± 6.05	38.2 ± 3.23
		UK 14,304	79.3 ± 7.37	37.1 ± 3.29
	Pre-test	Vehicle	93.8 ± 4.68	51.6 ± 5.71
		UK 14,304	88.8 ± 5.05	46.4 ± 6.42
2 (RS 79948)	Pre-sample	Vehicle	85.5 ± 5.19	50.5 ± 4.79
		RS79488	76.5 ± 10.4	48.3 ± 7.33
	Pre-test	Vehicle	59.2 ± 4.44	44.6 ± 2.77
		RS79488	54.7 ± 4.57	42.0 ± 3.27
3 (Prazosin and propranolol)	Pre-sample	Vehicle	74.2 ± 10.7	47.5 ± 5.29
		Prazosin	83.2 ± 6.40	47.5 ± 7.90
		Propranolol	84.7 ± 6.30	49.5 ± 6.48
	Pre-test	Vehicle	89.7 ± 4.37	41.7 ± 2.54
		Prazosin	92.9 ± 7.74	48.2 ± 6.12
		Propranolol	99.6 ± 3.46	45.4 ± 3.91

4.3.1.2.2 Experiment 2: Blockade of nucleus reuniens α2 adrenergic receptors has no effect on object-in-place memory

Infusion of the α2 antagonist RS 79948 into the NRe, before the sample or test phase had no effect on memory performance (Figure 4.2D). Statistical analysis confirmed

this observation with non-significant drug x infusion timing interaction ($F(1, 16) = .001$, $p = .978$); and non-significant main effects of drug ($F(1,16) = .073$, $p = .790$) and infusion timing ($F(1,16) = .857$, $p = .368$)). Accordingly, one-sample analyses revealed that following either pre-sample or pre-test infusions, both the vehicle and drug treated animals performed significantly above chance levels, vehicle (pre-sample: ($t(8) = 4.17$, $p = .003$); pre-test: ($t(8) = 3.47$, $p = .008$)) and RS 79948 (pre-sample: ($t(8) = 5.25$, $p = .001$); pre-test: ($t(8) = 4.44$, $p = .002$)).

Analysis of total exploration time in the sample phase revealed no significant main effect of drug ($F(1,16)= 1.89$, $p = .188$) and drug x infusion interaction ($F(1,16) = .293$, $p = .596$). A significant main effect of infusion timing was however observed ($F(1,16) = 10.3$, $p = .006$). Further analysis indicated that the main effect of infusion timing was due to both vehicle and drug treated animals demonstrating more exploration following pre-sample infusions. Finally, analysis of total test phase exploration found no significant differences between conditions (drug x infusion timing interaction: ($F(1,16) = .521$, $p = .481$); main effect of drug: ($F(1,16)= .001$, $p = .982$); main effect of infusion timing: ($F(1,16) = 3.33$, $p = .087$) (Table 4.2).

Overall, the results from Experiment 1 and 2 suggest that $\alpha 2$ adrenoceptors modulate noradrenaline release in the NRe via a pre-synaptic mechanism that is critical for the retrieval but not encoding of object-in-place memory.

4.3.1.3 Experiment 3: Blockade of nucleus reuniens $\alpha 1$ but not β adrenergic receptors impairs retrieval of object-in-place memory

In Experiment 3 the effect of $\alpha 1$ adrenergic and β adrenergic receptor antagonism on acquisition and retrieval of object-in-place performance was compared (Figure 4.2E). A mixed model ANOVA revealed a significant drug x infusion timing interaction ($F(2,36) = 4.09$, $p = .025$); and significant main effects of drug ($F(2,36) = 5.30$, $p = .010$) and infusion timing ($F(1,18) = 4.82$, $p = .041$). Post-hoc comparisons of performance following the pre-test infusions revealed a significant difference between vehicle and prazosin: ($p = .006$) and prazosin and propranolol: ($p = .011$), but not between vehicle and propranolol: ($p = 1.00$). One-sample t-tests revealed that

both the vehicle and propranolol-infused animals explored the novel object-in-place configuration above chance levels at both infusion timepoints, vehicle (pre-sample: ($t(9) = -4.10$, $p = .003$); pre-test: ($t(9) = 3.10$, $p = .013$)); and propranolol (pre-sample: ($t(9) = 3.17$, $p = .011$); pre-test: ($t(9) = 3.66$, $p = .005$)). In contrast, prazosin-infused animals demonstrated significant discrimination between the novel and familiar object-in-place configuration when the infusions were given before the sample phase but not the test phase (pre-sample: ($t(9) = 4.48$, $p = .001$); pre-test: ($t(9) = -1.70$, $p = .123$)).

Analysis of total exploration time in the sample phase revealed no drug x infusion timing interaction ($F(2,36) = .085$, $p = .918$) and no main effect of drug ($F(2,36) = 1.24$, $p = .301$). There was a significant main effect of infusion timing ($F(1,18) = 6.00$, $p = .025$), with greater levels of exploration observed following pre-test infusions in all drugs. Total exploration time during the test phase did not significantly differ between conditions (drug x infusion timing interaction: ($F(2,36) = .268$, $p = .766$); main effect of drug: ($F(2,36) = .295$, $p = .747$); main effect of infusion timing ($F(1,18) = .267$, $p = .612$) (Table 4.2).

These results indicate a critical role for $\alpha 1$ adrenergic receptors in the NRe for the retrieval but not encoding of object-in-place memory, while β adrenergic receptors in the NRe were found not to be involved in modulating associative recognition memory.

4.3.2 Noradrenergic neurotransmission in the hippocampus and medial prefrontal cortex

4.3.2.1 Hippocampus and medial prefrontal cortex histology

Histological analysis revealed that all cannulae were located in the HPC and mPFC. Schematic representation of the location of the cannula tips is shown in Figure 4.3 for cohort 2 and Figure 4.4 for cohort 3.

4.3.2.2 Comparison of hippocampus and medial prefrontal cortex saline-infused animals

In experiments 4, 5, 6 and 7, as stated in Section 4.2.5, saline infusions were made either into the HPC or mPFC, and that for a given drug, if an animal received a pre-sample infusion of saline into the HPC, then the same animal received a pre-test infusion of saline into the mPFC or vice versa. As saline infusions were made into two different brain regions, to test whether there were any significant differences in performance between HPC and mPFC saline infused animals at each infusion timepoint, a 2-way ANOVA was performed for each experiment with infusion region (HPC vs mPFC) and infusion timing (encoding vs retrieval) as between-subject factors. Analysis revealed that for each experiment there were no significant main effects of infusion region, main effects of infusion timing or infusion region x infusion timing interaction: (Experiment 4 (UK 14,304): main effect of infusion region ($F(1,20) = .067$, $p = .798$); main effect of infusion timing ($F(1,20) = .093$, $p = .764$); infusion region x infusion timing interaction ($F(1,20) = 1.42$, $p = .248$)); (Experiment 5 (RS 79948): main effect of infusion region ($F(1,20) = .126$, $p = .726$); main effect of infusion timing ($F(1,20) = .594$, $p = .450$); infusion region x infusion timing interaction ($F(1,20) = .002$, $p = .963$)); (Experiment 6 (Prazosin): main effect of infusion region ($F(1,20) = .456$, $p = .507$); main effect of infusion timing ($F(1,20) = .183$, $p = .674$); infusion region x infusion timing interaction ($F(1,20) = .483$, $p = .495$)); (Experiment 7 (Propranolol): main effect of infusion region ($F(1,18) = .004$, $p = .953$); main effect of infusion timing ($F(1,18) = 1.78$, $p = .199$); infusion region x infusion timing interaction ($F(1,18) = .017$, $p = .897$)). Therefore, for all subsequent analysis, for each experiment, discrimination ratios for HPC and mPFC saline-infused animals were combined and herein referred to as "control".

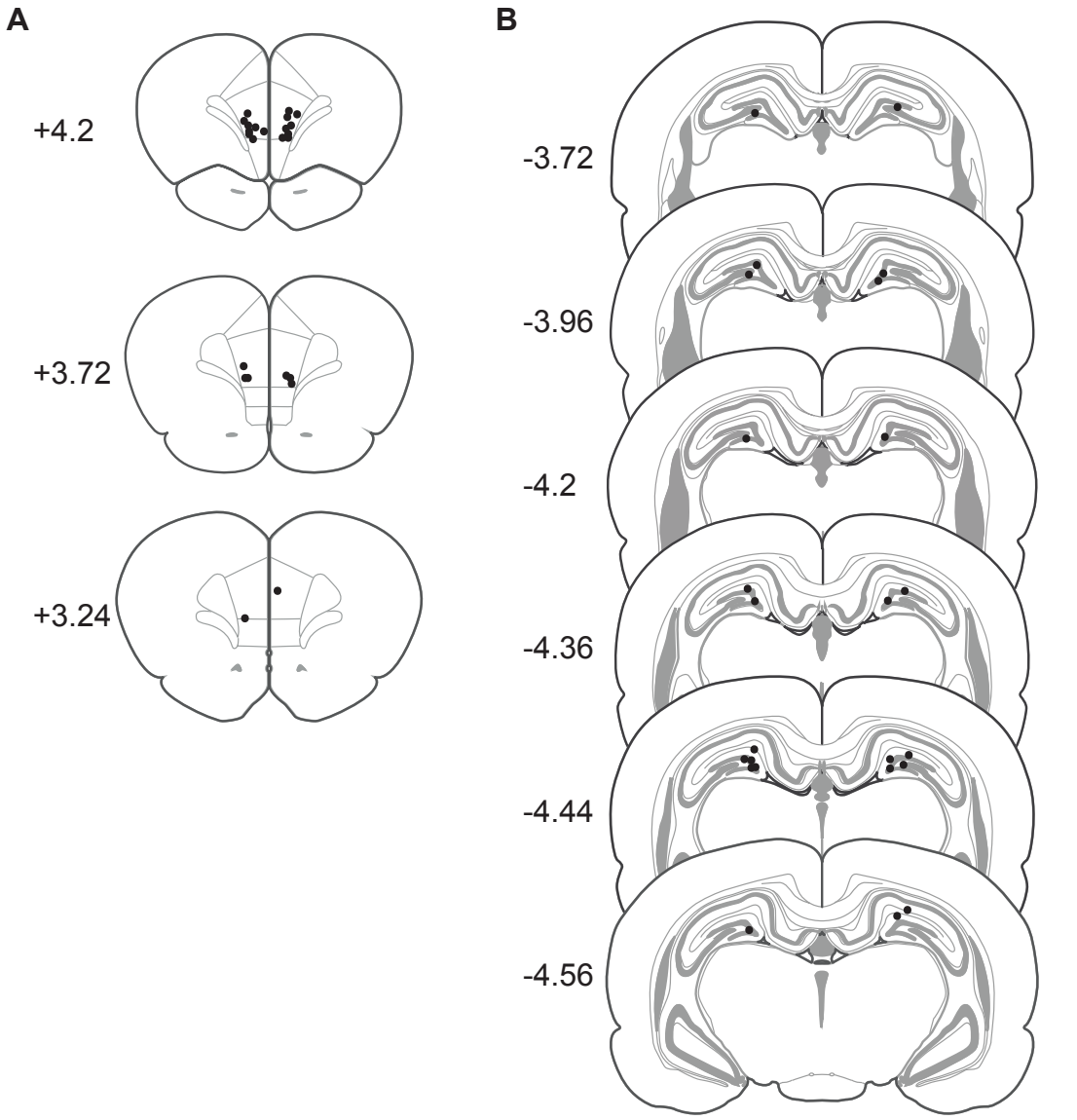

Figure 4.3. Schematic representation of placements of individual cannula for each animal targeting the HPC and mPFC in cohort 2. (A) mPFC. (B) HPC. Numbers indicate distance from bregma, and black dots indicate location of the tips of the cannula. Figures adapted from Paxinos & Watson (2006).

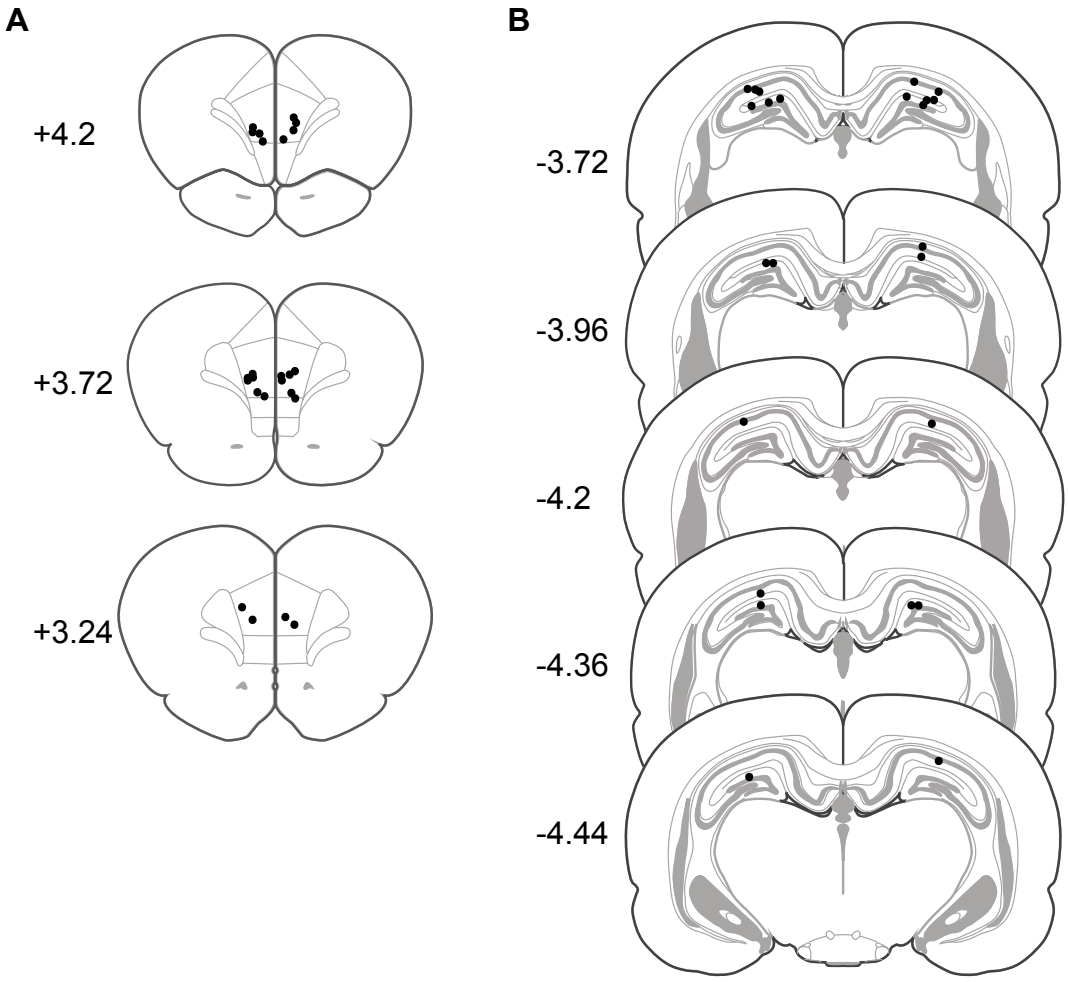

Figure 4.4. Schematic representation of placements of individual cannula for each animal targeting the HPC and mPFC in cohort 3. (A) mPFC. (B) HPC. Numbers indicate distance from bregma, and black dots indicate location of the tips of the cannula. Figures adapted from Paxinos & Watson (2006).

4.3.2.3 The role of α2 adrenergic receptors in the hippocampus and medial prefrontal cortex in object-in-place memory

4.3.2.3.1 Experiment 4: Activation of α2 adrenergic receptors in the hippocampus but not the medial prefrontal cortex impairs the encoding of object-in-place memory

The effects of infusion of UK 14,304 into the mPFC or HPC, either before the sample or the test phase on discrimination performance can be seen in Figure 4.5C. ANOVA revealed a non-significant infusion region x infusion timing interaction ($F(2,44) =$

2.67, p = .080); and non-significant main effects of infusion region (F(2,44) = 1.68, p = .198) or infusion timing (F(1,22) = 3.00, p = .098). Further analyses revealed that the discrimination ratios of the control and mPFC infused animals was significantly above chance when the infusions were made either before the sample or before the test phase, control (pre-sample: (t(11) = 4.19, p = .002); pre-test: (t(11) = 3.98, p = .002)); and mPFC (pre-sample: (t(11) = 5.69, p < .001); pre-test (t(11) = 3.20, p = .008)). Infusion of UK 14,304 into the HPC produced a somewhat different pattern of results. Pre-sample phase infusions impaired discrimination, while pre-test phase were without effect (pre-sample: (t(11) = 1.45 p = .176); pre-test (t(11) = 5.41, p < .001). These results suggest that $\alpha 2$ adrenoceptor mediated neurotransmission in the HPC is critical for the acquisition of object-in-place memory but not the retrieval (Figure 4.5C).

Analysis of total amount of object exploration during the sample phase revealed no significant differences between conditions (infusion region x infusion timing interaction: (F(2,44) = .341, p = .713); main effect of infusion region: (F(2,44)= .423, p = .658); main effect of infusion timing: (F(1,22) = 2.68, p = .116). Analysis of exploration during the test phase revealed no significant main effect of infusion region (F(1.45, 31.9) = .571, p = .517) or infusion region x infusion timing interaction (F(1.45, 31.9) = 1.82, p = .175). However, analyses did find a significant main effect of infusion timing (F(1,22) = .491, p = .037). Further analysis revealed that the main effect of infusion timing was due to greater amount of exploration observed in all infusion regions when pre-sample infusions were given (Table 4.4).

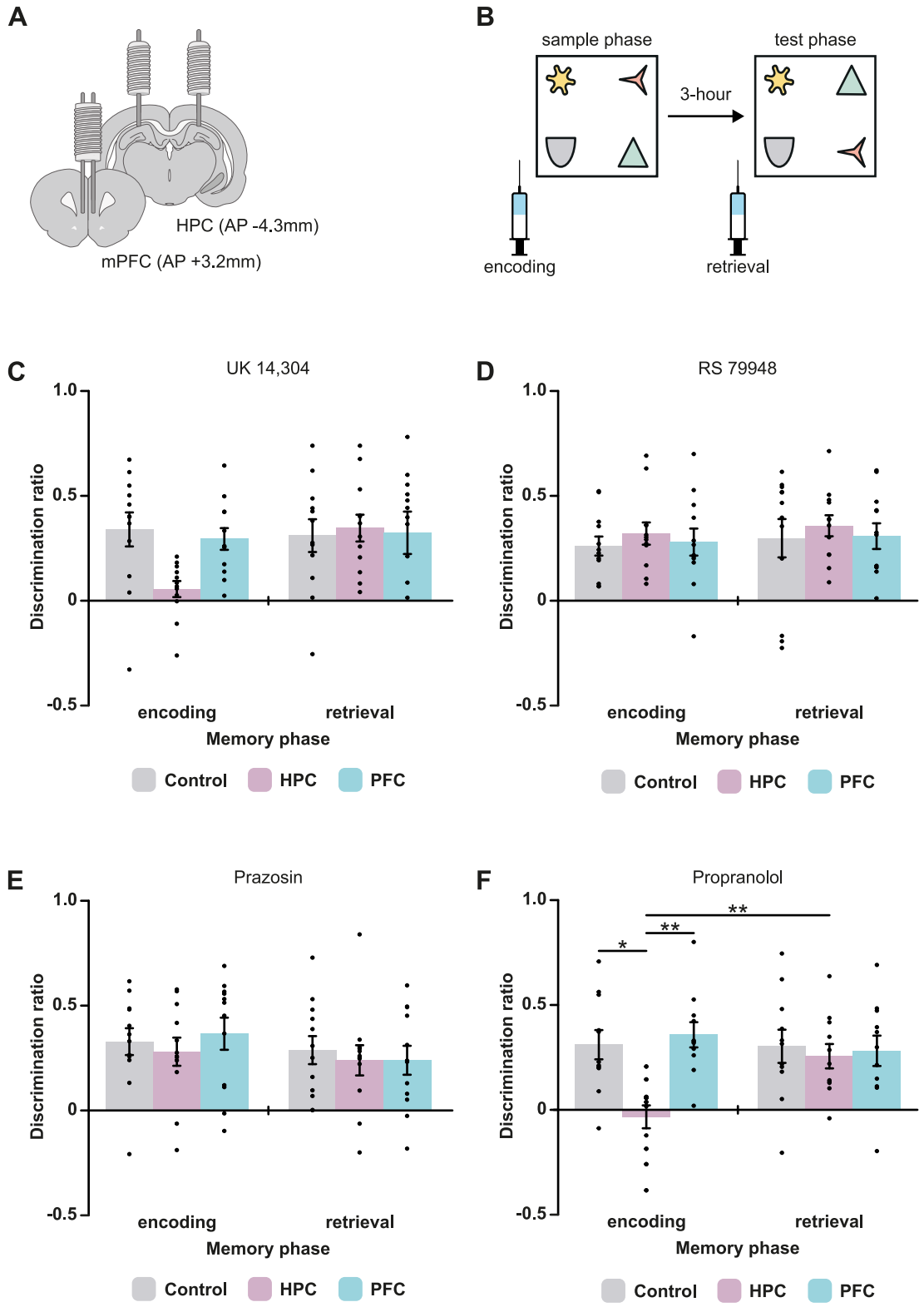

Figure 4.5. Noradrenergic neurotransmission in the HPC is critical for the encoding but not retrieval of object-in-place memory. Infusions into the mPFC had no effect. (A) Schematic of experiment. Infusions were made into the HPC or mPFC. (B) Schematic of the object-in-place task. Drugs were infused either before the sample phase or before the test phase. (C) Pre-sample but not pre-test infusion of UK 14,304 into the HPC impaired

Figure 4.5 ***(continued).*** memory. (D) Infusion of RS 79948 into either the HPC or mPFC did not affect memory. (E) Prazosin infusion into either the HPC or mPFC had no effect on memory. (F) Pre-sample but not pre-test infusion of propranolol into the HPC impaired memory. Data are represented as mean ± SEM. * $p < .05$, **$p < .01$.

Table 4.3. Mean exploration times ± SEM in the sample and test phases of HPC and mPFC-infused animals in the object-in-place task.

Experiment no.	Infusion timing	Infusion region	Exploration in sample phase (s) (300s max)	Exploration in test phase (s) (180s max)
4 (UK 14,304)	Pre-sample	Control	71.9 ± 5.65	46.9 ± 4.07
		HPC	69.4 ± 4.97	46.9 ± 3.69
		mPFC	65.6 ± 5.87	40.8 ± 3.89
	Pre-test	Control	59.3 ± 4.07	31.3 ± 3.72
		HPC	60.0 ± 5.61	36.7 ± 3.77
		MPFC	59.1 ± 3.93	36.9 ± 4.85
5 (RS 79948)	Pre-sample	Control	69.4 ± 5.17	36.1 ± 3.77
		HPC	71.1 ± 4.19	38.5 ± 4.83
		mPFC	67.3 ± 5.08	39.6 ± 3.61
	Pre-test	Control	60.4 ± 3.72	40.9 ± 3.00
		HPC	57.2 ± 4.97	42.5 ± 2.69
		mPFC	62.6 ± 5.51	39.4 ± 4.13
6 (Prazosin)	Pre-sample	Control	87.0 ± 5.33	53.1 ± 4.12
		HPC	90.9 ± 6.88	51.2 ± 4.13
		mPFC	76.7 ± 6.23	47.0 ± 3.82
	Pre-test	Control	92.5 ± 6.57	52.6 ± 3.01
		HPC	93.8 ± 4.86	57.7 ± 3.66
		mPFC	94.0 ± 3.65	56.5 ± 4.85
7 (Propranolol)	Pre-sample	Control	52.4 ± 4.05	34.9 ± 3.90
		HPC	54.5 ± 4.15	28.7 ± 2.98
		mPFC	50.2 ± 4.69	27.0 ± 2.62
	Pre-test	Control	55.9 ± 5.97	38.5 ± 5.36
		HPC	71.6 ± 8.48	40.6 ± 5.16
		mPFC	61.6 ± 10.0	35.0 ± 5.47
10 (Propranolol)	Pre-sample	Vehicle	66.6 ± 5.47	40.0 ± 4.32
		Propranolol	66.5 ± 3.43	38.4 ± 3.19

4.3.2.3.2 Experiment 5: Blockade of hippocampus and medial prefrontal cortex $\alpha 2$ adrenergic receptors has no effect on object-in-place memory

Both pre-sample and pre-test infusion of the $\alpha 2$ antagonist RS 79948 into the HPC or mPFC had no effect on object-in-place memory (Figure 4.5D). Statistical analysis revealed a non-significant infusion region x infusion timing interaction ($F(2,44) = .003$, $p = .997$); and non-significant main effects of infusion region ($F(2,44) = .465$, $p = .631$) or infusion timing ($F(1,22) = .499$, $p = .487$). Further analysis comparing performance against zero indicated that following pre-sample infusion all groups had mean discrimination ratios significantly above zero, (control: ($t(11) = 5.74$, $p < .001$); HPC: ($t(11) = 6.04$, $p < .001$); mPFC: ($t(11) = 4.34$, $p = .001$)). Similarly, following pre-test infusion all animals performed significantly above chance levels, (control: ($t(11) = 3.26$, $p = .008$); HPC: ($t(11) = 7.13$, $p < .001$); mPFC: ($t(11) = 5.03$, $p < .001$).

Analysis of total exploration time during the sample phase revealed a non-significant main effect of infusion region ($F(2,44)= .026$, $p = .974$), and non-significant infusion region x infusion timing interaction ($F(2,44) = .516$, $p = .600$). However, a significant main effect of infusion timing was found ($F(1,22) = 4.83$, $p = .039$). Further analysis revealed that when infusions were given before the sample phase animals demonstrated more exploration compared to when infusions were given before the test phase. Crucially, increased exploration during pre-sample infusion was observed in all infusion regions. Analysis of total exploration time in the test phase revealed no significant differences between conditions (infusion region x infusion timing interaction: ($F(2, 44) = .003$, $p = .997$; main effect of infusion region: ($F(2,44) = .465$, $p = .631$); main effect of infusion timing ($F(1,22) = .499$, $p = .487$)) (Table 4.3).

Altogether while the results suggest that pre-sample infusion of UK 14,304 into the HPC impaired the ability to differentiate between the novel and familiar object configuration, the mixed model ANOVA revealed no significant differences, thus this finding is inconclusive. Moreover, these results show that activation of mPFC

α2 adrenergic receptors are not required for either memory stage of object-in-place memory and that antagonism of α2 adrenoceptors in both the HPC and mPFC had no effect on memory.

4.3.2.4 Experiment 6: α1 adrenergic receptors in the hippocampus and medial prefrontal cortex are not required for encoding or retrieval of object-in-place memory

There was no effect of prazosin infusions into the HPC or mPFC following either pre-sample infusion or pre-test infusion (Figure 4.5E). Statistical analysis confirmed this observation (infusion region x infusion timing interaction: ($F(2,44) = .222$, $p = .802$); main effect of infusion region: ($F(2,44) = .254$, $p = .777$); main effect of infusion timing: ($F(1,22) = 2.14$, $p = .158$)). Additional analysis revealed that discrimination in all groups was significantly above chance levels following either pre-sample infusion (control: ($t(11) = 5.13$, $p < .001$); HPC: ($t(11) = 4.18$, $p = .002$); mPFC ($t(11) = 4.78$, $p = .001$)) or pre-test infusion (control: ($t(11) = 4.31$, $p = .001$); HPC: ($t(11) = 3.32$, $p = .007$); mPFC ($t(11) = 3.47$, $p = .005$)).

Analysis of total object exploration during the sample phase indicated no significant differences between conditions (infusion region x infusion timing interaction: ($F(2,44) = 1.31$, $p = .281$); main effect of infusion region: ($F(2,44)= 1.09$, $p = .345$); main effect of infusion timing: ($F(1,22) = 2.10$, $p = .161$)). Similarly, no significant differences between conditions were found following analysis of total test phase exploration (infusion region x infusion timing interaction: ($F(2, 44) = 1.38$, $p = .262$); main effect of infusion region: ($F(2,44) = .481$, $p = .621$); main effect of infusion timing ($F(1,22) = 1.66$, $p = .211$)) (Table 4.3).

The results indicate that α1 adrenergic receptors in the HPC and mPFC are not involved in object-in-place memory during either the encoding or retrieval phase.

4.3.2.5 Experiment 7: β adrenergic receptors in the hippocampus but not the medial prefrontal cortex are required for the encoding of object-in-place memory

Pre-sample infusion of the β adrenergic antagonist propranolol into the HPC disrupted object-in-place memory. Infusion into the mPFC had no effect on memory (Figure 4.5F). Statistical analysis confirmed that pre-sample but not pre-test intra-HPC infusions impaired memory while intra-mPFC infusions had no effect (infusion region x infusion timing interaction: ($F(2, 40) = 3.73$, $p = .033$); Bonferroni corrected post-hoc comparisons at the pre-sample infusion timepoint: (control versus HPC: ($p = .017$)), (control versus mPFC: ($p = 1.00$), (HPC versus mPFC: ($p = .006$)). A significant main effect of infusion region ($F(2,40) = 5.53$, $p = .008$) but not infusion timing ($F(1,20) = 2.03$, $p = .170$) was observed. Further analysis comparing performance against chance indicated that control animals or animals receiving infusions into the mPFC were able discriminate significantly above chance, while HPC infused animals did not (control: ($t(10) = 4.45$, $p = .001$); mPFC: ($t(10) = 5.10$, $p < .001$); HPC ($t(10) = -.615$, $p = .553$)). Animals receiving pre-test infusions into either the HPC or mPFC showed discrimination which was significantly above chance (control: ($t(10) = 3.82$, $p = .003$); HPC: ($t(10) = 4.40$, $p = .001$); mPFC: ($t(10) = 3.88$, $p = .003$)).

Analysis of the overall amount of exploration revealed no significant differences between conditions during the sample phase (infusion region x infusion interaction: ($F(2,40) = .868$, $p = .482$); main effect of infusion region: ($F(2,40)= 1.63$, $p = .208$); main effect of infusion timing: ($F(1,20) = 2.38$, $p = .138$)). However, during the test phase, while there was no significant main effect of infusion region ($F(2,40)= 1.81$, $p = .176$) and infusion region x infusion interaction ($F(2,40) = .915$, $p = .409$), there was a significant main effect of infusion timing ($F(1,20) = 7.43$, $p = .013$). Further analysis indicated that the significant main effect of infusion timing was due to greater levels of total object exploration observed in all conditions when infusions were given before the test phase (Table 4.3).

The results indicate that β adrenoceptors in the HPC are required for the

acquisition but not retrieval of object-in-place memory. Furthermore, it was also revealed that β adrenoceptors in the mPFC are not required for successful object-in-place memory.

4.3.2.6 Experiment 8: The role of $\alpha 2$ and β adrenergic receptors in the hippocampus in object location memory

Previous studies employing a number of experimental manipulations, e.g. lesions, pharmacology and optogenetics, have indicated that the HPC is involved in object location memory (Barker & Warburton, 2011; López et al., 2016; Mumby et al., 2002; Tuscher et al., 2018). Therefore, the next set of experiments sought to explore whether noradrenergic neurotransmission in the HPC is involved in object location memory. The $\alpha 2$ agonist UK 14,304 and the β antagonist propranolol were infused as previous experiments demonstrated that intra-HPC infusion of these two drugs result in encoding deficits in the object-in-place task (Figure 4.5).

4.3.2.6.1 Activation of $\alpha 2$ adrenergic receptors in the hippocampus is not required for object location memory

Pre-sample and pre-test infusion of UK 14,304 into the HPC did not disrupt object location memory (Figure 4.6C). These observations were confirmed with a mixed model ANOVA which revealed a non-significant drug x infusion timing interaction ($F(1,22) = .248$, $p = .624$); and non-significant main effects of drug ($F(1,22) = .040$, $p = .843$) or infusion timing ($F(1,22) = .636$, $p = .434$). Both conditions exhibited discrimination ratios significantly above chance at both pre-sample (vehicle: ($t(11) = 3.25$, $p = .008$); UK 14,304: ($t(11) = 5.71$, $p < .001$)); and pre-test infusion timepoints (vehicle: ($t(11) = 4.43$, $p = .001$); UK 14,304, ($t(11) = 3.32$, $p = .007$)).

Analysis of overall object exploration during the sample phase revealed no significant differences between conditions when infusions were given at the pre-sample timepoint, as shown by a non-significant interaction between drug x infusion timing interaction ($F(1,22) = .333$, $p = .570$); and non-significant main effects of drug ($F(1,22)= .167$, $p = .687$) or infusion timing ($F(1,22) = .167$, $p = .687$). While

analysis of total object exploration during the test phase revealed no significant drug main effect ($F(1,22) = .891$, $p = .356$) and drug x infusion timing interaction ($F(1, 22) = .077$, $p = .784$), there was a significant main effect of infusion timing ($F(1,22) = 16.63$, $p < .001$). Further analysis revealed that the significant main effect of infusion timing was due to greater levels of total object exploration observed in both groups when infusions were delivered before the test phase (Table 4.4).

The results indicate that noradrenergic neurotransmission in the HPC, mediated via the $\alpha 2$ adrenergic receptors, are not required for successful object location memory.

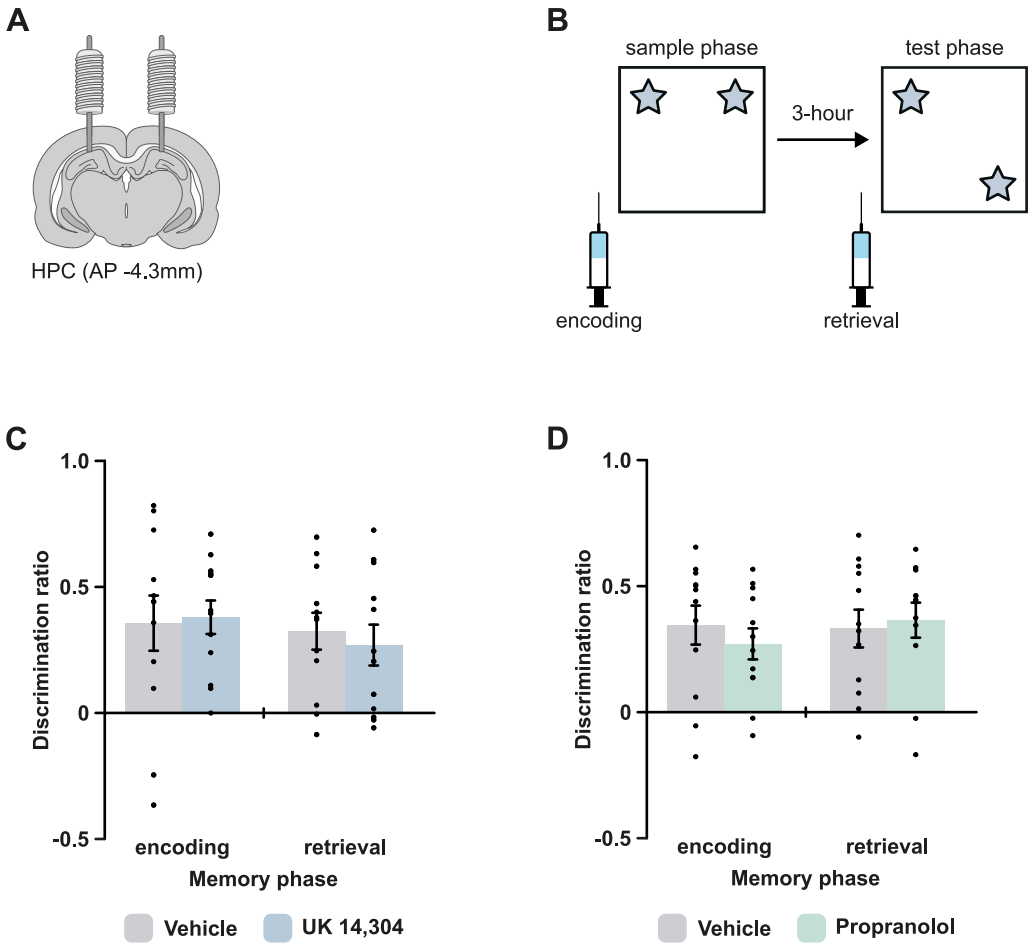

Figure 4.6. Infusion of $\alpha 2$ agonist and β antagonist in the HPC have no effect on object location memory. (A) Schematic of experiment. Infusions were made into the HPC. (B) Schematic of the object location task. Drugs were infused either before the sample phase or before the test phase. (C) Both pre-sample and pre-test infusions of UK 14,304 into the HPC were without effect in the object location task. (D) Both pre-sample and pre-test infusions of propranolol into the HPC did not affect object location memory. Data are represented as mean ± SEM.

Table 4.4. Mean exploration times ± SEM in the sample and test phases of HPC-infused animals in the object location and object recognition tasks.

Task	Infusion timing	Condition	Exploration in sample phase (s) (300s max)	Exploration in test phase (s) (180s max)
Object location	Pre-sample	Vehicle	50.1 ± 7.82	25.6 ± 1.35
		UK 14,304	49.1 ± 6.13	27.8 ± 3.09
	Pre-test	Vehicle	48.8 ± 3.62	36.3 ± 2.93
		UK 14,304	55.0 ± 5.24	40.3 ± 4.24
Object location	Pre-sample	Vehicle	48.9 ± 4.73	34.3 ± 3.06
		Propranolol	46.2 ± 3.73	29.7 ± 2.43
	Pre-test	Vehicle	42.8 ± 4.32	39.0 ± 2.92
		Propranolol	50.2 ± 2.86	38.0 ± 5.29
Object recognition	Pre-sample	Vehicle	71.4 ± 6.40	51.6 ± 5.11
		UK 14,304	68.1 ± 6.07	53.2 ± 3.81
Object recognition	Pre-sample	Vehicle	83.7 ± 5.43	53.2 ± 3.81
		Propranolol	72.1 ± 4.43	45.2 ± 4.56

4.3.2.6.2 β adrenergic receptors in the hippocampus are not required for object location memory

Both pre-sample and pre-test infusion of propranolol into the HPC did not affect object location memory (Figure 4.6D). These observations were confirmed with a mixed model ANOVA (drug x infusion timing interaction: ($F(2,44) = .417$, $p = .525$); main effect of drug: ($F(1,22) = .061$, $p = .808$); main effect of infusion timing: ($F(1,22) = .517$, $p = .480$). Animals that received either vehicle or drug infusions both exhibited discrimination that was significantly above chance at both pre-sample (vehicle: ($t(11) = 4.466$, $p = .001$); propranolol: ($t(11) = 4.40$, $p = .001$)); and pre-test infusion timepoints (vehicle: ($t(11) = 4.42$, $p = .001$); propranolol ($t(11) = 5.24$, $p < .001$)).

Analysis of overall object exploration in the sample phase revealed no significant differences between conditions (drug x infusion timing interaction: ($F(1,22) = 2.40$, $p = .136$); main effect of drug: ($F(1,22) = .522$, $p = .478$); main effect of infusion timing: ($F(1,22) = .051$, $p = .824$)). Analysis of test phase exploration revealed no significant differences in the total amount of object exploration (drug x infusion timing interaction: ($F(1, 22) = .393$, $p = .537$); main effect of drug: ($F(1,22) = .953$, $p = .340$); main effect of infusion timing ($F(1,22) = 2.43$, $p = .133$)) (Table 4.4).

Taken together, the above data indicates that β adrenergic receptors in the HPC are not involved in object location memory during either the encoding or retrieval phase.

4.3.2.7 Experiment 9: α2 and β adrenergic receptors in the hippocampus are not involved in object recognition memory

It could be argued that the impairments found in the object-in-place task but not object location task following intra-HPC infusions could be due to non-specific factors. For instance, the object-in-place task requires animals to encode four distinct objects while the object location task involves the encoding of two identical objects, thus any differences in the results in the two tasks could be due to stimulus load. To ensure the observed encoding deficits following intra-HPC infusions in the object-in-place task were not due to such non-specific effects, animals were tested on an object recognition task based on the object-in-place task, which consists of four distinct objects (Figure 4.7B). It was predicted that pharmacological manipulation of the HPC should result in no memory deficits as the HPC is not required for object recognition memory (see Section 1.1.2.2) and would therefore indicate that the object-in-place deficits are due to specific memory deficits.

Animals infused with the α2 adrenergic agonist UK 14,304 or the β adrenergic antagonist propranolol prior to the sample phase demonstrated no memory deficits (Figure 4.7). This was confirmed by a paired samples t-test indicating no significant differences in discrimination ratios between vehicle and UK 14,304-infused animals ($t(11) = -.564$, $p = .584$) and between vehicle and propranolol-infused animals

($t(11) = .646$, $p = .531$). Additional analysis comparing performance against chance confirmed these results, indicating that for the UK 14,304 experiment both vehicle and UK 14,304-infused animals demonstrated significant discrimination (vehicle: $t(11) = 4.55$, $p = .001$); UK 14,304: ($t(11) = 3.79$, $p = .003$). In addition, both vehicle and propranolol-infused animals also discriminated significantly above chance (vehicle: ($t(11) = 4.84$, $p = .001$); propranolol: ($t(11) = 3.21$, $p = .008$).

No significant differences in the total amount of object exploration during the sample phase ($t(11) = .465$, $p = .651$) or test phase ($t(11) = 1.28$, $p = .228$) were observed between vehicle and UK 14,304-infused animals. Similarly, no differences in exploration between vehicle and propranolol-infused animals were observed during the sample phase ($t(11) = 1.43$, $p = .181$) or test phase ($t(11) = 1.26$, $p = .235$) (Table 4.4).

Overall, the lack of impairment during the object-recognition task following pre-sample intra-HPC infusions of UK 14,304 or propranolol indicates that the impairments found in the object-in-place task were not due to stimulus or memory load.

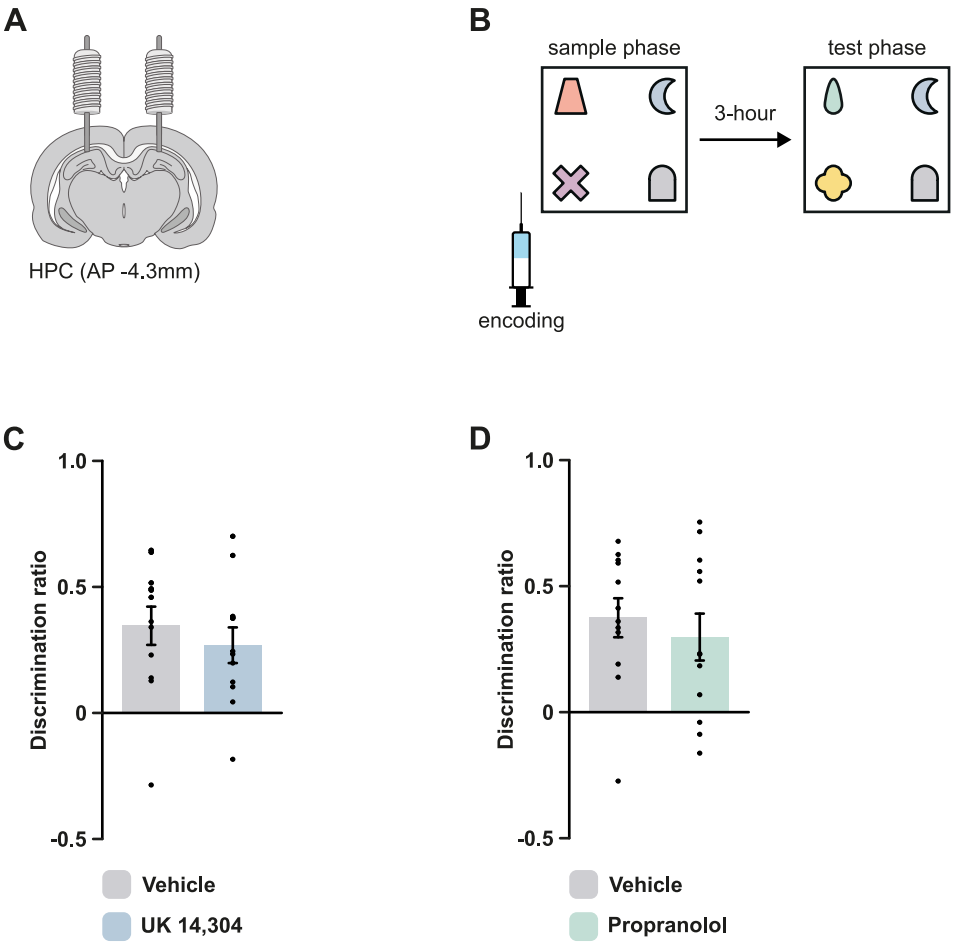

Figure 4.7. Pre-sample infusion of the $\alpha 2$ agonist and β antagonist in the HPC have no effect on object recognition memory. (A) Schematic of experiment. Infusions were made into the HPC. (B) Schematic of the object recognition task. Drugs were infused before the sample phase. (C) Pre-sample infusion of UK 14,304 into the HPC was without effect in the object recognition task. (D) Pre-test infusion of propranolol into the HPC was without effect in the recognition task. Data are represented as mean ± SEM.

4.3.2.8 Experiment 10: Replication of the study investigating the role of β adrenergic receptors in the hippocampus in object-in-place memory

This experiment sought to reproduce the behavioural deficit observed from cohort 2 animals in cohort 3 animals. This additional experiment was conducted as thus far the experiments conducted in cohort 3 animals have revealed no memory deficits (see Table 4.1 for summary of cohorts used in each experiment). The β adrenoceptor

antagonist propranolol experiment was replicated, however, only pre-sample intra-HPC infusions were conducted as robust deficits were observed under these conditions (see Section 4.3.2.5). To this end, it was revealed that pre-sample infusion of propranolol into the HPC resulted in impairments in memory (Figure 4.8C). A paired samples t-test confirmed this effect and revealed a significant difference between vehicle and propranolol-infused animals ($t(11) = 2.40$, $p = .035$). Additional analysis comparing performance against chance indicated that vehicle-infused animals demonstrated significantly greater discrimination of the novel object configuration over the familiar object configuration while propranolol-infused animals did not (vehicle: ($t(11) = 3.31$, $p = .007$); propranolol: ($t(11) = .412$, $p = .688$). The total amount of object exploration was also not significantly different between vehicle and HPC infusions in the sample phase ($t(11) = .014$, $p = .989$) or test phase ($t(11)$ .321, $p = .754$) (Table 4.4).

Together, these data provide further evidence that β adrenergic mediated neurotransmission in the HPC is crucial for the encoding of object-in-place memory. Furthermore, as this deficit was produced in the second HPC and mPFC cohort (cohort 3), this indicates that the lack of behavioural deficits observed up until this point in cohort 3 are not due to non-specific effects.

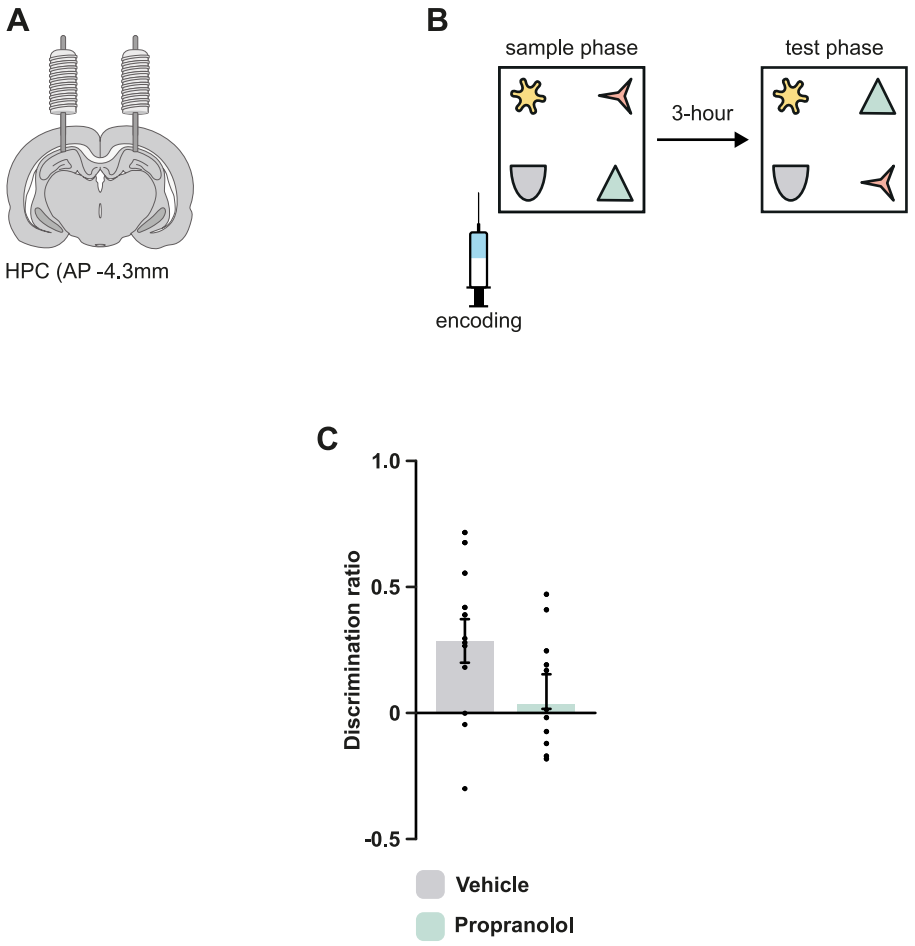

Figure 4.8. β adrenergic mediated neurotransmission in the HPC in cohort 3 is required for object-in-place memory. (A) Schematic of experiment. Infusions were made into the HPC. (B) Schematic of the object-in-place task. Drugs were infused before the sample phase. (C) Pre-sample infusion of propranolol into the HPC impaired object-in-place memory. Data are represented as mean ± SEM.

4.4 Discussion

The present study revealed a brain region and receptor subtype specific effect at different memory phases of the object-in-place task for noradrenergic neurotransmission. In the NRe, noradrenergic neurotransmission, mediated via the α1 and α2 but not β adrenoceptors, was shown to be required for the retrieval but not encoding of object-in-place recognition memory. In the HPC, the α2 and β but not α1 adrenoceptors, were found to be critical for the encoding but not retrieval of object-in-place memory. Furthermore, it was also revealed that neither α2 or

β adrenoceptors in the HPC are involved in object location or object recognition memory. Finally, pharmacological manipulation of the adrenergic receptors in the mPFC did not disrupt object-in-place memory. Importantly, total exploration time in the sample and test phases were unaltered between groups in all experiments, indicating that the deficits observed were not due to non-specific effects such as changes in motor function.

4.4.1 Noradrenergic modulation of the nucleus reuniens

The results of the current chapter extend recent findings revealing that the NRe is required for long-term object-in-place memory (Barker & Warburton, 2018), and demonstrate that noradrenergic modulation of the NRe is important for the retrieval of such memory. Based on behavioural and anatomical evidence, Barker & Warburton (2018) proposed that the NRe serves as a critical component of a recognition memory neural circuit which includes the HPC and mPFC. Furthermore, given the time-dependent action of the NRe in object-in-place memory it was also suggested that the NRe does not simply serve to convey information between the HPC and mPFC but instead is important in directly coordinating communication between the HPC and mPFC. Indeed, recent unpublished findings have provided empirical evidence for this proposal, demonstrating that distinct projections between the NRe, HPC and mPFC are engaged at different timepoints of associative recognition memory processing (Barker et al., unpublished data). Taken together, the current results add to the emerging picture that the NRe plays a pivotal role in cognitive processes that require both the HPC and mPFC but extend this notion and suggest that the ability of the NRe to support communication between the HPC and mPFC may be modulated, in part, by the noradrenergic system. This proposal that noradrenergic neurotransmission in the NRe modulates its connections with the HPC and mPFC is discussed further in Section 6.2.

Previous experiments examining the distribution of adrenergic receptors in the central nervous system have demonstrated that the NRe displays moderate to dense levels of expression of the α1 and α2 adrenergic receptors but only lightly expresses

the β adrenergic receptors (see Section 1.3.3.1). Therefore, the apparent lack of involvement of the β adrenoceptors may be due to the weak expression levels of these receptors in the NRe. To date, no direct functional evidence for the role of noradrenergic modulation of the NRe has been provided, however, in one study, correlative evidence suggested the existence of a relationship between the density of $\alpha 2$ adrenergic receptor expression in the NRe and feeding behaviour (Wilmot et al., 1988). The limited number of functional studies investigating the involvement of the adrenergic system in the NRe is likely due to the only rather recent appreciation that the NRe serves as a key structure in higher-order functions (Cassel et al., 2013; Dolleman-van der Weel et al., 2019). Given that the NRe displays moderate/dense expression levels of the α adrenergic receptors, and the results of the current chapter providing direct functional evidence that the $\alpha 1$ and $\alpha 2$ adrenergic receptors in the NRe are involved in associative recognition memory, it is reasonable to suggest that other NRe-dependent functions are also modulated by noradrenaline. Thus, more research is required to provide further insights into noradrenergic modulation of the NRe in other cognitive behaviours.

Although the precise synaptic distribution of the $\alpha 2$ adrenoceptors in the NRe has not been established, in other brain regions, $\alpha 2$ adrenergic receptor mediated effects are thought to have a primarily pre-synaptic locus of action, such that activation of pre-synaptically located $\alpha 2$ adrenoceptors results in inhibition of noradrenaline release (Langer, 1974; Starke, 2001; Talley et al., 1996). The current finding that agonism by UK 14,304 but not antagonism by RS 79948 impaired memory, suggests that pre-synaptic $\alpha 2$ adrenoceptors were engaged, and that a decrease in noradrenaline release in the NRe may underlie the memory deficits observed. Following this logic, it would be expected that antagonism by RS 79948 would have a faciliatory effect on memory, however, we found no effect following infusion of RS 79948. This lack of memory enhancement does not necessarily contradict our results however, it is likely that the current protocol employed in the object-in-place task is not sensitive enough to detect a facilitatory effect on memory. The use of a more difficult testing procedure, such as reducing the maximum sample phase exploration time to reduce

discrimination would allow any faciliatory effects on memory to become detectable.

4.4.2 Noradrenergic modulation of the hippocampus

The current finding that hippocampal noradrenaline is required for some forms of recognition memory is in agreement with previous literature. For example, Lemon et al. (2009) tested rats on an episodic-like memory task based on the spontaneous exploration task and demonstrated that pre-sample intra-HPC infusion of the β adrenergic antagonist propranolol, impaired the spatial component of the task. In contrast, a recent study suggested that dopamine release, acting via the D1-like receptors, from the LC, but not noradrenaline, acting via the β adrenergic receptors, enhanced spatial recognition memory (Kempadoo et al., 2016). The former study conducted by Lemon et al. (2009) required animals to discriminate the novel spatial location of objects while other non-identical objects were also present during the test phase, therefore it is likely that discriminations were not based purely on object location and required associations between object identity and their relative spatial locations. While the latter study conducted by Kempadoo et al. (2016), animals were only presented with identical objects during the sample and test phase, therefore the task required animals to discriminate based on the location of objects alone. These findings suggest that distinct neuromodulatory systems may underlie performance in each task, such that hippocampal noradrenaline is critical for object-place associations while hippocampal dopamine is required for object location memory. In addition, it is likely that hippocampal dopamine is only required for the encoding of longer-term object location memory (tested at a 24-hour delay) but not shorter-term object location as previous reports have indicated no role for dopaminergic neurotransmission in the HPC when object location is tested at a 1-hour delay (Savalli et al., 2015). We revealed that hippocampal noradrenaline is required for the encoding of object-in-place memory but not object location memory, thus the current findings agree with the above proposal that HPC noradrenaline is required for discriminations which require the binding of object-place associations but not for discriminations which require recognition of the location of the object

only.

Several studies have indicated a pivotal role for β adrenergic receptors in the HPC in regulating synaptic plasticity and hippocampal-dependent learning and memory functions (Hansen & Manahan-Vaughan, 2015; Ji et al., 2003; Kemp & Manahan-Vaughan, 2008; Lemon et al., 2009; Murchison et al., 2004; Straube et al., 2003). For example, antagonism of β adrenoceptors in the HPC impaired the retrieval of contextual fear memory (Murchison et al., 2004), while long term potentiation (LTP) in the HPC is enhanced following activation of β adrenergic receptors - a process thought to be critical for memory consolidation (Gelinas et al., 2008). While activation and inhibition of hippocampal β adrenergic receptors has been shown to have beneficial and detrimental effects on learning and memory processes, respectively, α1 adrenergic receptors seem to have an opposing effect in the HPC. Studies have demonstrated that while the majority of β adrenoceptors are expressed in CA1 pyramidal cells, α1 adrenoceptors are primarily expressed in CA1 interneurons (Hillman, Doze, et al., 2005, 2007; Hillman, Knudson, et al., 2005). Accordingly, electrophysiological evidence has indicated that noradrenaline acting via the α1 adrenoceptors decreases excitability in the HPC by depolarising CA1 interneurons, which subsequently inhibits neighbouring CA1 pyramidal neurons (Bergles et al., 1996; Hillman et al., 2009; Ul Haq et al., 2012). Interestingly, intra-DG infusions of α1 adrenoceptor agonist and antagonists have been demonstrated to slow and accelerate learning, respectively, when animals were tested on an active-avoidance learning paradigm (Lv et al., 2016). Collectively, these studies indicate that agonism of hippocampal α1 adrenoceptors has a negative effect on memory. Given that in the current study no effect on memory was found following intra-HPC infusion of the α1 adrenergic receptor antagonist prazosin, it is possible that such infusion caused inhibition of HPC interneurons, which, based on the above evidence, would be predicted to have a facilitatory effect on memory. However, any potential memory enhancing, as stated above, would be undetectable with the current paradigm used. Taken together, it is possible that α1 adrenergic receptors in the HPC are involved in associative recognition memory, however, additional experiments are required to

fully investigate this proposal.

Only a small number of studies have explored the involvement of $\alpha 2$ mediated neurotransmission in the HPC, however, studies conducted thus far have revealed that activation of $\alpha 2$ adrenergic receptors has a detrimental effect on memory while inactivation has a facilitatory effect, consistent with a pre-synaptic site of action. For instance, antagonism of $\alpha 2$ adrenergic receptors in the HPC has been demonstrated to increase freezing in a contextual fear condition paradigm, indicating enhanced memory. Furthermore, activation of $\alpha 2$ adrenoceptors in the HPC has been demonstrated to suppress sharp wave-ripple complexes - an electrophysiological correlate for memory consolidation (Ul Haq et al., 2012). While the current results did not find statistical significance between control versus animals infused with UK 14,304 into the HPC in the object-in-place task, animals subject to intra-HPC infusions of UK 14,304 were unable to make object-in-place discriminations based on their inability to show preferential exploration of the novel configuration over the familiar configuration, thus the current results are consistent with the notion that activation of $\alpha 2$ adrenoceptors in the HPC causes memory impairments via a pre-synaptic mechanism.

4.4.3 Noradrenergic modulation of the medial prefrontal cortex

Extensive research over the years has established through permanent lesions and temporary inactivation's that the mPFC is pivotal for associative recognition memory (Barker et al., 2007; Barker & Warburton, 2011; Benn et al., 2016). The mPFC is strongly innervated with noradrenergic fibres, and there is dense expression of all adrenergic receptor subtypes (see Section 1.3.3.3). Noradrenergic neurotransmission in the mPFC is critical in modulating a number of prefrontal cortical dependant cognitive functions (see review (Berridge & Spencer, 2016)). It is therefore surprising that in the current study no apparent role for noradrenergic neurotransmission in the mPFC in long-term associative recognition memory was found. The present null results however do not rule out a role for prefrontal noradrenaline in recognition

memory entirely. For instance, Nelson et al. (2011) found that 6-OHDA lesions of the mPFC disrupted temporal order recognition memory but spared object recognition and object location memory. While the authors do attempt to separate out the effects of dopamine from noradrenaline by pre-treating animals with the noradrenaline reuptake inhibitor desipramine, their high-pressure liquid chromatography with electrochemical detection (HPLC-ECD) analysis revealed that both dopamine and noradrenaline levels were reduced in the mPFC. Therefore, there is a possibility that noradrenergic modulation of the mPFC is required for temporal order memory. Moreover, in the present study animals were only tested following a 3-hour delay, thus a possible delay-dependent effect for noradrenergic neurotransmission in the mPFC in recognition memory may exist. Taken together, it is evident that further testing is warranted to fully investigate under what conditions, noradrenergic neurotransmission in the mPFC modulates recognition memory.

As mentioned above, consistent with a pre-synaptic mechanism of action, the $\alpha 2$ agonist UK 14,304 has been demonstrated to reduce noradrenaline levels (Dalley & Stanford, 1995; Van Veldhuizen et al., 1993), while the $\alpha 2$ antagonist RS 79948 has been shown to increase noradrenaline release in the frontal cortex (Devoto et al., 2005). Therefore, the present finding that UK 14,304 did not impair memory suggests that pre-synaptic $\alpha 2$ adrenergic receptors in mPFC are not required for associative recognition memory. Interestingly, it is worth noting that in the mPFC, studies have indicated that behavioural functions, such as working memory, engage post-synaptic $\alpha 2$ adrenergic receptors. This is in contrast to other brain regions such as the HPC and amygdala where the actions of the $\alpha 2$ adrenergic receptors are classically considered to have a pre-synaptic site of action (Caetano et al., 2013; Davies et al., 2004; Ferry & McGaugh, 2008; Ferry et al., 2015; Torkaman-Boutorabi et al., 2014). More specifically, it has been proposed that mPFC noradrenaline has an inverted-U shaped relationship in working memory, i.e., too low or high levels of noradrenaline release result in memory impairments. In addition, this inverted-U shape of noradrenergic modulation has been suggested to involve the opposing actions of the post-synaptic $\alpha 2$ and $\alpha 1$ adrenoceptors. Thus, under conditions of

moderate levels of noradrenaline release, such as during task engagement, high affinity $\alpha 2$ adrenergic receptors are engaged, whereas under conditions of high levels of noradrenaline release, such as periods of distractibility, low affinity $\alpha 1$ adrenergic receptors are engaged. Accordingly, functional studies have revealed that agonism of the $\alpha 2$ adrenergic receptors in the mPFC enhances working memory, and such enhancement of memory can be reversed by $\alpha 2$ adrenergic receptor antagonists (Arnsten, 1998; Franowicz et al., 2002; Mao et al., 1999; Ramos & Arnsten, 2007; Tanila et al., 1996; Wang et al., 2007). Furthermore, agonism of mPFC $\alpha 1$ adrenergic receptors has been revealed to impair working memory, and such deficits can be reversed by antagonism of $\alpha 1$ adrenergic receptors (Arnsten et al., 1999; Birnbaum et al., 1999; Mao et al., 1999). Given the outlined evidence, it is tempting to suggest that post-synaptic $\alpha 2$ adrenergic receptors in the mPFC may be involved in associative recognition memory processing, and that perhaps following infusion of drugs that target post-synaptic $\alpha 2$ adrenergic receptors, such as guanfacine, alterations in memory performance may be observed. However, it is also important to note that this inverted-U shape relationship of noradrenergic modulation has mainly been demonstrated in tests of working memory and in aged or catecholamine depleted animals. For example, in a previous study it was revealed that in contrast to the detrimental effects reported above following activation of $\alpha 1$ adrenergic receptors in working memory, activation of mPFC $\alpha 1$ adrenoceptors can enhance attentional set shifting (Lapiz & Morilak, 2006). Thus, it seems that factors such as the specific cognitive process tested, and baseline noradrenaline levels may govern the specific adrenergic receptors engaged in the mPFC. It is therefore unclear under what conditions, if any, would engage post-synaptic $\alpha 2$ adrenoceptors in young healthy rats with baseline levels of noradrenaline (as used in the current study), in recognition memory processing.

4.4.4 Time course of drugs

The current experimental approach undertaken, i.e., intra-cerebral infusion of drugs at various timepoints of a behavioural task, is often associated with the issue of

determining the phase of memory processing that may be impacted by a drug. However, multiple lines of evidence suggest that it is unlikely that in the current set of experiments that infusion of a given drug at a specific timepoint of the recognition memory task interfered with other stages of memory processing. For instance, in a retrodialysis study conducted in the basolateral amygdala, it was demonstrated that the decrease in noradrenaline release observed following infusion of 10μM UK 14,304 (same concentration used in the current chapter), only lasted 30 minutes (Ferry et al., 2015). Thus given that the current chapter tested animals at a delay of 3-hours between sample and test, it is unlikely that infusion of UK 14,304 had an impact on other stages of memory processing than the one being directly tested. In addition, the pattern of results observed in the current chapter, i.e., deficits at either the encoding or retrieval phase but not both, make it unlikely that the effects of the drugs tested persisted for longer than 3-hours. For instance, in the NRe experiments it was revealed that noradrenaline is critical for the retrieval but not encoding of object-in-place memory, therefore, if the effect of a given drug did in fact persist for longer than 3-hours, then it would be expected that pre-sample infusion of a drug into the NRe would cause memory impairments as the drug would also be effective during the retrieval phase, however this was not the case. Taken together, the above evidence indicates that it is unlikely that the drugs used in the current chapter were effective for more than 3-hours and it can therefore be concluded that under the current testing parameters used, infusion of a given drug did not interfere with other phases of memory processing other than the memory phase that was under direct investigation.

4.4.5 Conclusion

The results of this chapter indicate that noradrenergic neurotransmission has region specific effects at distinct memory stages of long-term associative recognition memory. In the NRe, noradrenergic neurotransmission is required during the retrieval of long-term object-in-place memory, while in the HPC it is critical for memory encoding. In contrast, in the mPFC, noradrenergic neurotransmission had no observable effects in

long-term associative recognition memory. Given that the LC provides the exclusive source of noradrenaline to the NRe, HPC and mPFC, it is likely that inputs from the LC are responsible for modulating the current behavioural results. The next chapter will test this proposal by inhibiting projections from the LC to the NRe and HPC using optogenetics during recognition memory.

5 Investigating the role of locus coeruleus projections to the nucleus reuniens and hippocampus in recognition memory

5.1 Introduction

In Chapter 4, it was established using specific pharmacological manipulations that noradrenergic neurotransmission has region-specific effects at distinct memory phases of associative recognition memory. More specifically, it was revealed that: in the NRe, noradrenaline is involved in the retrieval but not encoding; in the HPC, it is involved in the encoding but not retrieval; while in the mPFC, noradrenaline has no effect on memory performance. In Chapter 3, experiments revealed that the sole source of noradrenaline to the NRe originates from the LC, which is also the exclusive source of noradrenaline to the HPC and mPFC (Agster et al., 2013; Berridge & Waterhouse, 2003; Loy et al., 1980). Collectively, these findings suggest that afferents from the LC are responsible for the region-specific effects observed in Chapter 4.

To investigate the involvement of LC projections to the NRe and HPC (but not mPFC, as no behavioural deficits were found, see Chapter 4) in distinct phases of recognition memory, experiments in the current chapter employed an optogenetic approach. Traditionally, techniques to selectively target a specific subpopulation of cells involve the use of transgenic animals and site-specific recombinase technology (i.e., injecting a Cre-dependent virus into a Cre transgenic animal line) (Gompf et al., 2015; Stauffer et al., 2016). However, in recent years, viruses containing cell-type specific promoters injected into wild-type animals have been demonstrated to be successful in transducing neurons of a particular cell-type, and thus act as a feasible alternative to transgenic animals (Gompf et al., 2015; Stauffer et al., 2016).

Thus, this chapter has two aims, the first objective was to evaluate different viral

vector approaches in order to selectively transduce noradrenergic LC neurons and their axonal projections to the NRe and HPC. The second part of this chapter sought to investigate the function of LC projections to the NRe and HPC by inhibiting these projections during distinct phases of recognition memory using optogenetics.

5.2 Methods

5.2.1 Animals

33 male Lister hooded rats (Harlan Laboratories, UK) weighing ∼350g at the start of experimentation were used. See Section 2.1 for full details about animals. 9 animals were used for piloting of viruses, and 24 animals were used for behavioural testing (see Table 5.1 for an overview of which animals were used in each experiment).

Table 5.1. Overview of animals used for piloting of viruses and behavioural experiments.

Experiment	No. of animals	Virus	Brain region	Co-ordinates
Combinatorial pilot	1	AAV9-TH-Cre (1×10^{13}) + AAV5-EF1a-DIO-eArch3.0-EYFP (1×10^{12})	LC	AP: -9.6, ML: ±1.4, DV: -7.4
	1	AAV9-TH-Cre (1×10^{12}) + AAV5-EF1a-DIO-eArch3.0-EYFP (1×10^{12})	LC	AP: -9.6, ML: ±1.4, DV: -7.4
	1	AAV5-EF1a-DIO-eArch3.0-EYFP (1×10^{12})	LC	AP: -9.6, ML: ±1.4, DV: -7.4

	1	AAV9-TH-Cre (1×10^{13}) + AAV5-EF1a-DIO-eArch3.0-EYFP (1×10^{11})	LC	AP: -9.6, ML: ±1.4, DV: -7.4
	1	AAV9-TH-Cre (1×10^{12}) + AAV5-EF1a-DIO-eArch3.0-EYFP (1×10^{12})	VTA	AP: -5.6, ML: ±1.0, DV: -7.8
PRSx8 pilot	4	AAV9-PRSX8-eArchT3.0-EYFP	LC	AP: -9.6, ML: ±1.4, DV: -7.4
Behaviour	12	AAV5-Camkii-eArch3.0-EYFP	LC	AP: -9.6, ML: ±1.4, DV: -7.4
		Optical fibre	NRe	AP: -1.8, ML: ±2 (15°), DV: -6.6
		Optical fibre	HPC	AP: -5.4 (25°), ML: ±2.7, DV: -2.8
	12	AAV5-Camkii-EYFP	LC	AP: -9.6, ML: ±1.4, DV: -7.4
		Optical fibre	NRe	AP: -1.8, ML: ±2 (15°), DV: -6.6
		Optical fibre	HPC	AP: -5.4 (25°), ML: ±2.7, DV: -2.8

5.2.2 Surgery

All animals underwent surgical procedures as described in Section 2.2. For details concerning the viruses used, see Table 2.2. For an overview of which virus was injected into each animal and details of the co-ordinates used, see Table 5.1 for an overview. Animals in the combinatorial virus experiment were bilaterally injected with either a cocktail of viruses (AAV9-TH-Cre and AAV5-Ef1a-DIO-eArch3.0-EYFP) or a single

virus (AAV5-Ef1a-DIO-eArch3.0-EYFP) at various titres into the LC. An additional injection of (AAV9-TH-Cre and AAV5-Ef1a-DIO-eArch3.0-EYFP) was made into the VTA to investigate whether the specificity of the combinatorial viral approach was affected by brain region (see Section 5.3.1.1). Viral dilutions were made by adding virus buffer (350mM NaCl + 5% D-Sorbitol in PBS) to the virus solution. Animals were given 4 weeks to recover before histological processing. Animals in the PRSx8 experiment were bilaterally injected with 1μl per hemisphere of AAV9-PRSX8-eArchT3.0-EYFP into the LC. Animals were given 6 weeks to recover before histological processing. For the behavioural cohort animals, animals were randomly assigned into 2 groups, those that received the control virus, AAV5-CaMKII-EYFP (YFP, n = 12) and those that received the virus that expresses the inhibitory opsin Arch, AAV5-CaMKII-eArch3.0-EYFP (Arch, n = 12). Both YFP and Arch animals received a bilateral injection of 1μl per hemisphere of virus into the LC and were bilaterally implanted with optical fibres to target both the NRe and HPC. Therefore, for a given animal 4 optical fibres were implanted (2 aimed at the NRe and 2 aimed at the HPC). Animals were single housed 7 days post-surgery and given 6 weeks to recover before behavioural testing commenced.

5.2.3 Behavioural testing

The following spontaneous exploration tasks were used to test different types of recognition memory: object-in-place (3-hour delay) (Figure 5.7A and B), object-in-place task with 2 test phases (3-hour delay) (Figure 5.8A), object location (3-hour delay) (Figure 5.9A and B) and novel object preference task based on the object-in-place task (3-hour delay) (Figure 5.10A and B). Optical stimulation, to inhibit the LC terminals was either given during the sample phase to test the effects on encoding or during the test phase to test the effect on retrieval. Laser stimulation was delivered at a frequency of 30 Hz and a duration of 10ms using a custom protocol on WinLTP (2.20 M/X-Series, WinLTP Ltd.). See Section 2.3 for full details of habituation procedure, objects used, apparatus, testing procedures and optical stimulation parameters.

5.2.4 Data acquisition, scoring and analysis

For full details see Section 2.3.7. The experiments were run with a cross over design with each animal tested with both optical stimulation on and off conditions. In all behavioural experiments mixed model ANOVAs were conducted to compare discrimination ratios and exploration times (sample and test) between conditions, with stimulation condition (light off versus NRe light on versus HPC light on) as the within-subjects factor and virus (YFP versus Arch) as the between-subjects factor. When appropriate, Bonferroni-correct post-hoc comparisons were performed. In all experiments to determine whether discrimination ratios for each condition were significantly different from chance (a discrimination ratio of zero), one-sample t-tests were used. Alpha was set at 0.05. All statistical analysis was conducted with IBM SPSS Statistics 25 software (IBM, USA).

5.2.5 Histology

Following sufficient recovery time all animals were sacrificed and underwent immunohistochemical procedures as described in Section 2.4. For an overview of antibodies used see Table 2.4. For all viral injections, sections were stained with a cocktail of antibodies: primary antibodies anti-TH (rabbit, 1:1000, Chemicon, AB152) and anti-GFP (chicken, 1:1000, Aves Labs, GFP-1020); and secondary antibodies anti-rabbit Alexa Fluor 594 (goat, 1:500, Invitrogen, A-11037) and anti-chicken Alexa Fluor 488, (goat, 1:500, Invitrogen, A-11039).

5.2.6 Figures

Figures were edited using Adobe Illustrator (version 25.4.1, San Jose, CA, USA) and graphs were created using the R package ggplot2 (Hadley, 2016). Brain atlas figures are adapted from the rat brain atlas of Paxinos & Watson (2006).

5.3 Results

5.3.1 Piloting of viruses

5.3.1.1 Piloting of combinatorial viral vector approach

To achieve cell-type specificity in the LC, a combinatorial viral vector approach was piloted. This involved the co-infusion of two viruses, one virus (AAV9-TH-Cre) contains the TH-promoter fragment which drives the expression of Cre recombinase, and the other virus (AAV5-Ef1a-DIO-eArch3.0-EYFP) is a Cre dependent virus (herein, referred to as TH-Cre and DIO-YFP, respectively). Therefore, co-infusion of both viruses into the same brain region should result in Arch expression restricted to TH-positive neurons in the targeted brain region. To determine the optimal conditions to obtain cell-type specificity, various injection parameters were altered (see Table 5.1 and Figure 5.1 for an overview of parameters changed). Once the animals had been sacrificed, the brains were removed and sectioned on the cryostat, the sections were co-stained with antibodies against TH and GFP. Due to histological processing errors, quantification was not conducted, thus all observations are based on visual inspection. Figures 5.1B and C show representative cases in which the viral titre of the TH-Cre virus was altered while the viral titre of the DIO-YFP virus was kept constant at a titre of 5×10^{12} vg/ml. The combinatorial viral vector approach was observed to be very non-specific, regardless of the viral titre of the TH-Cre virus injected. For example, viral expression was consistently observed in areas outside of the LC, in fact, as illustrated in Figure 5.1B and C, very low levels of virus were expressed in TH-positive LC neurons with the majority of virus observed in non-TH-positive neurons. Thus, decreasing the viral titre of the TH-Cre virus did not affect specificity but instead significantly reduced the number of transduced neurons.

Cre-dependent AAV viral vectors can sometimes be the cause of off-target expression, as the LoxP sites in Cre-dependent plasmids can spontaneously recombine at the plasmid production stage or during DNA amplification, as a result, non-subtype

specific transgene expression occurs (Fischer et al., 2019). To investigate whether the DIO-YFP virus was the potential cause for the non-cell-type specific expression observed, the DIO-YFP virus was either injected alone (in the absence of the TH-Cre virus) or diluted to a concentration of 5×10^{11} vg/ml and co-injected with the TH-Cre virus. It was found that following injection of the DIO-YFP virus alone, no immunopositive cells were observed in the LC or any surrounding brain regions (Figure 5.1D). Furthermore, diluting the DIO-YFP virus and co-injecting it with the TH-Cre virus did not increase specificity of viral transduction, however, it did dramatically decrease the number of transduced neurons (Figure 5.1E). The evidence outlined above indicates that it is unlikely that the DIO-YFP virus is the major source for the off-target expression observed.

Previous reports using the same TH-Cre virus as used in the present study have demonstrated that co-infusion of the TH-Cre virus with a Cre-dependent virus into the VTA results in restricted expression in TH-positive neurons of the VTA in mice and monkeys (Stauffer et al., 2016). Therefore, the next experiment investigated the possibility that the combination of viruses used in the present chapter provides greater transduction specificity to TH-positive neurons of the VTA but not the LC. Thus, injections of the TH-Cre and DIO-YFP virus, both at a viral titre of 1×10^{12} vg/ml (as used in Stauffer et al. (2016)) were made into the VTA. However, it was found that similar to that observed following injections into the LC, viral expression was non-specific, with many non-TH-positive neurons demonstrating viral expression (Figure 5.2B).

Taking the results of these pilot experiments into consideration, given that various parameters have been altered but each have resulted in non-specific expression of TH-positive neurons, the combinatorial viral approach was not further investigated and therefore not used for behavioural experiments.

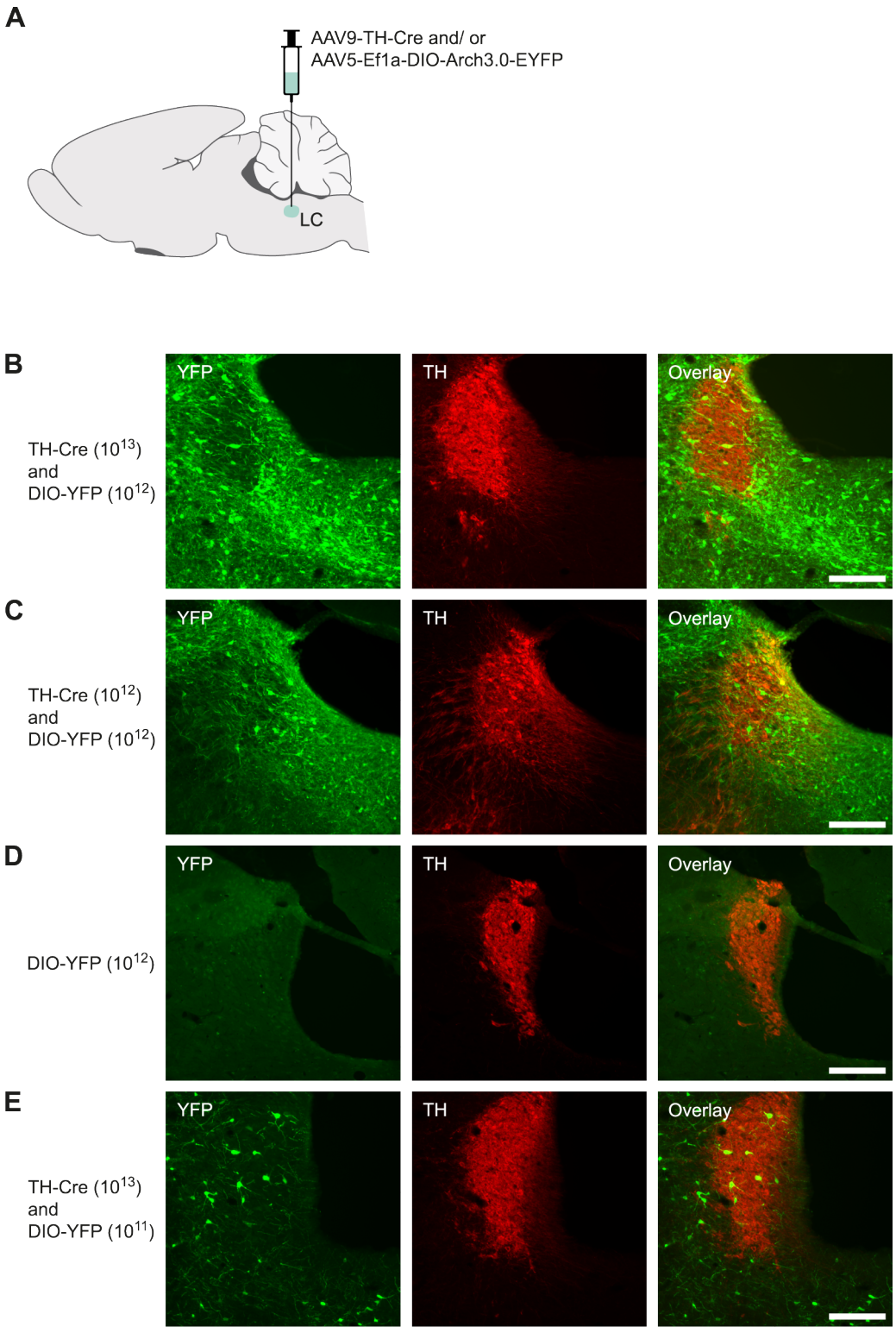

Figure 5.1. Combinatorial viral vector approach results in off-target expression in the LC. (A) Schematic of experiment. (B) Infusion of the TH-Cre virus at a viral titer of 1×10^{13} vg/ml and DIO-YFP virus at a titre of 5×10^{12} vg/ml resulted in off-target expression, the virus was predominantly expressed in TH-negative cells. (C) Infusion of the TH-Cre virus at a viral titer of 1×10^{12} vg/ml and DIO-YFP virus at a titre of 5×10^{12} vg/ml also resulted in off-target expression,

Figure 5.1 ***(continued).*** the majority of viral expression was in non-TH-positive neurons. (D) Infusion of the DIO-YFP virus only at a titre of 5×10^{12} vg/ml resulted in no viral expression. (E) Infusion of the DIO-YFP at a diluted titre of 5×10^{11} vg/ml reduced the number of transduced neurons but did not increase specificity. Scale bars: 200μM.

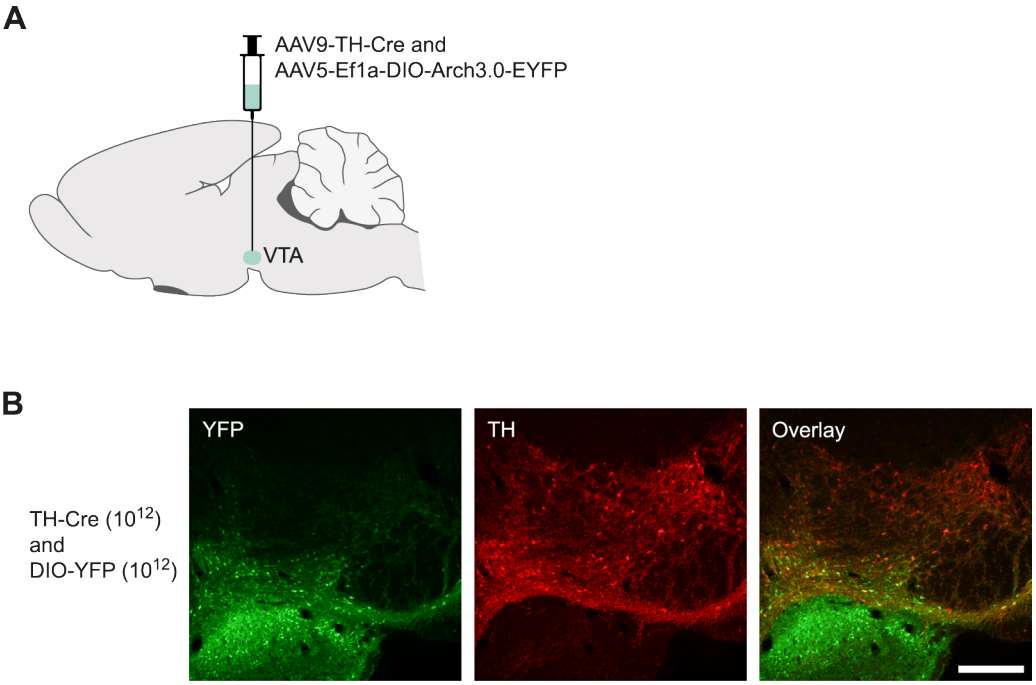

Figure 5.2. Combinatorial viral vector approach results in off-target expression in the VTA. (A) Schematic of experiment. Viral injections were made bilaterally into the VTA. (B) Infusion of the TH-Cre virus and DIO-YFP virus, both at a viral titer of 1×10^{12} vg/ml, resulted in off-target expression in the VTA. Scale bar: 200μm.

5.3.1.2 Piloting of the synthetic noradrenaline promoter (PRSx8) driven virus

In a further attempt to achieve cell-type specific expression of noradrenergic LC neurons, a custom-made virus (see Table 2.2 for details) expressing the inhibitory opsin Arch under the PRSx8 promoter – a synthetic noradrenaline promoter – was injected into the LC. Previous use of the PRSx8 promoter has demonstrated that a high degree of cell-type specific expression can be achieved using this promoter (Borodovitsyna et al., 2020; Campese et al., 2017; Giustino et al., 2019; Hirschberg

et al., 2017). Stereotaxic injection of the PRSx8 virus into the LC resulted in viral expression restricted to TH-positive neurons. Quantification revealed that 97.5 ± 1.01% of neurons were counted as double-labelled (i.e., the number of virus expressing neurons that co-stained for TH), however, examination of viral expression in the NRe and HPC revealed no transport of the virus (Figure 5.3). Furthermore, additional inspection of viral transport in other brain regions, such as the amygdala (which receives a strong projection from the LC (Jones & Yang, 1985; Samuels & Szabadi, 2008); data not shown), also revealed a lack of viral expression. Taken together, although the current PRSx8 virus resulted in robust expression in LC noradrenaline neurons, given that the aim of the behavioural experiments is to inhibit terminal projections from the LC to the HPC and NRe, the PRSx8 virus was not used for behavioural experiments.

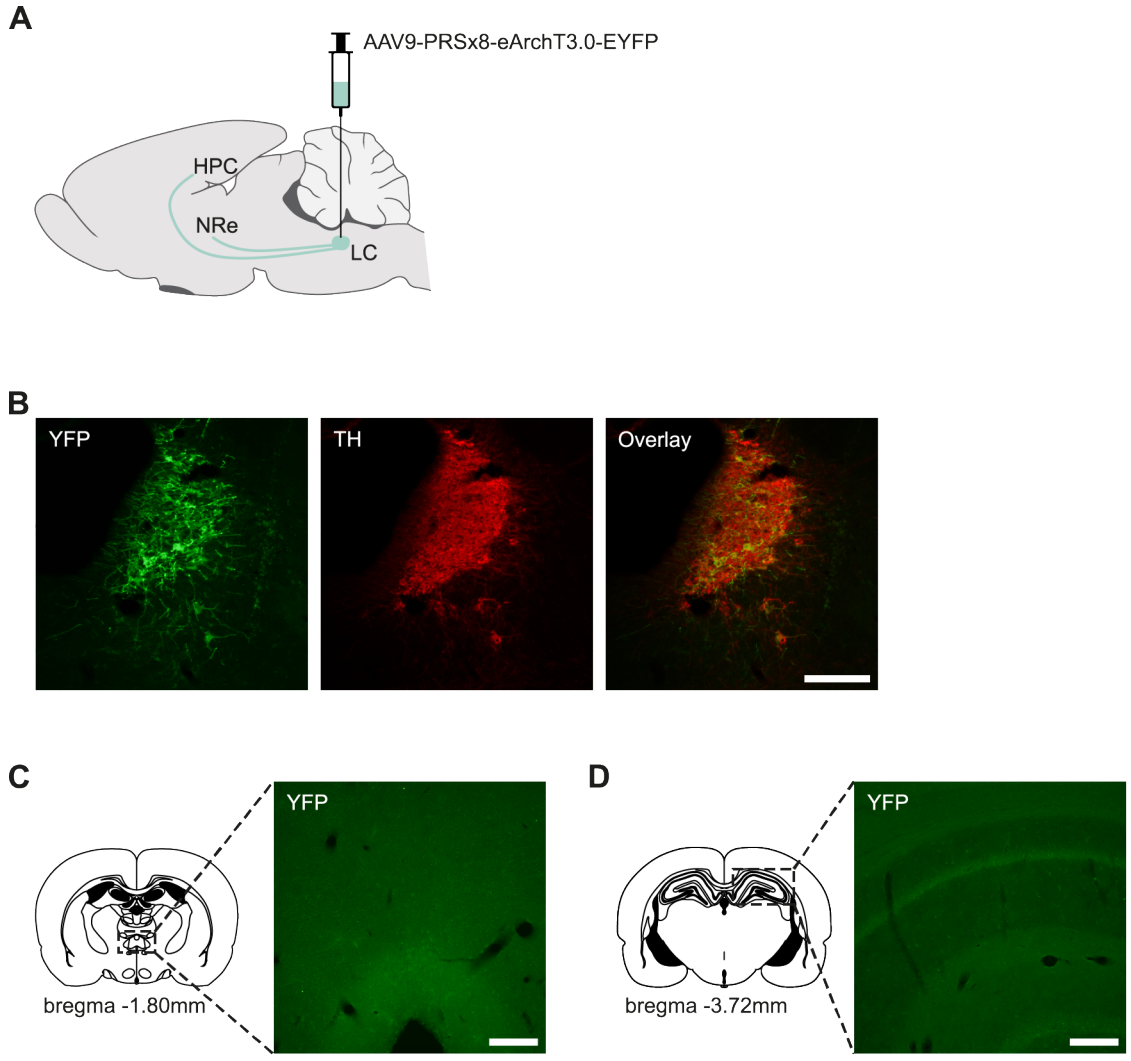

Figure 5.3. PRSx8 virus demonstrates cell-type specific expression in the LC but does not anterogradely transport to axon terminals. (A) Schematic of experiment. Viral injections were made bilaterally into the LC. (B) The PRSx8 virus is expressed almost exclusively in TH-positive neurons. (C) No transport of virus is observed in the NRe. (D) No transport of virus is observed in the HPC. Scale bars: 200μM. Figures adapted from Paxinos & Watson (2006).

5.3.2 Behavioural experiments

As an alternative approach to enable optogenetic investigation of the role of LC inputs to the NRe and HPC during recognition memory, a virus expressing the inhibitory opsin Arch under a CaMKII promoter was injected into the LC. LC noradrenaline neurons have been demonstrated to co-express with markers for excitatory neurons,

and previous studies have used a virus under a CaMKII promoter to target the LC. Thus the use of a virus under the control of the CaMKII promoter still serves as viable alternative to target the LC (Fung et al., 1994; Glennon et al., 2019; Nakamura et al., 2000; Yang et al., 2021). Pilot experiments (data not shown) revealed that injection of the CaMKII virus into the LC resulted in robust expression of LC TH-positive neurons. Moreover, axonal terminal expression of the virus was observed in the NRe and HPC. As the pilot experiments revealed that the injection site was centred in the LC and that axonal expression was observed in the NRe and HPC, the CaMKII virus was considered as an appropriate tool to inhibit LC projections to the NRe and HPC during recognition memory processing. Thus, for the behavioural experiments, either a Arch or YFP virus expressed under the CaMKII promoter was bilaterally injected into the LC. In addition, in the same surgery, animals were bilaterally implanted with optical fibres aimed at both the NRe and HPC to allow for optogenetic inhibition of LC terminals in the respective brain regions. Behavioural testing began 6 weeks after surgery (see Figure 5.4 for schematic of behavioural experiments).

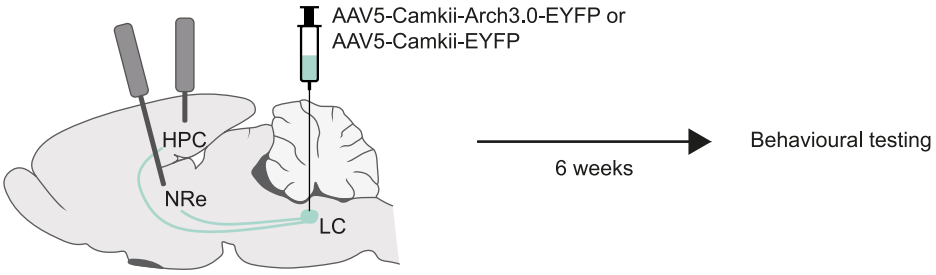

Figure 5.4. Schematic of experimental setup for behavioural experiments. Arch or YFP-expressing virus under the control of the CaMKII promoter was injected into the LC and optical fibres were bilaterally implanted in the NRe and HPC. Behavioural testing began 6 weeks after surgery.

5.3.2.1 Histological analysis

The core of viral expression was observed in the LC with diffuse expression of the virus observed in neighbouring brain regions to the LC in the behavioural cohort animals (Figure 5.5). Figure 5.5 schematically illustrates the maximum (light green) and minimum (dark green) of viral expression in the LC in the behavioural cohort

animals. Axonal transport of the virus was observed in the NRe and HPC in all animals (Figure 5.5C and D, respectively). Based on the optogenetic setup which was employed in the current study, (i.e., stimulation with a 515nm wavelength of light, fibre NA of 0.22, fibre core radius of 200μM and a light power of 10mW measured at the tip of the optical cannula), it is predicted that 10mW/mm^2 of light can be produced up to 0.5mm from the tip of the optical fibre (Deisseroth, 2012; Gradinaru et al., 2009). Thus, histological analysis revealed that in all animals optical fibres were correctly positioned to enable opto-inhibition of the NRe or HPC. Schematic representation of the location of the optical fibres and photomicrographs of representative cases are shown in Figure 5.6.

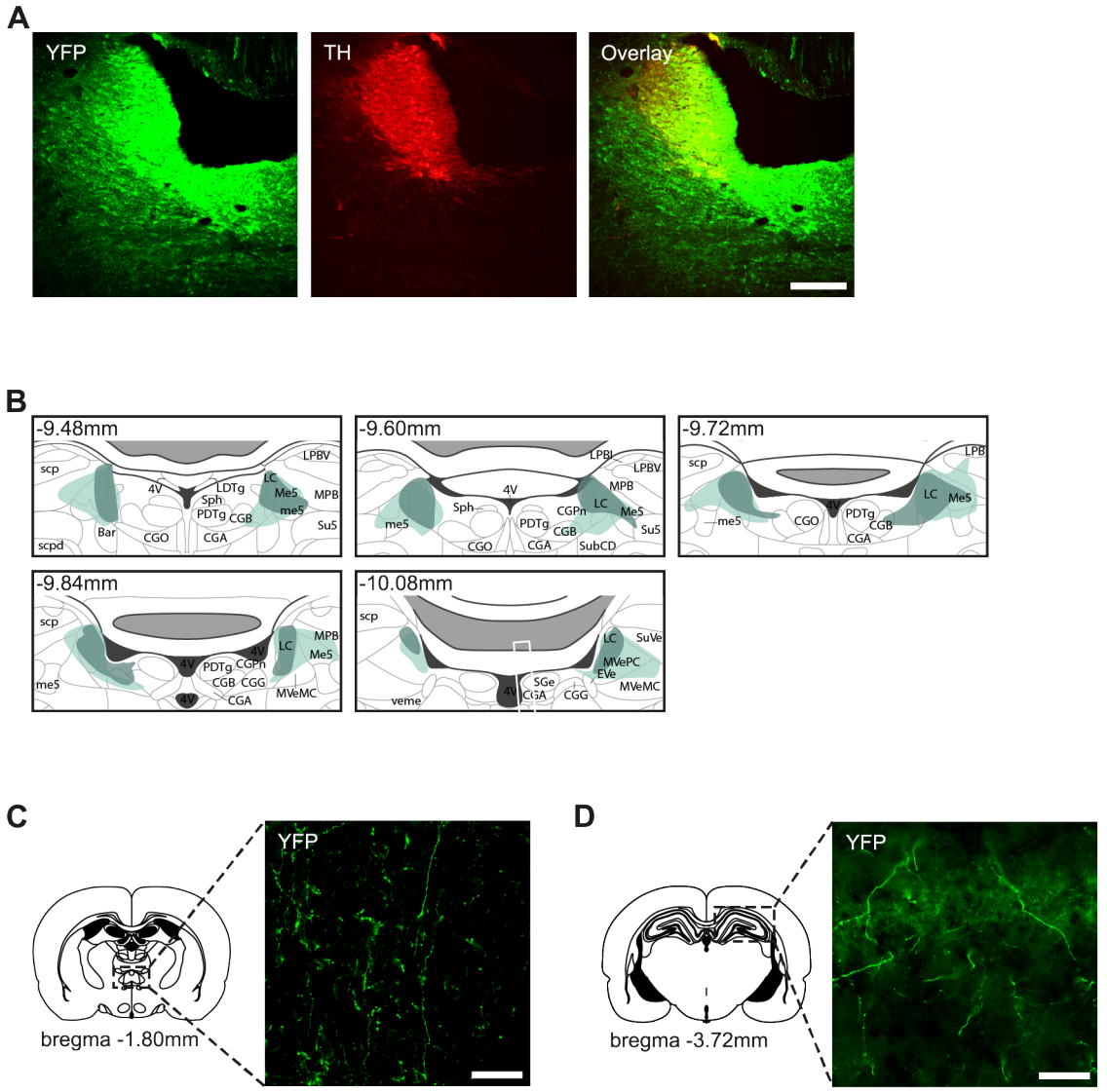

Figure 5.5. CaMKII virus results in robust transduction of LC neurons and their axon terminals. (A) The CaMKII virus robustly transduces LC neurons. (B) Schematic reconstruction demonstrating the maximum (light green) and minimum (dark green) expression of virus across different anterior-posterior levels relative to bregma. (C) Transport of virus is observed in the NRe. (D) Transport of virus is observed in the HPC. Scale bars: 200μM. 4V, 4th ventricle; Bar, Barrington's nucleus; CGA, central gray, alpha part; CGB, central gray, beta part; CGO, central gray, nucleus O; CGPn, central gray of the pons; Eve, nucleus of origin of efferents of the vestibular nerve; LC, locus coeruleus; LDTg, Laterodorsal tegmental nucleus; LPB Lateral parabrachial nucleus; LPBI, lateral parabrachial nucleus, internal part; LPbV, lateral parabrachial nucleus, ventral part; Me5, mesencephalic trigeminal nucleus; MPB, medial parabrachial nucleus; MVeMC, medial vestibular nucleus, magnocellular part; MVePC Medial vestibular nucleus, parvicellular part; PDTg, posterodorsal tegmental nucleus;

Figure 5.5 ***(continued).*** scp, superior cerebellar peduncle (brachium conjunctivum); Scpd, Superior cerebellar peduncle, descending limb; Sph, sphenoid nucleus; Su5, supratrigeminal nucleus; SubCD, subcoeruleus nucleus, dorsal part; SGe, supragenual nucleus; SuVe, Superior vestibular nucleus; Veme, Vestibulomesencephalic tract. Figures adapted from Paxinos & Watson (2006).

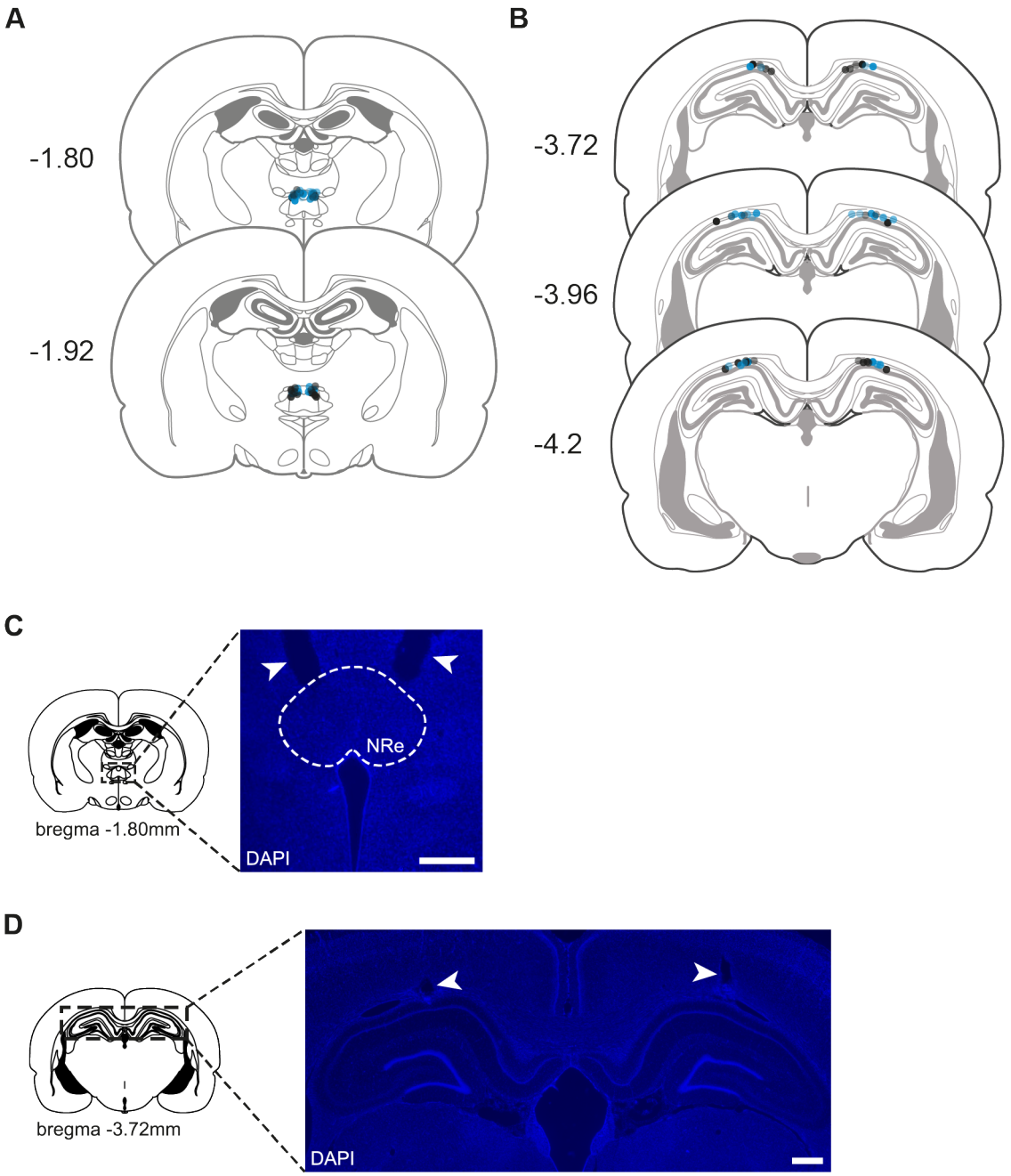

Figure 5.6. Optical fibre placement in the NRe and HPC. Schematic representation of the placement of individual optical fibre for each animal targeting the (A) NRe and (B) HPC. Numbers indicate distance from bregma. Black and blue dots indicate the location of the tips of the optical fibres in Arch and YFP animals, respectively. Representative photomicrographs of optical fibres targeting the (C) NRe and (D) HPC. White arrowheads indicate location of optical fibre tract. Scale bars: 500μM. Figures adapted from Paxinos & Watson (2006).

5.3.2.2 Optogenetic inhibition of locus coeruleus axonal terminals in the hippocampus or the nucleus reuniens selectively impairs distinct phases of object-in-place memory

5.3.2.2.1 Inhibition during the encoding phase of the object-in-place task

Inhibition of LC input to the HPC during the encoding phase of the object-in-place task impaired memory. In contrast, inhibition of LC input to the NRe in the object-in-place task during the encoding phase did not impair memory (Figure 5.7A). These observations were confirmed with a mixed model ANOVA (stimulation condition x virus interaction ($F(2,44) = 4.06$, $p = .024$); Bonferroni corrected post-hoc analysis comparing performance of the Arch group: (Off versus NRe: ($p = 1.00$)), (Off versus HPC: ($p = .003$), (NRe versus HPC: ($p = .013$)). A significant main effect of stimulation condition ($F(2,44) = 7.12$, $p = .002$) but not virus was found ($F(1,22) = 3.48$, $p = .075$). Analysis comparing performance against chance revealed that all animals, except for the Arch group receiving stimulation in the HPC ($t(11) = -.425$, $p = .679$), exhibited discrimination ratios significantly above chance (YFP Off: ($t(11) = 7.28$, $p < .001$); YFP NRe: ($t(11) = 4.17$, $p = .002$); YFP HPC: ($t(11) = 3.95$, $p = .002$); Arch Off: ($t(11) = 3.44$, $p = .006$); Arch NRe: ($t(11) = 5.63$, $p < .001$)).

Analysis of the overall amount of object exploration completed during the sample phase revealed no significant differences between conditions (stimulation condition x virus interaction: ($F(2,44) = 2.70$, $p = .079$); main effect of stimulation condition: ($F(2,44) = 1.87$, $p = .166$); main effect of virus: ($F(1,22) = .831$, $p = .372$)). In addition, no significant differences were found in total object exploration completed in the test phase between animals (stimulation condition x virus interaction: ($F(1.54,33.9) = .572$, $p = .526$); main effect of stimulation condition: ($F(1.54,33.9) = 1.69$, $p = .204$); main effect of virus: ($F(1,22) = .124$, $p = .728$)) (Table 5.2).

Together these results indicate that LC input to the HPC but not NRe is required for the encoding of object-in-place memory.

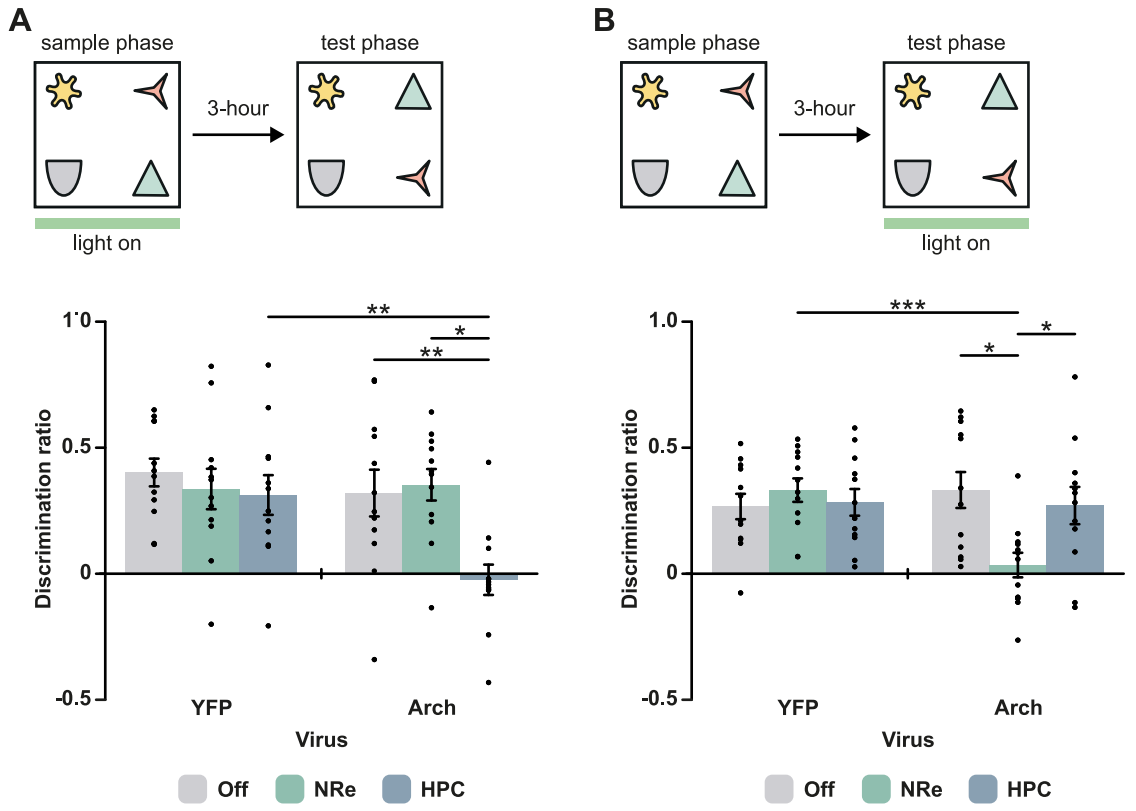

Figure 5.7. LC input to the HPC is critical for the encoding of object-in-place memory while LC input to the NRe is critical for the retrieval of object-in-place memory. (A) Top, schematic of object-in-place task. Light was delivered during the sample phase, as depicted by the green line. Bottom, Arch HPC but not Arch NRe animals were impaired. (B) Top, schematic of object-in-place task. Light was delivered during the test phase, as depicted by the green line. Bottom, Arch NRe but not Arch HPC animals were impaired. Data are represented as mean ± SEM. * $p < .05$, **$p < .01$, ***$p < .001$.

Table 5.2. Mean exploration times ± SEM in the sample and test phases in the object-in-place task.

Task	Virus	Stimulation condition	Exploration in sample phase (s) (300s max)	Exploration in test phase 1 (s) (300s max)	Exploration in test phase 2 (s) (180s max)
Object-in-place (encoding stimulation)	YFP	Off	57.9 ± 4.18	32.0 ± 4.10	
		NRe	49.7 ± 4.76	28.2 ± 3.16	
		HPC	41.9 ± 2.52	28.7 ± 3.03	
	Arch	Off	45.5 ± 3.90	31.1 ± 3.29	
		NRe	47.5 ± 3.52	29.9 ± 1.98	
		HPC	47.0 ± 4.29	24.6 ± 3.01	
Object-in-place (retrieval stimulation)	YFP	Off	71.5 ± 5.54	31.8 ± 4.17	
		NRe	68.0 ± 5.34	33.9 ± 4.28	
		HPC	66.3 ± 3.55	28.8 ± 3.28	
	Arch	Off	62.3 ± 4.15	32.6 ± 2.77	
		NRe	65.1 ± 4.39	29.7 ± 3.22	
		HPC	64.1 ± 3.00	31.4 ± 3.48	
Object-in-place (two test phases)	YFP	Off	71.0 ± 4.36	48.4± 4.40	34.9 ± 2.22
		NRe	72.5 ± 5.37	47.8 ± 4.49	38.6 ± 3.41
		HPC	69.8 ± 6.41	45.6 ± 3.54	37.4 ± 2.71
	Arch	Off	68.2 ± 5.71	55.3 ± 5.49	37.6 ± 3.83
		NRe	70.6 ± 3.42	54.5 ± 5.35	34.3 ± 1.92
		HPC	67.6 ± 4.74	56.8 ± 4.33	35.9 ± 3.20

5.3.2.2.2 Inhibition during the retrieval phase of the object-in-place task

Optogenetic inhibition of LC axonal terminals in the NRe but not HPC, delivered during the retrieval phase of the object-in-place task impaired memory (Figure 5.7B). Statistical analysis confirmed this pattern of results (stimulation condition x virus interaction: ($F(2,44) = 5.64$, $p = .007$); Bonferroni corrected post-hoc analysis

comparing performance of the Arch group: (Off versus NRe: (p = .029)), (Off versus HPC: (p = 1.00), (NRe versus HPC: (p = .024)). No significant main effects of stimulation condition ($F(2,44) = 2.36$, $p = .107$) or virus ($F(1,22) = 2.66$, $p = .117$) were found. Further one-sample analyses revealed that all animals, except for Arch group receiving stimulation in the NRe ($t(11) = .704$, $p = .496$), performed significantly above chance levels (YFP Off: ($t(11) = 5.30$, $p < .001$); YFP NRe: ($t(11) = 7.12$, $p < .001$); YFP HPC: ($t(11) = 5.35$, $p < .001$); Arch Off: ($t(11) = 4.66$, $p = .001$); Arch HPC: ($t(11) = 3.66$, $p = .004$)).

Analysis of total amount of object exploration during the sample phase revealed no significant differences (stimulation condition x virus interaction: ($F(2,44) = .687$, $p = .508$); main effect of stimulation condition: ($F(2,44) = .146$, $p = .865$); main effect of virus: ($F(1,22) = .907$, $p = .351$)). Total test phase object exploration also did not significantly differ between animals (stimulation condition x virus interaction: ($F(2,44) = 1.11$, $p = .338$); main effect of stimulation condition: ($F(2,44) = .438$, $p = .648$); main effect of virus: ($F(1,22) = .004$, $p = .950$)) (Table 5.2).

Taken together, these results indicate that LC input to the NRe but not HPC is required for the retrieval of object-in-place memory.

5.3.2.2.3 Inhibition during test phase one of the object-in-place task with two test phases

The experiments above tested the role of LC input to the NRe or HPC on the acquisition and retrieval stages of object-in-place memory, using optogenetics to inhibit LC terminals during the sample or test phase, respectively. However, encoding and retrieval processes are not distinct but in fact overlap and occur simultaneously. That is, during the test phase of the object-in-place task, as well as retrieving old associations from the sample phase, the animal is also encoding the novel object-place configurations. To manipulate encoding and retrieval processes simultaneously, the object-in-place task was adapted to include two test phases, and optogenetic inhibition was delivered during test phase 1 (Figure 5.8A). Therefore, if a pathway is required for the retrieval of object-in-place memory, it is predicted that performance

in test phase 1 should be impaired, conversely, if a pathway is required for the encoding of object-in-place memory, it is predicted that performance in test phase 2 should be impaired.

Optogenetic inhibition of LC axonal terminals in the NRe but not HPC, during test phase 1 of the object-in-place task impaired memory (Figure 5.8B). This observation was confirmed with statistical analysis (stimulation condition x virus interaction: $F(2,44) = 6.03$, $p = .005$)); Bonferroni corrected post-hoc analysis comparing performance of the Arch animals: (Off versus NRe: ($p = .002$)), (Off versus HPC: ($p = 1.00$), (NRe versus HPC: ($p = .004$)). Furthermore, significant main effects of stimulation condition ($F(2,44) = 9.95$, $p < .001$) and virus ($F(1,22) = 8.32$, $p = .009$), were found. One-sample analyses comparing discrimination ratios against chance revealed that all animals, except for Arch NRe animals ($t(11) = -.853$, $p = .412$), performed significantly above chance levels (YFP Off: ($t(11) = 5.52$, $p < .001$); YFP NRe: ($t(11) = 4.17$, $p = .001$); YFP HPC: ($t(11) = 3.95$, $p = .001$); Arch Off: ($t(11) = 6.54$, $p < .001$); Arch HPC: ($t(11) = 7.97$, $p < .001$)).

In contrast, optogenetic inhibition of LC axonal terminals in the HPC but not NRe, delivered during test phase 2 of the object-in-place task impaired memory (Figure 5.8C). A mixed model ANOVA confirmed these results (stimulation condition x virus interaction: $F(2,44) = 3.48$, $p = .040$); Bonferroni corrected post-hoc analysis comparing performance of the Arch animals: (Off versus NRe: ($p = 1.00$), (Off versus HPC: ($p = .043$), (NRe versus HPC: ($p = .020$)). No significant main effects of stimulation condition ($F(2,44) = 2.59$, $p = .086$) or virus ($F(1,22) = 3.25$, $p = .085$) were found. Further analysis revealed that all animals, except for Arch HPC animals ($t(11) = -2.49$, $p = .808$), demonstrated discrimination ratios significantly above zero (YFP Off: ($t(11) = 3.59$, $p = .004$); YFP NRe: ($t(11) = 3.63$, $p = .004$); YFP HPC: ($t(11) = 4.22$, $p = .001$); Arch Off: ($t(11) = 4.35$, $p = .001$); Arch NRe: ($t(11) = 4.20$, $p = .001$)).

Analysis of overall object exploration during the sample phase, test phase 1 and test phase 2 revealed no significant differences between animals. Sample phase (stimulation condition x virus interaction: ($F(2,44) = .006$, $p = .994$); main effect of

stimulation condition: ($F(2,44) = .273$, $p = .762$); main effect of virus: ($F(1,22) = .166$, $p = .688$)). Test phase 1 (stimulation condition x virus interaction: ($F(2,44) = .184$, $p = .833$); main effect of stimulation condition: ($F(2,44) = .014$, $p = .986$); main effect of virus: ($F(1,22) = 3.66$, $p = .069$)). Test phase 2 (stimulation condition x virus interaction: ($F(2,44) = .663$, $p = .521$); main effect of stimulation condition: ($F(2,44) = .006$, $p = .994$); main effect of virus: ($F(1,22) = .232$, $p = .635$)) (Table 5.2).

Together, these results corroborate the above evidence that LC input to the HPC and NRe are critical for different stages of object-in-place memory, the encoding and retrieval phases, respectively.

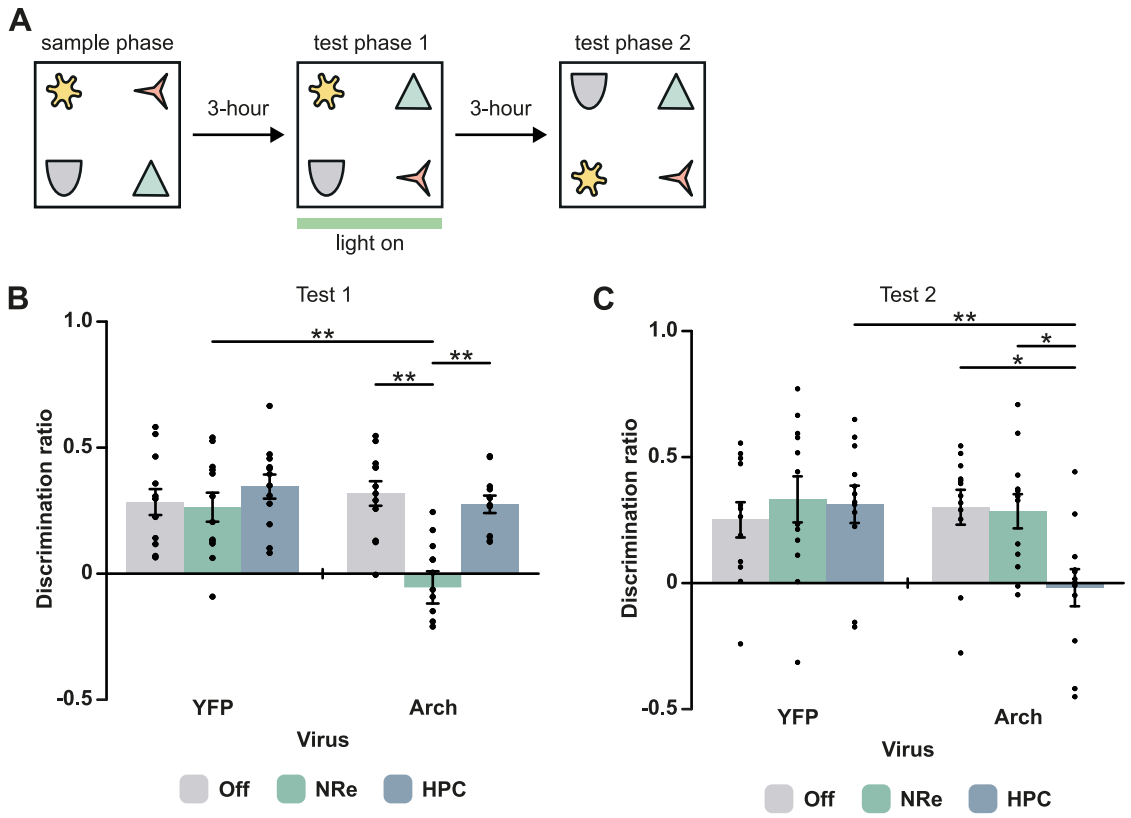

Figure 5.8. LC input to the HPC and NRe is critical for different memory stages of object-in-place memory. (A) Schematic of object-in-place task. Light was delivered during test phase 1, as depicted by the green line. (B) In test phase 1, Arch NRe but not Arch HPC animals were impaired. (C) In test phase 2, Arch HPC but not Arch NRe animals were impaired. Data are represented as mean ± SEM. * $p < .05$, **$p < .01$.

5.3.2.3 Silencing of locus coeruleus input to the hippocampus or nucleus reuniens has no effect on object location memory

5.3.2.3.1 Inhibition during the encoding phase of the object location task

The effects of optogenetic inhibition of LC input to the HPC or NRe during the encoding phase of the object location task on discrimination performance is shown in Figure 5.9A. A mixed model ANOVA revealed a non-significant stimulation condition x virus interaction ($F(2,44) = .378$, $p = .688$); and non-significant main effect of stimulation condition ($F(2,44) = .083$, $p = .921$); or virus ($F(1,22) = .194$, $p = .664$). Further analysis revealed that all animals performed significantly above chance levels (YFP Off: ($t(11) = 2.93$, $p = .014$); YFP NRe: ($t(11) = 3.44$, $p = .006$); YFP HPC: ($t(11) = 3.67$, $p = .004$); Arch Off: ($t(11) = 4.08$, $p = .002$); Arch NRe: ($t(11) = 6.10$, $p < .001$); Arch HPC: ($t(11) = 2.97$, $p = .013$)).

Statistical analysis of total exploration completed during the sample phase found no significant differences between animals (stimulation condition x virus interaction: ($F(2,44) = .828$, $p = .444$); main effect of stimulation condition: ($F(2,44) = .066$, $p = .936$); main effect of virus: ($F(1,22) = .006$, $p = .937$)). Similarly, analysis of total object exploration during the test phase revealed no significant differences between animals (stimulation condition x virus interaction: ($F(2,44) = .047$, $p = .954$); main effect of stimulation condition: ($F(2,44) = .098$, $p = .907$); main effect of virus: ($F(1,22) = 4.08$, $p = .056$)) (Table 5.3).

Overall, the lack of memory impairment indicates that LC inputs to the NRe and HPC are not involved in the encoding of object location memory.

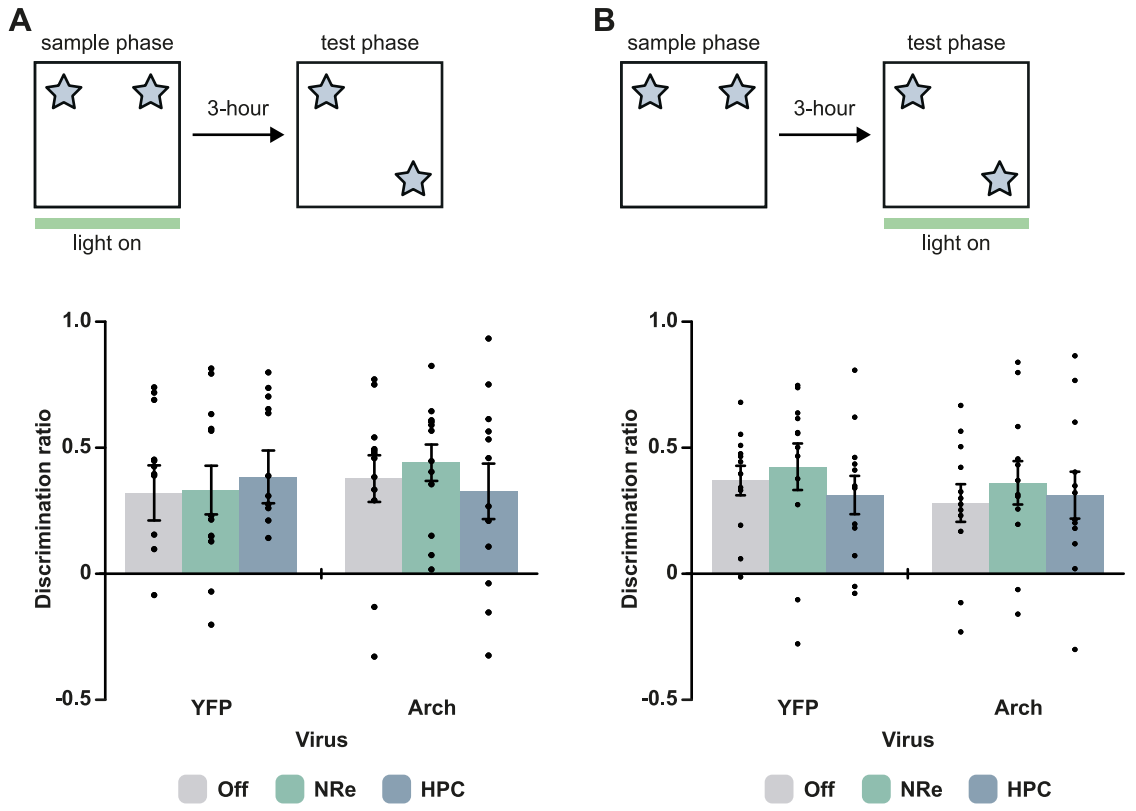

Figure 5.9. LC input to the HPC and NRe is not required for object-location memory. (A) Top, schematic of object location task. Light was delivered during the sample phase, as depicted by the green line. Bottom, optogenetic inhibition of LC to HPC or NRe inputs had no effect on performance. (B) Top, schematic of object location task. Light was delivered during the test phase, as depicted by the green line. Bottom, both inhibition of LC input to the HPC and NRe did not impair memory. Data are represented as mean ± SEM.

5.3.2.3.2 Inhibition during the retrieval phase of the object location task

Optogenetic inhibition of LC axonal terminals in the HPC or the NRe during the retrieval phase did not impair memory (Figure 5.9B). This observation was confirmed by a mixed model ANOVA which revealed no significant differences in discrimination ratios between animals (stimulation condition x virus interaction: ($F(2,44) = .133$, $p = .876$); main effect of stimulation condition: ($F(2,44) = .476$, $p = .625$); main effect of virus: ($F(1,22) = .994$, $p = .330$)). Additional analysis comparing performance against chance revealed that all animals demonstrated significant discrimination (YFP Off: ($t(11) = 6.32$, $p < .001$); YFP NRe: ($t(11) = 4.60$, $p = .001$); YFP HPC:

($t(11) = 4.11$, $p = .002$); Arch Off: ($t(11) = 3.75$, $p = .003$); Arch NRe: ($t(11) = 4.19$, $p = .002$); Arch HPC: ($t(11) = 3.35$, $p = .006$)).

Analysis of total amount of object exploration completed during the sample phase found no significant differences between animals (stimulation condition x virus interaction: ($F(2,44) = .268$, $p = .766$); main effect of stimulation condition: ($F(2,44) = .662$, $p = .521$); main effect of virus: ($F(1,22) = .011$, $p = .919$)). Similarly, analysis of total amount of exploration during the test phase also found no statistical differences between animals (stimulation condition x virus interaction: ($F(2,44) = .753$, $p = .872$); main effect of stimulation condition: ($F(2,44) = .027$, $p = .974$); main effect of virus: ($F(1,22) = .083$, $p = .775$)) (Table 5.3).

Taken together, the current results indicate that LC inputs to the NRe and HPC are not involved in the retrieval of object location memory.

Table 5.3. Mean exploration times ± SEM in the sample and test phases in the object location and object recognition tasks.

Task	Virus	Stimulation condition	Exploration in sample phase (s) (300s max)	Exploration in test phase (s) (180s max)
Object location (encoding stimulation)	YFP	Off	39.8 ± 3.74	27.3 ± 3.05
		NRe	36.8 ± 4.13	26.5 ± 2.51
		HPC	39.0 ± 4.07	25.7 ± 2.72
	Arch	Off	37.2 ± 1.81	31.6 ± 2.76
		NRe	40.1 ± 3.06	32.1 ± 2.64
		HPC	39.3 ± 3.19	31.3 ± 2.03
Object location (retrieval stimulation)	YFP	Off	39.8 ± 4.46	28.4 ± 2.93
		NRe	41.2 ± 4.17	28.2 ± 3.85
		HPC	38.9 ± 2.71	30.3 ± 2.40
	Arch	Off	38.2 ± 2.83	28.2 ± 2.36
		NRe	42.3 ± 3.19	29.3 ± 2.74
		HPC	40.8 ± 3.64	25.6 ± 2.69
Object recognition (encoding stimulation)	YFP	Off	62.7 ± 3.62	36.9 ± 2.81
		NRe	64.8 ± 2.59	41.8 ± 2.90
		HPC	59.4 ± 3.13	36.0 ± 2.75
	Arch	Off	61.3 ± 5.26	36.3 ± 3.08
		NRe	63.2 ± 3.05	41.8 ± 5.23
		HPC	59.1 ± 4.52	43.1 ± 2.19
Object recognition (retrieval stimulation)	YFP	Off	67.2 ± 4.99	39.6 ± 3.11
		NRe	79.5 ± 3.95	35.0 ± 4.33
		HPC	72.0 ± 4.82	36.9 ± 4.04
	Arch	Off	69.5 ± 5.31	43.0 ± 3.33
		NRe	74.8 ± 4.03	39.5 ± 4.71
		HPC	77.0 ± 4.08	39.4 ± 4.61

5.3.2.4 Inhibition of locus coeruleus input to the hippocampus or nucleus reuniens has no effect on object recognition memory

For the same reasons already outlined in Section 4.3.2.7, a novel object recognition task based on the object-in-place task was conducted to ensure that the object-in-place deficits were not due to non-specific factors such as stimulus or memory load.

5.3.2.4.1 Inhibition during the encoding phase of the object recognition task

Performance following optogenetic inhibition of LC input to the HPC or NRe during the encoding phase is shown in Figure 5.10A. Statistical analysis revealed no significant differences between animals (stimulation condition x virus interaction: ($F(2,42) = .089$, $p = .915$); main effect of stimulation condition: ($F(2,42) = .009$, $p = .991$); main effect of virus: ($F(1,21) = .183$, $p = .673$)). Further analysis revealed that all animals demonstrated discrimination ratios significantly above chance (YFP Off: ($t(11) = 4.59$, $p = .001$); YFP NRe: ($t(11) = 4.18$, $p = .002$); YFP HPC: ($t(11) = 4.40$, $p = .001$); Arch Off: ($t(11) = 3.72$, $p = .003$); Arch NRe: ($t(11) = 5.27$, $p < .001$); Arch HPC: ($t(10) = 3.31$, $p = .008$)).

Statistical analysis of overall object exploration revealed no significant differences between animals during the sample phase (stimulation condition x virus interaction: ($F(2,42) = .041$, $p = .959$); main effect of stimulation condition: ($F(2,42) = 1.84$, $p = .171$); main effect of virus: ($F(1,21) = .005$, $p = .947$)). Similarly, analysis of total object exploration in the test phase also revealed no statistical differences between animals (stimulation condition x virus interaction: ($F(2,42) = .671$, $p = .517$); main effect of stimulation condition: ($F(2,42) = 1.77$, $p = .183$); main effect of virus: ($F(1,21) = 1.05$, $p = .318$)) (Table 5.3).

The results indicate that LC inputs to the NRe and HPC are not involved in the encoding of object recognition memory.

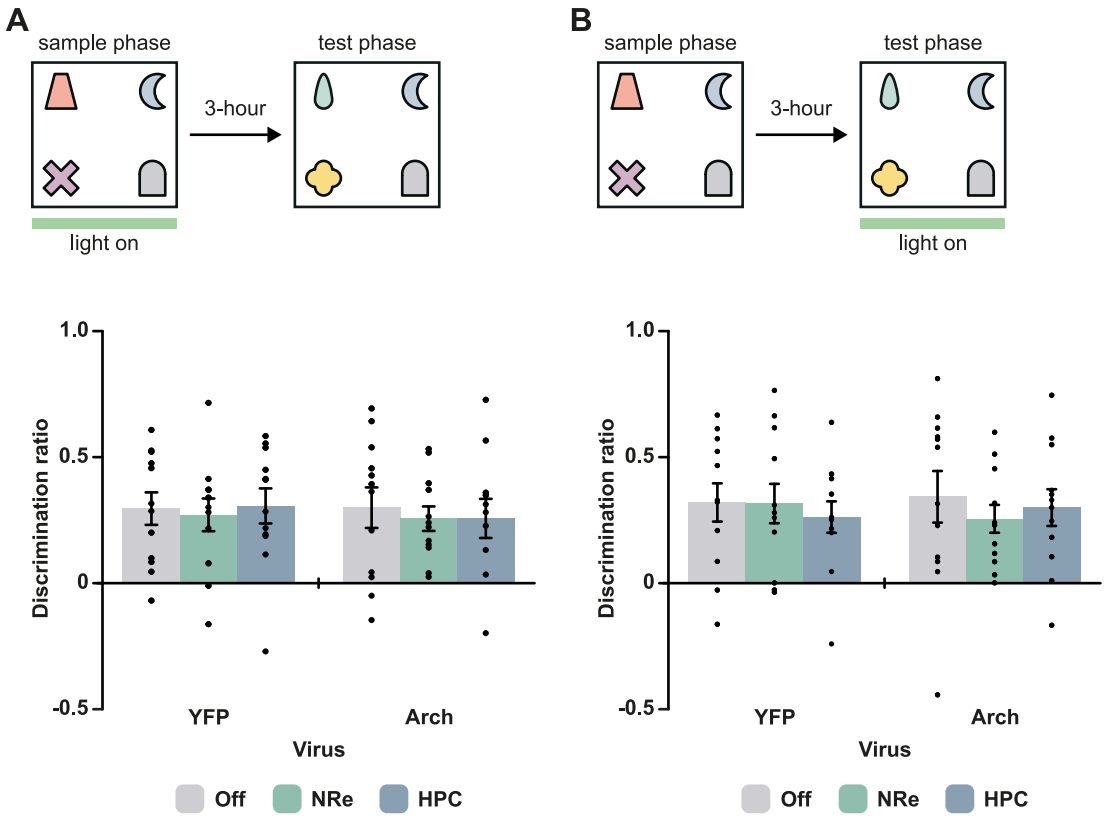

Figure 5.10. Inhibition of LC axonal terminals in HPC or NRe has no effect on object recognition memory. (A) Top, schematic of object recognition task. Light was delivered during the sample phase, as depicted by the green line. Bottom, both inhibition of LC to HPC and LC to NRe inputs did not impair memory. (B) Top, schematic of object recognition task. Light was delivered during the test phase, as depicted by the green line. Bottom, optogenetic inhibition of LC inputs into either the HPC or mPFC did not affect memory. Data are represented as mean ± SEM.

5.3.2.4.2 Inhibition during the retrieval phase of the object recognition task

Inhibition of LC to HPC or NRe input during the retrieval phase had no effect on object recognition memory (Figure 5.10B). Statistical analysis confirmed these observations (stimulation condition x virus interaction: ($F(2,44) = .343$, $p = .711$); main effect of stimulation condition: ($F(2,44) = .383$, $p = .684$); main effect of virus: ($F(1,22) < .001$, $p = .998$)). All animals demonstrated discrimination ratios significantly above chance levels (YFP Off: ($t(11) = 4.22$, $p = .001$); YFP NRe: ($t(11) = 4.04$, $p = .002$); YFP HPC: ($t(11) = 4.21$, $p = .001$); Arch Off: ($t(11) =$

3.35, p = .007); Arch NRe: (t(11) = 4.62, p = .001); Arch HPC: (t(11) = 4.11, p = .002)).

Overall object exploration during the sample phase did not significantly differ (stimulation condition x virus interaction: (F(2,44) = .919, p = .407); main effect of stimulation condition: (F(2,44) = 2.95, p = .063); main effect of virus: (F(1,22) = .033, p = .858)). Analysis of object exploration during the test phase did not reveal any significant differences (stimulation condition x virus interaction: (F(2,44) = .035, p = .966); main effect of stimulation condition: (F(2,44) = .623, p = .541); main effect of virus: (F(1,22) = .869, p = .361)) (Table 5.3).

Taken together, the lack of impairment following optogenetic inhibition of LC input to the NRe or HPC indicates that neither pathway is required for the retrieval of object recognition memory.

5.4 Discussion

The current chapter tested whether inputs from the noradrenergic nucleus, the LC, to the NRe or HPC are involved in associative recognition memory. An optogenetic approach was chosen, due to the unprecedented level of spatiotemporal specificity that this technique affords (Boyden et al., 2005), thus allowing for manipulation of specific LC pathways during distinct phases of recognition memory. As a first step, the specificity of two viral approaches was explored in order to achieve subtype-specific expression of noradrenergic neurons. It was demonstrated that both viral approaches (i.e., combinatorial viral technique and the PRSx8 virus) were unsuccessful in efficiently transducing noradrenergic LC neurons and their axonal projections. Thus, both viral approaches were rejected as options for the behavioural experiments. Instead, a virus in which the inhibitory opsin Arch, under the control of the CaMKII promoter was used. To this end, by inhibiting projections from the LC to the NRe and HPC during distinct phases of recognition memory processing it was revealed that LC to NRe projections are pivotal for the retrieval but not encoding of object-in-place memory, conversely, LC to HPC projections were found to be required for

the encoding but not retrieval of object-in-place memory - echoing the results from the pharmacological interventions conducted in Chapter 4. In addition, optogenetic inhibition of LC projections to either the NRe or HPC were demonstrated to not disrupt the encoding or retrieval of object recognition and object location memory.

5.4.1 Non-specific expression with the combinatorial viral vector approach

The combinatorial viral vector approach tested involved co-infusion of two viruses, AAV9-TH-Cre and AAV5-EF1a-DIO-eArch3.0-EYFP into the LC at various titres. An additional injection to target the VTA in one animal was also made. The combinatorial viral vector approach has been previously reported to be successful in targeting TH-positive neurons (Gompf et al., 2015; Stauffer et al., 2016). For instance, Stauffer et al. (2016) using the same TH-Cre virus that was used in the present study, found that 95% of virus expressing neurons were colocalised with TH-positive neurons, when viral injections were made into the VTA of monkeys and mice. Similarly, Gompf et al. (2015) using a TH-Cre virus (which contained a 2.5kb TH-promoter fragment) in combination with a Cre-dependent ChR2 or hM3Dq virus into the VTA or LC of rats, respectively, observed that 93% of virus expressing neurons demonstrated TH-immunoreactivity.

There are several possible reasons that may explain the discrepancy between the current observations and the abovementioned studies, such as differences in animal species, promoter size and viral titre. For instance, although the current study piloted the same parameters as Stauffer et al. (2016) (i.e., injection of the AAV9-TH-Cre into the VTA at a viral titre of 1×10^{12} particles of virus), the authors conducted their experiments in monkeys and mice while the current study used rats. To explore whether the discrepancies could be due to differences between species, additional piloting of the virus in mice is required. Another cause for the low levels of cell-type specific expression observed in the current chapter could be related to the size of the TH-promoter fragment that was inserted into the AAV9-TH-Cre virus. AAVs have a limited packaging capacity of 5kb (Grieger & Samulski, 2005), thus

due to the packaging limit of AAVs, partial fragments of cell-type specific promoters are often used, however, partial fragments of the promoter are typically less sensitive than the full promoter with the loss of key regulatory elements. Gompf et al. (2015), used a virus with the 2.5kb rat TH-promoter sequence, which is much larger than the TH-promoter fragment used in the present study and by Stauffer et al. (2016). It therefore seems possible that the low levels of cell-type specific expression achieved in the present study could be due to the small size of the TH-promoter fragment, and that perhaps specifically in rats and not other species (given that Stauffer et al. (2016) was able to achieve high levels of expression in monkeys and mice with the same 300bp TH-promoter used in the current study), that to achieve higher levels of subtype-specific expression, larger fragments of the TH-promoter in the viral construct are required.

The current study also manipulated the titre of the virus to increase the specificity of the virus. Previous evidence indicates that the specificity of cell-type specific viruses is often determined by the titre of the virus, such that the higher the titre of the virus the greater the number of genomic copies of a transgene enter the cell, resulting in weaker promoter activity and thus increasing the likelihood of off-target expression (Kakava-Georgiadou et al., 2019; Sjulson et al., 2016). However, it was found that decreasing viral titre did not impact specificity of virus expression, as a large majority of viral transduction was still observed in TH-negative cells.

Taken together, while the exact reason for the low percentage of transduced TH-positive neurons is unknown, comparison to previous studies indicates that perhaps the small fragment size of the TH-promoter fragment used in the current study may be the cause for non-specific expression in the rat brain. This possibility could be explored by directly comparing the degree of cell-type specific expression following injection into the rat brain of the TH-Cre virus with the 2.5kb TH-promoter sequence (Gompf et al., 2015) and the TH-Cre virus with the 300bp TH-promoter that was used in the present study.

5.4.2 Lack of axonal transduction with the PRSX8 virus

The second viral approach tested in the current chapter involved injection of a single virus with an AAV9 serotype, in which expression of the inhibitory opsin Arch was driven by the synthetic noradrenaline promoter, PRSx8. Thus, in contrast to the combinatorial approach, the PRSx8 promoter is driving the expression of Arch directly instead of Cre recombinase. Previous studies using viral vectors under the PRSx8 promoter with an AAV9 serotype at titre of 1×10^{12} particles of virus (as used in the present study), have indicated this is promoter results in robust transduction of noradrenergic neurons in the LC and their axonal projections, that are capable of eliciting effects at both the electrophysiological and behavioural level (Borodovitsyna et al., 2020; Campese et al., 2017; Giustino et al., 2019). While the current study managed to achieve almost 100% cell-type specific expression in LC-noradrenaline neurons, expression in axonal terminals was not achieved. In the current study, the animals were left to recover for 6 weeks, which based on previous literature using this promoter, serotype and titre combination, is sufficient time to observe axonal expression (Borodovitsyna et al., 2020; Campese et al., 2017; Giustino et al., 2019). It is therefore unclear why no expression in axonal terminals was achieved, however, as production of the virus was outsourced, factors such as production methods employed by the company (e.g. purification processes), may be the cause for the lack of axonal expression (Kakava-Georgiadou et al., 2019). Given that the aim of the current behavioural experiments is to inhibit axonal projections from the LC to the NRe and HPC using optogenetics, the virus containing the PRSx8 promoter was not used for further behavioural experiments.

5.4.3 Transgenic animals to achieve cell-type specificity

An alternative approach to target a specific subset of cells would be to use transgenic animals. In the present study, rats expressing Cre recombinase under the control of the TH promoter would be the most appropriate animal line to target the noradrenergic neurons of the LC. To achieve cell-type expression in Cre-driver transgenic animals,

a Cre-dependent AAV is often injected into the brain region of interest to transduce a specific cell subtype. However, variable degrees of selectivity have been reported in TH-Cre rats across studies (Quinlan et al., 2019; Witten et al., 2011), therefore additional piloting of viruses to find the optimal parameters to achieve high levels of specific expression would be required. Due to the significant extra time and resources required to optimise and use transgenic animals, they were not used in the present study.

5.4.4 CaMKII virus as an alternative approach to target locus coeruleus neurons

The current study used a virus under the CaMKII promoter to inhibit projections from the LC to the NRe and HPC. While the CaMKII virus is not ideal for the targeting of LC neurons, given that the LC contains excitatory neurons that co-express with noradrenergic neurons (Fung et al., 1994; Nakamura et al., 2000; Yang et al., 2021), the CaMKII virus still serves as a viable alternative to target the noradrenergic neurons of the LC. Indeed, the pilot experiments (data not shown) and histological analysis of the behavioural cohort conducted in the present study revealed that injection of the CaMKII virus into the LC was successful in targeting TH-positive neurons and their axonal projections to the NRe and HPC, unlike the virus containing the PRSx8 promoter which was only expressed in cell bodies and the combinatorial approach, which predominantly transduced TH-negative neurons. However, by using the CaMKII virus, precise targeting of the LC is sacrificed as CaMKII-positive neurons are also present in brain regions adjacent to the LC. Furthermore, some of these brain regions neighbouring the LC do send afferents to the NRe and HPC (Krout et al., 2002; Riley & Moore, 1981). For instance, brain regions which send afferents to the NRe and demonstrated viral expression are the parabrachial nucleus, laterodorsal tegmental nucleus, superior cerebellar peduncle (brachium conjunctivum), subcoeruleus nucleus (dorsal part) and dorsomedial tegmental area. For the HPC, only the lateral dorsal tegmental nucleus sends afferents to the HPC and demonstrated viral expression (Riley & Moore, 1981).

It should be noted that although viral expression was observed in these brain regions adjacent to the LC, expression was minimal and diffuse with the core of the injection centred in the LC. Moreover, given that the current optogenetic results mimicked the pharmacology results from Chapter 4, this strongly suggests that the results from the current behavioural study are specific to LC projections to the HPC and NRe.

Evidence suggests that most LC neurons are noradrenergic in nature (Schwarz & Luo, 2015) but as well as co-expression of glutamate in LC neurons (as discussed above) (Fung et al., 1994; Nakamura et al., 2000; Yang et al., 2021), the LC contains a subset of cells which also co-express other neurotransmitters and neuropeptides, such as galanin and Neuropeptide Y (Holets et al., 1988; McCall et al., 2015). Given the neurochemical diversity of LC neurons, it has been proposed that these subset of LC neurons which demonstrate immunoreactivity for these neurotransmitters and neuropeptides may subserve specialised functions (Schwarz & Luo, 2015). Thus, it was possible that by targeting the LC with the CaMKII virus, that only a subset of LC neurons would be targeted which may result in a different behavioural outcome to the pharmacological results reported in Chapter 4. However, based on the evidence in this thesis, this explanation seems unlikely, as the current optogenetic results using a CaMKII promoter echoes the pharmacological results found in Chapter 4. Furthermore, in another study, it was demonstrated that targeting of Gal-positive neurons in the LC (which only occupy a portion of LC neurons), resulted in similar functional consequences as stimulation of all the TH-positive neurons in the LC (McCall et al., 2015). Altogether, these findings suggest that although other neurotransmitters and neuropeptides are present in the LC, and only occupy a portion of LC neurons, they may not necessarily subserve a specialised function in recognition memory.

5.4.5 Optogenetic and pharmacologic techniques act as complementary tools

The current chapter utilised a viral construct which contained the inhibitory outward proton pump Arch. Given the well established inhibitory nature of Arch it is likely

that in the current chapter that the effect of Arch stimulation resulted in the desired silencing of neural activity in the pathways targeted. Moreover, given that the current optogenetic results recapitulated the pattern of results observed in Chapter 4, it provides further evidence that the current optogenetic setup resulted in pathway specific inhibition. However, it is important to note that because direct measures of neural activity were not conducted in the current chapter, there is a possibility that as well as the inhibitory effects in downstream structures, that excitatory or a mixture of excitatory and inhibitory effects also occurred. To ultimately determine the resultant net effect on neural activity following Arch stimulation, further experiments are required. For instance, one such approach could involve the use of c-fos immunohistochemistry (an indirect measure of neuronal activity) to histologically analyse the changes in c-fos expression in target brain structures following optogenetic stimulation (Benn et al., 2016; Zhu et al., 1996).

By employing an optogenetic approach in the current chapter, it builds on the findings of the previous chapter which employed pharmacological interventions. By utilising these complementary techniques in the current thesis, a more complete understanding of neural circuit function was provided. The pharmacological interventions identified the specific adrenergic receptors critical for mediating noradrenaline while the optogenetic experiments identified the precise pathways involved. In addition, given that optogenetic techniques have a higher degree of temporal specificity (millisecond range), compared to pharmacological manipulations (minutes to hours range). The optogenetic technique (given that the optogenetic results were in accordance with the pharmacology results), was able to fully confirm that the drugs infused in Chapter 4 were unlikely to interfere with other phases of memory processing than the current memory phase manipulated (see Section 4.4.4).

The optogenetic and pharmacology interventions conducted in the current thesis were performed separately in a different cohort of animals. However, perhaps a more appropriate strategy to fully corroborate the results would be to perform combined optogenetics and pharmacology in the same animal. For instance, future studies using opto-stimulation of LC axons in the NRe or HPC with concurrent infusion

of pharmacological agents to decrease noradrenaline release in the NRe or HPC would directly link the optogenetic and pharmacology results (Kempadoo et al., 2016; Takeuchi et al., 2016). Regardless, the current optogenetic results provide causal evidence that the LC was responsible for the behavioural effects observed in Chapter 4, revealing that distinct LC pathways are differentially involved in recognition memory. The implications of these results in relation to theories of LC function are discussed further in the general discussion (Section 6.3).

5.4.6 Locus coeruleus-noradrenaline and implications in NRe-associated behavioural functions

As stated in the general introduction (see Section 1.3), the LC-noradrenaline system has been implicated in a number of behavioural functions and an increase in LC firing has been observed in response to salient stimuli, during arousal, attention and more (Berridge, 2008; Sara, 2009; Schwarz & Luo, 2015). Given that the spontaneous recognition memory paradigm is neither stressful nor aversive, it seems that LC-noradrenaline may be directly involved in providing a salience signal to the NRe during object-in-place memory. For instance, as previously stated, LC neurons respond to salient novel stimuli and contexts by firing in a phasic manner that rapidly habituates over time (Vankov et al., 1995). Thus, release of noradrenaline from the LC to the NRe during a precise timepoint of the associative recognition memory task could act as a critical novelty induced salience signal to facilitate the NRe during memory retrieval (this proposal is discussed in more detail in Section 6). Moreover, release of noradrenaline in the NRe could act to promote on-going exploration of novelty (Beerling et al., 2011).

While the current thesis only provides a functional exploration of recognition memory, the NRe has also been shown to be involved in other behavioural functions that are modulated by the LC-noradrenaline system. For instance, a number of studies have demonstrated that the NRe has a critical role in fear memory (Troyner et al., 2018; Xu & Südhof, 2013). However, it is likely that noradreneraline provides differential modulation of the NRe during fear memory versus recognition memory.

For instance, instead of facilitating novelty-induced arousal that occurs during the low stress conditions of the recognition memory tasks, during the high threat and anxiety inducing conditions of the contextual fear conditioning paradigm, noradrenaline is likely to be involved in modulating aversive arousal in the NRe. Thus, it is likely that the effect of noradrenaline in the NRe is behavioural task-dependent. It evident that an important avenue for future research is to begin evaluation of the role of noradrenaline in the NRe in other behavioural functions that are associated with the NRe.

5.4.7 The locus coeruleus and its involvement in HPC-dependent recognition memory

In recent years, the notion that LC neurons are able to co-release both dopamine and noradrenaline has garnered a lot of attention (Kempadoo et al., 2016; McNamara & Dupret, 2017; Takeuchi et al., 2016). Initial studies demonstrated that upon LC electrical stimulation, both dopamine and noradrenaline release was observed in the cerebral cortex (Devoto & Flore, 2006). While more recent studies, combining optogenetic and pharmacologic techniques have demonstrated that projections from the LC to the HPC are capable of releasing dopamine as well as noradrenaline and that such release of dopamine is critical in modulating certain aspects of learning and memory (Kempadoo et al., 2016; McNamara & Dupret, 2017; Takeuchi et al., 2016; Wagatsuma et al., 2018). It was therefore a possibility in the current study, that following optogenetic manipulation of LC axons in the NRe or HPC, that dopamine and/or noradrenaline release would be inhibited. However, the current chapter found no indication for the involvement of dopamine following LC axonal terminal stimulation as the pattern of results observed in the optogenetic experiments is in accordance with the behavioural results from the pharmacological experiments conducted in Chapter 4. Moreover, this notion that the LC can co-release both noradrenaline and dopamine has only been found in a handful of brain regions, such as the cortex, striatum and HPC (Devoto & Flore, 2006; Devoto et al., 2005; Kempadoo et al., 2016; Takeuchi et al., 2016), therefore whether this proposal of

co-release of neurotransmitters applies to all brain regions under current investigation, such as the NRe, is unknown. Overall, the data in the current thesis indicate that the optogenetic results were a consequence of manipulation of the noradrenergic and not dopaminergic system.

In a previous study, (described in Section 4.4.2), Kempadoo et al. (2016) demonstrated that LC projections to the HPC are crucial for object location memory when tested at a 24-hour delay (Kempadoo et al., 2016). The current chapter adds to this finding, suggesting that the LC to HPC pathway has a delay-dependent involvement in the encoding of object location memory, such that the LC to HPC pathway is involved in the encoding of longer term (24-hour) but not shorter term (3-hour) object location memory.

In Chapter 4 (see Section 4.4.2), it was suggested that distinct neuromodulatory systems in the HPC are involved in distinct aspects of recognition memory, i.e., dopamine is required for the encoding of object location memory while noradrenaline is crucial for the encoding of object-in-place memory. Given that the current chapter provides causal evidence that noradrenaline originating from the LC is required for object-in-place memory and work by Kempadoo et al. (2016) indicates that the LC is the functional source of dopamine to the HPC during object-location memory, it seems that the previous proposal that dopaminergic and noradrenergic systems differentially modulate the HPC during different aspects of recognition memory should be updated to include the LC. Thus, it seems that dependent on the neurotransmitter released by the LC, the LC provides differential modulation of hippocampal function during recognition memory processing.

5.4.8 Conclusion

Overall, the current results demonstrate that distinct projections from the LC differentially contribute to different stages of recognition memory processing. Moreover, it was also demonstrated that the combinatorial viral approach and the PRSx8 virus piloted were not suitable tools to achieve both cell-type specific expression of noradrenergic neurons and efficiently transduce noradrenergic axonal terminals.

6 General Discussion

6.1 Overview of key findings

The experiments presented in this thesis had three aims: to re-evaluate the anatomy of the catecholaminergic system in the NRe; to explore the role of noradrenergic neurotransmission mediated via the adrenergic receptors in the NRe, HPC and mPFC in recognition memory; and to investigate the role of LC inputs to the NRe and HPC in recognition memory.

The results from Chapter 3 extended observations from previous studies demonstrating that the entire rostro-caudal axis of the NRe is innervated with catecholaminergic fibres. It was also revealed that the sole source of dopaminergic and noradrenergic inputs to the NRe originates from the A13 cell group and LC, respectively.

In Chapter 4 it was revealed that antagonism of α1- or agonism of α2-adrenergic receptors in the NRe selectively impaired the retrieval of associative recognition memory. Conversely, in the HPC, agonism of α2- or antagonism of β-adrenoceptors selectively impaired the encoding of associative recognition memory. However, in the mPFC, pharmacological manipulation of the adrenergic receptors did not disrupt object-in-place memory. Furthermore, it was also revealed that noradrenergic neurotransmission in the HPC was not necessary for object recognition or object location memory (for summary of results, see Table 6.1).

In Chapter 5 optogenetic inactivation of LC inputs to NRe significantly disrupted the retrieval of object-in-place memory but did not impair the acquisition. Inactivation of LC inputs to the HPC impaired the acquisition but not retrieval of object-in-place memory (for summary of results, see Table 6.1). In addition, it was also demonstrated that both LC projections to the NRe or HPC are not required for object location and object recognition memory.

Table 6.1. Summary of results following pharmacological or optogenetic manipulations presented in chapter 4 and 5, respectively, in the object-in-place task.

Brain region	Memory stage	Manipulation			
		Pharmacology			Optogenetic
		α1	α2	β	
NRe	Encoding	-	-	-	-
	Retrieval	x	x	-	x
HPC	Encoding	-	x	x	x
	Retrieval	-	-	-	-
mPFC	Encoding	-	-	-	N/A
	Retrieval	-	-	-	N/A

"x" indicates a memory impairment, and "-" indicates no effect.

6.2 Implications of noradrenergic modulation of the nucleus reuniens within brain circuits of associative recognition memory

Recent evidence employing chemogenetic and optogenetic tools have unravelled the precise anatomical pathways between the HPC, mPFC and NRe, involved in different memory stages of associative recognition memory (Barker et al., unpublished data). The authors revealed that projections from the mPFC to the NRe and NRe to the HPC are pivotal for the retrieval of object-in-place memory. Thus, the finding in this thesis that the adrenergic receptors in the NRe are only required for the retrieval of associative recognition memory may correspond to these retrieval-specific pathways reported by Barker et al. (unpublished data).

As highlighted in Section 1.2.3, anatomical data indicates that the mPFC projects strongly to the NRe (Jayachandran et al., 2019; Vertes et al., 2007). In addition, it has also been revealed that hippocampal projecting NRe neurons receive inputs

from the mPFC (Vertes et al., 2007). Moreover, as previously stated (see Section 3.4.5.2), LC afferents to the NRe seem to be well organised to target hippocampal projecting NRe neurons, as data from this thesis (see Chapter 3) and previous literature (Hoover & Vertes, 2012) have demonstrated that LC inputs to the NRe and hippocampal projecting NRe neurons are predominantly located in the rostral NRe. The anatomical arrangement highlighted above presents an emerging picture wherein corticothalamic and LC pathways could converge on hippocampal projecting NRe neurons, which may in turn have implications for the modulation of the retrieval of object-in-place memory. It is therefore proposed that during the test phase of the object-in-place task that novelty-related firing that is observed in LC neurons (Sara et al., 1994; Vankov et al., 1995) releases noradrenaline in the NRe. At the same time, information concerning the stored object-place representation in the mPFC is relayed to the NRe. Thus, the NRe acts to integrate external novelty cues with internally stored details about the previous representation and relay these signals as a unified output to the HPC. As a result, in the HPC, activation sequences in neuronal firing are initiated for the successful retrieval of the object-place association (Dolleman-van der Weel et al., 2019).

However, it is noteworthy to mention that it is currently unknown whether noradrenaline modulates NRe neurons directly or affects inputs to the NRe. Given that mPFC inputs to the NRe are glutamatergic and a recent in vivo electrophysiological experiment revealed that mPFC afferents can control the firing pattern of the NRe neurons (Jayachandran et al., 2019; Vertes et al., 2007; Zimmerman & Grace, 2018), it is possible that release of noradrenaline elicited by novelty, acts at the mPFC-NRe synapse. Under this model, activation of adrenergic receptors would induce glutamate release at mPFC-NRe synapses to enhance excitatory transmission. Such modulation of the mPFC-NRe input would act to facilitate integration of top-down and bottom-up signals in the NRe as suggested above (this proposed neural circuit is illustrated in Figure 6.1). However, whether mPFC afferents to the NRe are sensitive to modulation by noradrenaline in the first instance is not known. In addition, this hypothesis also relies on the fact that the mPFC-NRe-HPC pathway is involved in

the retrieval of object-in-place memory, which to date, has not been directly tested, it has only been indirectly suggested through manipulation of the separate pathways, (i.e., mPFC to NRe and NRe to HPC) (Barker et al., unpublished data).

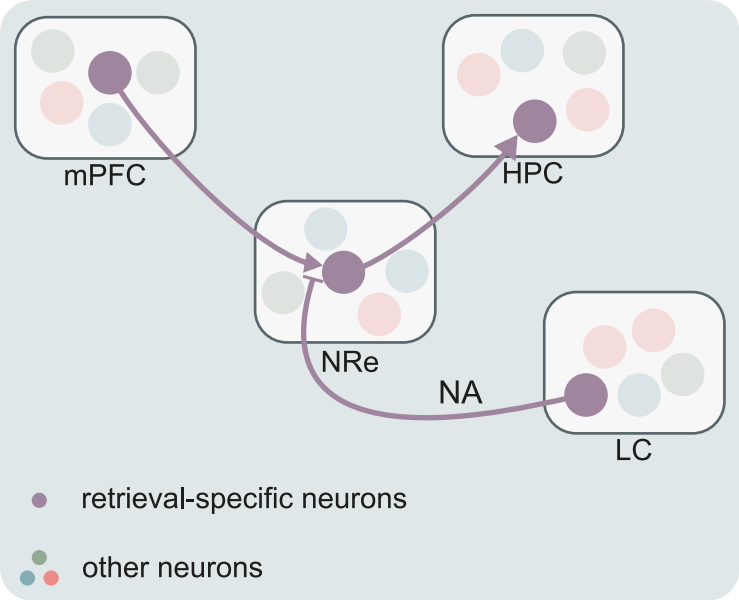

Figure 6.1. Schematic diagram of proposed neural circuit by which noradrenaline modulates retrieval-specific pathways during associative recognition memory. During the retrieval of long-term associative recognition memory, noradrenaline, originating from the LC acts on mPFC-NRe synapses to enhance synaptic transmission and thus affect hippocampal projecting NRe neurons.

Alternatively, it is also possible that LC-noradrenaline directly modulates NRe neurons. For instance, it has been demonstrated in the guinea pig and cat thalamus, in other thalamic nuclei (the lateral geniculate nucleus, the medial geniculate nucleus, thalamic reticular nucleus (TRN), anteroventral medial thalamic nucleus and paratenial nucleus), that bath application of noradrenaline in thalamic slices reduced burst firing and promoted tonic firing and that these effects were intrinsic to the thalamus and not due to synaptic input (McCormick & Prince, 1988). In addition, in a in vivo electrophysiology study, it was revealed that LC activation of the ventral posteromedial nucleus (VPm) and the TRN of the thalamus enhances information transmission in the VPm and TRN by directly altering intrinsic firing properties of these thalamic nuclei (Rodenkirch et al., 2019). More specifically, Rodenkirch et

al. (2019) demonstrated that LC-noradrenaline induces a switch in neural firing in the VPm and TRN, causing firing to change from a burst to tonic mode. Moreover, LC-induced changes in neural firing of the thalamus were demonstrated to be dependent on modulation of T-type calcium channels (Rodenkirch et al., 2019). The state of thalamic neuronal firing has been proposed to be governed by T-type calcium channels (i.e., burst and tonic modes of firing are associated with the activation and suppression of T-type calcium channel activity, respectively). In addition, classical models have suggested that burst firing in the thalamus represents a "wake-up call" while tonic firing acts to facilitate information transfer (Sara et al., 1994; Sherman, 2001; Steriade & Llinás, 1988). Taken the above into consideration, it is therefore possible that activation of LC-noradrenaline in the NRe blocks T-type calcium channels, which are found in the NRe (Walsh et al., 2017), and causes a decrease in NRe burst firing. Thus, this change in NRe firing to a more tonic pattern of activity could act to enhance information transmission in the NRe. Such a mechanism could enable the NRe to integrate and amplify signals related to details about the stored object-spatial association incoming from the mPFC and relay this information to the HPC to promote the retrieval of object-in-place memory. However, whether these changes in neuron firing reported above in other thalamic nuclei following LC-noradrenaline activation can be generalised to the NRe remains to be determined.

As previously mentioned (see Section 1.2.2), the NRe contains the calcium binding proteins, CB and CR (Arai et al., 1994; Bokor et al., 2002; Viena et al., 2021), and it has been recently proposed that dependent on the neurochemical identity of thalamic midline neurons (NRe included), they are differentially involved in different stages of memory processing (Lara-Vásquez et al., 2016). This notion was based on the observation that CR-positive and CR-negative neurons of the midline thalamus display different firing properties during distinct stages of hippocampal network oscillations that have been implicated with different memory stages (i.e., hippocampal theta with memory encoding and sharp wave-ripples with memory consolidation). Thus, it is possible that cellular heterogeneity in the NRe provides a means by which a subpopulation of NRe neurons could be specifically engaged during

the retrieval of associative recognition memory. However, the exact neurochemical composition of these NRe neurons involved in retrieval is not known.

Taken together, it is evident that more experimentation is required to provide a more detailed understanding of the underlying mechanisms of noradrenergic neuromodulation of the NRe and its input pathways. Such experiments would provide greater insight into how noradrenaline facilitates the mPFC-NRe-HPC memory retrieval circuit (see Section 6.4 for future experiments).

6.3 Manipulation of noradrenergic neurotransmission and projections from the locus coeruleus result in region-specific effects

The experiments presented in this thesis revealed that noradrenaline, originating from the LC has different roles in the NRe, HPC and mPFC during associative recognition memory. It was demonstrated that LC-noradrenaline in the HPC is crucial for the acquisition of associative recognition memory, while LC-noradrenaline in the NRe is specifically involved in the retrieval of associative object-in-place recognition memory. In contrast, LC-noradrenaline in the mPFC has no effect on memory performance. Thus, it seems that the region-specific effects observed at distinct phases of associative recognition memory can be explained at the level of LC processing.

Classical theories of LC function consider the LC as a homogeneous population of broadly projecting neurons which predominantly sends outputs via axon collaterals. Accordingly, the LC was proposed to provide a global signal that alters brain-wide noradrenaline concentration and functional specificity is achieved by local processes within the target brain structure (Agster et al., 2013; Berridge, 2008; Chandler et al., 2019; Loughlin et al., 1986; Uematsu et al., 2015; Uematsu et al., 2017). On the other hand, recent studies (at both the anatomical and functional level) indicate that the LC is a heterogenous brain region where separate populations of LC neurons

send selective projections to target brain structures to provide functional specificity (Borodovitsyna et al., 2020; Chandler et al., 2019; Chandler et al., 2014; Chandler & Waterhouse, 2012; Giustino et al., 2019; Hirschberg et al., 2017; Ranjbar-Slamloo & Fazlali, 2020; Totah et al., 2019; Uematsu et al., 2015; Uematsu et al., 2017). However, another recent experiment using a genetic anatomical technique revealed that although the majority of LC neurons demonstrate projection specificity, some LC neurons were found to also send projections to many brain regions (Kebschull et al., 2016), thus it is becoming apparent that the LC cannot be classed as either simply homogeneous or heterogeneous but demonstrates both patterns of cell organisation and is therefore capable of providing both global and targeted modulation. Further supporting this notion, recent evidence employing anatomical tract tracing techniques have revealed that most, but not all, LC projections to the mPFC and basolateral amygdala (BLA) arise from a different subpopulation of LC neurons and optogenetic inactivation showed that these distinct afferents from the LC to the mPFC or BLA are implicated in different aspects of fear conditioning: fear extinction or fear learning, respectively (Uematsu et al., 2017). In addition, the authors also demonstrate, using in vivo electrophysiological recordings, that during exposure to an intense aversive stimulus, elicited by an unconditioned footshock, global LC activation is observed, however, during more refined cognitive processes (such as during fear extinction and learning phases) distinct sub-populations of LC neurons are activated. Accordingly, the ability of LC to change from a global firing pattern to a more discrete mode of firing has been termed context-dependent modular coding (Likhtik & Johansen, 2019; Poe et al., 2020).

In regard to the results in this thesis, the finding that LC noradrenaline has brain region-specific effects at specific stages of associative recognition memory could be explained by any one of the theories of LC function mentioned above (i.e., a homogeneous LC where region-specific effects are due to local processes within the target brain region or a heterogeneous LC/ mixed population of homogenous and heterogeneous LC neurons where distinct LC modules with specific efferent connectivity provide targeted modulation). Interestingly, recent in vitro electrophysiological

evidence has revealed that distinct groups of LC neurons project to the ventral HPC and mPFC and that these populations demonstrate differential physiological properties when the $\alpha 2$ adrenergic agonist clonidine is bath applied (Wagner-Altendorf et al., 2019). Thus, it is likely that dorsal HPC (as studied in the present thesis), similar to the ventral HPC (as demonstrated by Wagner-Altendorf et al. (2019)), receives afferents from a separate population of LC neurons to that of the mPFC. Therefore, suggesting that heterogeneity within the LC may provide an explanation for the distinct role of LC-noradrenaline in the HPC and mPFC for object-in-place memory.

However, as mentioned above, the LC cannot be simply classed as a heterogeneous structure as it has also been shown to provide global modulation under certain behavioural contexts. Thus, how can the ability of the LC to provide both global and discrete modes of modulation be incorporated to explain the underlying mechanisms of LC-noradrenergic modulation of associative recognition memory? As previously mentioned, it has been demonstrated that when an animal is first exposed to a novel stimulus or context, that the majority of LC neurons initially respond to novelty with a brief phasic discharge which rapidly habituates (Sara et al., 1994; Vankov et al., 1995). Interestingly, although Vankov et al. (1995) suggests that in general, LC neurons display diminished firing rates upon second exposure to the novel stimulus, the authors do note (but do not fully consider) the heterogeneous firing patterns of LC neurons. The authors state that compared to the first exposure, that during the second exposure to the novel stimulus that although the majority of LC neurons show a weak response, some neurons completely cease firing and other neurons demonstrate equally robust firing responses. Together, this indicates that during exposure to novelty and subsequent exploration, as occurs during the spontaneous recognition memory tasks, LC neurons display differential modes of firing – a homogeneous mode where almost all LC neurons respond during first exposure to the novel stimulus and a heterogeneous pattern of neural responses following second exposure to the stimulus. Thus, these observations could be consistent with the context-dependent modular coding view of the LC described above (Likhtik & Johansen, 2019; Poe et al.,

2020). Under this framework, it is possible therefore that during initial exposure to novelty, as occurs in the object-in-place recognition memory task during both the sample phase when all objects encountered are novel and the test phase when specific object configurations are novel, that global activation of the LC occurs, sending a brain-wide noradrenaline signal. However, following this initial exposure and during continued exploration of the objects, distinct LC modules become activated at different timescales, such that LC neurons that project to either the HPC or NRe are differentially engaged in the sample or test phase of the object-in-place task to support the encoding or retrieval of associative recognition memory, respectively (this hypothetical model is illustrated in Figure 6.2).

While the literature reviewed suggests that the findings of this thesis are largely in accordance with the context-dependent modulation model of LC neuromodulation. It is important to note that this proposal is purely speculative as even basic questions, such as the anatomical organisation of LC afferents to the dorsal HPC, mPFC, and NRe, have not been answered. Thus, to test this proposed framework of LC-noradrenergic modulation of associative recognition memory, further experiments utilising anatomical, electrophysiological and behavioural techniques are required (see Section 6.4 for future experiments).

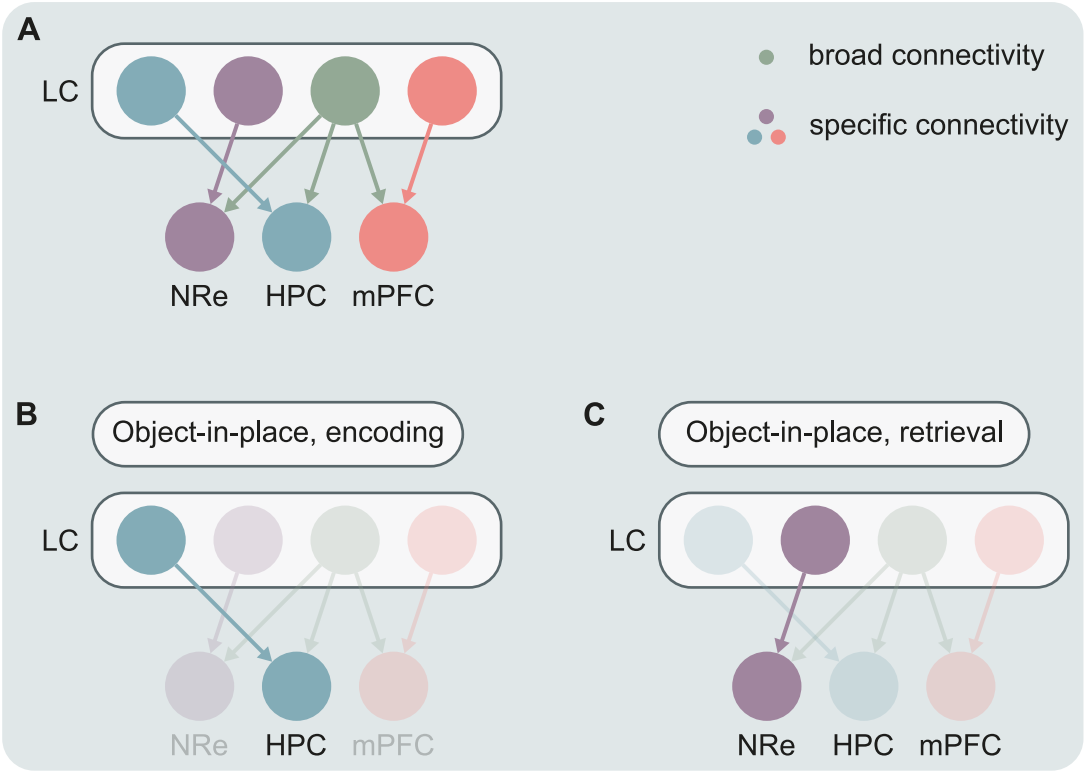

Figure 6.2. Hypothetical model for context-dependent modulation of associative recognition memory by the LC. The context-dependent modulation model proposes that some LC neurons display a broad pattern of connectivity and provide afferents to many brain regions, while some LC neurons project to a specific brain region. This anatomical arrangement allows the LC to provide both global and targeted modulation, respectively. In the context of recognition memory processing, it is proposed that upon initial exposure to a novel stimulus, populations of both broadly projecting LC neurons and afferent specific LC neurons are activated and thus capable of transmitting a global noradrenaline signal (A). However, during continued exploration of the objects, distinct LC subpopulations become active that engage specific afferents for targeted noradrenergic modulation. Thus, during the encoding of associative recognition memory, LC neurons projecting to the HPC are active (B), while during memory retrieval, LC neurons projecting to the NRe are active (C). Figure adapted from Poe et al. (2020) and Likhtik & Johansen (2019).

6.4 Future directions

The experiments in this thesis provide the first steps into understanding the catecholaminergic system in the NRe and the functional role of noradrenergic modulation

of the NRe, HPC and mPFC in recognition memory. In doing so, questions have arisen from these results that warrant further investigation. While not a comprehensive list, a number of further experiments are suggested below:

- Experiments revealed that the origin of dopaminergic input to the NRe arises from the A13 cell group, thus further experiments should functionally investigate the role of the dopaminergic system in the NRe in recognition memory. Further studies should firstly focus on characterising the distribution of the D1-like and D2-like receptors in the rat NRe before functional analysis is conducted. Behavioural studies could involve combined optogenetic and pharmacological manipulations during different times points of the spontaneous recognition memory tasks. Such experiments would involve opto-stimulation of A13 projections to the NRe with intra-NRe infusions of D1-like or D2-like antagonists. These experiments would reveal the specific dopamine receptors involved in mediating dopamine release from the A13 cell group in the NRe during distinct phases of recognition memory.

- Additional experiments employing in vitro electrophysiological techniques should also be performed in order to characterise the neurophysiological effects of noradrenaline, mediated via the adrenoceptors, in the NRe. Moreover, it would also be interesting to determine whether rostro-caudal differences exist in the NRe at the cellular level given that the present thesis indicates that the rostral NRe receives a denser noradrenergic input. In addition, to investigate whether mPFC-NRe synapses are sensitive to adrenergic modulation (see Section 6.2), an optogenetic approach could be employed. This would involve injection of an anterogradely transported virus expressing an excitatory opsin (such as channelrhodopsin-2; ChR2) into the mPFC and preparing acute NRe slices. Opto-stimulation of mPFC terminals in the NRe combined with bath application of adrenergic agonists and antagonists would reveal whether adrenoceptors modulate mPFC-NRe synapses.

- The optogenetic experiments performed in the current study should be repeated

using a cell-type specific approach. As previously stated, the current use of a virus under the CaMKII promoter is not the ideal virus to target the LC. Therefore future experiments should involve the use of approaches that can achieve cell-type specificity, such as the readily available TH-Cre transgenic rat line (Witten et al., 2011).

- As a first step to determine whether theories of LC function regarding discrete/ global modes of modulation are applicable to neural circuits involved in recognition memory, an anatomical approach should be employed. The anatomical study would determine whether, and to what extent, LC neurons send collateralised projections or display projection specificity to the NRe, HPC and mPFC. This could be achieved by pairwise injection of retrograde tracers/ viruses into the NRe, HPC and/or mPFC and quantifying the presence of double-labelled and single-labelled cells in the LC.

- Another avenue for future experiments would be to utilise newly developed technologies that can measure neurotransmitter release with a high temporal resolution (millisecond range) in the awake behaving animal, such as the G protein-coupled receptor-activation-based (GPCR) neurotransmitter sensors (Feng et al., 2019; Sun et al., 2020). Utilisation of the noradrenaline based GPCR sensor ($GRAB_{NE}$) (Feng et al., 2019), combined with fibre photometry would allow measurement of the dynamics of noradrenaline release in the NRe, HPC and LC, simultaneously, during the sample and test phase of the object-in-place task. In addition, the $GRAB_{NE}$ sensor would enable one to visualise in real-time the effect of LC optogenetic perturbation on noradrenaline release. Moreover, the use of dual-colour fibre photometry would allow simultaneous measurement of dopamine and noradrenaline release (using a red fluorescent GRAB dopamine sensor ($GRAB_{DA}$) (Sun et al., 2020) and green fluorescent $GRAB_{NE}$ sensor), and thus allow direct visualisation of the precise conditions during behaviour in which release of dopamine and/or noradrenaline, from the LC, occurs in certain brain regions (e.g., in the hippocampus during object

location memory).

6.5 Conclusion

The anatomical and functional investigation of the catecholaminergic system in the NRe suggests that the NRe receives a more substantial catecholaminergic input than previously described. In addition, the NRe was found to receive its dopaminergic and noradrenergic inputs from the A13 cell group and LC, respectively. At the functional level, noradrenergic neurotransmission in the NRe and projections from the LC to the NRe were found to be important for the retrieval of object-in-place memory. Together, these results further confirm the importance of the NRe in neural circuits in associative recognition memory and demonstrates that noradrenergic modulation of the NRe is critical for such process.

In addition to functional analysis of the NRe, experiments conducted in this thesis analysed the function of noradrenergic neurotransmission in the HPC and mPFC. These experiments revealed no apparent role for noradrenaline in the mPFC in associative recognition memory, while in the HPC, noradrenergic neurotransmission in the HPC and projections from the LC to the HPC were found to be specifically involved in the acqusition but not retrieval of object-in-place memory.

Overall, these differential effects in the NRe, HPC and mPFC at distinct time points of object-in-place memory processing, following manipulation of the noradrenergic system or projections from the LC, support the emerging view that modularity within the LC-noradrenaline system may explain these region-specific effects.

References

Adlam, A.-L. R., Malloy, M., Mishkin, M., & Vargha-Khadem, F. (2009). Dissociation between recognition and recall in developmental amnesia. *Neuropsychologia*, *47*(11), 2207–2210.

Aggleton, J. P., & Nelson, A. J. (2020). Distributed interactive brain circuits for object-in-place memory: A place for time? *Brain and Neuroscience Advances*, *4*, 2398212820933471.

Agster, K. L., Mejias-Aponte, C. A., Clark, B. D., & Waterhouse, B. D. (2013). Evidence for a regional specificity in the density and distribution of noradrenergic varicosities in rat cortex. *Journal of Comparative Neurology*, *521*(10), 2195–2207.

Ainge, J. A., Heron-Maxwell, C., Theofilas, P., Wright, P., de Hoz, L., & Wood, E. R. (2006). The role of the hippocampus in object recognition in rats: Examination of the influence of task parameters and lesion size. *Behavioural brain research*, *167*(1), 183–195.

Alexander, R. W., Davis, J. N., & Lefkowitz, R. J. (1975). Direct identification and characterisation of β-adrenergic receptors in rat brain. *Nature*, *258*(5534), 437–440.

Ameen-Ali, K., Easton, A., & Eacott, M. (2015). Moving beyond standard procedures to assess spontaneous recognition memory. *Neuroscience & Biobehavioral Reviews*, *53*, 37–51.

Arai, R., Jacobowitz, D. M., & Deura, S. (1994). Distribution of calretinin, calbindin-d28k, and parvalbumin in the rat thalamus. *Brain research bulletin*, *33*(5), 595–614.

Arnsten, A. F. (1998). Catecholamine modulation of prefrontal cortical cognitive function. *Trends in cognitive sciences*, *2*(11), 436–447.

Arnsten, A. F., Mathew, R., Ubriani, R., Taylor, J. R., & Li, B.-M. (1999). α-1 noradrenergic receptor stimulation impairs prefrontal cortical cognitive function. *Biological psychiatry*, *45*(1), 26–31.

Aston-Jones, G., & Waterhouse, B. (2016). Locus coeruleus: From global projection system to adaptive regulation of behavior. *Brain research*, *1645*, 75–78.

Aston-Jones, G., Zhu, Y., & Card, J. P. (2004). Numerous gabaergic afferents to locus ceruleus in the pericerulear dendritic zone: Possible interneuronal pool. *Journal of Neuroscience*, *24*(9), 2313–2321.

Atlas, D., Steer, M. L., & Levitzki, A. (1974). Stereospecific binding of propranolol and catecholamines to the β-adrenergic receptor. *Proceedings of the National Academy of Sciences*, *71*(10), 4246–4248.

Atzori, M., Cuevas-Olguin, R., Esquivel-Rendon, E., Garcia-Oscos, F., Salgado-Delgado, R. C., Saderi, N., Miranda-Morales, M., Treviño, M., Pineda, J. C., & Salgado, H. (2016). Locus ceruleus norepinephrine release: A central regulator of cns spatio-temporal activation? *Frontiers in synaptic neuroscience*, *8*, 25.

Ayano, G. (2016). Dopamine: Receptors, functions, synthesis, pathways, locations and mental disorders: Review of literatures. *J Ment Disord Treat*, *2*(120), 2.

Baddeley, A., Vargha-Khadem, F., & Mishkin, M. (2001). Preserved recognition in a case of developmental amnesia: Implications for the acaquisition of semantic memory? *Journal of Cognitive Neuroscience*, *13*(3), 357–369.

Barker, G. R., Banks, P. J., Scott, H., Ralph, G. S., Mitrophanous, K. A., Wong, L.-F., Bashir, Z. I., Uney, J. B., & Warburton, E. C. (2017). Separate elements of episodic memory subserved by distinct hippocampal–prefrontal connections. *Nature neuroscience*, *20*(2), 242–250.

Barker, G. R., Bird, F., Alexander, V., & Warburton, E. C. (2007). Recognition memory for objects, place, and temporal order: A disconnection analysis of the role of the medial prefrontal cortex and perirhinal cortex. *Journal of Neuroscience*, *27*(11), 2948–2957.

Barker, G. R., & Warburton, E. C. (2009). Critical role of the cholinergic system for object-in-place associative recognition memory. *Learning & Memory*, *16*(1), 8–11.

Barker, G. R., & Warburton, E. C. (2011). When is the hippocampus involved in recognition memory? *Journal of Neuroscience*, *31*(29), 10721–10731.

Barker, G. R., & Warburton, E. C. (2018). A critical role for the nucleus reuniens in long-term, but not short-term associative recognition memory formation. *Journal of Neuroscience*, *38*(13), 3208–3217.

Bastin, C., Linden, M. V. d., Charnallet, A., Denby, C., Montaldi, D., Roberts, N., & Andrew, M. R. (2004). Dissociation between recall and recognition memory performance in an amnesic patient with hippocampal damage following carbon monoxide poisoning. *Neurocase*, *10*(4), 330–344.

Beerling, W., Koolhaas, J., Ahnaou, A., Bouwknecht, J., de Boer, S., Meerlo, P., & Drinkenburg, W. (2011). Physiological and hormonal responses to novelty exposure in rats are mainly related to ongoing behavioral activity. *Physiology & behavior*, *103*(3-4), 412–420.

Bell, A. H., & Bultitude, J. H. (2018). Methods matter: A primer on permanent and reversible interference techniques in animals for investigators of human neuropsychology. *Neuropsychologia*, *115*, 211–219.

Benn, A., Barker, G. R., Stuart, S. A., Roloff, E. v. L., Teschemacher, A. G., Warburton, E. C., & Robinson, E. S. (2016). Optogenetic stimulation of prefrontal glutamatergic neurons enhances recognition memory. *Journal of Neuroscience*, *36*(18), 4930–4939.

Bentivoglio, M., & Morelli, M. (2005). Chapter i the organization and circuits of mesencephalic dopaminergic neurons and the distribution of dopamine receptors in the brain. *Handbook of chemical neuroanatomy* (pp. 1–107). Elsevier.

Bergles, D. E., Doze, V. A., Madison, D. V., & Smith, S. J. (1996). Excitatory actions of norepinephrine on multiple classes of hippocampal ca1 interneurons. *Journal of Neuroscience*, *16*(2), 572–585.

Berridge, C. W. (2008). Noradrenergic modulation of arousal. *Brain research reviews*, *58*(1), 1–17.

Berridge, C. W., & Spencer, R. C. (2016). Differential cognitive actions of norepinephrine a2 and a1 receptor signaling in the prefrontal cortex. *Brain research*, *1641*, 189–196.

Berridge, C. W., & Waterhouse, B. D. (2003). The locus coeruleus–noradrenergic system: Modulation of behavioral state and state-dependent cognitive processes. *Brain research reviews*, *42*(1), 33–84.

Birnbaum, S., Gobeske, K. T., Auerbach, J., Taylor, J. R., & Arnsten, A. F. (1999). A role for norepinephrine in stress-induced cognitive deficits: α-1-adrenoceptor mediation in the prefrontal cortex. *Biological psychiatry*, *46*(9), 1266–1274.

Björklund, A., & Dunnett, S. B. (2007). Dopamine neuron systems in the brain: An update. *Trends in neurosciences*, *30*(5), 194–202.

Björklund, A., Moore, R. Y., Nobin, A., & Stenevi, U. (1973). The organization of tubero-hypophyseal and reticulo-infundibular catecholamine neuron systems in the rat brain. *Brain research*, *51*, 171–191.

Blackstad, T. W., Fuxe, K., & Hökfelt, T. (1967). Noradrenaline nerve terminals in the hippocampal region of the rat and the guinea pig. *Zeitschrift für Zellforschung und Mikroskopische Anatomie*, *78*(4), 463–473.

Bokor, H., Csáki, Á., Kocsis, K., & Kiss, J. (2002). Cellular architecture of the nucleus reuniens thalami and its putative aspartatergic/glutamatergic projection to the hippocampus and medial septum in the rat. *European Journal of Neuroscience*, *16*(7), 1227–1239.

Bolton, A. D., Murata, Y., Kirchner, R., Kim, S.-Y., Young, A., Dang, T., Yanagawa, Y., & Constantine-Paton, M. (2015). A diencephalic dopamine source provides input to the superior colliculus, where d1 and d2 receptors segregate to distinct functional zones. *Cell reports*, *13*(5), 1003–1015.

Booze, R. M., Crisostomo, E. A., & Davis, J. N. (1993). Beta-adrenergic receptors in the hippocampal and retrohippocampal regions of rats and guinea pigs: Autoradiographic and immunohistochemical studies. *Synapse*, *13*(3), 206–214.

Borodovitsyna, O., Duffy, B. C., Pickering, A. E., & Chandler, D. J. (2020). Anatomically and functionally distinct locus coeruleus efferents mediate opposing effects on anxiety-like behavior. *Neurobiology of Stress*, *13*, 100284.

Bouthenet, M.-L., Souil, E., Martres, M.-P., Sokoloff, P., Giros, B., & Schwartz, J.-C. (1991). Localization of dopamine d3 receptor mrna in the rat brain using in situ hybridization histochemistry: Comparison with dopamine d2 receptor mrna. *Brain research*, *564*(2), 203–219.

Bowles, B., Crupi, C., Mirsattari, S. M., Pigott, S. E., Parrent, A. G., Pruessner, J. C., Yonelinas, A. P., & Köhler, S. (2007). Impaired familiarity with preserved recollection after anterior temporal-lobe resection that spares the hippocampus. *Proceedings of the National Academy of Sciences*, *104*(41), 16382–16387.

Boyajian, C., Loughlin, S., & Leslie, F. (1987). Anatomical evidence for alpha-2 adrenoceptor heterogeneity: Differential autoradiographic distributions of [3h] rauwolscine and [3h] idazoxan in rat brain. *Journal of Pharmacology and Experimental Therapeutics*, *241*(3), 1079–1091.

Boyden, E. S., Zhang, F., Bamberg, E., Nagel, G., & Deisseroth, K. (2005). Millisecond-timescale, genetically targeted optical control of neural activity. *Nature neuroscience*, *8*(9), 1263–1268.

Breton-Provencher, V., & Sur, M. (2019). Active control of arousal by a locus coeruleus gabaergic circuit. *Nature neuroscience*, *22*(2), 218–228.

Broadbent, N. J., Gaskin, S., Squire, L. R., & Clark, R. E. (2010). Object recognition memory and the rodent hippocampus. *Learning & memory*, *17*(1), 5–11.

Brown, M. W., & Aggleton, J. P. (2001). Recognition memory: What are the roles of the perirhinal cortex and hippocampus? *Nature Reviews Neuroscience*, *2*(1), 51–61.

Buzsáki, G., & da Silva, F. L. (2012). High frequency oscillations in the intact brain. *Progress in neurobiology*, *98*(3), 241–249.

Bylund, D. (2005). Adrenergic receptors: Historical perspectives from the 20th century. *The Adrenergic Receptors in the 21st Century, edited by Perez DM. Totowa: Humana*, 3–21.

Bylund, D., & Snyder, S. H. (1976). Beta adrenergic receptor binding in membrane preparations from mammalian brain. *Molecular pharmacology*, *12*(4), 568–580.

Caetano, M. S., Jin, L. E., Harenberg, L., Stachenfeld, K. L., Arnsten, A. F., & Laubach, M. (2013). Noradrenergic control of error perseveration in medial prefrontal cortex. *Frontiers in integrative neuroscience*, *6*, 125.

Cain, R. E., Wasserman, M. C., Waterhouse, B. D., & McGaughy, J. A. (2011). Atomoxetine facilitates attentional set shifting in adolescent rats. *Developmental cognitive neuroscience*, *1*(4), 552–559.

Calzada, B. C., & de Artiñano, A. A. (2001). Alpha-adrenoceptor subtypes. *Pharmacological Research*, *44*(3), 195–208.

Campese, V. D., Soroeta, J. M., Vazey, E. M., Aston-Jones, G., LeDoux, J. E., & Sears, R. M. (2017). Noradrenergic regulation of central amygdala in aversive pavlovian-to-instrumental transfer. *eneuro*, *4*(5).

Carli, M., Robbins, T., Evenden, J., & Everitt, B. (1983). Effects of lesions to ascending noradrenergic neurones on performance of a 5-choice serial reaction task in rats; implications for theories of dorsal noradrenergic bundle function based on selective attention and arousal. *Behavioural brain research*, *9*(3), 361–380.

Cassel, J.-C., De Vasconcelos, A. P., Loureiro, M., Cholvin, T., Dalrymple-Alford, J. C., & Vertes, R. P. (2013). The reuniens and rhomboid nuclei: Neuroanatomy, electrophysiological characteristics and behavioral implications. *Progress in neurobiology*, *111*, 34–52.

Cerpa, J.-C., Marchand, A. R., & Coutureau, E. (2019). Distinct regional patterns in noradrenergic innervation of the rat prefrontal cortex. *Journal of chemical neuroanatomy*, *96*, 102–109.

Chandler, D. J., Jensen, P., McCall, J. G., Pickering, A. E., Schwarz, L. A., & Totah, N. K. (2019). Redefining noradrenergic neuromodulation of behavior: Impacts of a modular locus coeruleus architecture. *Journal of Neuroscience*, *39*(42), 8239–8249.

Chandler, D. J., Gao, W.-J., & Waterhouse, B. D. (2014). Heterogeneous organization of the locus coeruleus projections to prefrontal and motor cortices. *Proceedings of the National Academy of Sciences*, *111*(18), 6816–6821.

Chandler, D. J., & Waterhouse, B. D. (2012). Evidence for broad versus segregated projections from cholinergic and noradrenergic nuclei to functionally and anatomically discrete subregions of prefrontal cortex. *Frontiers in behavioral neuroscience*, *6*, 20.

Chao, O. Y., de Souza Silva, M. A., Yang, Y.-M., & Huston, J. P. (2020). The medial prefrontal cortex-hippocampus circuit that integrates information of object, place and time to construct episodic memory in rodents: Behavioral, anatomical and neurochemical properties. *Neuroscience & Biobehavioral Reviews*, *113*, 373–407.

Cholvin, T., Loureiro, M., Cassel, R., Cosquer, B., Geiger, K., Nogueira, D. D. S., Raingard, H., Robelin, L., Kelche, C., de Vasconcelos, A. P., & Cassel, J.-C. (2013). The ventral midline thalamus contributes to strategy shifting in a memory task requiring both prefrontal cortical and hippocampal functions. *Journal of Neuroscience*, *33*(20), 8772–8783.

Churchwell, J. C., & Kesner, R. P. (2011). Hippocampal-prefrontal dynamics in spatial working memory: Interactions and independent parallel processing. *Behavioural brain research*, *225*(2), 389–395.

Cipolotti, L., Bird, C., Good, T., Macmanus, D., Rudge, P., & Shallice, T. (2006). Recollection and familiarity in dense hippocampal amnesia: A case study. *Neuropsychologia*, *44*(3), 489–506.

Clark, R. E., Zola, S. M., & Squire, L. R. (2000). Impaired recognition memory in rats after damage to the hippocampus. *Journal of Neuroscience*, *20*(23), 8853–8860.

Cohen, S. J., Munchow, A. H., Rios, L. M., Zhang, G., Ásgeirsdóttir, H. N., & Stackman Jr, R. W. (2013). The rodent hippocampus is essential for nonspatial object memory. *Current Biology*, *23*(17), 1685–1690.

Condé, F., Maire-lepoivre, E., Audinat, E., & Crepel, F. (1995). Afferent connections of the medial frontal cortex of the rat. ii. cortical and subcortical afferents. *Journal of Comparative Neurology*, *352*(4), 567–593.

Cox, D. J., Racca, C., & Lebeau, F. E. (2008). β-adrenergic receptors are differentially expressed in distinct interneuron subtypes in the rat hippocampus. *Journal of Comparative Neurology*, *509*(6), 551–565.

Dahlström, A., & Fuxe, K. (1964). Localization of monoamines in the lower brain stem. *Experientia*, *20*(7), 398–399.

Dalley, J., & Stanford, S. (1995). Contrasting effects of the imidazol (in) e alpha 2-adrenoceptor agonists, medetomidine, clonidine and uk 14,304 on extra-neuronal levels of noradrenaline in the rat frontal cortex: Evaluation using in vivo microdialysis and synaptosomal uptake studies. *British journal of pharmacology*, *114*(8), 1717.

Danet, L., Pariente, J., Eustache, P., Raposo, N., Sibon, I., Albucher, J.-F., Bonneville, F., Peran, P., & Barbeau, E. J. (2017). Medial thalamic stroke and its impact on familiarity and recollection. *Elife*, *6*, e28141.

Daubner, S. C., Le, T., & Wang, S. (2011). Tyrosine hydroxylase and regulation of dopamine synthesis. *Archives of biochemistry and biophysics*, *508*(1), 1–12.

Davies, M. F., Tsui, J., Flannery, J. A., Li, X., DeLorey, T. M., & Hoffman, B. B. (2004). Activation of α 2 adrenergic receptors suppresses fear conditioning: Expression of c-fos and phosphorylated creb in mouse amygdala. *Neuropsychopharmacology*, *29*(2), 229–239.

Day, H. E., Campeau, S., Watson Jr, S. J., & Akil, H. (1997). Distribution of α1a-, α1b-and α1d-adrenergic receptor mrna in the rat brain and spinal cord. *Journal of chemical neuroanatomy*, *13*(2), 115–139.

de Vasconcelos, A. P., & Cassel, J.-C. (2015). The nonspecific thalamus: A place in a wedding bed for making memories last? *Neuroscience & Biobehavioral Reviews*, *54*, 175–196.

Devoto, P., & Flore, G. (2006). On the origin of cortical dopamine: Is it a co-transmitter in noradrenergic neurons? *Current neuropharmacology*, *4*(2), 115–125.

Devoto, P., Flore, G., Saba, P., Fà, M., & Gessa, G. L. (2005). Co-release of noradrenaline and dopamine in the cerebral cortex elicited by single train and repeated train stimulation of the locus coeruleus. *BMC neuroscience*, *6*(1), 1–11.

Dix, S. L., & Aggleton, J. P. (1999). Extending the spontaneous preference test of recognition: Evidence of object-location and object-context recognition. *Behavioural brain research*, *99*(2), 191–200.

Dolleman-van der Weel, M. J., Griffin, A. L., Ito, H. T., Shapiro, M. L., Witter, M. P., Vertes, R. P., & Allen, T. A. (2019). The nucleus reuniens of the thalamus sits at the nexus of a hippocampus and medial prefrontal cortex circuit enabling memory and behavior. *Learning & Memory*, *26*(7), 191–205.

Dolleman-Van der Weel, M. J., & Witter, M. P. (2000). Nucleus reuniens thalami innervates γ aminobutyric acid positive cells in hippocampal field ca1 of the rat. *Neuroscience letters*, *278*(3), 145–148.

Domyancic, A. V., & Morilak, D. A. (1997). Distribution of α1a adrenergic receptor m rna in the rat brain visualized by in situ hybridization. *Journal of Comparative Neurology*, *386*(3), 358–378.

Eacott, M. J., & Norman, G. (2004). Integrated memory for object, place, and context in rats: A possible model of episodic-like memory? *Journal of Neuroscience*, *24*(8), 1948–1953.

Eaton, M., Wagner, C., Moore, K., & Lookingland, K. (1994). Neurochemical identification of a 13 dopaminergic neuronal projections from the medial zona incerta to the horizontal limb of the diagonal band of broca and the central nucleus of the amygdala. *Brain research*, *659*(1-2), 201–207.

Ego-Stengel, V., & Wilson, M. A. (2010). Disruption of ripple-associated hippocampal activity during rest impairs spatial learning in the rat. *Hippocampus*, *20*(1), 1–10.

Eichenbaum, H., Otto, T., & Cohen, N. J. (1994). Two functional components of the hippocampal memory system. *Behavioral and Brain Sciences*, *17*(3), 449–472.

Eichenbaum, H., Yonelinas, A. P., & Ranganath, C. (2007). The medial temporal lobe and recognition memory. *Annu. Rev. Neurosci.*, *30*, 123–152.

Ennaceur, A. (2010). One-trial object recognition in rats and mice: Methodological and theoretical issues. *Behavioural brain research*, *215*(2), 244–254.

Ennaceur, A., & Aggleton, J. P. (1994). Spontaneous recognition of object configurations in rats: Effects of fornix lesions. *Experimental brain research*, *100*(1), 85–92.

Ennaceur, A., & Delacour, J. (1988). A new one-trial test for neurobiological studies of memory in rats. 1: Behavioral data. *Behavioural brain research*, *31*(1), 47–59.

Ennaceur, A., Neave, N., & Aggleton, J. P. (1997). Spontaneous object recognition and object location memory in rats: The effects of lesions in the cingulate cortices, the medial prefrontal cortex, the cingulum bundle and the fornix. *Experimental brain research*, *113*(3), 509–519.

Farovik, A., Dupont, L. M., Arce, M., & Eichenbaum, H. (2008). Medial prefrontal cortex supports recollection, but not familiarity, in the rat. *Journal of Neuroscience*, *28*(50), 13428–13434.

Feng, J., Zhang, C., Lischinsky, J. E., Jing, M., Zhou, J., Wang, H., Zhang, Y., Dong, A., Wu, Z., Wu, H., Chen, W., Zhang, P., Zou, J., Hires, S. A., Zhu, J. J., Cui, G., Lin, D., Du, J., & Li, Y. (2019). A genetically encoded fluorescent sensor for rapid and specific in vivo detection of norepinephrine. *Neuron*, *102*(4), 745–761.

Fernández-Pastor, B., & Meana, J. J. (2002). In vivo tonic modulation of the noradrenaline release in the rat cortex by locus coeruleus somatodendritic α2-adrenoceptors. *European journal of pharmacology*, *442*(3), 225–229.

Ferry, B., & McGaugh, J. L. (2008). Involvement of basolateral amygdala α2-adrenoceptors in modulating consolidation of inhibitory avoidance memory. *Learning & Memory*, *15*(4), 238–243.

Ferry, B., Parrot, S., Marien, M., Lazarus, C., Cassel, J.-C., & McGaugh, J. L. (2015). Noradrenergic influences in the basolateral amygdala on inhibitory avoidance memory are mediated by an action on α2-adrenoceptors. *Psychoneuroendocrinology*, *51*, 68–79.

Ferry, B., Roozendaal, B., & McGaugh, J. L. (1999a). Basolateral amygdala noradrenergic influences on memory storage are mediated by an interaction between β-and α1-adrenoceptors. *Journal of Neuroscience*, *19*(12), 5119–5123.

Ferry, B., Roozendaal, B., & McGaugh, J. L. (1999b). Involvement of α1-adrenoceptors in the basolateral amygdala in modulation of memory storage. *European journal of pharmacology*, *372*(1), 9–16.

Finch, A. M., Sarramegna, V., & Graham, R. M. (2006). Ligand binding, activation, and agonist trafficking. *The adrenergic receptors* (pp. 25–85). Springer.

Fischer, K. B., Collins, H. K., & Callaway, E. M. (2019). Sources of off-target expression from recombinase-dependent aav vectors and mitigation with cross-over insensitive atg-out vectors. *Proceedings of the National Academy of Sciences*, *116*(52), 27001–27010.

Floresco, S. B., Block, A. E., & Maric, T. (2008). Inactivation of the medial prefrontal cortex of the rat impairs strategy set-shifting, but not reversal learning, using a novel, automated procedure. *Behavioural brain research*, *190*(1), 85–96.

Forwood, S. E., Winters, B., & Bussey, T. (2005). Hippocampal lesions that abolish spatial maze performance spare object recognition memory at delays of up to 48 hours. *Hippocampus*, *15*(3), 347–355.

Frankland, P. W., & Bontempi, B. (2005). The organization of recent and remote memories. *Nature reviews neuroscience*, *6*(2), 119–130.

Franowicz, J. S., Kessler, L. E., Borja, C. M. D., Kobilka, B. K., Limbird, L. E., & Arnsten, A. F. (2002). Mutation of the α2a-adrenoceptor impairs working memory performance and annuls cognitive enhancement by guanfacine. *Journal of Neuroscience*, *22*(19), 8771–8777.

Frassoni, C., Spreafico, R., & Bentivoglio, M. (1997). Glutamate, aspartate and co-localization with calbindin in the medial thalamus an immunohistochemical study in the rat. *Experimental brain research*, *115*(1), 95–104.

Fung, S., Reddy, V., Liu, R.-H., Wang, Z., & Barnes, C. (1994). Existence of glutamate in noradrenergic locus coeruleus neurons of rodents. *Brain research bulletin*, *35*(5-6), 505–512.

Fuxe, D. (1964). Evidence for existence of monoamine-containing neurons in central nervous system. i. demonstration of monoamines in the cell bodies of brain stem neurons. *Acta physiol. scand.*, *62*, 1–55.

Garcıa-Cabezas, M. Á., Martınez-Sánchez, P., Sánchez-González, M. Á., Garzón, M., & Cavada, C. (2009). Dopamine innervation in the thalamus: Monkey versus rat. *Cerebral Cortex*, *19*(2), 424–434.

Garcıa-Cabezas, M. Á., Rico, B., Sánchez-González, M. Á., & Cavada, C. (2007). Distribution of the dopamine innervation in the macaque and human thalamus. *Neuroimage*, *34*(3), 965–984.

Gasbarri, A., Sulli, A., & Packard, M. G. (1997). The dopaminergic mesencephalic projections to the hippocampal formation in the rat. *Progress in Neuro-Psychopharmacology and Biological Psychiatry*, *21*(1), 1–22.

Gelinas, J. N., Tenorio, G., Lemon, N., Abel, T., & Nguyen, P. V. (2008). β-adrenergic receptor activation during distinct patterns of stimulation critically modulates the pka-dependence of ltp in the mouse hippocampus. *Learning & Memory*, *15*(5), 281–289.

Giustino, T. F., Fitzgerald, P. J., Ressler, R. L., & Maren, S. (2019). Locus coeruleus toggles reciprocal prefrontal firing to reinstate fear. *Proceedings of the National Academy of Sciences*, *116*(17), 8570–8575.

Glennon, E., Carcea, I., Martins, A. R. O., Multani, J., Shehu, I., Svirsky, M. A., & Froemke, R. C. (2019). Locus coeruleus activation accelerates perceptual learning. *Brain research*, *1709*, 39–49.

Gompf, H. S., Budygin, E. A., Fuller, P. M., & Bass, C. E. (2015). Targeted genetic manipulations of neuronal subtypes using promoter-specific combinatorial aavs in wild-type animals. *Frontiers in behavioral neuroscience*, *9*, 152.

Good, M. A., Barnes, P., Staal, V., McGregor, A., & Honey, R. C. (2007). Context-but not familiarity-dependent forms of object recognition are impaired following excitotoxic hippocampal lesions in rats. *Behavioral neuroscience*, *121*(1), 218.

Greengrass, P., & Bremmer, R. (1979). Binding characteristics of 3h-prazosin to rat brain α-adrenergic receptors. *European journal of pharmacology*, *55*(3), 323–326.

Grieger, J. C., & Samulski, R. J. (2005). Packaging capacity of adeno-associated virus serotypes: Impact of larger genomes on infectivity and postentry steps. *Journal of virology*, *79*(15), 9933–9944.

Groenewegen, H. J., & Witter, M. P. (2004). Chapter 17 - thalamus. In G. Paxinos (Ed.), *The rat nervous system (third edition)* (Third Edition, pp. 407–453). Academic Press. https://doi.org/https://doi.org/10.1016/B978-012547638-6/50018-3

Groenewegen, H. (1988). Organization of the afferent connections of the mediodorsal thalamic nucleus in the rat, related to the mediodorsal-prefrontal topography. *Neuroscience*, *24*(2), 379–431.

Groenewegen, H., & Berendse, H. (1994). The specificity of the 'nonspecific'midline and intralaminar thalamic nuclei. *Trends in neurosciences*, *17*(2), 52–57.

Guo, N.-N., & Li, B.-M. (2007). Cellular and subcellular distributions of β1-and β2-adrenoceptors in the ca1 and ca3 regions of the rat hippocampus. *Neuroscience*, *146*(1), 298–305.

Hadley, W. (2016). *Ggplot2: Elegrant graphics for data analysis*. Springer.

Hallock, H. L., Wang, A., & Griffin, A. L. (2016). Ventral midline thalamus is critical for hippocampal–prefrontal synchrony and spatial working memory. *Journal of Neuroscience*, *36*(32), 8372–8389.

Hallock, H. L., Wang, A., Shaw, C. L., & Griffin, A. L. (2013). Transient inactivation of the thalamic nucleus reuniens and rhomboid nucleus produces deficits of

a working-memory dependent tactile-visual conditional discrimination task. *Behavioral neuroscience*, *127*(6), 860.

Hammond, R. S., Tull, L. E., & Stackman, R. W. (2004). On the delay-dependent involvement of the hippocampus in object recognition memory. *Neurobiology of learning and memory*, *82*(1), 26–34.

Hannesson, D. K., Howland, J. G., & Phillips, A. G. (2004). Interaction between perirhinal and medial prefrontal cortex is required for temporal order but not recognition memory for objects in rats. *Journal of Neuroscience*, *24*(19), 4596–4604.

Hansen, N., & Manahan-Vaughan, D. (2015). Locus coeruleus stimulation facilitates long-term depression in the dentate gyrus that requires activation of β-adrenergic receptors. *Cerebral Cortex*, *25*(7), 1889–1896.

Hembrook, J. R., & Mair, R. G. (2011). Lesions of reuniens and rhomboid thalamic nuclei impair radial maze win-shift performance. *Hippocampus*, *21*(8), 815–826.

Hembrook, J. R., Onos, K. D., & Mair, R. G. (2012). Inactivation of ventral midline thalamus produces selective spatial delayed conditional discrimination impairment in the rat. *Hippocampus*, *22*(4), 853–860.

Herkenham, M. (1978). The connections of the nucleus reuniens thalami: Evidence for a direct thalamo-hippocampal pathway in the rat. *Journal of Comparative Neurology*, *177*(4), 589–609.

Hillman, K. L., Doze, V. A., & Porter, J. E. (2005). Functional characterization of the β-adrenergic receptor subtypes expressed by ca1 pyramidal cells in the rat hippocampus. *Journal of Pharmacology and Experimental Therapeutics*, *314*(2), 561–567.

Hillman, K. L., Doze, V. A., & Porter, J. E. (2007). α1a-adrenergic receptors are functionally expressed by a subpopulation of cornu ammonis 1 interneurons in rat hippocampus. *Journal of Pharmacology and Experimental Therapeutics*, *321*(3), 1062–1068.

Hillman, K. L., Knudson, C. A., Carr, P. A., Doze, V. A., & Porter, J. E. (2005). Adrenergic receptor characterization of ca1 hippocampal neurons using real time single cell rt-pcr. *Molecular brain research*, *139*(2), 267–276.

Hillman, K. L., Lei, S., Doze, V. A., & Porter, J. E. (2009). Alpha-1a adrenergic receptor activation increases inhibitory tone in ca1 hippocampus. *Epilepsy research*, *84*(2-3), 97–109.

Hirschberg, S., Li, Y., Randall, A., Kremer, E. J., & Pickering, A. E. (2017). Functional dichotomy in spinal-vs prefrontal-projecting locus coeruleus modules splits descending noradrenergic analgesia from ascending aversion and anxiety in rats. *Elife*, *6*, e29808.

Hokfelt, T. (1984). Distribution maps of tyrosinehydroxylase-immunoreactive neurons in the rat brain. *Handbook of Chemical Neuroanatomy, Classical Transmitters in the CNS*, *2*, 277–379.

Holets, V., Hökfelt, T., Rökaeus, Å., Terenius, L., & Goldstein, M. (1988). Locus coeruleus neurons in the rat containing neuropeptide y, tyrosine hydroxylase or galanin and their efferent projections to the spinal cord, cerebral cortex and hypothalamus. *Neuroscience*, *24*(3), 893–906.

Hoover, W. B., & Vertes, R. P. (2012). Collateral projections from nucleus reuniens of thalamus to hippocampus and medial prefrontal cortex in the rat: A single and double retrograde fluorescent labeling study. *Brain Structure and Function*, *217*(2), 191–209.

Horrillo, I., Ortega, J. E., Diez-Alarcia, R., Urigüen, L., & Meana, J. J. (2019). Chronic fluoxetine reverses the effects of chronic corticosterone treatment on α2-adrenoceptors in the rat frontal cortex but not locus coeruleus. *Neuropharmacology*, *158*, 107731.

Hotte, M., Naudon, L., & Jay, T. M. (2005). Modulation of recognition and temporal order memory retrieval by dopamine d1 receptor in rats. *Neurobiology of learning and memory*, *84*(2), 85–92.

Huerta-Ocampo, I., Hacioglu-Bay, H., Dautan, D., & Mena-Segovia, J. (2020). Distribution of midbrain cholinergic axons in the thalamus. *Eneuro*, *7*(1).

Hur, E. E., & Zaborszky, L. (2005). Vglut2 afferents to the medial prefrontal and primary somatosensory cortices: A combined retrograde tracing in situ hybridization. *Journal of Comparative Neurology*, *483*(3), 351–373.

Jay, T. M., & Witter, M. P. (1991). Distribution of hippocampal ca1 and subicular efferents in the prefrontal cortex of the rat studied by means of anterograde transport of phaseolus vulgaris-leucoagglutinin. *Journal of Comparative Neurology*, *313*(4), 574–586.

Jayachandran, M., Linley, S. B., Schlecht, M., Mahler, S. V., Vertes, R. P., & Allen, T. A. (2019). Prefrontal pathways provide top-down control of memory for sequences of events. *Cell reports*, *28*(3), 640–654.

Jentsch, J. D., Aarde, S. M., & Seu, E. (2009). Effects of atomoxetine and methylphenidate on performance of a lateralized reaction time task in rats. *Psychopharmacology*, *202*(1), 497–504.

Ji, J.-Z., Zhang, X.-H., & Li, B.-M. (2003). Deficient spatial memory induced by blockade of beta-adrenoceptors in the hippocampal ca1 region. *Behavioral neuroscience*, *117*(6), 1378.

Johnson, R. D., & Minneman, K. P. (1985). α1-adrenergic receptors and stimulation of [3h] inositol metabolism in rat brain: Regional distribution and parallel inactivation. *Brain research*, *341*(1), 7–15.

Jones, B. E., & Yang, T.-Z. (1985). The efferent projections from the reticular formation and the locus coeruleus studied by anterograde and retrograde axonal transport in the rat. *Journal of Comparative Neurology*, *242*(1), 56–92.

Kafkas, A., Migo, E. M., Morris, R. G., Kopelman, M. D., Montaldi, D., & Mayes, A. R. (2017). Material specificity drives medial temporal lobe familiarity but not hippocampal recollection. *Hippocampus*, *27*(2), 194–209.

Kakava-Georgiadou, N., Bullich-Vilarrubias, C., Zwartkruis, M., Luijendijk, M. M., Garner, K., & Adan, R. (2019). Considerations related to the use of short neuropeptide promoters in viral vectors targeting hypothalamic neurons. *Scientific reports*, *9*(1), 1–11.

Kebschull, J. M., da Silva, P. G., Reid, A. P., Peikon, I. D., Albeanu, D. F., & Zador, A. M. (2016). High-throughput mapping of single-neuron projections by sequencing of barcoded rna. *Neuron*, *91*(5), 975–987.

Kemp, A., & Manahan-Vaughan, D. (2008). β-adrenoreceptors comprise a critical element in learning-facilitated long-term plasticity. *Cerebral Cortex*, *18*(6), 1326–1334.

Kempadoo, K. A., Mosharov, E. V., Choi, S. J., Sulzer, D., & Kandel, E. R. (2016). Dopamine release from the locus coeruleus to the dorsal hippocampus promotes spatial learning and memory. *Proceedings of the National Academy of Sciences*, *113*(51), 14835–14840.

Köhler, S., & Martin, C. B. (2020). Familiarity impairments after anterior temporal-lobe resection with hippocampal sparing: Lessons learned from case nb. *Neuropsychologia*, *138*, 107339.

Krout, K. E., Belzer, R. E., & Loewy, A. D. (2002). Brainstem projections to midline and intralaminar thalamic nuclei of the rat. *Journal of Comparative Neurology*, *448*(1), 53–101.

Kvetnansky, R., Sabban, E. L., & Palkovits, M. (2009). Catecholaminergic systems in stress: Structural and molecular genetic approaches. *Physiological reviews*, *89*(2), 535–606.

Langer, S. Z. (1974). Presynaptic regulation of catecholamine release. *Biochemical pharmacology*.

Langston, R. F., & Wood, E. R. (2010). Associative recognition and the hippocampus: Differential effects of hippocampal lesions on object-place, object-context and object-place-context memory. *Hippocampus*, *20*(10), 1139–1153.

Lapiz, M., & Morilak, D. (2006). Noradrenergic modulation of cognitive function in rat medial prefrontal cortex as measured by attentional set shifting capability. *Neuroscience*, *137*(3), 1039–1049.

Lara-Vásquez, A., Espinosa, N., Durán, E., Stockle, M., & Fuentealba, P. (2016). Midline thalamic neurons are differentially engaged during hippocampus network oscillations. *Scientific reports*, *6*(1), 1–16.

Layfield, D. M., Patel, M., Hallock, H., & Griffin, A. L. (2015). Inactivation of the nucleus reuniens/rhomboid causes a delay-dependent impairment of spatial working memory. *Neurobiology of learning and memory*, *125*, 163–167.

Lefkowitz, R. J., Limbird, L. E., Mukherjee, C., & Caron, M. G. (1976). The ß-adrenergic receptor and adenylate cyclase. *Biochimica et Biophysica Acta (BBA)-Reviews on Biomembranes*, *457*(1), 1–39.

Lein, E. S., Hawrylycz, M. J., Ao, N., Ayres, M., Bensinger, A., Bernard, A., Boe, A. F., Boguski, M. S., Brockway, K. S., Byrnes, E. J., et al. (2007). Genome-wide atlas of gene expression in the adult mouse brain. *Nature*, *445*(7124), 168–176.

Lemon, N., Aydin-Abidin, S., Funke, K., & Manahan-Vaughan, D. (2009). Locus coeruleus activation facilitates memory encoding and induces hippocampal ltd that depends on β-adrenergic receptor activation. *Cerebral cortex*, *19*(12), 2827–2837.

Likhtik, E., & Johansen, J. P. (2019). Neuromodulation in circuits of aversive emotional learning. *Nature neuroscience*, *22*(10), 1586–1597.

Lindvall, O. (1983). Dopamine and norepinephrine containing neuron system: Their anatomy in the rat brain. *Chemical neuroanatomy*, 229–255.

Lindvall, O., Björklund, A., Nobin, A., & Stenevi, U. (1974). The adrenergic innervation of the rat thalamus as revealed by the glyoxylic acid fluorescence method. *Journal of comparative Neurology*, *154*(3), 317–347.

Liu, Y., Liang, X., Ren, W.-W., & Li, B.-M. (2014). Expression of β1-and β2-adrenoceptors in different subtypes of interneurons in the medial prefrontal cortex of mice. *Neuroscience*, *257*, 149–157.

López, A. J., Kramár, E., Matheos, D. P., White, A. O., Kwapis, J., Vogel-Ciernia, A., Sakata, K., Espinoza, M., & Wood, M. A. (2016). Promoter-specific effects of dreadd modulation on hippocampal synaptic plasticity and memory formation. *Journal of Neuroscience*, *36*(12), 3588–3599.

Loughlin, S., Foote, S., & Bloom, F. (1986). Efferent projections of nucleus locus coeruleus: Topographic organization of cells of origin demonstrated by three-dimensional reconstruction. *Neuroscience*, *18*(2), 291–306.

Loureiro, M., Cholvin, T., Lopez, J., Merienne, N., Latreche, A., Cosquer, B., Geiger, K., Kelche, C., Cassel, J.-C., & de Vasconcelos, A. P. (2012). The ventral midline thalamus (reuniens and rhomboid nuclei) contributes to the persistence of spatial memory in rats. *Journal of Neuroscience*, *32*(29), 9947–9959.

Loy, R., Koziell, D. A., Lindsey, J. D., & Moore, R. Y. (1980). Noradrenergic innervation of the adult rat hippocampal formation. *Journal of Comparative Neurology*, *189*(4), 699–710.

Lv, J., Zhan, S.-Y., Li, G.-X., Wang, D., Li, Y.-S., & Jin, Q.-H. (2016). α1-adrenoceptors in the hippocampal dentate gyrus involved in learning-dependent long-term potentiation during active-avoidance learning in rats. *Neuroreport*, *27*(16), 1211–1216.

MacDonald, E., Kobilka, B. K., & Scheinin, M. (1997). Gene targeting—homing in on α2-adrenoceptor-subtype function. *Trends in pharmacological sciences*, *18*(4), 211–219.

Mair, R. G., Burk, J. A., & Porter, M. C. (1998). Lesions of the frontal cortex, hippocampus, and intralaminar thalamic nuclei have distinct effects on remembering in rats. *Behavioral neuroscience*, *112*(4), 772.

Maisson, D. J.-N., Gemzik, Z. M., & Griffin, A. L. (2018). Optogenetic suppression of the nucleus reuniens selectively impairs encoding during spatial working memory. *Neurobiology of Learning and Memory*, *155*, 78–85.

Manns, J. R., Hopkins, R. O., Reed, J. M., Kitchener, E. G., & Squire, L. R. (2003). Recognition memory and the human hippocampus. *Neuron*, *37*(1), 171–180.

Mansour, A., Meador-Woodruff, J., Bunzow, J., Civelli, O., Akil, H., & Watson, S. (1990). Localization of dopamine d2 receptor mrna and d1 and d2 receptor binding in the rat brain and pituitary: An in situ hybridization-receptor autoradiographic analysis. *Journal of neuroscience*, *10*(8), 2587–2600.

Mao, Z.-M., Arnsten, A. F., & Li, B.-M. (1999). Local infusion of an α-1 adrenergic agonist into the prefrontal cortex impairs spatial working memory performance in monkeys. *Biological psychiatry*, *46*(9), 1259–1265.

Mason, S. T., & Fibiger, H. C. (1979). Regional topography within noradrenergic locus coeruleus as revealed by retrograde transport of horseradish peroxidase. *Journal of comparative neurology*, *187*(4), 703–724.

Mathis, C. (2018). The value of the object recognition paradigm in investigating animal models of alzheimer's disease: Advances and future directions. *Handbook of behavioral neuroscience* (pp. 307–330). Elsevier.

Mayes, A., Holdstock, J., Isaac, C., Hunkin, N., & Roberts, N. (2002). Relative sparing of item recognition memory in a patient with adult-onset damage limited to the hippocampus. *Hippocampus*, *12*(3), 325–340.

McCall, J. G., Al-Hasani, R., Siuda, E. R., Hong, D. Y., Norris, A. J., Ford, C. P., & Bruchas, M. R. (2015). Crh engagement of the locus coeruleus noradrenergic system mediates stress-induced anxiety. *Neuron*, *87*(3), 605–620.

McCormick, D. A., & Prince, D. A. (1988). Noradrenergic modulation of firing pattern in guinea pig and cat thalamic neurons, in vitro. *Journal of Neurophysiology*, *59*(3), 978–996.

McCune, S., Voigt, M., & Hill, J. (1993). Expression of multiple alpha adrenergic receptor subtype messenger rnas in the adult rat brain. *Neuroscience*, *57*(1), 143–151.

McDonald, R. J., & White, N. M. (2013). A triple dissociation of memory systems: Hippocampus, amygdala, and dorsal striatum.

McKenna, J. T., & Vertes, R. P. (2004). Afferent projections to nucleus reuniens of the thalamus. *Journal of comparative neurology*, *480*(2), 115–142.

McNamara, C. G., & Dupret, D. (2017). Two sources of dopamine for the hippocampus. *Trends in neurosciences*, *40*(7), 383–384.

Mello-Carpes, P. B., de Vargas, L. d. S., Gayer, M. C., Roehrs, R., & Izquierdo, I. (2016). Hippocampal noradrenergic activation is necessary for object recog-

nition memory consolidation and can promote bdnf increase and memory persistence. *Neurobiology of learning and memory*, *127*, 84–92.

Messanvi, F., Eggens-Meijer, E., Roozendaal, B., Der Want, V., & Jacobus, J. (2013). A discrete dopaminergic projection from the incertohypothalamic a13 cell group to the dorsolateral periaqueductal gray in rat. *Frontiers in neuroanatomy*, *7*, 41.

Milner, T. A., Lee, A., Aicher, S. A., & Rosin, D. L. (1998). Hippocampal α2a-adrenergic receptors are located predominantly presynaptically but are also found postsynaptically and in selective astrocytes. *Journal of Comparative Neurology*, *395*(3), 310–327.

Minneman, K. P., Hegstrand, L. R., & Molinoff, P. B. (1979). Simultaneous determination of beta-1 and beta-2-adrenergic receptors in tissues containing both receptor subtypes. *Molecular pharmacology*, *16*(1), 34–46.

Mitchell, J. B., & Laiacona, J. (1998). The medial frontal cortex and temporal memory: Tests using spontaneous exploratory behaviour in the rat. *Behavioural brain research*, *97*(1-2), 107–113.

Moreno-Castilla, P., Pérez-Ortega, R., Violante-Soria, V., Balderas, I., & Bermúdez-Rattoni, F. (2017). Hippocampal release of dopamine and norepinephrine encodes novel contextual information. *Hippocampus*, *27*(5), 547–557.

Morris, R. G., Garrud, P., Rawlins, J. a., & O'Keefe, J. (1982). Place navigation impaired in rats with hippocampal lesions. *Nature*, *297*(5868), 681–683.

Mumby, D. G., Gaskin, S., Glenn, M. J., Schramek, T. E., & Lehmann, H. (2002). Hippocampal damage and exploratory preferences in rats: Memory for objects, places, and contexts. *Learning & memory*, *9*(2), 49–57.

Mumby, D. G., Tremblay, A., Lecluse, V., & Lehmann, H. (2005). Hippocampal damage and anterograde object-recognition in rats after long retention intervals. *Hippocampus*, *15*(8), 1050–1056.

Murchison, C. F., Zhang, X.-Y., Zhang, W.-P., Ouyang, M., Lee, A., & Thomas, S. A. (2004). A distinct role for norepinephrine in memory retrieval. *Cell*, *117*(1), 131–143.

Nagatomo, T., Tsuchihashi, H., Sasaki, S., Nakagwa, Y., Nakahara, H., & Imai, S. (1985). Displacement by α-adrenergic agonists and antagonists of 3h-prazosin bound to the α-adrenoceptors of the dog aorta and the rat brain. *The Japanese Journal of Pharmacology*, *37*(2), 181–187.

Nakamura, Y., Kitani, T., Okuno, S., Otake, K., Sato, F., & Fujisawa, H. (2000). Immunohistochemical study of the distribution of ca2+/calmodulin-dependent protein kinase phosphatase in the rat central nervous system. *Molecular brain research*, *77*(1), 76–94.

Nelson, A. J., Cooper, M. T., Thur, K. E., Marsden, C. A., & Cassaday, H. J. (2011). The effect of catecholaminergic depletion within the prelimbic and infralimbic medial prefrontal cortex on recognition memory for recency, location, and objects. *Behavioral neuroscience*, *125*(3), 396.

Nicholas, A. P., Pieribone, V., & Hökfelt, T. (1993a). Cellular localization of messenger rna for beta-1 and beta-2 adrenergic receptors in rat brain: An in situ hybridization study. *Neuroscience*, *56*(4), 1023–1039.

Nicholas, A. P., Pieribone, V., & Hökfelt, T. (1993b). Distributions of mrnas for alpha-2 adrenergic receptor subtypes in rat brain: An in situ hybridization study. *Journal of Comparative Neurology*, *328*(4), 575–594.

Ogundele, O. M., Lee, C. C., & Francis, J. (2017). Thalamic dopaminergic neurons projects to the paraventricular nucleus-rostral ventrolateral medulla/c1 neural circuit. *The Anatomical Record*, *300*(7), 1307–1314.

O'Keefe, J., & Nadel, L. (1978). *The hippocampus as a cognitive map*. Oxford university press.

Oleskevich, S., Descarries, L., & Lacaille, J.-C. (1989). Quantified distribution of the noradrenaline innervation in the hippocampus of adult rat. *Journal of Neuroscience*, *9*(11), 3803–3815.

Palacios, J., & Kuhar, M. J. (1982). Beta adrenergic receptor localization in rat brain by light microscopic autoradiography. *Neurochemistry international*, *4*(6), 473–490.

Papadopoulos, G. C., & Parnavelas, J. G. (1990). Distribution and synaptic organization of serotoninergic and noradrenergic axons in the lateral geniculate nucleus of the rat. *Journal of Comparative Neurology*, *294*(3), 345–355.

Paschalis, A., Churchill, L., Marina, N., Kasymov, V., Gourine, A., & Ackland, G. (2009). β1-adrenoceptor distribution in the rat brain: An immunohistochemical study. *Neuroscience letters*, *458*(2), 84–88.

Patai, E. Z., Gadian, D. G., Cooper, J. M., Dzieciol, A. M., Mishkin, M., & Vargha-Khadem, F. (2015). Extent of hippocampal atrophy predicts degree of deficit in recall. *Proceedings of the National Academy of Sciences*, *112*(41), 12830–12833.

Paxinos, G., & Franklin, K. B. (2019). *Paxinos and franklin's the mouse brain in stereotaxic coordinates*. Academic press.

Paxinos, G., & Watson, C. (2006). *The rat brain in stereotaxic coordinates: Hard cover edition*. Elsevier.

Pérez-Santos, I., Palomero-Gallagher, N., Zilles, K., & Cavada, C. (2021). Distribution of the noradrenaline innervation and adrenoceptors in the macaque monkey thalamus. *Cerebral Cortex*, *31*(9), 4115–4139.

Pieribone, V. A., Nicholas, A. P., Dagerlind, A., & Hokfelt, T. (1994). Distribution of alpha 1 adrenoceptors in rat brain revealed by in situ hybridization experiments utilizing subtype-specific probes. *Journal of Neuroscience*, *14*(7), 4252–4268.

Poe, G. R., Foote, S., Eschenko, O., Johansen, J. P., Bouret, S., Aston-Jones, G., Harley, C. W., Manahan-Vaughan, D., Weinshenker, D., Valentino, R., Berridge, C., Chandler, D. J., Waterhouse, B., & Sara, S. J. (2020). Locus coeruleus: A new look at the blue spot. *Nature Reviews Neuroscience*, *21*(11), 644–659.

Porter, M. C., Burk, J. A., & Mair, R. G. (2000). A comparison of the effects of hippocampal or prefrontal cortical lesions on three versions of delayed non-matching-to-sample based on positional or spatial cues. *Behavioural brain research*, *109*(1), 69–81.

Porter, M. C., & Mair, R. G. (1997). The effects of frontal cortical lesions on remembering depend on the procedural demands of tasks performed in the radial arm maze. *Behavioural brain research*, *87*(2), 115–125.

Prakash, N., & Wurst, W. (2006). Development of dopaminergic neurons in the mammalian brain. *Cellular and Molecular Life Sciences CMLS*, *63*(2), 187–206.

Qu, L.-L., Guo, N.-N., & Li, B.-M. (2008). β1-and β2-adrenoceptors in basolateral nucleus of amygdala and their roles in consolidation of fear memory in rats. *Hippocampus*, *18*(11), 1131–1139.

Quet, E., Majchrzak, M., Cosquer, B., Morvan, T., Wolff, M., Cassel, J.-C., de Vasconcelos, A. P., & Stéphan, A. (2020). The reuniens and rhomboid nuclei are necessary for contextual fear memory persistence in rats. *Brain Structure and Function*, *225*(3), 955–968.

Quinlan, M. A., Strong, V. M., Skinner, D. M., Martin, G. M., Harley, C. W., & Walling, S. G. (2019). Locus coeruleus optogenetic light activation induces long-term potentiation of perforant path population spike amplitude in rat dentate gyrus. *Frontiers in systems neuroscience*, *12*, 67.

Ragozzino, M. E., Kim, J., Hassert, D., Minniti, N., & Kiang, C. (2003). The contribution of the rat prelimbic-infralimbic areas to different forms of task switching. *Behavioral neuroscience*, *117*(5), 1054.

Rainbow, T. C., Parsons, B., & Wolfe, B. B. (1984). Quantitative autoradiography of beta 1-and beta 2-adrenergic receptors in rat brain. *Proceedings of the National Academy of Sciences*, *81*(5), 1585–1589.

Rajasethupathy, P., Sankaran, S., Marshel, J. H., Kim, C. K., Ferenczi, E., Lee, S. Y., Berndt, A., Ramakrishnan, C., Jaffe, A., Lo, M., Liston, C., & Deisseroth, K. (2015). Projections from neocortex mediate top-down control of memory retrieval. *Nature*, *526*(7575), 653–659.

Ramos, B. P., & Arnsten, A. F. (2007). Adrenergic pharmacology and cognition: Focus on the prefrontal cortex. *Pharmacology & therapeutics*, *113*(3), 523–536.

Ranjbar-Slamloo, Y., & Fazlali, Z. (2020). Dopamine and noradrenaline in the brain; overlapping or dissociate functions? *Frontiers in molecular neuroscience*, *12*, 334.

Rieck, R. W., Ansari, M., Whetsell, W. O., Deutch, A. Y., & Kessler, R. M. (2004). Distribution of dopamine d 2-like receptors in the human thalamus: Autoradiographic and pet studies. *Neuropsychopharmacology*, *29*(2), 362–372.

Riley, J. N., & Moore, R. Y. (1981). Diencephalic and brainstem afferents to the hippocampal formation of the rat. *Brain research bulletin*, *6*(4-6), 437–444.

Robinson, E. S. (2012). Blockade of noradrenaline re-uptake sites improves accuracy and impulse control in rats performing a five-choice serial reaction time tasks. *Psychopharmacology*, *219*(2), 303–312.

Rodenkirch, C., Liu, Y., Schriver, B. J., & Wang, Q. (2019). Locus coeruleus activation enhances thalamic feature selectivity via norepinephrine regulation of intrathalamic circuit dynamics. *Nature neuroscience*, *22*(1), 120–133.

Rosin, D. L., Talley, E. M., Lee, A., Stornetta, R. L., Gaylinn, B. D., Guyenet, P. G., & Lynch, K. R. (1996). Distribution of α2c-adrenergic receptor-like immunoreactivity in the rat central nervous system. *Journal of Comparative Neurology*, *372*(1), 135–165.

Sabec, M. H., Wonnacott, S., Warburton, E. C., & Bashir, Z. I. (2018). Nicotinic acetylcholine receptors control encoding and retrieval of associative recognition memory through plasticity in the medial prefrontal cortex. *Cell reports*, *22*(13), 3409–3415.

Saleeba, C., Dempsey, B., Le, S., Goodchild, A., & McMullan, S. (2019). A student's guide to neural circuit tracing. *Frontiers in neuroscience*, *13*, 897.

Samuels, E. R., & Szabadi, E. (2008). Functional neuroanatomy of the noradrenergic locus coeruleus: Its roles in the regulation of arousal and autonomic function part i: Principles of functional organisation. *Current neuropharmacology*, *6*(3), 235–253.

Sánchez-González, M. Á., Garcıa-Cabezas, M. Á., Rico, B., & Cavada, C. (2005). The primate thalamus is a key target for brain dopamine. *Journal of Neuroscience*, *25*(26), 6076–6083.

Santana, N., & Artigas, F. (2017). Laminar and cellular distribution of monoamine receptors in rat medial prefrontal cortex. *Frontiers in neuroanatomy*, *11*, 87.

Santana, N., Mengod, G., & Artigas, F. (2013). Expression of α1-adrenergic receptors in rat prefrontal cortex: Cellular co-localization with 5-ht2a receptors. *International Journal of Neuropsychopharmacology*, *16*(5), 1139–1151.

Sara, S. J. (2009). The locus coeruleus and noradrenergic modulation of cognition. *Nature reviews neuroscience*, *10*(3), 211–223.

Sara, S. J., Vankov, A., & Hervé, A. (1994). Locus coeruleus-evoked responses in behaving rats: A clue to the role of noradrenaline in memory. *Brain research bulletin*, *35*(5-6), 457–465.

Sargent, L., Gauger, L., & Davis, J. (1984). Anatomy of brain alpha,-adrenergic receptors: In vitro autoradiography with [125i]-heat. *J. Comp. Neurol*, *231*, 190–208.

Savalli, G., Bashir, Z. I., & Warburton, E. C. (2015). Regionally selective requirement for d1/d5 dopaminergic neurotransmission in the medial prefrontal cortex in object-in-place associative recognition memory. *Learning & Memory*, *22*(2), 69–73.

Scheinin, M., Lomasney, J. W., Hayden-Hixson, D. M., Schambra, U. B., Caron, M. G., Lefkowitz, R. J., & Fremeau Jr, R. T. (1994). Distribution of α2-adrenergic receptor subtype gene expression in rat brain. *Molecular Brain Research*, *21*(1-2), 133–149.

Schindelin, J., Arganda-Carreras, I., Frise, E., Kaynig, V., Longair, M., Pietzsch, T., Preibisch, S., Rueden, C., Saalfeld, S., Schmid, B., Tinevez, J.-Y., White, D. J., Hartenstein, V., Eliceiri, K., Tomancak, P., & Cardona, A. (2012). Fiji: An open-source platform for biological-image analysis. *Nature methods*, *9*(7), 676–682.

Schofield, B. R. (2008). Retrograde axonal tracing with fluorescent markers. *Current protocols in neuroscience*, *43*(1), 1–17.

Schwarz, L. A., & Luo, L. (2015). Organization of the locus coeruleus-norepinephrine system. *Current Biology*, *25*(21), R1051–R1056.

Sesack, S. R., Deutch, A. Y., Roth, R. H., & Bunney, B. S. (1989). Topographical organization of the efferent projections of the medial prefrontal cortex in the rat: An anterograde tract-tracing study with phaseolus vulgaris leucoagglutinin. *Journal of Comparative Neurology*, *290*(2), 213–242.

Sharma, S., Kim, L. H., Mayr, K. A., Elliott, D. A., & Whelan, P. J. (2018). Parallel descending dopaminergic connectivity of a13 cells to the brainstem locomotor centers. *Scientific reports*, *8*(1), 1–15.

Sherman, S. M. (2001). Tonic and burst firing: Dual modes of thalamocortical relay. *Trends in neurosciences*, *24*(2), 122–126.

Sherman, S., & Guillery, R. (2006). Exploring the role of the thalamus and its role in cortical function.

Sita, L., Elias, C., & Bittencourt, J. (2007). Connectivity pattern suggests that incerto-hypothalamic area belongs to the medial hypothalamic system. *Neuroscience*, *148*(4), 949–969.

Sjulson, L., Cassataro, D., DasGupta, S., & Miesenböck, G. (2016). Cell-specific targeting of genetically encoded tools for neuroscience. *Annual review of genetics*, *50*, 571–594.

Sontag, T., Hauser, J., Kaunzinger, I., Gerlach, M., Tucha, O., & Lange, K. (2008). Effects of the noradrenergic neurotoxin dsp4 on spatial memory in the rat. *Journal of Neural Transmission*, *115*(2), 299–303.

Squire, L. R., Wixted, J. T., & Clark, R. E. (2007). Recognition memory and the medial temporal lobe: A new perspective. *Nature Reviews Neuroscience*, *8*(11), 872–883.

Staresina, B. P., Fell, J., Do Lam, A. T., Axmacher, N., & Henson, R. N. (2012). Memory signals are temporally dissociated in and across human hippocampus and perirhinal cortex. *Nature neuroscience*, *15*(8), 1167–1173.

Staresina, B. P., Fell, J., Dunn, J. C., Axmacher, N., & Henson, R. N. (2013). Using state-trace analysis to dissociate the functions of the human hippocampus and perirhinal cortex in recognition memory. *Proceedings of the National Academy of Sciences*, *110*(8), 3119–3124.

Starke, K. (2001). Presynaptic autoreceptors in the third decade: Focus on α2-adrenoceptors. *Journal of neurochemistry*, *78*(4), 685–693.

Stauffer, W. R., Lak, A., Yang, A., Borel, M., Paulsen, O., Boyden, E. S., & Schultz, W. (2016). Dopamine neuron-specific optogenetic stimulation in rhesus macaques. *Cell*, *166*(6), 1564–1571.

Steriade, M., & Llinás, R. R. (1988). The functional states of the thalamus and the associated neuronal interplay. *Physiological reviews*, *68*(3), 649–742.

Straube, T., Korz, V., Balschun, D., & Uta Frey, J. (2003). Requirement of β-adrenergic receptor activation and protein synthesis for ltp-reinforcement by novelty in rat dentate gyrus. *The Journal of physiology*, *552*(3), 953–960.

Summers, R., Papaioannou, M., Harris, S., & Evans, B. (1995). Expression of β3-adrenoceptor mrna in rat brain. *British journal of pharmacology*, *116*(6), 2547–2548.

Sun, F., Zhou, J., Dai, B., Qian, T., Zeng, J., Li, X., Zhuo, Y., Zhang, Y., Wang, Y., Qian, C., Tan, K., Feng, J., Dong, H., Lin, D., Cui, G., & Li, Y. (2020). Next-generation grab sensors for monitoring dopaminergic activity in vivo. *Nature methods*, *17*(11), 1156–1166.

Swanson, L. (2004). *Brain maps: Structure of the rat brain*. Gulf Professional Publishing.

Swanson, L., & Hartman, B. (1975). The central adrenergic system. an immunofluorescence study of the location of cell bodies and their efferent connections in the rat utilizing dopamine-b-hydroxylase as a marker. *Journal of Comparative Neurology*, *163*(4), 467–505.

Szabadi, E. (2013). Functional neuroanatomy of the central noradrenergic system. *Journal of psychopharmacology*, *27*(8), 659–693.

Tait, D. S., Brown, V. J., Farovik, A., Theobald, D. E., Dalley, J. W., & Robbins, T. W. (2007). Lesions of the dorsal noradrenergic bundle impair attentional set-shifting in the rat. *European Journal of Neuroscience*, *25*(12), 3719–3724.

Takeuchi, T., Duszkiewicz, A. J., Sonneborn, A., Spooner, P. A., Yamasaki, M., Watanabe, M., Smith, C. C., Fernández, G., Deisseroth, K., Greene, R. W., & Morris, R. G. (2016). Locus coeruleus and dopaminergic consolidation of everyday memory. *Nature*, *537*(7620), 357–362.

Talley, E. M., Rosin, D. L., Lee, A., Guyenet, P. G., & Lynch, K. R. (1996). Distribution of α2a-adrenergic receptor-like immunoreactivity in the rat central nervous system. *Journal of comparative neurology*, *372*(1), 111–134.

Tanila, H., Rämä, P., & Carlson, S. (1996). The effects of prefrontal intracortical microinjections of an alpha-2 agonist, alpha-2 antagonist and lidocaine on the delayed alternation performance of aged rats. *Brain research bulletin*, *40*(2), 117–119.

Tayrien, M. W., & Loy, R. (1984). Computer-assisted image analysis to quantify regional and specific receptor ligand binding: Upregulation of [3h] qnb and [3h] wb4101 binding in denervated hippocampus. *Brain research bulletin*, *13*(6), 743–750.

Torkaman-Boutorabi, A., Danyali, F., Oryan, S., Ebrahimi-Ghiri, M., & Zarrindast, M.-R. (2014). Hippocampal α-adrenoceptors involve in the effect of histamine on spatial learning. *Physiology & behavior*, *129*, 17–24.

Totah, N. K., Logothetis, N. K., & Eschenko, O. (2019). Noradrenergic ensemble-based modulation of cognition over multiple timescales. *Brain research*, *1709*, 50–66.

Troyner, F., Bicca, M. A., & Bertoglio, L. J. (2018). Nucleus reuniens of the thalamus controls fear memory intensity, specificity and long-term maintenance during consolidation. *Hippocampus*, *28*(8), 602–616.

Turriziani, P., Serra, L., Fadda, L., Caltagirone, C., & Carlesimo, G. A. (2008). Recollection and familiarity in hippocampal amnesia. *Hippocampus*, *18*(5), 469–480.

Tuscher, J. J., Taxier, L. R., Fortress, A. M., & Frick, K. M. (2018). Chemogenetic inactivation of the dorsal hippocampus and medial prefrontal cortex, individually and concurrently, impairs object recognition and spatial memory consolidation in female mice. *Neurobiology of learning and memory*, *156*, 103–116.

Uematsu, A., Tan, B. Z., & Johansen, J. P. (2015). Projection specificity in heterogeneous locus coeruleus cell populations: Implications for learning and memory. *Learning & memory*, *22*(9), 444–451.

Uematsu, A., Tan, B. Z., Ycu, E. A., Cuevas, J. S., Koivumaa, J., Junyent, F., Kremer, E. J., Witten, I. B., Deisseroth, K., & Johansen, J. P. (2017). Modular organization of the brainstem noradrenaline system coordinates opposing learning states. *Nature neuroscience*, *20*(11), 1602–1611.

Ul Haq, R., Liotta, A., Kovacs, R., Rösler, A., Jarosch, M., Heinemann, U., & Behrens, C. (2012). Adrenergic modulation of sharp wave-ripple activity in rat hippocampal slices. *Hippocampus*, *22*(3), 516–533.

U'Prichard, D. C., Charness, M. E., Robertson, D., & Snyder, S. H. (1978). Prazosin: Differential affinities for two populations of α-noradrenergic receptor binding sites. *European journal of pharmacology*, *50*(1), 87–89.

Van Meel, J., De Jonge, A., Timmermans, P., & Van Zwieten, P. (1981). Selectivity of some alpha adrenoceptor agonists for peripheral alpha-1 and alpha-2 adrenoceptors in the normotensive rat. *Journal of Pharmacology and Experimental Therapeutics*, *219*(3), 760–767.

Van Veldhuizen, M., Feenstra, M. G., Heinsbroek, R. P., & Boer, G. J. (1993). In vivo microdialysis of noradrenaline overflow: Effects of α-adrenoceptor agonists and antagonists measured by cumulative concentration-response curves. *British journal of pharmacology*, *109*(3), 655–660.

Vankov, A., Hervé-Minvielle, A., & Sara, S. J. (1995). Response to novelty and its rapid habituation in locus coeruleus neurons of the freely exploring rat. *European Journal of Neuroscience*, *7*(6), 1180–1187.

Varela, C., Kumar, S., Yang, J., & Wilson, M. A. (2014). Anatomical substrates for direct interactions between hippocampus, medial prefrontal cortex, and the thalamic nucleus reuniens. *Brain Structure and Function*, *219*(3), 911–929.

Venkataraman, A., Hunter, S. C., Dhinojwala, M., Ghebrezadik, D., Guo, J., Inoue, K., Young, L. J., & Dias, B. G. (2021). Incerto-thalamic modulation of fear via gaba and dopamine. *Neuropsychopharmacology*, 1–11.

Versteeg, D. H., Van der Gugten, J., De Jong, W., & Palkovits, M. (1976). Regional concentrations of noradrenaline and dopamine in rat brain. *Brain research*, *113*(3), 563–574.

Vertes, R. P. (2002). Analysis of projections from the medial prefrontal cortex to the thalamus in the rat, with emphasis on nucleus reuniens. *Journal of Comparative Neurology*, *442*(2), 163–187.

Vertes, R. P. (2004). Differential projections of the infralimbic and prelimbic cortex in the rat. *Synapse*, *51*(1), 32–58.

Vertes, R. P. (2006). Interactions among the medial prefrontal cortex, hippocampus and midline thalamus in emotional and cognitive processing in the rat. *Neuroscience*, *142*(1), 1–20.

Vertes, R. P., Hoover, W. B., Do Valle, A. C., Sherman, A., & Rodriguez, J. (2006). Efferent projections of reuniens and rhomboid nuclei of the thalamus in the rat. *Journal of comparative neurology*, *499*(5), 768–796.

Vertes, R. P., Hoover, W. B., Szigeti-Buck, K., & Leranth, C. (2007). Nucleus reuniens of the midline thalamus: Link between the medial prefrontal cortex and the hippocampus. *Brain research bulletin*, *71*(6), 601–609.

Vertes, R. P., Linley, S. B., & Hoover, W. B. (2015). Limbic circuitry of the midline thalamus. *Neuroscience & Biobehavioral Reviews*, *54*, 89–107.

Vetere, G., Kenney, J. W., Tran, L. M., Xia, F., Steadman, P. E., Parkinson, J., Josselyn, S. A., & Frankland, P. W. (2017). Chemogenetic interrogation of a brain-wide fear memory network in mice. *Neuron*, *94*(2), 363–374.

Viena, T. D., Linley, S. B., & Vertes, R. P. (2018). Inactivation of nucleus reuniens impairs spatial working memory and behavioral flexibility in the rat. *Hippocampus*, *28*(4), 297–311.

Viena, T. D., Rasch, G. E., Silva, D., & Allen, T. A. (2021). Calretinin and calbindin architecture of the midline thalamus associated with prefrontal–hippocampal circuitry. *Hippocampus*, *31*(7), 770–789.

Wagatsuma, A., Okuyama, T., Sun, C., Smith, L. M., Abe, K., & Tonegawa, S. (2018). Locus coeruleus input to hippocampal ca3 drives single-trial learning of a novel context. *Proceedings of the National Academy of Sciences*, *115*(2), E310–E316.

Wagner-Altendorf, T. A., Fischer, B., & Roeper, J. (2019). Axonal projection-specific differences in somatodendritic α2 autoreceptor function in locus coeruleus neurons. *European Journal of Neuroscience*, *50*(11), 3772–3785.

Wais, P. E., Wixted, J. T., Hopkins, R. O., & Squire, L. R. (2006). The hippocampus supports both the recollection and the familiarity components of recognition memory. *Neuron*, *49*(3), 459–466.

Walsh, D. A., Brown, J. T., & Randall, A. D. (2017). In vitro characterization of cell-level neurophysiological diversity in the rostral nucleus reuniens of adult mice. *The Journal of physiology*, *595*(11), 3549–3572.

Wanaka, A., Kiyama, H., Murakami, T., Matsumoto, M., Kamada, T., Malbon, C., & Tohyama, M. (1989). Immunocytochemical localization of β-adrenergic receptors in the rat brain. *Brain research*, *485*(1), 125–140.

Wang, G.-W., & Cai, J.-X. (2006). Disconnection of the hippocampal–prefrontal cortical circuits impairs spatial working memory performance in rats. *Behavioural brain research*, *175*(2), 329–336.

Wang, M., Ramos, B. P., Paspalas, C. D., Shu, Y., Simen, A., Duque, A., Vijayraghavan, S., Brennan, A., Dudley, A., Nou, E., Mazer, J. A., McCormick, D. A., & Arnsten, A. F. (2007). α2a-adrenoceptors strengthen working memory networks by inhibiting camp-hcn channel signaling in prefrontal cortex. *Cell*, *129*(2), 397–410.

Warburton, E. C., Barker, G. R., & Brown, M. W. (2013). Investigations into the involvement of nmda mechanisms in recognition memory. *Neuropharmacology*, *74*, 41–47.

Wilmot, C., Sullivan, A., & Levin, B. (1988). Effects of diet and obesity on brain α1-and α2-noradrenergic receptors in the rat. *Brain research*, *453*(1-2), 157–166.

Winters, B. D., Forwood, S. E., Cowell, R. A., Saksida, L. M., & Bussey, T. J. (2004). Double dissociation between the effects of peri-postrhinal cortex and hippocampal lesions on tests of object recognition and spatial memory: Heterogeneity of function within the temporal lobe. *Journal of Neuroscience*, *24*(26), 5901–5908.

Witten, I. B., Steinberg, E. E., Lee, S. Y., Davidson, T. J., Zalocusky, K. A., Brodsky, M., Yizhar, O., Cho, S. L., Gong, S., Ramakrishnan, C., Stuber, G. D., Tye, K. M., Janak, P. H., & Deisseroth, K. (2011). Recombinase-driver rat lines: Tools, techniques, and optogenetic application to dopamine-mediated reinforcement. *Neuron*, *72*(5), 721–733.

Wouterlood, F. G., Aliane, V., Boekel, A. J., Hur, E. E., Zaborszky, L., Barroso-Chinea, P., Härtig, W., Lanciego, J. L., & Witter, M. P. (2008). Origin of calretinin-containing, vesicular glutamate transporter 2-coexpressing fiber terminals in the entorhinal cortex of the rat. *Journal of Comparative Neurology*, *506*(2), 359–370.

Wouterlood, F. G., Saldana, E., & Witter, M. P. (1990). Projection from the nucleus reuniens thalami to the hippocampal region: Light and electron microscopic tracing study in the rat with the anterograde tracer phaseolus vulgaris-leucoagglutinin. *Journal of Comparative Neurology*, *296*(2), 179–203.

Xu, W., & Südhof, T. C. (2013). A neural circuit for memory specificity and generalization. *Science*, *339*(6125), 1290–1295.

Yang, B., Sanches-Padilla, J., Kondapalli, J., Morison, S. L., Delpire, E., Awatramani, R., & Surmeier, D. J. (2021). Locus coeruleus anchors a trisynaptic circuit controlling fear-induced suppression of feeding. *Neuron*, *109*(5), 823–838.

Young, W. S., & Kuhar, M. J. (1980). Noradrenergic alpha 1 and alpha 2 receptors: Light microscopic autoradiographic localization. *Proceedings of the National Academy of Sciences*, *77*(3), 1696–1700.

Zhang, H.-T., Whisler, L. R., Huang, Y., Xiang, Y., & O'donnell, J. M. (2009). Postsynaptic α-2 adrenergic receptors are critical for the antidepressant-like effects of desipramine on behavior. *Neuropsychopharmacology*, *34*(4), 1067–1077.

Zhu, X.-O., McCabe, B. J., Aggleston, J. P., & Brown, M. W. (1996). Mapping visual recognition memory through expression of the immediate early gene c-fos. *Neuroreport: An International Journal for the Rapid Communication of Research in Neuroscience*.

Zimmerman, E. C., & Grace, A. A. (2018). Prefrontal cortex modulates firing pattern in the nucleus reuniens of the midline thalamus via distinct corticothalamic pathways. *European Journal of Neuroscience*, *48*(10), 3255–3272.